2013-05-13

Dopaminergic Modulation of Mammalian Locomotor Networks

Humphreys, Jennifer

UNIVERSITY OF CALGARY

Dopaminergic Modulation of Mammalian Locomotor Networks

by

Jennifer Marie Humphreys

A THESIS

SUBMITTED TO THE FACULTY OF GRADUATE STUDIES

IN PARTIAL FULFILMENT OF THE REQUIREMENTS FOR THE

DEGREE OF DOCTOR OF PHILOSOPHY

DEPARTMENT OF NEUROSCIENCE

CALGARY, ALBERTA

MAY, 2013

Abstract

Central pattern generators (CPGs), which are intrinsic to the spinal cord, contain sufficient circuitry to generate complex and coordinated muscle activities necessary for locomotion. A class of neurotransmitters termed monoamines (dopamine, serotonin, noradrenaline) exerts neuromodulatory effects on mammalian CPGs. Monoamines are released within the spinal cord during walking and can change the excitability of neurons that comprise the CPG. In contrast with the other monoamines, the neuromodulatory role of dopamine (DA) on locomotor CPGs has been largely neglected in the mammal. Therefore, the goal of my work was to examine the multiple changes in locomotor CPG network output induced by DA. I have employed a "systems" to "cells" approach. Utilizing the neonatal mouse isolated spinal cord preparation and electrophysiological techniques, I first characterized how DA modulates locomotor patterns evoked by either drug application or electrical stimulation. I found that while DA application boosts the stability of a fictive drug-evoked locomotor rhythm, it functions to depress the activation of locomotor networks following ventral root stimulation. By examining disinhibited rhythms, where the Renshaw cell pathway was blocked, I found that DA depresses a putative recurrent excitatory pathway that projects onto rhythm generating circuitry of the spinal cord. These data demonstrate that DA can potentiate network activity, while at the same time, reducing the gain of recurrent excitatory feedback loops from motoneurons onto the network. Next, at the motoneuronal level I examined the ability of DA to modulate the intrinsic membrane property of postinhibitory rebound (PIR), which has been shown to play an important role in producing stable rhythmic locomotor patterns. I found that DA boosts the PIR response in motoneurons, which may account for part of the mechanism by which DA exerts a modulatory role during drug-evoked locomotion. Finally, using a pharmacological approach, I confirm that the primary

ionic conductance underlying the observed PIR response in motoneurons, T-type calcium conductance, also plays an important role at the level of the CPG network. Collectively, my work demonstrates that in a mammalian system, DA exerts complex modulatory actions at the level of the CPG network and ultimately contributes to the sculpting of motor output.

Acknowledgements

First and foremost, I would like to acknowledge the support and guidance of my supervisor Dr. Patrick Whelan, whose pure passion and enthusiasm for Science is truly inspiring. I appreciate your continuous encouragement and understanding throughout the tough times, and I thank you for giving me the opportunity to think differently. I would also like to acknowledge my committee members Dr. Richard Wilson and Dr. Ray Turner, for their continuous support, advice, and feedback.

I would like to thank the past and present members of the Whelan Lab including Dr. Mary Dunbar for her inspiring work ethic; Dr. Sravan Mandadi for his genuine willingness to help whenever I needed it (which was very very often); Dr. Stan Nakanishi for his enthusiasm, honesty and advice – Stan, I simply never would have gotten through this if it wasn't for you; Dr. Kathrin Koblinger and Dr. Aleks Krajacic for their sharp European minds and for making lab such an enjoyable place to be – I admire you both so much; and Simon Sharples and Jillian Ejdrygiewicz for their camaraderie and support.

Thank you to all my amazing friends who have always supported me throughout the years. I would especially like to thank Lauren Turnquist, Ashley Gergel, and Therese Cormier for your understanding, humor and loyalty. You are my favorite people.

Last but certainly not least; I would like to thank my wonderful family. To my incredible parents, Donna and Flynn, I would not be who I am today without your continuous love, patience and support. You have always given me the encouragement and foundation to be successful. To my sister Kari, and her husband Vance, you both inspire me to do good things, and to be better. Finally, a very special thank-you to my boyfriend Matthew, for his love, never-ending support, and for continuously proving to me that there are still good and honest people left in this world.

To all the families and individuals who have experienced the devastation and loss caused by spinal cord injury. May the work presented in this thesis be a small piece of the puzzle in the long journey to recovery and healing.

Table of Contents

List of Tables

List of Figures and Illustrations

List of Symbols, Abbreviations, and Nomenclature

Symbol	Definition
5-HT	- 5-Hydroxytryptamine, used interchangeably with serotonin
A11	- area 11
AB	- anterior burster
aCSF	- artificial cerebral spinal fluid
AHP	- afterhyperpolarization
AMP	- adenosine monophosphate
AP	- action potential
ATP	- adenosine triphosphate
Ca^{2+}	- calcium ion
cAMP	- cyclic adenosine monophosphate
CaV3	- T-type calcium channel
CINs	- commissural interneurons
CNS	- central nervous system
CPG	- central pattern generator
DA	- dopamine
dCINs	- descending commissural interneurons
E	- extensor
F	- flexor
G-protein	- guanine nucleotide-binding protein
GABA	- gamma amino butyric acid
GPe	- globus pallidus externa

GPi - globus pallidus interna

GIRK - G-protein regulated inwardly rectifying potassium current

HCN - hyperpolarization activated, cyclic nucleotide

HEK - human embryonic kidney cells

HVA - high voltage activated

I_A - transient potassium current

IC_{50} - half maximal inhibitory concentraion

I_h - hyperpolarization activated non-specific cation current

I_{Nap} - persistent sodium current

ISI - interspike interval

I_t - T-type calcium current

K^+ - potassium ion

L# - refers to a lumbar spinal root or segment

LVA - low voltage activated

mGluR - metabotropic glutamate receptor

MLR - mesencephalic locomotor region

NA - noradrenalin

Na^+ - sodium ion

Ni^{2+} - nickel

NMA - N-methyl-(DL)-aspartate

NMDA - N-methyl-D-aspartate

P# - postnatal day

PD - Parkinson's disease

PD - pyloric dilator

PFA - paraformaldehyde

PIR - postinhibitory rebound

PKA - protein kinase A

S# - refers to sacral ventral root or segment

sAHP - slow afterhyperpolarization

sCINs - segmental commissural interneurons

SD - standard deviation

siRNA - small interfering ribonucleic acid

SK_{Ca} - small conductance calcium dependent potassium current

SNc - substantia nigra pars compacta

STG - stomatogastric ganglion

STN - subthalamic nuclei

TTX - tetrodotoxin

VLF - ventral lateral funiculus

Chapter One: Introduction

1.1 INTRODUCTION

1.1.1 General remarks

Locomotor behaviors such as walking, flying, and swimming, are essential motor acts that allow animals to move. The generation of such rhythmic locomotor behaviors requires a sophisticated activation of many muscles. Dedicated neuronal networks localized within the spinal cord termed central pattern generators (CPGs), contain sufficient timing and pattern information to recruit motoneurons in the appropriate sequence and with enough intensity to generate basic stepping patterns (Grillner, 2003). Remarkably, the production of basic stepping patterns can be achieved in the absence of phasic input (Grillner, 1981). Although spinal CPG networks support basic locomotor rhythmogenesis, it should be noted that these networks are normally recruited by supraspinal command centers (Grillner, 1981; Shapovalov, 1975). Furthermore, valuable sensory input generated by ongoing movements is utilized for the refinement of CPG activity (Grillner, 2003).

CPG networks are capable of producing a wide variety of locomotor outputs in which the intensity, duration, cycle frequency, and phasing are constantly changing. This flexibility inherent within the locomotor CPG is important because rhythmic motor behavior adapts to meet the demands of an ever-changing environment. Some of this flexibility in motor behavior is accomplished by inputs that arise from peripheral sensory feedback systems (Pearson, 2004). An additional level of flexibility arises from central mechanisms through neuromodulation of the spinal networks themselves (Gordon & Whelan, 2006a; Jankowska, Jukes, Lund, & Lundberg, 1967a; Kiehn & Kjaerulff, 1996; Kiehn, Sillar, Kjaerulff, & McDearmid, 1999; Madriaga, McPhee, Chersa, Christie, & Whelan, 2004; Miles & Sillar, 2011; Schmidt & Jordan, 2000). From a systems-level point of view, a “neuromodulator” can be distinguished from a

"neurotransmitter" based upon function, and the spatial-temporal scale to which the signaling agent acts. If a signaling agent rapidly conveys information regarding the current state of one network component to another, for example the excitatory post-synaptic current, then it is acting as a neurotransmitter. In contrast, neuromodulators act more slowly and globally on cellular and synaptic properties which alters the effect of subsequent neurotransmission (Brezina, 2010; Katz, 1995). Neuromodulatory actions are often mediated by the activation of metabotropic receptors, which initiate second messenger signaling cascades. While some sources of neuromodulation are local to the spinal cord, other types of neuromodulators originate in supraspinal centers (Katz, 1995). An important family of neuromodulators are the serotonergic (5-HT), noradrenergic (NA), and dopaminergic (DA) monoamines. Although the monoamines 5-HT and NA have been extensively investigated with respect to their roles in the descending control of mammalian locomotor CPGs, **the actions and mechanisms by which DA exerts neuromodulatory effects on mammalian CPG networks remain largely unknown.** In contrast, the actions of DA on invertebrate (Harris-Warrick et al., 1998) and lower vertebrate networks (Irons, Kelly, Hunter, Macphail, & Padilla, 2013; Lambert, Bonkowsky, & Masino, 2012; Svensson, Woolley, Wikström, & Grillner, 2003) are more completely understood. These studies highlight DA as a powerful and diverse modulator of CPG networks. Therefore, the goal of the current study was to examine how DA modulates locomotor CPG network output in a developing mammalian system, the neonatal mouse. I have done this by using a "systems" to "cells" approach. I first examine how DA modulates CPG network output evoked by both pharmacological application (Chapter 3) and electrical stimulation (Chapter 4). Next, at the cellular level I investigate the specific effects of DA on the intrinsic membrane property of postinhibitory rebound (PIR) in motoneurons. I also investigate the actions of DA on the underlying ionic conductances, namely

the low voltage activated T-type calcium channel conductance (I_T) and the hyperpolarization activated cyclic-nucleotide gated (HCN) current (I_h), which give rise to PIR behavior (Chapter 5). Finally, I demonstrate that the I_T conductance, which I found to primarily contribute to the PIR response at the level of motor output, also exerts a crucial influence at the level of network function (Chapter 6).

1.1.2 Locomotor CPG circuits

1.1.2.1 Historical view of mammalian locomotor CPG circuits

Stepping behaviors have long been studied and analyzed with the hope of gaining valuable insight as to the structure and organization of the central nervous system. The pioneering work of Sir Charles Sherrington (1910) conducted over 100 years ago first described the stepping behaviors of spinal cord-transected cats and dogs to be the result of chains of reflex actions initiated from proprioceptors in the hindlimb and paw onto spinal centers (Sherrington, 1910). However, this idea of "reflex-stepping" was challenged by Sherrington's student, Thomas Graham-Brown who provided evidence that rhythmic locomotor-like stepping behaviors could be generated by intrinsic spinal cord networks (T. G. Brown, 1911). Specifically, Graham-Brown discovered that cats that underwent spinal transection maintained the ability to perform alternating stepping movements while under a level of anesthetic that sufficiently blocked all proprioceptive and exteroceptive reflex activity. The significance of this work was largely ignored until the late 1960's when Jankowska and Lundberg confirmed and extended upon Graham-Brown's seminal work by providing intracellular recordings of spinal interneurons that became rhythmically active in response to flexor afferent stimulation (Lundberg, 1969). Over

time, the underlying spinal circuitry that permits rhythmic activity to persist in the absence of phasic sensory input became known as the CPG network (Grillner, 1981).

Over the past 30 years, work in two non-mammalian vertebrate systems, the lamprey (Grillner, 2003) and the *Xenopus* tadpole (McLean, Merrywest, & Sillar, 2000; Roberts, Soffe et al., 1998) has provided valuable insight regarding the structure and function of the CPG network for swimming. Owing to the relative simplicity of the lamprey motor network when compared to mammals, it has been possible to map out interacting neurons, neurotransmitters, and cellular mechanisms underlying swimming CPG function and modulation. Additionally, many laboratories have begun taking advantage of the zebrafish preparation given the number of genetic tools available for the model system (Hughes, 2013). Comparatively less is known regarding mammalian CPG function despite the fact that the mammalian locomotor CPG was first studied over 100 years ago (Brownstone & Wilson, 2008; Kiehn, 2006). Fortunately, insight provided by the lower vertebrate CPG network can be extended to the mammalian spinal network because the vertebrate nervous system phylogeny is highly conserved (Grillner, 2003; Smith & Feldman, 1987; R. Wilson, Vasilakos, & Remmers, 2006). Additionally, the application of new and improved molecular and genetic strategies combined with classical electrophysiological approaches are rapidly advancing our knowledge of the mammalian CPG network (Goulding, 2009). Given that our current most promising approaches for the treatment of spinal cord injury such as pharmacological therapies, spinal cord stimulation, and rehabilitative activity-based motor training rely heavily on modulating the physiological state of the spinal cord circuitry (Fong et al., 2009), extending our current knowledge regarding the structure, function, and modulation of mammalian locomotor CPGs is an important step in designing more sophisticated treatment programs for spinal cord injured patients.

1.1.2.2 Hypothesized models for CPG coordination

1.1.2.2.1 The half-center model

Although the exact internal organization and location of the mammalian locomotor CPG remains unknown, early studies have demonstrated that the ventral lumbar enlargement is necessary and sufficient for generating rhythmic locomotor activity (Grillner, 1981; Kjaerulff & Kiehn, 1996). Our knowledge about the spinal circuits that reside within the lumbar enlargement has evolved over time. The first conceptual scheme of the mammalian locomotor CPG network was based on the pioneering work of Graham-Brown (1911) and later extended on by Lundberg and his collaborators (Hongo, Jankowska, & Lundberg, 1965). Graham-Brown proposed the "half-center" concept to explain how rhythmic activity between ipsilateral flexor and extensor muscle groups was achieved. Briefly, he described the existence of a single network composed of two tonically active excitatory neuronal populations (called flexor and extensor half-centers), which he hypothesized to be reciprocally coupled together by inhibitory connections. This would ensure that when one half-center was active, the other remained quiescent. The switch between half-center activity was hypothesized to occur via one, or as a combination of, two mechanisms: (1) synaptic fatigue; or (2) by some mechanism in place that would permit the half-center neurons the intrinsic ability to escape their inhibition (the latter will be expanded upon in section 1.1.8.2.2). Although the architecture of the CPG network has been somewhat refined over the last 30 years (Grillner, 1981; McCrea & Rybak, 2007), elements of the classical "half-center" model are still present today in most CPG models (McCrea & Rybak, 2007).

1.1.2.2.2 The unit-burst generator

Although the notion of the simple half-center oscillator has been around for over 100 years, one draw back of this system is that it assumes a strict alternation between flexor and extensor activity. In reality, the alternation of flexor and extensor muscle activity is far more complex, as there are differences in the precise onset and offset of individual flexor – extensor motoneuronal pools (Engberg & Lundberg, 1969; McCrea & Rybak, 2008). Additionally, during locomotion it has been found that some motoneuronal pools are active during both flexion and extension (Rossignol et al., 1996). Therefore, the architecture for a CPG model in which separate modules or "unit-burst generators" was proposed, which assumed that there were multiple unit-burst generators which govern synergistic muscle groups across one joint (e.g. the hip flexors) (Grillner, 1981; 2006). Moreover, interconnections between unit-burst generators provided the delicate timing information necessary for the appropriate phasing between different muscle groups during locomotion. However, it has since been recognized that the unit-burst generator concept alone would not account for more complex sequences of motoneuron activation (McCrea & Rybak, 2008).

1.1.2.2.3 Multiple layer models for CPG networks

Recently, revised models of CPG structure have been introduced to account for more complex locomotor activities. One organizational principle that has received much attention over the years is the idea that the CPG network may comprise multiple layers. Indeed, there is compelling experimental evidence to support the existence of a "rhythm-generating" layer and a "pattern formation" layer of the CPG network (Fig 1.1) (Burke, Degtyarenko, & Simon, 2001;

Kriellaars, Brownstone, Noga, & Jordan, 1994; Lafreniere-Roula & McCrea, 2005). Such a multiple layer CPG model has been proposed by McCrea and colleagues (2006).

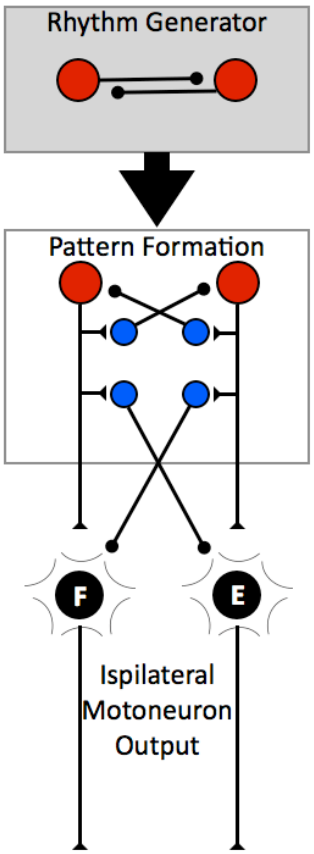

Figure 1.1: Schematic diagram illustrating the multiple level CPG concept.

Represented in this schematic are two separate layers of CPG organization: (1) the rhythm generating layer and (2) the pattern formation layer. Flexor (F) and Extensor (E) motoneurons receive excitatory input from last order interneurons (Red) which are reciprocally coupled via inhibitory interneuronal connections (Blue). An additional group of inhibitory interneurons ensure alternation between antagonistic motoneuron pools. Note: this diagram is simply meant to illustrate the idea of there being multiple layers to CPG organization, and is **not** meant to discount other models. Adapted from Brownstone and Wilson, 2008.

The two-level architecture consists of the first level as being a half-center rhythm generator, which acts as the "clock" as it is responsible for setting the speed and regularity of the rhythm.

The second level, which lies postsynaptic to the rhythm generating layer, is the pattern formation layer that coordinates the intricate activation sequences of different motoneuron populations to which it projects. This allows a separate control of the two levels. Therefore, incoming sensory signals or perturbations may only affect the one level of the CPG, without affecting the other. For example, non-resetting deletions can occur during the stepping cycle (Fig 1.2). The term "non-resetting deletions" describes the ability of the rhythm generating layer to maintain rhythmicity independently of a brief cessation, or deletion, in muscle activity caused by the pattern formation layer, since the rhythm resumes at the exact same frequency and does not change the phase of subsequent motor cycles (Lafreniere-Roula & McCrea, 2005). Another example can be drawn from the work of Kriellaars et al (1994), whereby they demonstrated that a change in the amplitude of locomotor output could happen independently of a change in locomotor speed. It should be noted that currently, the multiple layer model of CPG function has only been modeled to describe the activity of one limb thus far (Rybak, Shevtsova, Lafreniere-Roula, & McCrea, 2006).

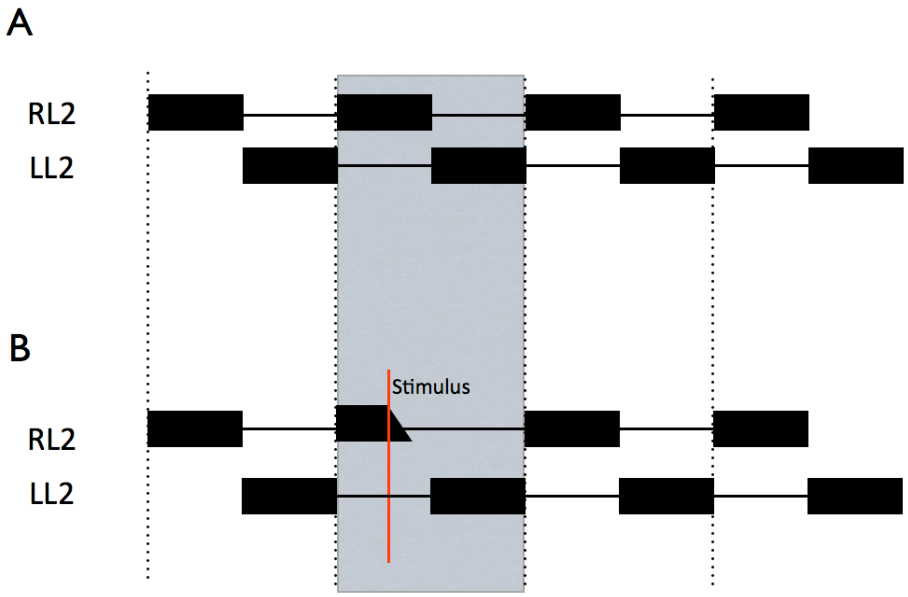

Figure 1.2: Schematic diagram illustrating non-resetting deletions.

A: control trace illustrating an alternating rhythm between the right and left lumber segment 2 (RL2 and LL2 respectively) neurogram recordings. B: Same trace as A, only interrupted briefly by a stimulus (red line) which causes a brief decline in burst amplitude in the RL2 recording only. Note: following the stimulus, the rhythm re-emerged with the precise frequency and with an unaltered phase in subsequent motor cycles.

1.1.3 Introduction to monoaminergic modulation of locomotor CPGs

1.1.3.1 5-HT modulation of locomotor CPG circuits

Since the pioneering work of Jankowska and colleagues in the late 1960's, it has been realized that monoamines contribute greatly to the control of locomotor CPGs (Jankowska, Jukes, Lund, & Lundberg, 1967b; 1967a). 5-HT has attracted the most attention, and therefore, it is not surprising that we know a great deal about how 5-HT influences CPG circuits (Alvarez et al., 1998; Basbaum, Zahs, Lord, & Lakos, 1988; Bras, Cavallari, Jankowska, & McCrea, 1989; Holstege et al., 1996; Jordan & Schmidt, 2002; Kjaerulff & Kiehn, 1996; Wang & Dun, 1990).

5-HT containing neurons originate in the medullary raphe nuclei, descend through the ventral and ventrolateral funiculus columns, and terminate in the ventral horn of the spinal cord where the motor circuits are located (Alvarez et al., 1998; Gerin, Hill, Hill, Smith, & Privat, 2010; Rekling, Funk, Bayliss, Dong, & Feldman, 2000; Steinbusch, 1981; Takeuchi, Kojima, Matsuura, & Sano, 1983). 5-HT-immunoreactive boutons have been found to make direct synaptic connections onto both spinal interneurons and motoneurons. Using the neonatal rat isolated spinal cord preparation, several reports demonstrated that application of 5-HT alone could activate CPG networks and induce rhythmic locomotor-like discharge of lumbar ventral roots (Cazalets, Sqalli-Houssaini, & Clarac, 1992; Cowley & Schmidt, 1994b). Furthermore, using the same preparation, ventral root reflexes were used to determine that 5-HT exerts a depolarizing influence on spinal motoneurons, a finding that was later verified with intracellular recordings (Akagi, Konishi, Otsuka, & Yanagisawa, 1985; Berger & Takahashi, 1990; Connell & Wallis, 1988; 1989; Saito, Ito, Kitazawa, & Ohga, 1982). In summary, it is recognized that 5-HT is a potent activator and modulator of locomotor circuits, both at the interneuronal and motoneuronal levels (Dunbar, Tran, & Whelan, 2010; Rekling et al., 2000; Schmidt & Jordan, 2000).

1.1.3.2 NA modulation of locomotor CPG circuits

In addition to 5-HT, NA has also been shown to exert neuromodulatory actions on spinal cord networks (Fedirchuk & Dai, 2004; Kiehn et al., 1999; Tartas et al., 2010). NAergic projections originate in the pons, primarily in the locus coeruleus, and terminate in the ventral horn of the lumbar spinal cord, similarly to 5-HT projections (Tartas et al., 2010). In 1973, Forssberg & Grillner provided a clear demonstration of NA's capability to operate as a

neuromodulator when they intravenously injected spinalized cats with clonidine, a specific noradrenergic receptor agonist, and saw a dramatic improvement in stepping function (Forssberg & Grillner, 1973). Additionally, using the isolated rat spinal cord preparation, Kiehn and colleagues (1999) demonstrated that application of NA could rescue rhythmic locomotor activity following a time-dependent deterioration of a 5-HT, NMDA-induced locomotor rhythm. These results suggest that NA contributes to locomotor activity, although it is not as potent as 5-HT at inducing locomotor-like activity. As a consequence of 5-HT and NA's ability to modulate locomotor CPGs, these monoamine transmitters continue to receive considerable attention fueled by the belief that they reserve the potential to facilitate recovery following spinal cord injury (Schmidt & Jordan, 2000; Tartas et al., 2010).

1.1.3.3 DA modulation of locomotor CPG circuits?

As previously discussed, the role for 5-HT and NA in the descending control and modulation of mammalian spinal locomotor circuits has been extensively investigated at the network and cellular level (Jankowska, 2001; Rekling et al., 2000; Schmidt & Jordan, 2000). On the other hand, much less is known about the monoamine transmitter DA. Much of what we do know regarding DA's ability to modulate locomotor CPGs has been derived from studies using nonterrestrial, lower vertebrate models such as the lamprey (Kemnitz, 1997; Kemnitz, Strauss, Hosford, & Buchanan, 1995; McPherson & Kemnitz, 1994; Schotland et al., 1995). Moreover, much of our knowledge regarding DA's ability to alter intrinsic and synaptic properties of neurons, and therefore neuronal output, has largely been derived from studies of its role in the brain (Y. Dong, Cooper, Nasif, Hu, & White, 2004; Gorelova, Seamans, & Yang, 2002; Missale, Nash, Robinson, Jaber, & Caron, 1998; Neve, Seamans, & Trantham-Davidson, 2004; Surmeier

& Kitai, 1993; Yang, Seamans, & Gorelova, 1999). Taken together, there is a large gap in our knowledge regarding DA's ability to modulate mammalian locomotor CPG output. Hence, we are left with the following question: ***what is the mechanistic basis by which DA exerts its effects on mammalian CPG circuits?***

1.1.4 Spinal DA origins and projections

Originally, it was thought that DA was directly released from A11 (posterior hypothalamus) projections, however a novel signaling system has recently been proposed (Barraud et al., 2010; Holstege et al., 1996; Qu, Ondo, Zhang, Xie, & Pan, 2006; Weil-Fugazza & Godefroy, 1993; Yoshida & Tanaka, 1988). A report from Barraud and colleagues, (2010) in which a detailed immunohistochemical analysis was completed, provided evidence that A11 neurons in the non-human primate lack a DA transporter system as well as dopa-decarboxylase (DDC), the enzyme necessary for the conversion of L-DOPA into DA. Major conclusions drawn from this report suggest the possibility that the A11 region may be a L-DOPAergic nuclei rather than a DAergic one. If this were the case, then it would represent the first instance of the precursor for DA being released synaptically. Contrary to these findings however, ongoing work in our lab has demonstrated that DDC is indeed present in the A11 region, and maintains that the A11 nuclei is DAergic, at least in the mouse (Koblinger, Krajacic, Nakanishi, & Whelan, 2012). Whichever mechanism is supported, it has been revealed that there is extensive DA fiber and receptor innervation of both the dorsal and ventral horns (Holstege et al., 1996; Qu et al., 2006; Weil-Fugazza & Godefroy, 1993; Yoshida & Tanaka, 1988; Zhu, Clemens, Sawchuk, & Hochman, 2007).

Interestingly, the results of Barraud and colleagues (2010) may explain the early findings of Jankowska and Lundberg (1967) which demonstrated that unanaesthetized cats injected with L-DOPA exhibited long-latency, long-lasting discharges evoked in ipsilateral flexor and contralateral extensor motoneurons in response to volleys in flexor reflex afferents. A few decades after these classical experiments it became clear that DA possessed a functional role during locomotion, highlighted by the finding that L-DOPA-elicited air stepping in neonatal rats is blocked by DAergic antagonists (McCrea, Stehouwer, & Van Hartesveldt, 1997; Sickles, Stehouwer, & Van Hartesveldt, 1992). In summary, multiple lines of evidence point to DA fibers and receptors being present in the spinal cord, and for a DAergic modulation of stepping behavior.

1.1.5 DAergic receptor families and signaling

1.1.5.1 Classification of DA receptor families

Based on what knowledge is available regarding the DAergic modulation of CPG circuits (Barriere, Mellen, & Cazalets, 2004; Gordon & Whelan, 2006b; Madriaga et al., 2004; Schotland et al., 1995; Whelan, Bonnot, & O'Donovan, 2000), it is well accepted that DA receptor isoforms exert diverse neuromodulatory effects over CPG networks. Similar to the 5-HTergic system, the diverse physiological actions of DA are mediated by at least five distinct receptor types, which are grouped into two families, or classes (Missale et al., 1998; Neve et al., 2004). The D_1 – like receptor class is composed of the D_1 and D_5 receptor subtypes. The D_2 – like receptor class is composed of the D_2, D_3, and D_4 receptor subtypes. All of the DA receptors are G-protein-coupled receptors (GPCRs) whose signaling cascade is determined by their interaction and activation of either a stimulatory or inhibitory G-protein.

1.1.5.2 DA receptor signaling pathways and downstream effects

Pharmacological and biochemical evidence has revealed that D_1 – like receptors couple to a stimulatory G-protein, $G\alpha_s$, which activate the effector protein adenylate cyclase (Neve et al., 2004). Once activated, adenylate cyclase catalyzes the conversion of adenosine triphosphate (ATP) to cyclic adenosine monophosphate (AMP). Increased cellular cyclic AMP levels preside over numerous downstream effects that determine many parameters of cellular behavior. For example, increased intracellular cyclic AMP levels initiate a protein kinase A (PKA)-dependent phosphorylation of numerous voltage and ligand-gated ion channels. In contrast, D_2 – like signaling is mediated primarily by activation of an inhibitory G-protein, $G\alpha_i$, which ultimately functions to reduce adenylate cyclase activity, and therefore reduce activity of the cyclic AMP signaling cascade pathway. The opposing effects of D_1 – like vs D_2 – like receptor activation on adenylate cyclase and cyclic AMP activity ensure that DA's actions through these receptor families are quite diverse. As a result of differential DA receptor signaling, DA can exercise different regulatory roles, which can ultimately affect cell excitability.

1.1.6 DAergic receptor expression and distribution within the mouse lumbar spinal cord

Until recently, the expression pattern of DA receptors within the spinal cord remained unclear. Fortunately, *in situ* hybridization studies in the mouse have revealed the presence and regional distribution of all DA receptors in the lumbar spinal cord. Generally, the D_2 – like receptor family was strongly expressed in the motoneurons and in lamina I-III of the dorsal horn (Neve et al., 2004; Zhu et al., 2007). The dominant expression of D_2 – like receptors in the dorsal horn supports several lines of evidence suggesting that D_2 – like receptor activation inhibits spinal neurons in the pain-encoding region of the dorsal horn (Fleetwood-Walker, Hope, &

Mitchell, 1988; Gallagher, Inokuchi, & Shinnick-Gallagher, 1980; Kiritsy-Roy et al., 1994; Tamae et al., 2005). Anti-nociceptive actions of DA have also been demonstrated on the primary afferent terminals via activation of the D_2 – like receptor based pathway (Fleetwood-Walker et al., 1988). D_1 – like receptors are expressed more ventrally, where the motor circuits reside (Zhu et al., 2007). Based on their location, D_1 – like receptors are optimally positioned to exert direct excitatory effects on the interneurons and motoneurons that comprise the CPG network. The D_3 and D_4 receptors were found to have the lowest expression within the mouse lumbar spinal cord. This may be explained by a predominant presynaptic expression of these isoforms on descending dopaminergic and primary afferents terminals rather than on postsynaptic spinal cord neurons themselves (Levant, 1997). The diverse expression of DA receptors within the spinal cord corresponds well with broad descending DAergic projections, and supports a widespread DAergic control over spinal CPG networks (Zhu et al., 2007).

1.1.7 DAergic modulation of multiple pathways that gain access to the locomotor CPG

1.1.7.1 Introduction to the activation of CPG networks

The spinal cord is the interface for sensory-motor integration during ongoing locomotion. Therefore, CPG networks can be recruited and modulated by a number of different sensory and motor pathways. For example, CPG networks become active in response to glutamatergic descending commands originating from reticulospinal and vestibulospinal regions (Clarac, Vinay, Cazalets, Fady, & Jamon, 1998; Grillner, 1975; Jordan, Brownstone, & Schmidt, 1992). Both low and high threshold-afferents carrying sensory information such as proprioceptive, cutaneous, and nociceptive signals, can access CPG networks (Jankowska, Jukes, Lund, & Lundberg, 1967b; Lundberg, 1979; Mandadi et al., 2009; Pearson, 2001; Whelan, Hiebert, &

Pearson, 1995). Recently, in the neonatal mouse it was discovered that antidromic stimulation of motoneuron axons can trigger locomotor-like activity, suggesting that the efferent projection system too has either direct access to CPG networks, or indirect access via interposed interneurons that project onto CPG networks (Bonnot, Chub, Pujala, & O'Donovan, 2009; Mentis et al., 2005). Taking into consideration that there are multiple avenues to access locomotor CPGs, and that there is a wide distribution of both excitatory D_1 – like and inhibitory D_2 – like DA receptors throughout the spinal cord, a logical next step would be to explore whether DA could exert differential modulatory effects that are dependent upon the mode of which the CPG becomes activated. Fortunately, the utility of the *in vitro* isolated spinal cord preparation offers a versatile and powerful experimental system to test for the potentially diverse effects of DA on the recruitment of CPG network. Furthermore, locomotor patterns can readily be elicited from this preparation using drugs or electrical stimulation and DA can easily be bath applied (Kudo & Yamada, 1987a; Smith, Feldman, & Schmidt, 1988; Whelan et al., 2000).

1.1.7.2 The in vitro isolated mouse spinal cord preparation

In the mid 1980's the isolated neonatal rat spinal cord became a popular *in vitro* preparation for the study of CPG activation because it allowed for the easy manipulation of the extracellular environment, while simultaneously recording locomotor output (Kudo & Yamada, 1987a; Smith et al., 1988; Whelan et al., 2000). Although the isolated neonatal rat spinal cord has generated a wealth of information regarding mammalian locomotor networks, another *in vitro* preparation, the isolated mouse spinal cord, has been adopted by many laboratories because it offers many advantages over the rat preparation (Gordon & Whelan, 2006a; Whelan et al., 2000). Compared to the rat, smaller mouse spinal cords can be maintained *in vitro* at later ages when the animal is

capable of performing weight-bearing locomotion (Jiang, Carlin, & Brownstone, 1999). Another advantage of using a smaller mouse cord is that the preparation is fully perfused with O_2 at all tissue depths, which is important because hypoxic conditions can alter neuronal firing characteristics (Wilson, Chersa, & Whelan, 2003). However, arguably the most attractive advantage of utilizing the mouse spinal cord is the possibility for investigating the locomotor patterns of genetically manipulated networks (Gordon & Whelan, 2006a; Gosgnach, Pierani, Jessell, & Goulding, 2004; Goulding, 2009; Kiehn, 2006) .

1.1.7.3 Signature of locomotion defined

As illustrated by Grillner in 1975, the limbs serve two important purposes during locomotion: (1) they support the body during ongoing movement and (2) they provide a propulsive force for movement to take place. Locomotor movements have long been analyzed based on how joint angles change throughout the step cycle (Philippson, 1905). Generally, the step cycle has been characterized by ipsilateral flexion of the knee, ankle, and hip which position the limb forward (flexion phase), followed by extension of the knee, ankle, and hip where by the foot contacts the ground, supports body weight during a brief stance, and eventually propels the animal forward (extension phase). In addition to flexor-extensor antisynchrony of ipsilateral muscle groups, locomotion requires a simultaneous antisynchrony between contralateral flexor-flexor and extensor-extensor muscle groups necessary for the left-right alternation of limbs. Although we can visually differentiate between "left-right" and "flexion-extension" phases of the step cycle in the intact animal, often times experimental systems are reduced in the sense that the limbs are absent, such as in the isolated spinal cord preparation. In this system, motor output is recorded directly from the level of the ventral roots, which in the intact animal would go on to

innervate flexor and extensor muscle groups of the lower limbs. To ascertain whether or not motor output from the isolated spinal cord preparation is actually representative of locomotion, Whelan and colleagues (2000) compared rhythmic discharges recorded from flexor muscle nerves such as the common peroneal, and extensor muscle nerves such as the lateral gastrocnemius-soleus with alternating discharge of parent lumbar (L) ventral roots L2 and L5/L6, respectively, and found that these two motor patters were correlated. Despite these exciting findings, one important caveat to be aware of is the fact that electrophysiological characterization of locomotor patterns acquired solely by monitoring ventral root activity may in fact be missing valuable information regarding phasic hindlimb flexor and extensor activity (Cowley & Schmidt, 1994a). However even with this caveat in mind, it became common practice within the motor community to record from left – right L2 ventral roots as they correlate predominately with flexor muscle activity, and from left – right L5 ventral roots as they correlate predominately with extensor muscle activity (Fortier, Smith, & Rossignol, 1987; Whelan et al., 2000). Therefore, we define motor output from the isolated spinal cord preparation as "locomotor-like" if there is an alternating discharge between the left and right lumbar ventral roots of the same spinal segment, and if there is alternation of the ipsilateral flexor and extensor muscles or muscle nerves (Whelan et al., 2000).

As previously mentioned, locomotor-like patterns or "fictive locomotor" patterns have traditionally been elicited for experimental observation in a number of ways such as bath application of rhythmogenic drugs, electrical afferent stimulation of the cauda equina or fourth sacral dorsal root, and electrical stimulation of the parapyramidal region of the brainstem (Kiehn & Kjaerulff, 1996; J. Liu & Jordan, 2005; Whelan et al., 2000). Recently using the isolated mouse spinal cord preparation, antidromic stimulation of lumbar ventral roots has also proven to

be another mode of CPG recruitment (Bonnot et al., 2009; Mentis et al., 2005). In the following section, I will further describe the advantages and disadvantages for each mode of CPG activation.

1.1.7.4 Drug-evoked locomotion

Using the isolated spinal cord preparation, my work has begun to elucidate how DA differentially modulates locomotor rhythms by employing different strategies to activate CPG networks (Chapters 3 and Chapter 4). The first experimental approach I utilized was to evoke locomotion using a combination of the rhythmogenic drugs 5-HT, NMDA, and DA. Drug-evoked locomotion is advantageous because it elicits sustainable rhythms that can last between 4 – 10 hours, making it easy to dissect out changes in the rhythm over time (Jiang et al., 1999; Whelan et al., 2000). It is arguable that this method of CPG recruitment is somewhat representative of the descending activation of CPG networks that occurs *in vivo*, as neuromodulators such as glutamate and monoamines are continuously being released and are present. However, there are several caveats to be aware of when using exogenous application of drugs to activate locomotor CPG networks. First, the locomotor-like pattern produced *in vitro* is maintained at a rate that is almost 10 times slower than that which is normally seen *in vivo* (Bonnot, Whelan, Mentis, & O'Donovan, 2002). Second, mice tend to move, in short relatively fast bouts of activity, while the drug-induced rhythms are highly sustainable and are rarely interrupted. Third, the exogenous administration of a few neuroactive agents may not accurately reflect the activation of CPG networks as it would normally occur *in vivo* (Cowley & Schmidt, 1994b). Finally, depending on the combination and concentration of the neuroactive agents administered, motor patterns elicited can be highly variable and difficult to distinguish between

"locomotor-like" and other possible motor patterns evoked from potentially overlapping components of the CPG network (Cowley & Schmidt, 1994b). Despite these caveats, many laboratories have adopted this approach to locomotor CPG network activation because it is a relatively simple experimental paradigm. Therefore, perhaps the main advantage of using the application of exogenous drugs as a means to recruit the locomotor CPG network is that this method has been used across many different laboratories and therefore provides a wealth of data to compare current findings with. Hence, I have utilized this approach to elucidate which DA receptor families contribute to modulation of sustainable locomotor rhythms over time (Chapter 3).

1.1.7.5 Electrically-evoked locomotion

1.1.7.5.1 Electrical stimulation of afferent projections with access to the CPG network

While the use of pharmacology to activate CPG networks has proven highly effective, another possible drawback from using this approach is that exogenously applied drugs may indiscriminately activate cells within the CPG network. Additionally, there is the risk of possibly activating extrasynaptic receptors not normally recruited *in vivo*. Therefore, one approach to help tackle this problem would be to employ the use of electrical stimulation of afferent projections that have access to CPG networks (Whelan et al., 2000). This technique of CPG recruitment is advantageous because it relies upon the release of endogenous neurotransmitters and neuromodulators to excite spinal circuits, perhaps arguing for a more physiological mode of activation.

Although it has been demonstrated that electrical stimulation of dorsal root or cauda equina afferents produces consistent and robust locomotor-like patterns (Bonnot et al., 2002; Whelan et

al., 2000) one must remain aware that activating the CPG network using this approach will recruit different sensory fibers, including nociceptive fibers (Mandadi et al., 2009). It is important to note that monoaminergic transmitters, including DA, have been demonstrated to powerfully inhibit incoming nociceptive information at the level of the dorsal horn (Garraway & Hochman, 2001; Kiritsy-Roy et al., 1994). Along these lines, work published by our lab has demonstrated that DA application during cauda-equina evoked locomotion will potently block the emergence of rhythmic activity (Gordon & Whelan, 2006b). Thus, although electrical stimulation of afferent pathways is effective at eliciting robust locomotor rhythms, this technique is not an ideal approach for exploring the effects of DA on locomotor CPG networks.

1.1.7.5.2 Electrical simulation of efferent projections with access to the CPG network

Historically, mammalian motoneurons were thought to be the major output source of the spinal cord, and they were assumed not to have a role in rhythmogenesis. This view was maintained because the only known functional collateral projections from motoneurons were to Renshaw cells, which serve as an inhibitory brake onto motoneurons (Renshaw, 1941). However, recent work in the developing mouse found that antidromic stimulation of ventral root motor axons could evoke bouts of locomotor activity, therefore suggesting a more important role for motoneurons in rhythmogenesis than previously thought (Mentis et al., 2005). This has opened up yet another avenue to explore how DA can modulate CPG activity. Although the circuit properties are not completely understood, stimulation of motoneuron axons activates recurrent collaterals that have access to CPG networks. These recurrent collateral projections are hypothesized to release an excitatory amino acid (likely glutamate) in addition to acetylcholine, onto CPG networks (Bonnot et al., 2009; Mentis et al., 2005; O'Donovan et al., 2010). Evidence

for this was demonstrated when locomotion evoked via ventral root stimulation persisted in the presence of cholinergic blockade (Mentis et al., 2005).

Utilizing ventral root stimulation to activate the locomotor CPG offers several advantages over drug-evoked rhythms when investigating the actions of different neuromodulators, such as DA. For example, just as with electrical stimulation of afferent pathways, electrical stimulation of efferent pathways is dependent upon the release of endogenous neurotransmitters and neuromodulators to excite spinal circuits. Another advantage is that these circuits offer a tractable electrophysiological method for identification of interposed interneurons by stimulation of recurrent collaterals. Unfortunately, when electrically stimulating either dorsal root afferent pathways or ventral root efferent pathways, it is necessary to provide a recovery period after each stimulus bout as the evoked locomotor activity is short lived, most likely due to synaptic fatigue (Mentis et al., 2005; Whelan et al., 2000).

While utilizing the ventral root stimulation paradigm, Machacek and Hochman (2006) discovered a novel excitatory recurrent pathway that was only unmasked by the presence of the monoaminergic neuromodulator NA. Specifically, it was found that during ventral root-evoked recruitment of adjacent motoneuron populations, recurrent excitation that was normally undetectable was uncovered by the presence of NA, as evident by increases in reflex amplitude. This, for the first time, indicates that motoneuron recurrent collateral pathways can be conditionally recruited by monoamines, which can ultimately affect CPG activity (Machacek & Hochman, 2006).

If novel circuitry supporting recurrent excitation can be unveiled by the presence of NA, then it is not unreasonable to assume that different monoamines, such as DA, can also modulate recurrent circuitry, especially considering the widespread distribution and expression of DA

receptors (Zhu et al., 2007). Therefore, I examined the possibility that DA could modulate CPG activity through recurrent collateral pathways (Chapter 4).

1.1.8 Intrinsic currents and properties of CPG networks

1.1.8.1 Introduction to rhythmogenic ion currents

Studies of CPG networks in both vertebrate and invertebrate models have shown that the firing characteristics of neurons are dependant upon the intrinsic ion currents they possess (Grillner, 2003; Harris-Warrick, 2010; Marder & Bucher, 2001). Different intrinsic membrane properties such as plateau potentials, PIR, endogenous bursting cells, and spike frequency adaptation govern the generation of rhythmic motor behavior. However, modulatory inputs such as the presence of monoamines can alter the activity of ion channel function and therefore have profound effects on the intrinsic properties of neurons that generate CPG network output. In the following text, I will briefly discuss a few of the currents that appear to be critical components of rhythmogenesis, as these currents are therefore targets for neuromodulation (Harris-Warrick, 2010). A special emphasis will be given to the low voltage-activated T-type calcium current.

1.1.8.2 Inward currents

1.1.8.2.1 Persistent inward Na^+ currents

The generation of action potentials is primarily due to the rapid opening of voltage dependent Na^+ channels. The majority of Na^+ channels subsequently rapidly inactivate resulting in an intense, but brief, depolarization (Hodgkin & Huxley, 1952). However, a small proportion of the Na^+ channels fail to inactivate, and give rise to a persistent inward Na^+ current, or $I_{NaP.}$ This can lead to the generation of plateau potentials, which is an intrinsic membrane property that

permits the cell to stay depolarized even after the depolarizing stimuli has been lifted (Harris-Warrick, 2010; Marder & Bucher, 2001). Neurons that express plateau potentials can act as "intrinsic memories" of their last synaptic input and subsequently produce discharge patterns that long outlast their excitatory input. Strong evidence for the involvement of I_{NaP} in the rodent locomotor CPG network was demonstrated by experiments in which blockade of this current with low concentrations of riluzole abolished fictive locomotion evoked by either pharmacological or electrical means (Tazerart et al., 2007; Zhong, Masino, & Harris-Warrick, 2007).

1.1.8.2.2 Low voltage activated calcium currents

Calcium ions are one of the most widespread intracellular signaling molecules and demonstrate their versatility among every excitable tissue found in the mammalian host (Grillner, 2003). In addition to acting as important second messenger molecules, calcium ions are necessary for synaptic transmission, and they are divalent cations (Ca^{2+}) that upon entry will depolarize the cellular membrane thereby activating other voltage sensitive ion channels (Hille, 2001).

Low voltage-activated (LVA) Ca^{2+} channels belong to the Cav3 family of calcium channels, and three isoforms have been identified (Cav3.1, Cav3.2, and Cav3.3) (Nowycky, Fox, & Tsien, 1985). Cav3 calcium currents (I_T collectively) are expressed in both vertebrate and invertebrate CPG network neurons and are important for maintaining oscillatory activity (Grillner, 2006; Perez-Reyes, 2003; Selverston & Moulins, 1985). Calcium entry through T-type Ca^{2+} channels following a period of membrane hyperpolarization boosts membrane depolarization to reach Na^+ channel activation, thus triggering a series of action potentials. This

phenomenon is appropriately termed the PIR.

As previously discussed, the "half-center" model of locomotor rhythm generation was proposed by Graham-Brown (1911) and provided an important conceptual and theoretical framework for studies investigating the underlying neural control of locomotion. Briefly, Brown's proposal put forth the notion that rhythmic activity between flexor and extensor muscle groups is produced by two symmetrically-organized half-centers that drive alternating activity between flexor and extensor motoneuronal pools. Furthermore, Brown proposed that these half-centers reciprocally inhibit each other via inhibitory interneuronal connections. In this context, PIR can contribute to the generation of a stable, alternating burst pattern by promoting a rebound bursting among the half-center neurons that are experiencing inhibition, thereby ensuring alternation between reciprocally connected networks.

The functional relevance of T-type Ca^{2+} currents has been well characterized in the lamprey, owing to the relative simplicity and reduced number of neurons within the lamprey CPG when compared with mammals (Matsushima, Tegnér, Hill, & Grillner, 1993; Tegnér, Hellgren-Kotaleski, Lansner, & Grillner, 1997). In the lamprey, calcium entry through T-type Ca^{2+} channels contributes to the depolarizing phase and subsequent onset of burst activity necessary during swimming behavior. Interestingly, my work and that of others (Anderson et al., 2012), has begun to reveal an important functional role for T-type Ca^{2+} channels within the mouse locomotor CPG. Briefly, I have demonstrated that when T-type Ca^{2+} currents are blocked with the channel antagonist Ni^{2+} during ongoing fictive locomotion, the alternating burst pattern becomes severely disrupted and eventually converts into a synchronous bursting pattern. This suggests that T-type Ca^{2+} channels, and the associated intrinsic properties supported by T-type Ca^{2+} activation, are involved in the emergence of left-right - flexor-extensor alternating behavior

of hindlimb activity necessary during locomotion.

1.1.8.2.3 HCN-gated currents

The HCN-gated current (I_h) is a non-selective cation current that becomes activated at subthreshold potentials around -50 to -60 mV, similarly to T-type Ca^{2+} channels (Biel, Wahl-Schott, Michalakis, & Zong, 2009; Pape, 1996). Together with I_T, I_h has been thought of as a "pacemaker current" as it provides a pacemaker like depolarization during the generation of rhythmic oscillatory behavior (Biel et al., 2009; Huguenard, 1996; Pape, 1996; Robinson & Siegelbaum, 2003). For example, I_h will become activated due to the accumulated hyperpolarization following a series of action potentials. Once activated, I_h will provide a depolarizing ramp current that will drive the next cycle of burst activity (Harris-Warrick, 2010).

During locomotion, the membrane potential of rat motoneurons fluctuates between bouts of depolarization and inhibition (Hochman & Schmidt, 1998). This rhythmic oscillation is thought to underlie the phasic transition between excitation and inhibition of muscle activity, and I_h has been implicated as one of the currents that help facilitate this switch. Work published by Kiehn and colleagues (2000) demonstrated that I_h depolarized the average resting membrane potential, which in turn gave rise to two subsequent effects of I_h in motoneurons during rhythmic activity. Specifically, the presence of I_h was found to (1) provide a depolarizing "boost" which largely contributed to the accelerated phase transition between excitation and inhibition and (2) decreased the onset to the first spike in the locomotor cycle. Collectively, these results suggest that I_h provided a tonic leak conductance during locomotion, contributing to the shaping of motoneuron activity during locomotion.

1.1.8.3 Outward Currents

Essential to rhythm generation, and therefore modulation, is the ability to terminate a burst of action potentials. I will briefly highlight two outward currents, both of which reserve important roles in burst termination and spike frequency regulation.

1.1.8.3.1 Ca^{2+} dependent K^+ currents

Ca^{2+}-activated K^+ channels are key mediators of neuronal excitability as they participate in determining intrinsic properties that govern inter-spike interval, and spike frequency adaptation (Vergara, Latorre, Marrion, & Adelman, 1998). During a burst of action potentials, cytosolic Ca^{2+} increases and leads to activation of Ca^{2+}-activated K^+ channels. One subfamily of Ca^{2+} - activated K^+ channels, the small conductance (SK_{Ca}) Ca^{2+} - activated K^+ channel, is sensitive to intracellular Ca^{2+} levels. Activation of SK_{Ca} channels contributes to membrane hyperpolarization, and contributes to a reduction in spike frequency within a burst. The intracellular Ca^{2+} accumulated during action potential firing decays relatively slowly, thereby permitting SK_{Ca} channel activation to generate a long lasting hyperpolarization termed the slow afterhyperpolarization (sAHP). Firing frequency of repetitive action potentials is limited during the sAHP. For example, in the lamprey model system, application of the SK_{Ca} channel blocker apamin, reduces the sAHP and as a result slows fictive swimming by prolonging each burst (Manira, Tegnér, & Grillner, 1994). This spike frequency adaptation is an intrinsic membrane property inherent to many CPG networks, as it protects rhythm-generating neurons from adverse effects of repetitive high frequency firing.

1.1.8.3.2 A-type K^+ current

The transient A-type K^+ (I_A) current helps to determine the rate of repolarization following a spike or a burst (Harris-Warrick, 2010). In the lamprey locomotor CPG, the high threshold catechol-sensitive A-type current was characterized (Hess & Manira, 2001). Activation of I_A was found to facilitate the recovery of Na^+ channels from inactivation, thereby assisting in repetitive firing. Furthermore, when the I_A was selectively blocked during fictive swimming, neurons were found to fire fewer spikes per burst, which ultimately accelerated cycle frequency. In addition to the high-threshold I_A currents, CPG networks also possess a low-threshold, fast-inactivating 4-AP-sensitive, I_A current component (Han, Nakanishi, Tran, & Whelan, 2007). Low threshold I_A currents are involved in determining the first spike latency of active neurons.

1.1.9 Monoaminergic modulation of intrinsic membrane properties that govern network output

1.1.9.1 The role of 5-HT and NA in the modulation of spinal neurons

Despite the demonstration that many ventral interneurons and motoneurons are rhythmically active during locomotor activity in the rodent (Butt, Harris-Warrick, & Kiehn, 2002; Dougherty & Kiehn, 2010; Kwan, Dietz, Webb, & Harris-Warrick, 2009; Nishimaru, Restrepo, & Kiehn, 2006; O'Donovan et al., 2010; Tresch & Kiehn, 2000; J. M. Wilson et al., 2005; Zhong et al., 2010), we only have a fragmented knowledge regarding these neurons' intrinsic and synaptic properties. What we do know is that these intrinsic and synaptic properties are targets for monoaminergic modulation. For example at the cellular level, 5-HT and NA produce a depolarization of spinal neurons, facilitate the expression of plateau potentials, reduce the AHP following an action potential, and enhance membrane oscillatory capacity (Berger &

Takahashi, 1990; Connell & Wallis, 1989; Elliott & Wallis, 1992; Hounsgaard, Hultborn, Jespersen, & Kiehn, 1988; MacLean, Cowley, & Schmidt, 1998). These cellular effects are mediated by an alteration of ion channels and their respective conductances previously discussed. Namely, the facilitation of I_h and NMDA currents, and the activation of I_T and I_{NaP}, are all key conductances that govern cell excitability (Berger & Takahashi, 1990; Kjaerulff & Kiehn, 2001; Takahashi & Berger, 1990; Wang & Dun, 1990). Additionally, at the level of motor output, it has been demonstrated that bath application of 5-HT and NA can facilitate locomotor output (Barbeau, Chau, & Rossignol, 1993; Cazalets et al., 1992; Cowley & Schmidt, 1994b; Kiehn et al., 1999; Kiehn, Hultborn, & Conway, 1992; Smith et al., 1988). Although I have only provided a snapshot of the literature available regarding the modulatory capacity of 5-HT and NA, the most valuable result from these studies is the fact that 5-HT and NA, either applied individually or as a "cocktail" of the two, appear to endow CPG networks with a broad range of cellular and motor output configurations.

1.1.9.2 DA modulation of CPG network properties and motor output

When compared with 5-HT and NA, studies regarding the capability of DA to modulate rhythmogenic ionic conductances that govern cellular intrinsic properties have largely been restricted to studies in the lamprey (Schotland et al., 1995; Wang, Grillner, & Wallén, 2011) and the pyloric network in the stomatogastric ganglion of the spiny lobster (Ayali, Johnson, & Harris-Warrick, 1998; Harris-Warrick et al., 1998; Harris-Warrick, Coniglio, Levini, Gueron, & Guckenheimer, 1995; Johnson, Kloppenburg, & Harris-Warrick, 2003; Johnson, Schneider, Nadim, & Harris-Warrick, 2005). Collectively, these studies have highlighted a rather complex modulatory role for DA. For example, in the 14-neuron pyloric network from the crustacean

stomatogastric ganglion, DA has been shown to affect each neuron independently and by different mechanisms (Harris-Warrick et al., 1998). In the lamprey, DA has been demonstrated to exert both excitatory (Schotland et al., 1995) and inhibitory (Wang et al., 2011) effects on the swimming CPG network. Consequently, it is logical to hypothesize that DA would exert a complex modulatory role within the more refined mammalian CPG network. Indeed, my work and that of others (Barriere et al., 2004; Gordon & Whelan, 2006b; Madriaga et al., 2004; Whelan et al., 2000), has begun to elucidate the importance of DA at the level of the CPG network in governing rhythm frequency and stability. Moreover, work published from our lab has revealed that DA can influence the shaping of motor output from the CPG networks (Han et al., 2007; Han & Whelan, 2009). Specifically, it was demonstrated that DA causes an increase in motoneuron excitability by reducing the fast inactivating I_A, decreasing the SK_{Ca}, and increasing the input resistance (Han et al., 2007). In addition, it was revealed that DA exerts a modulatory role over synaptic transmission of motoneurons, such that AMPA currents were enhanced through both pre-and postsynaptic mechanisms (Han & Whelan, 2009). **Therefore, it would be of great benefit to explore further how DA, in addition to 5-HT and NA, can modulate cellular properties of the interneurons and motoneurons that comprise the mammalian CPG locomotor network** (Barriere et al., 2004; Kiehn & Kjaerulff, 1996; Madriaga et al., 2004; Whelan et al., 2000).

1.1.10 Summary and hypothesis

1.1.10.1 Summary

Mammalian spinal circuits responsible for producing locomotor activity are strongly modulated by the presence of monoamines such as DA. We know that DA alters intrinsic and synaptic

properties to increase cell excitability of motoneurons that deliver network output from the CPG to the muscle. Currently, it remains unclear what DA's actions are within the CPG network. Additionally, there is a gap in our knowledge regarding the cellular mechanisms by which DA modulates locomotor output. Acknowledging the widespread expression and distribution of DA receptor subtypes within the spinal cord, and that there are multiple avenues to access the CPG network, it is likely DA's actions are highly complex. The goals of my work were to explore potential mechanisms of action of this important neuromodulator, whose direct effects on motor control are just starting to be understood. *Knowledge of the mechanisms and sites of modulation that are subject to DAergic influence will contribute to our understanding of DA's role within the spinal circuits that generate locomotion, and may help lay the foundation for more applied studies with the ultimate goal of developing highly targeted DAergic therapies for spinal cord injured patients*.

1.1.10.2 Hypothesis

Outlined in this thesis are the strategies I utilized to explore the DAergic modulation of mammalian locomotor circuits. My experiments were designed to test the following general hypothesis: **DA influences cellular mammalian locomotor behavior through diverse and complex modulations actions on locomotor-related spinal neurons.**

To obtain a better understanding of how DA contributes to the modulation of the CPG network, my approach was designed to identify different DA receptors and spinal neuronal populations that are subject to DAergic modulation during locomotor behavior and characterize the intrinsic conductances and properties by which DA exerts effects. Utilizing a combination of electrophysiological and pharmacological techniques, I targeted and manipulated network,

synaptic, and intrinsic properties to elucidate part of the mechanistic basis of DA's role during fictive locomotion. My general hypothesis was tested by the following specific hypotheses:

Specific Hypothesis 1: DA stabilizes a pre-existing 5-HT, N-methyl-(DL)-aspartate (NMA)-evoked locomotor rhythm by activating D_1 – like receptors.

Specific Hypothesis 2: DA facilitates ventral root-evoked locomotor activity by activating D_1 – like receptors.

Specific Hypothesis 3: DA enhances the intrinsic membrane property of PIR at the level of motoneurons, which may underlie DA's ability to facilitate CPG network function.

Specific Hypothesis 4: T-type Ca^{2+} currents play an important role in supporting rhythm generation evoked by 5-HT, NMA and DA application.

Chapter Two: Methods

2.1 GENERAL METHODS

Experiments were performed on Swiss Webster mice (Charles River Laboratories, Wilmington, MA), postnatal day 0 (P0) to P3 [weight 1.5 - 2.9 g; $n = 183$]. The animals were anaesthetized by hypothermia, decapitated and eviscerated using procedures approved by the University of Calgary Animal Care Committee which following the guidelines published by the Canadian Council on Animal Care.

2.1.1 Tissue preparation

2.1.1.1 Isolated spinal cord preparation

The remaining tissue was placed in a dissection chamber filled with carbogenated (95% O_2, 5% CO_2) artificial CSF (aCSF) (concentrations in mM: 128 NaCl, 4 KCl, 1.5 $CaCl_2$, 1 $MgSO_4$, 0.5 Na_2HPO_4, 21 $NaHCO_3$, and 30 D-glucose). A ventral laminectomy exposed the cord, and the ventral and dorsal roots were cut. The spinal cord was transversely transected at T5 and was gently removed from the vertebral column to the level of the cauda equina. Once dissections were complete, the aCSF containing the isolated spinal cord was allowed to warm up to room temperature (~24 – 25°C) in the dissection chamber (~30 min). Then, the preparation was transferred to the recording chamber and superfused with carbogenated aCSF (concentrations same as dissecting solution). The bath solution was then heated gradually from room temperature to 27˚C (Whelan et al., 2000). The spinal cords were then allowed another 30 min to recover in the recording chamber.

2.1.1.2 Isolated spinal cord with attached sciatic nerve preparation

In some preparations, the sciatic nerve was carefully dissected out and exposed several millimeters away from the spinal cord. Caution was taken to ensure that the sciatic nerve was dissected in continuity with the parent ventral roots (L3 – L6). All dorsal roots were cut.

2.1.1.3 Isolated spinal cord with dorsal horn-removed preparation

After following the dissection procedures outline in section 2.1.1.1 but prior to transecting the spinal cord at T5, the isolated spinal cord was immediately transferred to a pre-cooled (4°C) slicing chamber and stabilized dorsal side up in an horizontal position onto an agar block using 20% gelatin. The slicing chamber was then filled with ice-cold, oxygenated sucrose – aCSF (in mM: 25 NaCl, 188 sucrose, 1.9 KCl, 10 $MgSO_4$, 1.2 Na_2HPO_4, 26 $NaHCO_3$, and 25 D-Glucose) solution that was kept chilled and bubbled continuously with carbogen. Longitudinal sections (50 microns) were cut until approximately 100 – 250 microns were removed from the dorsal horn (Vibrotome VT1000S; Leica, Bussloch, Germany). Any sliced tissue was discarded. Following the slicing process, the isolated spinal cord was then gently transferred to the recording chamber and superfused with carbogenated aCSF (concentrations same as dissecting solution). The bath solution was then heated gradually from room temperature to 27˚C (Whelan et al., 2000). The spinal cords were then allowed another 30-60 min to recover in the recording chamber.

2.1.1.4 Isolated spinal cord – mid-sagittal sectioned preparation

In some experiments, the isolated spinal cord was mid-sagittally sectioned following the induction of fictive locomotion evoked by drug application. For these experiments, the isolated spinal cord preparation was completely hemisected so that the two halves of the spinal cord were

independent of one another. Once cut, between 20 and 30 minutes were allowed for the isolated cord to recover from spinal shock. In all preparations used, ipsilateral alternating activity resumed during the recovery time indicating the health of the cord was sufficient for experimentation. Once the rhythm resumed, another 10 minutes was allowed for stabilization prior to recording.

2.1.2.5 Slice preparations

The spinal cord was dissected free as described in section 2.2.1. Once free, the spinal cord was transected at T9/10 and then again at S1/2 and then immediately transferred to a pre-cooled (4°C) slicing chamber and stabilized in an upright position onto an agar block using 20% gelatin. The slicing chamber was then filled with ice-cold, oxygenated sucrose – aCSF solution (in mM: 25 NaCl, 188 sucrose, 1.9 KCl, 10 $MgSO_4$, 1.2 Na_2HPO_4, 26 $NaHCO_3$, and 25 D-Glucose) that was kept chilled and continuously oxygenated. Transverse sections (250 μm) were cut (Vibrotome VT1000S; Leica, Bussloch, Germany), and the slices were collected in a chamber containing prewarmed (36°C), oxygenated recovery ACSF (in mM: 119 NaCl, 1.9 KCl, 1 $CaCl_2$, 10 MgSO4, 1.2 Na_2HPO_4, 26 $NaHCO_3$, and 10 D-glucose) and equilibrated for at least 45 min before being moved into the recording rig.

2.1.2 Pharmacology

2.1.2.1 Pharmacology for DA studies

The effects of several dopaminergic (DAergic) agonists and antagonists were investigated on drug-evoked and ventral root/sciatic nerve evoked rhythmic activity. In this study, the D_1 – like (D_1/D_5) and D_2 – like subfamilies (D_2/$_3$/$_4$) which are present within the mouse spinal cord (Zhu et

al., 2007) were targeted. Specific DA agonists used were: D_1 – receptor: SKF-81297 (20 μM; Tocris). D_2 receptors quinpirole, (20 μM; Sigma-Aldrich). Additionally, the effects of DA during entrainment of disinhibited rhythms that were generated by bath application of the glycine receptor antagonist strychnine (2 μM; Sigma-Aldrich), the $GABA_A$ antagonist picrotoxin (50 μM; Sigma Aldrich) and the $GABA_B$ antagonist CGP-35348 (CGP, 50 μM; Sigma-Aldrich) (Mandadi et al., 2009) were also investigated. Disinhibited rhythms are slow synchronous rhythms that occur after GABA and glycinergic receptors are blocked.

2.1.2.2 Pharmacology for postinhibitory rebound studies

The synaptic blockers used in these experiments include the following: CNQX (AMPA/kainate receptor antagonist, 20 μM; Sigma-Aldrich), AP-5 (NMDA receptor antagonist, 50 μM; Sigma-Aldrich), strychnine hydrochloride (glycine receptor antagonist, 10 μM; Sigma-Aldrich), and picrotoxin ($GABA_A$ receptor, chloride channel blocker, 50 μM; Sigma-Aldrich). Additional channel blockers used were tetrodotoxin citrate (TTX) (Na^+ channel blocker; 1 μM; Tocris); nickel (Ni^{2+}) (T-type calcium channel blocker; 100 μM; Sigma-Aldrich) and ZD-7288 (hyperpolarization cyclic-nucleotide gated cation channel blocker; 50 μM; Sigma-Aldrich). DA concentrations were based on previous studies using this concentration range to modulate spinal networks in mouse (Christie & Whelan, 2005; Han et al., 2007; Hinckley, Hartley, Wu, Todd, & Ziskind-Conhaim, 2005; Jiang et al., 1999; Whelan et al., 2000). Washout time of drugs varied from 15 to 20 min, and recording recommenced when the membrane potential had stabilized. All the blockers and stimulants were dissolved and applied with the recording aCSF solution (in mM: 119 NaCl, 1.9 KCl, 1 $CaCl_2$, 10 $MgSO_4$, 1.2 Na_2HPO_4, 26 $NaHCO_3$, and 10 D-glucose [24 – 25°C]).

2.1.2.3 Pharmacology for T-type Ca^{2+} channel studies

The T-type antagonists used in these experiments included the following: Ni^{2+} (42 μM – 319 μM; Sigma-Aldrich), amiloride (500 μM; Sigma-Aldrich), mibefradil (2 – 10 μM), NNC 55-0396 (10 μM), TTA-P2 (3 – 10 μM). T-type agonist used in these experiments was L-Cysteine (100 – 200 μM). I would like to acknowledge Dr. Ray Turner's lab (University of Calgary, Canada) for generously providing aliquots of mibefradil, NNC 55-0396, and L-Cysteine, and to Dr. Victor Uebele (Merck, USA) for generously donating an aliquot of TTA-P2.

2.1.3 Identification of motoneurons

For experiments examining intrinsic properties of motoneurons (mixed flexor and extensor), motoneuron soma from lumbar spinal cord segments 2–4 were visually identified (Olympus BX51WI) using infrared differential interference contrast (IR-DIC) in the lateral ventral horn and had soma diameters >20 μm.

2.1.4 Electrophysiology and activation of locomotor networks

2.1.4.1 In vitro isolated spinal cord experiments

Tight fitting suction electrodes were used to record neurograms from the right and left lumbar ventral roots two (L2) and from a single lumbar five ventral root (L5). A locomotor-like rhythm exhibits a classic neurogram signature, evident by an alternating left/right L2 neurogram pattern, as well as an ipsilateral alternation between the L2 and L5 neurograms. When this pattern was observed I classified the evoked rhythm as locomotor-like. Neurograms were amplified (100 – 10,000 times), filtered (DC - 1 kHz), and digitized (Digidata 1322A, Molecular Devices, Sunnyvale, CA) for future analysis. All data collected were analyzed using custom written

programs (MatLab, Math Works, Natick, MA; SpinalCore, A. Lev-Tov) and commercially available programs (Clampfit, Molecular Devices & Spike2, CED, Cambridge, UK). Rhythmic activity was elicited by bath application of drugs or by stimulation of the ventral roots or sciatic nerve (Bonnot et al., 2009; Whelan et al., 2000).

2.1.4.2 Drug-evoked locomotion

In certain experiments, pharmacological agents were used to evoke rhythmicity (Jiang et al., 1999; Whelan et al., 2000). These drugs included N-methyl-D(L)-aspartic acid (NMA, 5 μM), and 5-HT (10 μM). To measure the modulatory effects of DA, 50 μM DA was added to the bath. Note this concentration of DA remained the same for all drug-evoked and ventral root/sciatic nerve stimulation experiments and was selected based on concentrations used by several labs to elicit robust bouts of rhythmicity (Jiang et al., 1999; Whelan et al., 2000).

2.1.4.3 Ventral root stimulation-evoked locomotion

Square – wave stimulation trains were delivered to the ventral roots (L5 or L6) to antidromically activate spinal motoneurons (stimulus duration: 500 μs, trains: 4 Hz, stimulus intensity: 2 - 10 μA, train duration: 10 s). In some preparations, antidromic stimulation of the sciatic nerve (stimulus duration: 500 μs, trains: 4 Hz, stimulus intensity: 50-100 μA, train duration: 10 s) was utilized. To determine the stimulus evoked response threshold (T), pulse trains were delivered at increasing intensities until a depolarization response could be detected (2 - 10 μA) in the ipsilateral L2 ventral root. Pulse trains were delivered once every three minutes at a constant intensity throughout an experiment (Whelan et al., 2000). Control rhythms were recorded for at least 15 min before pharmacological agents were added. For some experiments, stimuli were

delivered to the L5 ventral root (5 pulses, 50 - 100 μA, 200 μs duration, at 4 Hz) and neurogram recordings were made from the L6 ventral root.

2.1.4.4 Slice preparations

The lumbar spinal cord slice was placed into the recording chamber and superfused with oxygenated ACSF solution (in mM: 128 NaCl, 4 KCl, 1.5 $CaCl_2$, 1 $MgSO_4$, 0.5 Na_2HPO_4, 21 $NaHCO_3$, and 30 D-glucose) at an approximate rate of 2 ml/min. Electrodes were pulled from borosilicate glass on a P87 Flaming/Brown puller (Sutter Instruments, Novato, CA) and had resistances in the range of 3–8 MΩ. The internal pipette solution contained (in mM) 130 K-gluconate, 7 NaCl, 0.1 EGTA, 10 HEPES, 0.3 $MgCl_2$, 2 ATP, and 0.5 GTP, adjusted to pH 7.3 with KOH. Neurons were visualized for whole-cell patch using differential interference contrast optics and infrared light transmission. In certain experiments, glutamatergic and/or inhibitory fast neurotransmission were blocked. The data were low-pass filtered (10 kHz) and digitized (sampling rate of 20 kHz) for off-line analyses (Digidata 1322A, Clampex 8 and 10; Molecular Devices). The channel blockers and pharmacological reagents were dissolved in aCSF and prepared fresh before each experiment.

2.1.5 Data analyses

2.1.5.1 Analysis of frequency and spectral power using non-stationary analysis techniques

Spinalcore is a wavelet-based data analysis software developed by the Lev-Tov group (Mor & Lev-Tov, 2007) that was applied to neurogram signals recorded during fictive locomotion induced by pharmacology and by electrical stimulation. Briefly, the pairs of neurogram signals (Right L2 (RL2) - Left L2 (LL2)), were rectified, integrated, and low-pass filtered. The program

utilizes Wavelet Transformation (WT) and WT coherence approaches to analyze sections of the processed neurogram. Spectrograms were constructed to graphically represent the frequency components of the neurogram signals with respect to time. Illustrated in the spectrogram representations, the x-axis represents the time course of the recording, in seconds; the y-axis represents the range of frequencies where locomotor rhythms occur, from approximately 0.1 to 5 Hz. The colors that are plotted on the graph represent logarithmic power, which shows the amplitude of a given frequency component (y-axis) at that time (x-axis) in the recording. High-power regions are arbitrarily assigned "warm" colors (i.e., red and orange), and low-power regions are assigned "cool" colors (i.e., green and blue). The spectrograms show which frequencies are more strongly represented in the recording and how those frequency components may change over the course of the recording. Once the spectrograms were produced, a high power band representing the cross WT of the segmental L2 neurograms became apparent. This band was then selected in its entirety as a region of interest for further analysis. Regions of interest were segmented into 6 bins across the time course of the experiment, and analyzed to produce the following parameters: mean frequency, mean coherence, and mean power, for each bin. Bins were then averaged together, and resulting values were normalized to control conditions. Normalized values were calculated by dividing each sweep value by the maximum control value obtained in each experiment, leading to the generation of a mean control value hovering around 1 with an accompanying SD. Phase values were obtained for each experiment and plotted as a circular plot with length of the vector and phase (degrees) as variables (Oriana Software, Kovach Computing Services, UK). A Rayleigh test was performed to examine whether the distribution was random or clustered (*Biostatistical Analysis*, 2009). Significant values were in the range of $P < 0.001$ to $P < 0.05$ (GraphPad Software Inc, La Jolla, CA).

2.1.5.2 Analysis of burst amplitude

Burst amplitudes were calculated using Spike 2 software (CED, Cambridge, UK). Two ten minute segments of data were identified for analysis. One segment was taken immediately prior to drug administration while the other 10-minute segment was centered around the point where the DA drugs had the greatest effect. Neurograms were rectified, integrated and the peak amplitudes of the bursts were measured and binned (10 bins per 10 minute time segment). Data amplitudes were normalized to average control values for each experiment. A two-way analysis of variance was performed to measure the DAergic effect across time (GraphPad).

2.1.5.3 Intrinsic motoneuron properties

A collection of intrinsic electrical properties was recorded from each motoneuron (total $n = 25$) in this study. These properties were: action potential (AP) amplitude, AP half-width time, AP time-to-peak, AP threshold voltage, rheobase current, afterhyperpolarization (AHP) half – decay time, R_{in}, frequency–current slope (*f–I* gain), and postinhibitory rebound (PIR). AP amplitude was measured from the resting potential preceding an AP to that AP peak; AP half-width time was measured as the duration of the spike at 0.5 the AP amplitude; AP time-to-peak time was measured from the base of an AP to the peak. Rheobase current was quantified as the minimal depolarizing current step (2 Hz, 25 ms duration, 5 pA intervals) sufficient to elicit an AP. Averaged AP traces (10 consecutive sweeps) evoked by brief suprathreshold depolarizing current injections (0.5–1.0 ms) were used to quantify AP AHP half-decay times (AHP). AHP was measured as the duration from the most hyperpolarized potential following an AP to the time at which the membrane potential has returned halfway to the resting potential. AHP duration was calculated from the down-stroke of the AP to the return to baseline. Input resistance

(R_{in}) was measured by dividing the average voltage deflection (20 -30 consecutive sweeps) of the membrane potential by a hyperpolarizing 50 pA current step (250 ms). Two protocols were used to investigate the presence of PIR in putative motoneurons in the presence of synaptic blockers. First, the voltage dependency of PIR was tested by delivering a series of hyperpolarizing current steps (500 ms), of increasing amplitude (from -10 pA to -190 pA) at a constant holding potential of around -60 mV. Second, the time dependency of the hyperpolarizing current pulse was investigated by delivering a series of current steps, which hyperpolarized the cell to between -77 and -95 mV of increasing duration (200 ms to 2100 ms) from a set holding potential around -60 mV. Current levels were adjusted (from -50 to -200 pA) to reach and estimated voltage of -80 mV for all cells.

Chapter Three: Dopaminergic modulation of drug-evoked locomotor-like activity

3.1 INTRODUCTION

Neural circuits that produce basic rhythmic motor patterns reside primarily in the spinal cord and are subject to neuromodulation from a wide range of sources both intrinsic and extrinsic to the spinal cord (Dunbar et al., 2010; Gordon & Whelan, 2008; Jankowska, Jukes, Lund, & Lundberg, 1967a; 1967b; Katz, 1995; Kiehn et al., 1999; Kiehn & Kjaerulff, 1996; Madriaga et al., 2004; Schmidt & Jordan, 2000). Monoamines, an important group of neuromodulators, are released onto spinal cord circuits and are critical for the expression of locomotion. Additionally, monoamines also endow these circuits with the necessary flexibility to control the precision, timing, and constancy of locomotor behaviors in order to adapt to different external demands, essential for survival (Grillner, 2003; Miles & Sillar, 2011).

In contrast with the other monoamines, the role of DA in controlling spinal locomotor circuits has been largely neglected in the mammal. What we do know is that DA is released within the spinal cord during stepping activity (Gerin & Privat, 1998) to increase motor output (Barbeau & Rossignol, 1991; Clemens, Belin-Rauscent, Simmers, & Combes, 2012; Han et al., 2007; Lapointe, Rouleau, Ung, & Guertin, 2009; Madriaga et al., 2004; McCrea et al., 1997) and modulate sensory transmission in a variety of species. DA fibers and receptors projecting from the diencephalon (A11 area) are present in the ventral horn of the adult spinal cord (Holstege et al., 1996; Qu et al., 2006; Ridet, Sandillon, Rajaofetra, Geffard, & Privat, 1992; Weil-Fugazza & Godefroy, 1993; Yoshida & Tanaka, 1988), an area where motor circuits are located. Accordingly, mice with lesions of the A11 area show deficits in motor control (Clemens, Rye, & Hochman, 2006). Microdialysis measurements in both neonatal and adult rodents show release of DA and its metabolites in the ventral horn of neonatal rats during fictive locomotion (Gerin,

Becquet, & Privat, 1995; Jordan & Schmidt, 2002). The key role for DA transmission in locomotion is highlighted by the fact that L-DOPA-elicited air stepping in intact neonatal rats is blocked by DA receptor antagonists (McCrea et al., 1997) and that D_1 agonists can promote stepping in adult mice (Lapointe et al., 2009). Additionally, previous work has emphasized that DA can modulate ongoing drug-evoked locomotor rhythms (Barriere et al., 2004; Jiang et al., 1999; Madriaga et al., 2004; Schotland et al., 1995; Whelan et al., 2000). Collectively, these studies emphasize an important role for DA in the initiation and modulation of locomotor function in the developing and adult spinal cord.

An important step in understanding how DA exerts sustained neuromodulatory actions on CPG networks is to identify the receptors activated by DA. Two DA receptor families that have been distinguished based on biochemical studies, and are subdivided into five receptor subtypes (D_1 and D_5 receptors belonging to the D_1 – like family, and D_2, D_3 and D_4 belonging to the D_2 – like family) (Missale et al., 1998; Neve et al., 2004). Previous reports in the neonatal mouse have investigated the underlying DA receptors that contribute to ongoing locomotor rhythms evoked by either pharmacological application of 5-HT (Madriaga et al., 2004), or electrical stimulation of the afferents that reside in the cauda-equina (Gordon & Whelan, 2006b). These studies, as well as others in the rat, provide evidence that DA's excitatory effects are mainly mediated via a D_1 – like receptor based pathway (Barriere et al., 2004; Seth, Gajendiran, Maitra, Ross, & Ganguly, 1993). Interestingly, in contrast to the mammalian system, the lamprey appears to utilize a D_2 – receptor based pathway to promote excitability (Schotland et al., 1995). Despite that the mechanistic basis of DA's excitatory influence on locomotor CPGs appears to differ across species, the modulatory effects of DA on locomotion are qualitatively similar (Barriere et al., 2004; Grillner, 2003).

The aim of my current work was to build on and extend previous observations of the DAergic modulation of rhythmic activity in the neonatal mouse spinal cord, by investigating the effects of DA, and it's agonists on a pre-existing locomotor-like rhythm evoked by pharmacological application of 5-HT and NMA. In the rat spinal cord, application of 5-HT and NMA is sufficient to induce relatively stable, rhythmic activity (Cowley & Schmidt, 1995; 1997; Kjaerulff & Kiehn, 1996; Kremer & Lev-Tov, 1997). However in the mouse, application of 5-HT and NMA has been shown to generate uncoordinated rhythmic activity between the left and right sides of the spinal cord (Jiang et al., 1999; Whelan et al., 2000). Therefore, I made use of this relatively unstable locomotor-like rhythm to highlight which aspects of rhythmic activity were altered by DA application. My data demonstrate that DA application stabilized a pre-existing 5-HT, NMA-evoked locomotor-like rhythm, increased burst amplitude, and slowed the rhythm frequency. The underlying boost in excitation leading to a stabilization of rhythmic output was found to be D_1 – and D_2 – dependent, a finding consistent to what was demonstrated in the newborn rat (Barriere et al., 2004), while DA's ability to slow down the timing of the rhythm was likely mediated by D_2 – dependent signaling mechanisms. Moreover, I found that D_1 receptor activation is critical for the maintenance of an ongoing locomotor rhythm elicited by bath application of 5-HT, NMA, and DA. Finally, I provide additional support for the proposal that DA receptors are potentially cross-activated by the application of 5-HT (Madriaga et al., 2004). Therefore, regardless of whether DA receptor activation occurs by exogenously applied DA, endogenously released DA, or by the presence of 5-HT, my data highlights an important contribution for DA receptor activation in the maintenance and stability of ongoing CPG network activity.

3.2 RESULTS

3.2.1 DA modulation of drug-evoked locomotor activity

In the first set of experiments I evoked relatively unstable, rhythmic activity by bath application of 5-HT (10μM) and NMA (5 μM). Then, DA (50 μM) was added to the pre-existing rhythm in order to investigate which aspects of rhythmic activity were altered by the presence of DA. Note the drug concentrations remained the same in all subsequent experiments.

3.2.1.1 Addition of DA increases the stability, frequency, and burst amplitude of a 5-HT, NMA-evoked locomotor rhythm

Similar to previous reports (Barriere et al., 2004; Whelan et al., 2000), I observed that DA alters several aspects of rhythmic activity evoked by bath application of 5-HT and NMA. Figure 3.1B shows the bursting pattern recorded from the segmental L2 ventral root neurograms following bath application of 5-HT and NMA. Generally, the 5-HT, NMA-evoked activity was comprised of bouts of alternating bursts, with intermittent short pauses of tonic activity. Following application of DA for 10 minutes, the relatively unstable 5-HT, NMA-evoked rhythm began to convert into a more stable, alternating rhythm in 6/6 preparations. Normalized power scores increased following addition of DA (n = 6; $P < 0.05$; Fig 3.1Di). Burst amplitude significantly increased five minutes after the addition of DA and reached a peak 3 minutes later (n = 6; $P <$ 0.001 to 0.05; Fig 3.1E). Additionally, as the rhythmic bursting pattern became more stable in the presence of DA, the frequency of the rhythm slowed considerably from an average of ~0.4 Hz to ~0.3 Hz (n = 6; $P < 0.001$; Fig 3.1Dii). To summarize power and frequency changes over time, I produced a representative spectrogram illustrating a 5-HT, NMA-evoked rhythm

following application of DA at two different time points (Fig 3.1C). The advantage of this approach is that it allows one to examine an experiment in its entirety. Overall, bath application of DA facilitated 5-HT, NMA-evoked locomotor-like activity by increasing the burst amplitude, stabilizing the rhythm as indicated by an increase in power, and also decreasing the rhythm frequency.

3.2.2 Contribution of DA receptor families to the observed effects of DA on a pre-existing 5-HT, NMA-evoked locomotor rhythm

In the next set of experiments I examined which of the underlying DA receptors families (D_1 – like vs. D_2 – like) were responsible for the DAergic mediated effects on a pre-existing locomotor rhythm. My first question was whether application of D_1 – like or D_2 – like receptor agonists could mimic the effects of DA on rhythm stability and burst amplitude. Next, I sought to investigate whether activation of D_1 – like and/or D_2 – like receptors could replicate DA's ability to slow the frequency of an ongoing locomotor rhythm.

3.2.2.1 Both D_1 – like and D_2 – like receptor families contribute to the DA-induced increase in rhythm stability evoked by 5-HT, NMA

First, I tested whether the application of D_1 – like and/or D_2 – like receptor agonists could sufficiently reproduce DA's effects by increasing the rhythm stability of a pre-existing 5-HT, NMA-evoked rhythm. Application of specific D_1 – like agonist SKF-81297 (20 μM) significantly increased the stability of an ongoing 5-HT, NMA-evoked rhythm, evident by a significant increase in normalized power scores (n = 9; $P < 0.01$; Fig 3.2A and Bi), consistent with DA's effects. Wash with 500 ml aCSF containing 5-HT and NMA restored the rhythm to

control conditions.

In a separate set of experiments, addition of the D_2 – like agonist quinpirole (20 μM) also resulted in a significant increase in normalized power scores ($n = 7$; $P < 0.05$; Fig 3.2C and Di). The D_2 – like agonist activity persisted despite wash with 500-700 ml aCSF containing 5-HT and NMA (Fig 3.2Di and Dii), indicating the possibility for long lasting effects of D_2 – like receptor activation on rhythm stability. This finding was somewhat surprising and did not support specific hypothesis 1. However my work supports previous findings in the rat, and provides further evidence for the effectiveness of not only D_1 – like, but also D_2 – like receptor activation in the maintenance and stability of an ongoing locomotor rhythm (Barriere et al., 2004).

3.2.2.2 D_1 – like receptor activation increases burst amplitude

Next, I explored which DA receptor family may underlie DA's ability to increase burst amplitude by testing (1) whether D_1/D_2 – like agonists could excite populations of ventral lateral funiculus (VLF) projecting interneurons and (2) whether D_1/D_2 – like agonists could excite ventral root populations. I tested this by recording slow electrotonic DC potentials from the left VLF tissue, right L2 and right L5 (Fig 3.2E and F). Collectively, increases in slow electrotonic DC potentials reflect an average of passive membrane events from multiple cells that project axons into ventral roots or the VLF tissue being recorded, along with Na^+ spike activity. Additionally, previous work has established that the time course of the slow DC potential corresponds closely with the membrane potential trajectory recorded intracellularly (Fig3.2E and F) (O'Donovan, 1987). My work revealed that the D_1 – like agonist SKF-81297 (40 μM) increased the amplitude of the slow electrotonic DC potentials and also increased high frequency tonic bursting (Fig 3.2F). When these experiments were repeated with the D_2 agonist quinpirole,

there was no change in the amplitude or tonic bursting of neurogram activity (data not shown). Collectively, my data suggest that while the effects of DA on rhythm stability are mediated through activation of both D_1 and D_2 – like receptor based pathways, DA's effects on burst amplitude appear to be primarily D_1 – like based.

3.2.2.3 D_2 – like receptor activation slows the rhythm frequency of a 5-HT, NMA-evoked locomotor rhythm

As previously demonstrated, DA application increased stability while simultaneously slowing the frequency of a 5-HT, NMA-evoked rhythm (Fig 3.1C and D). Therefore, I tested whether D_1 – like and/or D_2 like receptor activation could mimic the effects of DA on rhythm frequency. When specific D_1 – like agonist SKF-81297 was applied to the ongoing 5-HT, NMA-evoked rhythm, there were no significant changes in rhythm frequency (Fig 3.2Bii). However, bath application of D_2 – like agonist quinpirole reproduced the effects of DA, resulting in a 21% decrease in the rhythm frequency (n = 7; $P < 0.01$; Fig 3.2C and Dii). Similar to my findings regarding rhythm stability, the effects of D_2 – like receptor activation on rhythm frequency persisted following wash with 500 – 700 ml aCSF containing 5-HT and NMA. This further provides evidence for the presence of a long-lasting downstream D_2 – mediated signaling mechanism. Collectively these experiments, as well as those completed in sections 3.2.1 and 3.2.2, reinforce the importance for D_1 – like receptor activation in mediating DA's excitatory effects on rhythm stability and burst amplitude (Barriere et al., 2004; Gordon & Whelan, 2006b; Madriaga et al., 2004; Seth et al., 1993), but also highlight a potential role for the contribution of D_2 – like receptor activation in mediating DA's actions on rhythm stability and frequency in the mammalian system.

3.2.2.4 Co-application of D_1/D_2 agonists to a 5-HT, NMA - evoked rhythm significantly decreased frequency but had no effect on power

In my final set of experiments, I co-applied the D_1 – like agonist SKF-81297 and D_2 – like agonist quinpirole to test if the combination of the two could directly reproduce the effect of DA on a pre-existing 5-HT, NMA rhythm. Upon co-application, I observed a significant decrease in rhythm frequency within 10-20 min of application ($n = 5$; $P < 0.001$; Fig 3.3B), consistent with DA application. However, this effect was transient as the rhythm frequency eventually returned back to control values within 20-30 min of application (Fig 3.3C). Interestingly, I observed no change in rhythm stability or burst amplitude. This finding is expanded upon in the discussion. It is important to note that in my personal observations during the course of these experiments, I observed that the 5-HT, NMA – evoked rhythm generated was much more regular and stable than what I had found in my previous experiments (compare Fig 3.1Bi with Fig 3.3Ai). I suspect this may have been a contributing factor as to why I did not see an increase in normalized power scores.

3.2.3 Contribution of DA receptors to 5-HT, NMA, DA-evoked locomotion

In the neonatal mouse, it has been established that monoaminergic activation of CPG networks by bath application of 5-HT, NMA, and DA is a highly reliable approach for generating stable, long lasting rhythms (Jiang et al., 1999; Whelan et al., 2000). Additionally, this combination of drug-evoked locomotor-like activity has been correlated with the alternating patterns of discharge between ipsilateral flexor and extensor hindlimb muscle nerves that occurs during treadmill walking (Whelan et al., 2000). Therefore, to further explore the role of DA during ongoing locomotor activity, I selectively blocked either D_1 – like or D_2 – like receptors during 5-

HT, NMA, DA-evoked locomotion.

3.2.3.1 Blocking D_1 – like receptors severely disrupts a 5-HT, NMA, DA-evoked locomotor rhythm

Following the establishment of a stable, regular rhythm by bath application of 5-HT, NMA and DA, I examined the effects of blocking the D_1 – like family of receptors. In all preparations, the sustained rhythm began to break down within 5 - 10 min following addition of D_1 – like receptor antagonist LE 300 (6 μM) (Fig 3.4A, B, and E; LE 300: $n = 5$; $P < 0.05$). This was evident by a 37% decrease in normalized power (Fig 3.4E). These results were replicated following addition of another D_1 antagonist, SCH-23390 (1-2 μM data not shown). Wash with 500 – 700 ml aCSF containing 5-HT, NMA and DA restored the rhythm to control conditions (Fig 3.4E; $n = 5$; $P < 0.05$).

In a separate set of experiments, I tested for the contribution of the D_2 – like receptor activation during an ongoing 5-HT, NMA, DA-evoked locomotor rhythm. Surprisingly, there was no effect upon application of the D_2 – like receptor antagonist L-741,626 (6 μM) (Fig 3.4C, D and F*;* $n = 5$). To test for the possibility of competitive binding between DA and L-741,626 I doubled the amount of L-741,626 applied (12 μM; $n = 3$), however I still observed no effect.

To further test the contribution of each DA receptor family to the maintenance of an ongoing 5-HT, NMA, DA-evoked locomotor rhythm, in two experiments I first applied the D_2 – like antagonist L-741,626 followed by the D_1 – like antagonist LE 300. Only upon subsequent addition of D_1 – like antagonist LE 300 were there any changes in the rhythm parameters (data not shown). I did not further test the application of adding LE 300 first, followed by application of L-741,626. Taken together, these data suggest that D_1 – like receptor activity is necessary for the maintenance of an ongoing 5-HT, NMA DA-evoked locomotor rhythm while D_2 – like

receptor activity appears to have far less impact.

3.2.4 5-HT application may cross-activate DA receptors

Several studies published by our lab suggest the possibility that cross activation of monoaminergic receptors by inappropriate ligands can occur in the neonatal mouse spinal cord (Gordon & Whelan, 2006b; Madriaga et al., 2004). Specifically, I was interested in the potential cross-reaction of 5-HT with DA receptors. Therefore, I ran a series of control experiments to test for this possibility.

3.2.4.1 Blocking D_1 – like receptors severely disrupts a 5-HT, NMA-evoked locomotor rhythm

To explore the potential cross-reactivity of 5-HT on DA receptors, I first generated a 5-HT, NMA-evoked locomotor rhythm, just as in previous experiments. Next, I applied either a D_1 – like or D_2 – like antagonist and observed if there were any changes in the rhythm parameters. Upon application of D_1 – like antagonist LE 300 (1 – 2 μM), the ongoing rhythm became severely disrupted, which was reflected by a significant decrease in power ($n = 6$; $P < 0.05$; Fig 3.5Bi, Bii, and D). Interestingly, the emergence of a second, very slow underlying rhythm became apparent (see Epoch 3 in Fig 3.5Ai and Bi). Atop this low frequency rhythm rode bouts of alternating bursts, which exhibited a similar frequency to that of the 5-HT, NMA - evoked rhythm (Fig 3.5E). Between bouts of bursts were intermittent periods of tonic activity (Fig 3.5Bii). The fact that I saw two rhythms emerge, which were governed by separate frequencies (Epoch 2 vs. Epoch 3; Fig 3.5Ai and Bi) adds to the existing evidence for the presence of multiple "clocks" within the CPG system (McCrea & Rybak, 2007).

Next, I tested the ability of DA to recover the 5-HT, NMA-evoked rhythm in the presence of a D_1 – like blockade. Upon application of DA, there was a depolarization in the baseline of the

neurogram activity (data not shown). Similar to my previous findings, DA application significantly increased normalized power scores (Fig 3.5D; $P < 0.001$) and decreased rhythm frequency ($P < 0.001$) suggesting the possibility that DA helped recover the rhythm via a D_2 – like mediated signaling mechanism. These results were replicated by application of another D_1 – like antagonist SCH-23390 ($n = 5$; data not shown).

In the next set of experiments, when I applied the D_2 – like antagonist L-741, 626 to a pre-existing 5-HT, NMA-evoked locomotor rhythm I did not observe any significant changes in rhythm parameters ($n = 5$; data not shown). However upon application of DA, once again I saw normalized power scores increase significantly ($P < 0.05$) and rhythm frequency significantly decrease ($P < 0.01$). Based on my findings, I conclude that 5-HT may possibly be cross-reacting with D_1 – like receptors preferentially, and may not exert an influence over D_2 – like signaling pathways. Additionally, my data suggests that DA functions to restore locomotor rhythms evoked by 5-HT, NMA by activating all receptor isoforms.

Chapter Three: FIGURES

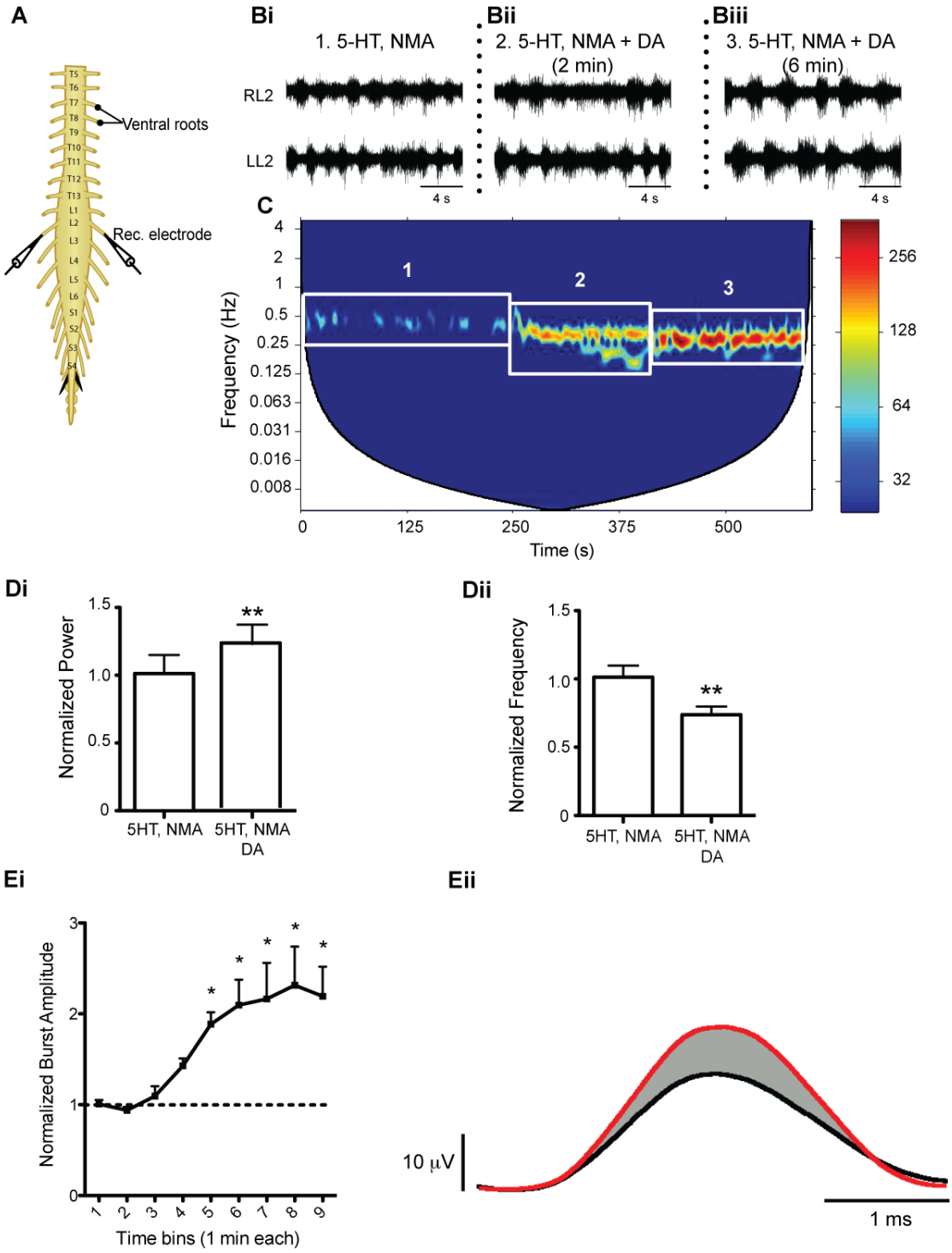

Figure 3.1: DA stabilizes a 5-HT, NMA-evoked locomotor rhythm.

A: schematic diagram of the isolated spinal cord preparation showing recording sites. B: raw traces from the L2-L2 neurogram recordings under conditions with 5-HT, NMA (Bi), two min after DA (50 μM) was added to the pre-existing locomotor rhythm (Bii), and six minutes after DA was added to the pre-existing locomotor rhythm. C: cross-wavelet spectrogram showing DA's effects over a 10 minute period. Epoch 1 illustrates the lower power region representing the 5-HT-NMA-evoked locomotor rhythm. Epoch 2 illustrates the increase in power associated with 2 min of DA application to the 5-HT, NMA-evoked rhythm. Epoch 3 illustrates the high power region associated with 6 min application of DA (Epoch 1 – 3 are the same experiment as Bi – Biii). D: graphs showing normalized power (Di) and normalized frequency (Dii) under 5-HT, NMA, and 5-HT, NMA, DA conditions ($P < 0.05$; paired t test; $n = 6$). Control 5-HT, NMA conditions were normalized to 1. Error bars represent the standard deviation (SD) Note: SD values were computed for all conditions, including control. E: graph displaying increase in burst amplitude over 10 minute time frame, taken immediately following the addition of DA to a pre-existing 5-HT-NMA-evoked rhythm. Each time point represents burst amplitude, normalized to 5-HT-NMA values, per bin ($n = 6$; Two-way repeated measures ANOVA; $P < 0.001$ to $P < 0.05$) (Ei). Graph showing the averaged L2 neurograms for one representative experiment (Eii). Graph was constructed by using a peak detection algorithm. Black line represents the averaged 5-HT, NMA burst amplitude across a ten minute time ($n = 6$); Red line represents the 5-HT, NMA, DA burst amplitude across a ten minute time ($n = 6$).

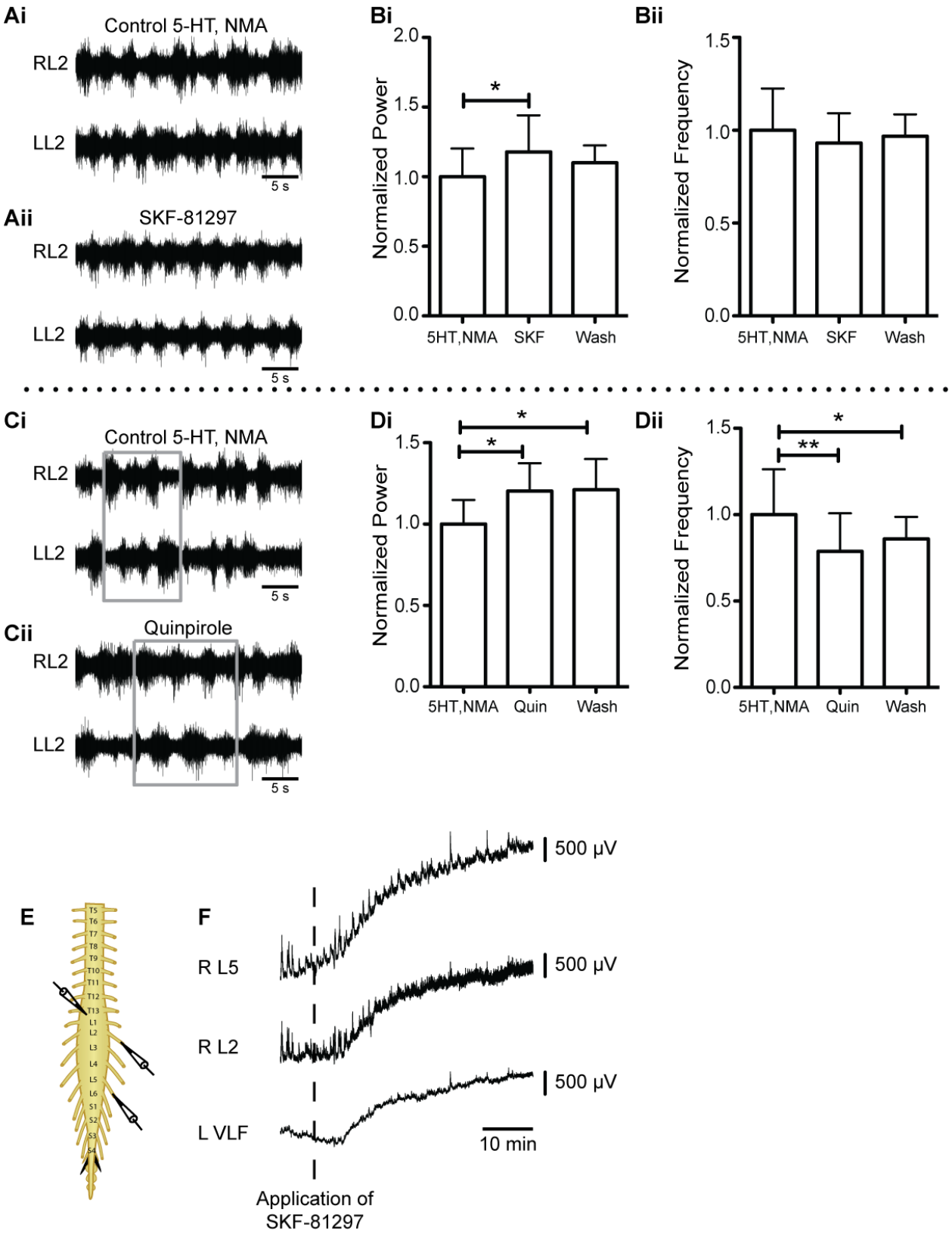
Ai
Control 5-HT, NMA
RL2
LL2
5 s
Aii
SKF-81297
RL2
LL2
5 s
Bi
Normalized Power
2.0
1.5
1.0
0.5
0.0
*
5HT,NMA
SKF
Wash
Bii
Normalized Frequency
1.5
1.0
0.5
0.0
5HT,NMA
SKF
Wash
Ci
Control 5-HT, NMA
RL2
LL2
5 s
Cii
Quinpirole
RL2
LL2
5 s
Di
Normalized Power
1.5
1.0
0.5
0.0
*
*
5HT,NMA
Quin
Wash
Dii
Normalized Frequency
1.5
1.0
0.5
0.0
*
**
5HT,NMA
Quin
Wash
E
T5
T6
T7
T8
T9
T10
T11
T12
T13
L1
L2
L3
L4
L5
L6
S1
S2
S3
S4
F
R L5
R L2
L VLF
500 µV
500 µV
500 µV
10 min
Application of
SKF-81297

Figure 3.2: Application of D_1 – like and D_2 – like receptor agonists alter power, but only D_2 – like receptor agonist alters frequency.

A: raw traces from the L2 neurogram recordings under control conditions with 5-HT, NMA (Ai) and D_1 - like receptor agonist SKF-81297 (20 μM) (Aii). B: graphs showing normalized power (Bi) and normalized frequency (Bii) under SKF-81297 conditions ($P < 0.05$; One-way repeated measures ANOVA). Control 5-HT, NMA conditions were normalized to 1. Error bars represent the SD. C: raw traces from the L2 neurogram recordings under control conditions with 5-HT, NMA (Ci) and D_2 – like receptor agonist quinpirole (20 μM) (Cii). Grey boxes indicate 3 consecutive alternating bursts between the RL2 and LL2 neurograms during 5-HT, NMA and quinpirole conditions. The reference point for the first of three consecutive bursts was taken from the RL2 for both conditions. D: graphs showing normalized power (Di) and normalized frequency (Dii) under quinpirole conditions (* $P < 0.05$; ** $P < 0.001$; One-way repeated measures ANOVA). E: schematic illustrates the recording arrangement (RL5, RL2, VLF). F: neurogram recordings from ventral roots or VLF tissue indicate that SKF-81297 can depolarize populations of motoneurons and interneurons. Neurogram recording from the VLF show that SKF-81297 depolarizes interneurons that project into white matter tracts. Recordings were obtained in DC mode and low-pass filtered to isolate slow potentials.

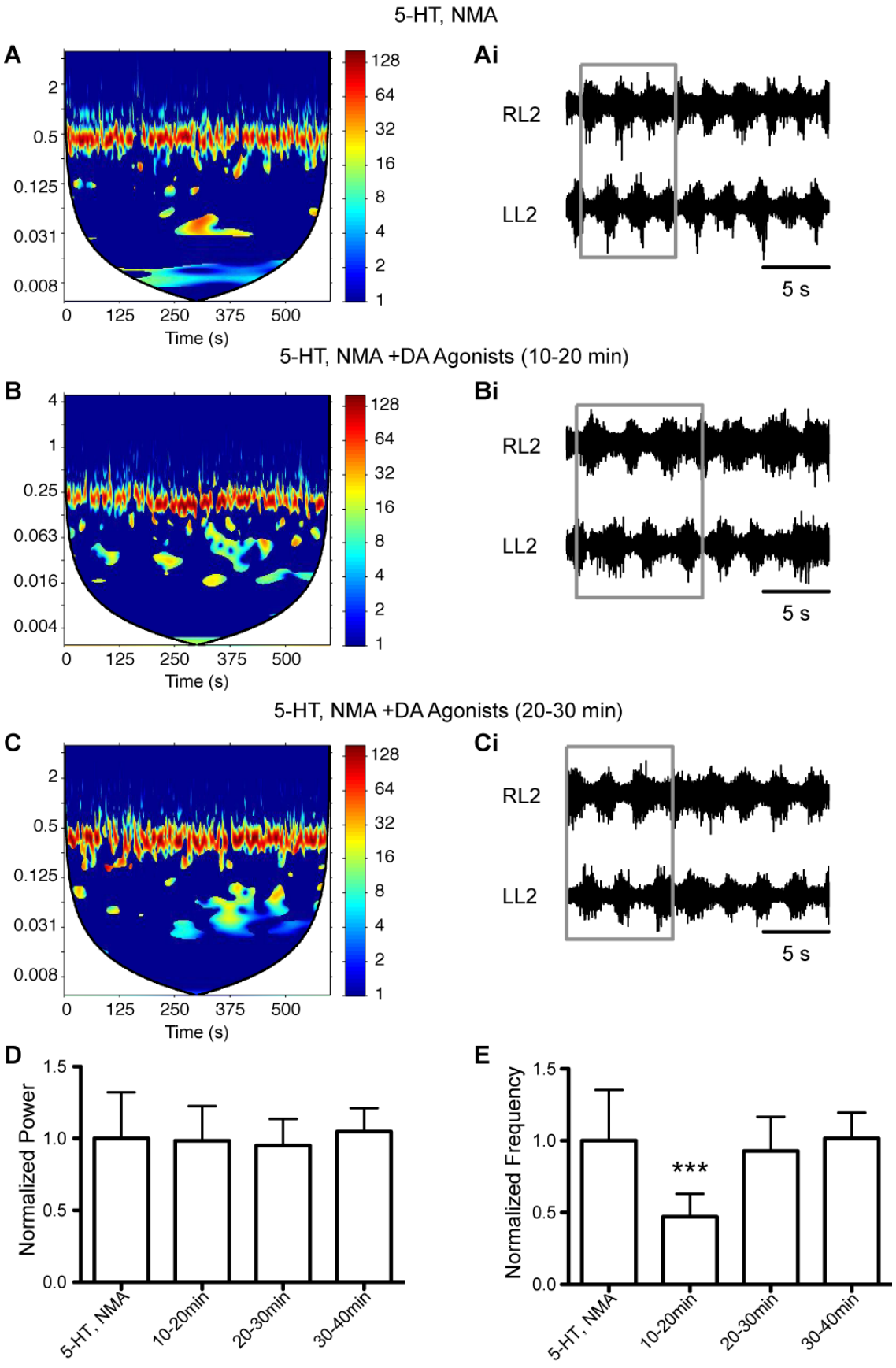
5-HT, NMA
A
Ai
RL2
LL2
5 s
2
0.5
0.125
0.031
0.008
0
125
250
375
500
Time (s)
128
64
32
16
8
4
2
1
5-HT, NMA +DA Agonists (10-20 min)
B
Bi
4
1
0.25
0.063
0.016
0.004
5-HT, NMA +DA Agonists (20-30 min)
C
Ci
D
E
Normalized Power
Normalized Frequency
1.5
1.0
0.5
0.0
***
5-HT, NMA
10-20min
20-30min
30-40min

Figure 3.3: Co-application of D_1/D_2 agonists initially slow the frequency of a 5-HT, NMA – evoked rhythm but do not affect power.

A: Cross-wavelet spectrogram depicting the control 5-HT, NMA-evoked locomotor rhythm over a 10 minute period (A) and raw traces from the L2 neurogram recordings under control conditions with 5-HT and NMA (Ai). Note this 5-HT, NMA rhythm is much more stable than what we have previously observed (compare Fig 3.1Bi). B: Cross-wavelet spectrogram depicting the first 10 – 20 minutes application of D_1/D_2 agonists to a 5-HT, NMA – evoked locomotor rhythm (B) and raw traces from the L2 neurogram recordings showing that the D_1/D_2 agonists slowed down the rhythm (Bi). C: Cross-wavelet spectrogram depicting the next 20 – 30 minutes application of D_1/D_2 agonists to a 5-HT, NMA-evoked locomotor rhythm (Ci) and raw traces from the L2 neurogram recordings showing that the D_1/D_2 agonists no longer slowed down the rhythm. D – E : graphs showing normalized power (D) and normalized frequency (E) under 5-HT, NMA and D_1/D_2 agonist conditions (*** $P < 0.001$; One-way repeated measures ANOVA).

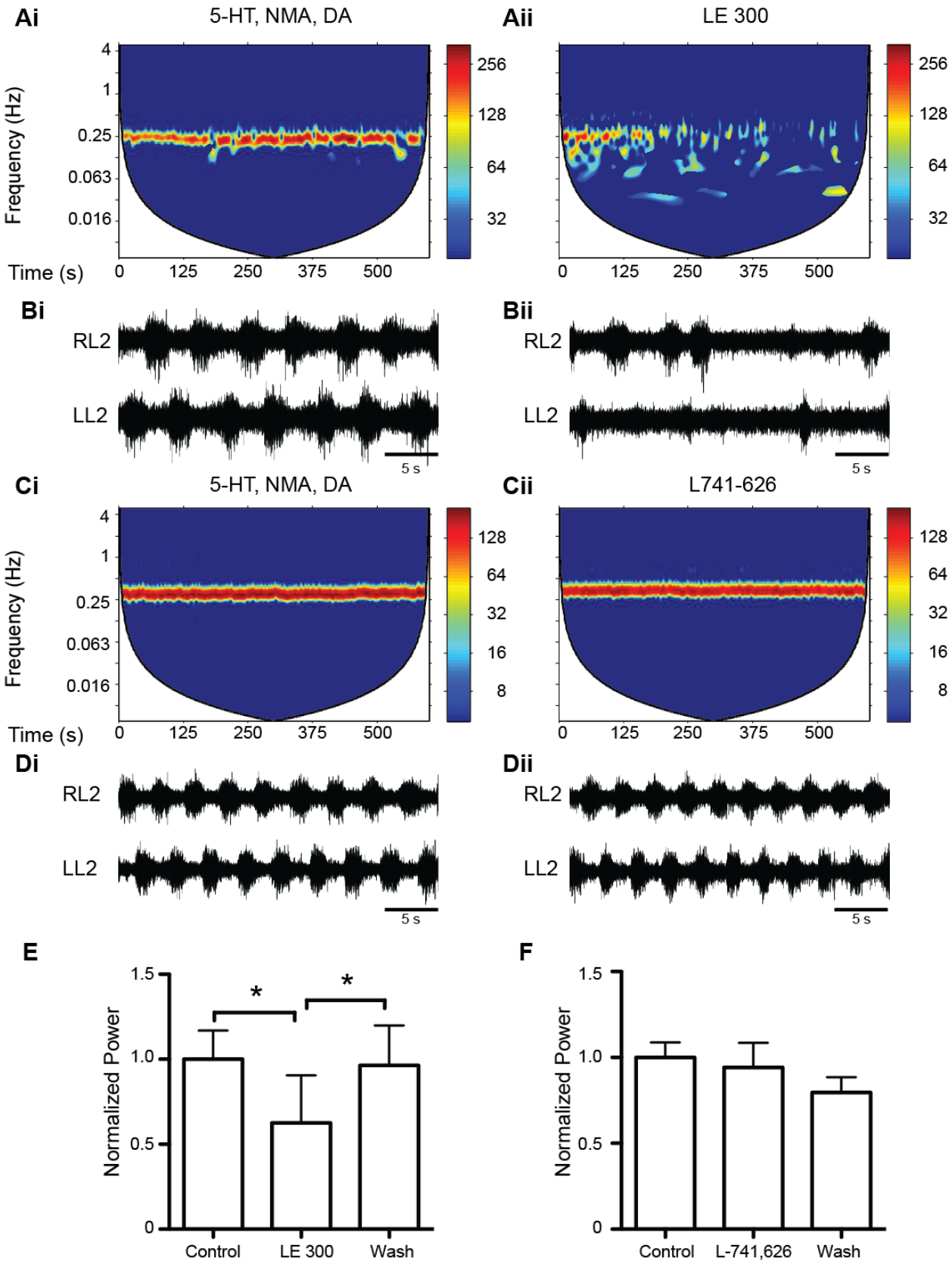
Ai
5-HT, NMA, DA
Aii
LE 300
Frequency (Hz)
4
1
0.25
0.063
0.016
Time (s)
0
125
250
375
500
256
128
64
32
Bi
Bii
RL2
LL2
5 s
Ci
5-HT, NMA, DA
Cii
L741-626
128
64
32
16
8
Di
Dii
E
F
Normalized Power
1.5
1.0
0.5
0
*
*
Control
LE 300
Wash
L-741,626

Figure 3.4: Locomotor rhythm becomes disrupted with application of D_1 – like receptor antagonist, but not D_2 – like receptor antagonist.

A: cross-wavelet spectrograms of L2-L2 neurogram recordings (10 min) following bath-application of 5-HT, NMA, DA (Ai) and with the addition of the D_1 – like receptor antagonist LE 300 (1-4 μM) (Aii). Note the high power frequency band becomes disrupted with the addition of LE 300, indicating a disruption of the rhythmic bursting pattern. B: raw traces from the L2 – L2 neurogram recordings under conditions with 5-HT, NMA, DA (Bi) and D_1 – like receptor antagonist LE 300 (Bii) (same experiment as A). C: cross-wavelet spectrograms of L2-L2 neurogram recordings (10 min) under 5-HT, NMA, DA conditions (Ci) and with the addition of the D_2 – like receptor antagonist L-741, 626 (6 μM) (Cii). Note the high power frequency band is not disrupted with the addition of L-741, 626. D: raw traces from the L2 – L2 neurogram recordings under conditions with 5-HT, NMA, DA (Di) and with the addition of the D_2 – like receptor antagonist L-741, 626 (Dii) (same experiment as C). E – F: graphs showing normalized power under SKF-81297 and L-741, 626 conditions. (One-way repeated measures ANOVA, $P < 0.05$; $n = 5$). Error bars represent standard deviation. Control 5-HT, NMA, DA conditions were normalized to 1.

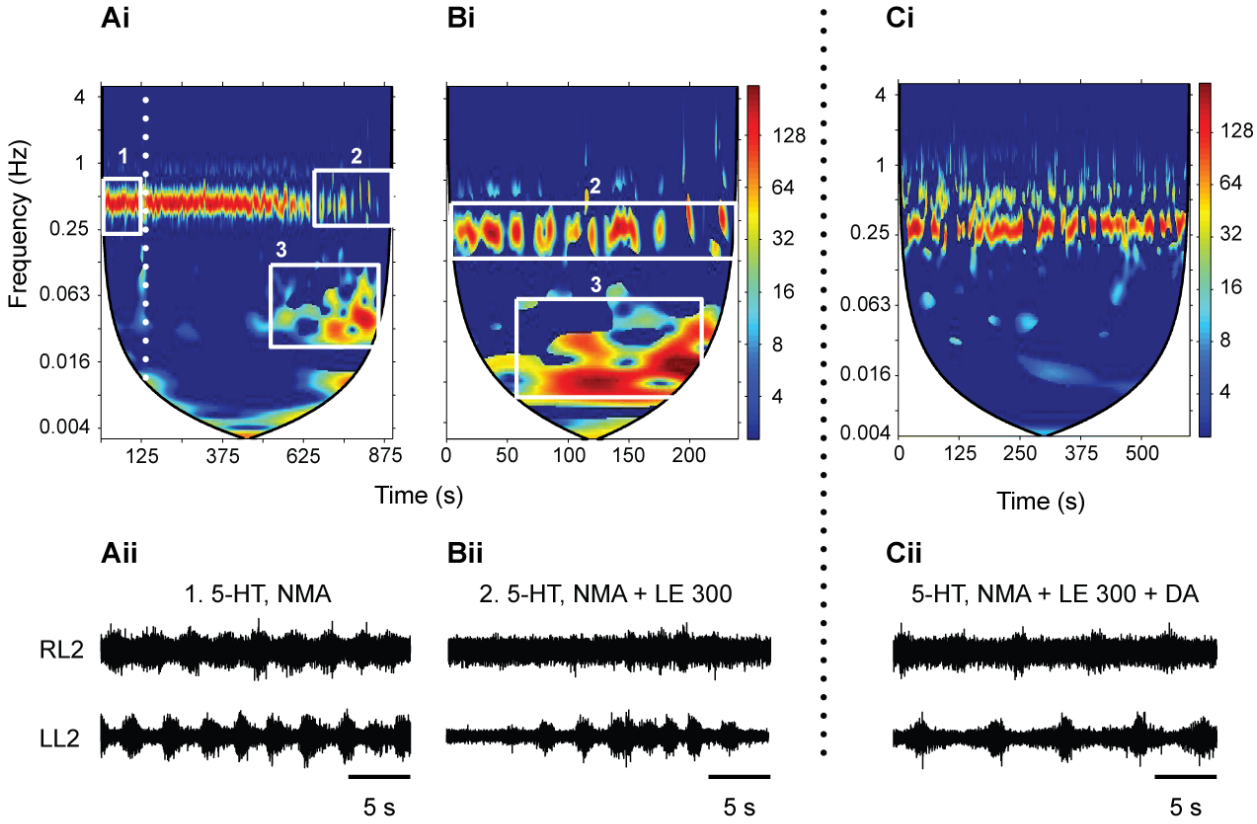
Ai
Bi
Ci
Frequency (Hz)
4
1
0.25
0.063
0.016
0.004
1
2
3
125
375
625
875
0
50
100
150
200
128
64
32
16
8
4
0
125
250
375
500
Time (s)
Aii
Bii
Cii
1. 5-HT, NMA
2. 5-HT, NMA + LE 300
5-HT, NMA + LE 300 + DA
RL2
LL2
5 s
5 s
5 s

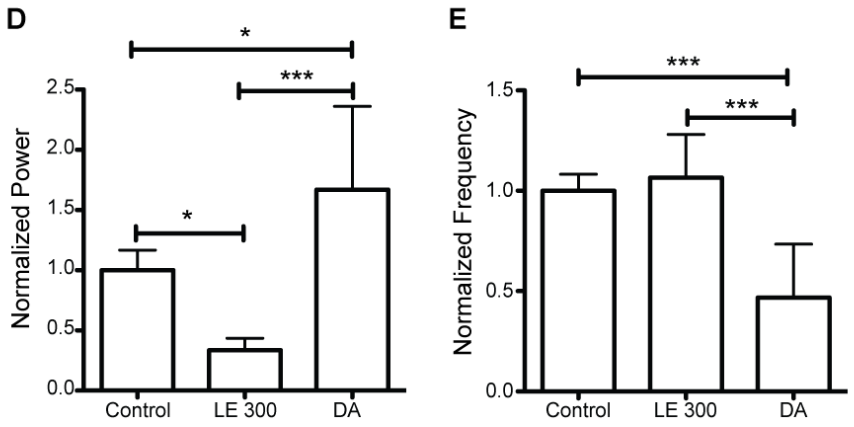
D
Normalized Power
2.5
2.0
1.5
1.0
0.5
0.0
*
***
*
Control
LE 300
DA
E
Normalized Frequency
1.5
1.0
0.5
0.0
***
***
Control
LE 300
DA

Figure 3.5: Application of 5-HT cross-activates D_1 – like receptors.

A: cross-wavelet spectrogram showing the addition of D_1 – like antagonist LE 300 to a 5-HT, NMA-evoked locomotor rhythm over a 15 minute period (Ai). Epoch 1 illustrates the power region representing the 5-HT-NMA-evoked locomotor rhythm. Epoch 2 illustrates the steady state effect and also the decreased power associated with LE 300 application to the 5-HT, NMA-evoked rhythm. Epoch 3 illustrates the emergence of a low frequency rhythm associated with application of LE 300. Raw traces from the L2-L2 neurogram recordings under 5-HT, NMA conditions (Aii). B: cross-wavelet spectrogram illustrating the expansion of Epoch's 2 and 3 from A. Note the change in time scale. Epoch 2 was used for further analysis. Raw traces from the L2-L2 neurogram recordings following the addition of LE 300 to a 5-HT, NMA-evoked rhythm taken from Epoch 2 (Bii). C: cross-wavelet spectrogram showing the addition of DA to a 5-HT, NMA + LE 300 - evoked locomotor rhythm over a 10 minute period (Ci). Raw traces from the L2-L2 neurogram recordings following the addition of DA to a 5-HT, NMA + LE 300 - evoked rhythm (Cii). D - E: graphs showing normalized power (D) and normalized frequency (E) under 5-HT, NMA (control) conditions, 5-HT, NMA + LE 300 conditions, and 5-HT, NMA, LE 300 + DA conditions (* $P < 0.05$; *** $P < 0.0001$; One-way repeated measures ANOVA; $n = 6$). Control 5-HT, NMA conditions were normalized to 1. Error bars represent the SD. Raw traces are taken from the same experiment as their associated cross-wavelet spectrograms.

3.3 DISCUSSION

3.3.1 General remarks

The ability for DA to initiate and modulate on going locomotor rhythms is of growing interest in the field of motor control. Over the past decade, work *in vivo* has implicated an important role for DA during the initiation and maintenance of stepping behavior (Clemens et al., 2006; Gerin et al., 1995; Gerin & Privat, 1998; Jordan & Schmidt, 2002; Lapointe et al., 2009; McCrea et al., 1997). Additionally, *in vitro* work has highlighted the ability of DA to modulate ongoing locomotor rhythms (Barriere et al., 2004; Gordon & Whelan, 2006b; Jiang et al., 1999; Madriaga et al., 2004; Schotland et al., 1995; Whelan et al., 2000). However, experimental protocols in the mouse have often relied upon fairly robust control rhythms induced either pharmacologically or by electrical stimulation, to test the effectiveness of DA. This has raised some questions regarding whether the effects of DA are somewhat "masked" by the presence of a fairly stable control rhythm. Therefore in the current study, I sought to expand upon an existing body of research (Barriere et al., 2004; Gordon & Whelan, 2006b; Kiehn & Kjaerulff, 1996; Madriaga et al., 2004; Whelan et al., 2000) and test what aspects of a fairly uncoordinated, pharmacologically induced rhythm were altered by the presence of DA. My results indicate that the presence of DA induced a much more stable, slower rhythm with enhanced burst amplitude. Indeed, I found that D_1 – like and D_2 – like receptors have distinct roles in controlling rhythm stability, frequency and burst amplitude. Moreover, a portion of my data provides additional evidence that 5-HT is sufficient to activate DA receptors, which may have important developmental implications.

3.3.2 Contribution of DA receptors to ongoing fictive locomotion in the neonatal mouse

The potential for DA to modulate ongoing locomotor rhythms *in vitro* was first recognized in the lamprey (Schotland et al., 1995) and later in the mammalian system (Barriere et al., 2004; Gordon & Whelan, 2006b; Kiehn & Kjaerulff, 1996; Madriaga et al., 2004; Whelan et al., 2000). Initial experiments described DA's ability to slow down the cycle frequency of swimming behavior (Schotland et al., 1995). More recent work in the isolated mouse has reported an excitatory role for DA on network output (Gordon & Whelan, 2006b; Madriaga et al., 2004; Whelan et al., 2000). My current work adds to this growing body of research in the following important ways: First, the number of studies investigating the DAergic modulation of ongoing locomotor rhythms in the neonatal mouse is limited. Although a report in the neonatal rat documenting DA's role during ongoing locomotor activity exists (Barriere et al., 2004), we cannot assume the underlying receptor subtypes activated during fictive locomotion are the same. Second, of the limited studies that do exist in the mouse, two of them have relied upon evoking robust control rhythms prior to investigating DA's modulatory effects (Gordon & Whelan, 2006b; Madriaga et al., 2004). Therefore it is arguable that the magnitude of DA's effect on a pre-existing stable rhythm was not fully revealed. The remaining study that did show DA's modulatory effects on an uncoordinated control rhythm (Whelan et al., 2000) did not further ascribe distinct roles for the underlying DA receptor families responsible for mediating DA's effects. In my current work, it appears that D_1 - like receptor pathways act synergistically with D_2 – like receptor pathways to increase the stability of a pre-existing 5-HT, NMA – induced rhythm. Evidence in the brain and spinal cord support the finding that a synergy between D_1 and D_2 receptor-based signaling pathways exists, and functions to produce appropriate behavioral output in the brain and spinal cord (Barriere et al., 2004; Braun & Chase, 1986;

LaHoste, Henry, & Marshall, 2000; Missale et al., 1998). However, it is important to note that application of the D_1 – like antagonist LE 300 resulted in the break down of the stable 5-HT, NMA, DA-evoked locomotor-like rhythm, while the D_2 – like antagonist L-741, 626 did not. Additionally, L-741, 626 exerted no effects on rhythm frequency. This was unexpected given that application of D_2 – like receptor agonist quinpirole decreased rhythm frequency (Fig 3.2). This finding may be explained by differences in receptor density, or distribution. In an attempt to rule out the possibility for competitive binding between DA and the D_2 – like antagonist, I doubled the concentration of L-741, 626 (from 6 μM to 12 μM) however I still saw no effect. Lack of diffusion into the spinal cord tissue is not likely, given that L-741, 626 has been shown to block 5-HT – evoked locomotor rhythms in the same preparation (Madriaga et al., 2004). Therefore, while it is conceivable that both receptor families contribute to rhythm stability, a heavier emphasis is placed on D_1 – like receptor activation to *maintain* ongoing locomotor rhythms.

Unexpectedly, the substantial effects on rhythm stability and burst amplitude observed by DA application to a pre-existing 5-HT, NMA-evoked locomotor rhythm were not reproduced by co-application of D_1 – like and D_2 – like agonists (Fig 3.3). Although co-application of DA agonists did significantly slow the frequency of the pre-existing locomotor rhythm, this effect was transient as frequency values eventually returned to control levels. Interestingly, this is not the first time that a mismatch between DA spinal responses and D_1/D_2 receptor responses has been reported. For example in the neonatal rat, DA application is sufficient to induce locomotor like activity, yet application of the non-selective D_1/D_2 agonist apomorphine or pergolide were unable to mimic the DA action (Barriere et al., 2004). Moreover, these authors also found that while both D_1 – like and D_2 – like antagonists blocked DA – induced activity, only the D_1 – like

agonist SKF – 81297 (50 μM) was able to induce locomotor-like activity. It should be noted that the concentration of SKF-81297 used by Barriere and colleagues (2004) to mimic DA – induced locomotion was two and half times higher than what I used in combination with D_2 – like agonist quinpirole in my attempt to reproduce DA's actions. Additionally, at the concentrations I used, SKF-81297 and quinpirole may have subthreshold effects that remain undetectable by my extracellular recording methods. Interestingly, when I increased my working concentration to 40 μM, I found that D_1 – like agonist SKF-81297 increased the amplitude of the slow electrotonic DC potentials and also increased high frequency tonic bursting recorded from VLF-projecting interneurons and ventral roots. Therefore, although it is unlikely that low drug concentrations explain the entirety of my findings, it very well may have contributed to the lack of effect.

It is also possible that, in addition to my experimental methodology, the observed mismatch between DA and DA agonists may be of biological origin. Indeed, it must be acknowledged that similar to reports in the 5-HT system (Cazalets et al., 1992; Connell & Wallis, 1989), spinal DA receptors may have slightly different binding characteristics from their DA receptor counterparts in the brain. Future studies with improved pharmacological tools will help clarify these issues.

3.3.3 Potential cross-reaction of 5-HT with DA receptors

Previous studies in the brain and spinal cord have reported that administering 5-HT or 5-HT receptor ligands can influence the DAergic system (Bortolozzi, Díaz-Mataix, Scorza, Celada, & Artigas, 2005; Hoyer, Hannon, & Martin, 2002; Madriaga et al., 2004). The potential for high concentrations of 5-HT (20 – 40 μM) to interact with DA receptors has been described in the mouse (Madriaga et al., 2004). In my current work, I extended on these data by demonstrating

that even low levels of exogenously applied 5-HT (10 μM) may potentially activate DA receptors, specifically D_1 – like receptors (Fig 3.5). While this is a plausible explanation, it is useful to explore other possibilities.

Recent evidence from the non-human primate suggests that the diencephalic A11 region, which was originally thought to be a DAergic nuclei and the sole source for spinal DA, lacks a DA transporter system as well as the enzyme necessary for the conversion of L-DOPA into DA, DDC (Barraud et al., 2010). The authors conclude that the A11 region is likely a major source of spinal L-DOPA, rather than DA. Perhaps even more fascinating is the fact that this finding suggests that the release and conversion of L-DOPA can occur at the level of the spinal cord, rather than the brain. Indeed, cells containing dopa-decarboxylase (DDC), have been described throughout the rat spinal cord at all ages, and have been appropriately named "D-cells" (Jaeger et al., 1983). In this usage, the "D" classification means decarboxylation. The presence of D-cells has two important implications for my work. First, D-cells may simply boost endogenous levels of DA in the isolated spinal cord (Komori, Fujii, Karasawa, & Yamada, 1991), even if by just a few micromoles, which may contribute to the activation of the CPG. However, if this were the case, then one would expect some effect of D_2 – like antagonist L-741, 626 on the 5-HT, NMA-evoked rhythm given that DA binds with highest affinity to the D_3 member of the D_2 – like family of receptors (Freedman et al., 1994; Sautel et al., 1995; Sokoloff et al., 1992). Secondly, D-cells produce trace amines which are structurally related to amine transmitters such DA and NA(Burchett & Hicks, 2006). Because of their structural similarities, the presence of trace amines may serve as substitute or false neurotransmitters in central DA and NA systems (Baldessarini & Fischer, 1978; Berry, 2004; Fischer & Baldessarini, 1971; Kopin, Fischer, Musacchio, & Horst, 1964). That said, D-cell expression in the rat spinal cord was found to be

highest in the cervical region, and much more sparse in the thoracolumbar region where the CPG circuits that I studied reside (Jaeger et al., 1983). Therefore, it is questionable that the endogenous concentration of trace amines, at least those produced by D-cells, would be high enough to modulate or activate DA receptors or CPG activity in the isolated spinal cord preparation. These caveats are interesting in their own right, and deserve future studies for further elucidation.

The role for 5-HT activation of spinal circuits has been well documented in several species (Manira, Pombal, & Grillner, 1997; Nishimaru, Takizawa, & Kudo, 2000; Noga, Kettler, & Jordan, 1988; Schmidt & Jordan, 2000; Steeves & Jordan, 1980). Indeed, 5-HT fibers and receptors are present at birth in the mouse (Ballion, Branchereau, Chapron, & Viala, 2002) and the release of endogenous 5-HT has been demonstrated to modulate fictive locomotion (Dunbar et al., 2010). Several lines of evidence suggest that the early presence of 5-HT in the spinal cord contributes to the maturation of spinal CPG circuits (Cazalets, Gardette, & Hilaire, 2000; Nakajima, Matsuyama, & Mori, 1998; Schmidt & Jordan, 2000). If this were true, then it is possible that by cross-activating DA receptors, in addition to 5-HT's own native receptors, that the 5-HTergic system reinforces the maturation of CPG networks through multiple avenues. In future studies, it will be important to test the signaling mechanisms underlying the possible cross-reaction between 5-HT and DA receptors at the cellular level.

Chapter Four: Dopaminergic modulation of ventral root-evoked locomotor-like activity

4.1 INTRODUCTION

Critical for the expression and control of locomotion is the release of monoamines onto spinal cord networks (Miles & Sillar, 2011). A great deal of insight regarding the rhythmogenic and modulatory capabilities of monoamines has been generated experimentally by bath application of drugs to neonatal *in vitro* spinal cord preparations (Jiang et al., 1999; Kiehn & Kjaerulff, 1996; Whelan et al., 2000). My previous work (Chapter 3) and that of others has emphasized a role for DA in modulating on-going drug-evoked locomotor rhythms (Barriere et al., 2004; Jiang et al., 1999; Schotland et al., 1995; Whelan et al., 2000). Although drug-evoked locomotion has proven advantageous when studying monoaminergic modulation because it elicits sustainable long lasting rhythms making it easy to dissect out changes in the rhythm over time (Jiang et al., 1999; Whelan et al., 2000), there are caveats to using this approach. For example, the interpretation of the precise modulatory capabilities of drugs such as DA becomes complicated by the fact that additional monoamines are used to elicit the rhythm. Another caveat related to the use of externally applied drugs to activate CPG networks is the possibility of activating extrasynaptic receptors not normally recruited *in vivo*. Therefore, in order to further our understanding regarding the DAergic modulation of drug-evoked locomotor rhythms, it is important to contrast these findings with other distinct modes of CPG activation.

In an attempt to avoid excessive pharmacology to produce a baseline locomotor rhythm, several studies have employed the use of electrical simulation of sacral-caudal afferents *in vitro* to readily evoke rhythmic locomotor-like activity in the neonatal mouse and rat preparations (Delvolvé, Gabbay, & Lev-Tov, 2001; Gordon & Whelan, 2006b; Strauss & Lev-Tov, 2003; Whelan et al., 2000). This pathway consists of both low and high threshold afferents that convey

proprioceptive, cutaneous, and nociceptive information to the spinal cord. Additionally, we know that afferent pathways have access to the CPG network (Mandadi et al., 2009). One advantage of electrically stimulating the sacral afferents is that the circuitry necessary for producing locomotion is contained entirely within the spinal cord (Strauss & Lev-Tov, 2003). Additionally, because descending projections are cut, it is unlikely that there is any monoaminergic modulation of this self-contained circuit. Interestingly, under these conditions when DA was applied alone, the electrically-evoked locomotor rhythm was abolished (Gordon & Whelan, 2006b) which is opposite to what I see during drug-evoked rhythms (Chapter 3). This finding suggests that DA's actions on the CPG network are more complex than originally thought, and appear to be dependent upon the mode of activation.

Evidence over the last decade suggests that antidromic stimulation of recurrent collaterals from motoneurons cause excitatory activation of motor networks and can elicit locomotion (Machacek & Hochman, 2006; Mentis et al., 2005; O'Donovan et al., 2010) likely independently of the Renshaw circuit (Bonnot et al., 2009; Delpy, Allain, & Meyrand, 2008). While the function of this pathway is not fully understood, one possibility is that it could act to reinforce ongoing network activity. The gain of recurrent positive feedback circuits needs to be carefully controlled (Douglas, Koch, Mahowald, Martin, & Suarez, 1995; Staley, Longacher, Bains, & Yee, 1998). While postsynaptic GABAergic and glycinergic mechanisms control the gain of the Renshaw pathway, less is known about the recurrent excitatory pathway. Machacek and colleagues (2006) showed that NA could promote excitability in a recurrent excitatory pathway. Interestingly, 5-HT appeared to inhibit activity of this excitatory pathway.

Our lab's previous work in the lumbar slice preparation demonstrated an excitatory effect of DA on motoneuronal spike rates that are due to changes in intrinsic neuronal properties and

increased glutamatergic synaptic transmission (Han et al., 2007; Han & Whelan, 2009). Overall, my data (Chapter 3), and that of others, has established that DA exerts a net excitatory effect on neurons within the ventral spinal cord (Barriere et al., 2004; Jiang et al., 1999; Schotland et al., 1995; Whelan et al., 2000). In my current work, I add to the previous findings (Gordon & Whelan, 2006b) that DA exerts more complex neuromodulatory effects on rhythmic activity that are dependent upon the mode of evoking CPG activity. I examine the effects of DA on the modulation of ventral root-evoked locomotor activity, and establish that DA attenuates this activity. My data suggest that DA inhibits an excitatory recurrent circuit via a D_2 – mediated signaling pathway. Interestingly, this work contrasts my data demonstrating that DA potentiates locomotor-like activity by boosting the amplitude of 5-HT, NMA-evoked bursts and by decreasing rhythm frequency (Chapter 3). Collectively, these data suggest that DA exerts complex activation-dependent modulation of locomotor networks and acts to decrease the gain of the recurrent excitatory pathway.

4.2 RESULTS

4.2.1 DA modulation of ventral root-evoked locomotor-like activity

In the neonatal rodent, antidromic stimulation of motoneuron axons can trigger alternating rhythmic activity via non-Renshaw cell pathways (Mentis et al., 2005). Therefore, I made use of this approach to test the modulatory role of DA on recurrent pathway-elicited rhythmic activity.

4.2.1.1 Establishment of ventral root-evoked locomotor-like activity

I was able to evoke rhythmic activity recorded with extracellular suction electrodes from segmental L2 and contralateral L5 ventral roots of the isolated neonatal mouse spinal cord, by applying a brief train of stimuli (4Hz, 5-10 μA, 10s) to either the L5 or L6 ventral root (Bonnot et al., 2009; Mentis et al., 2005). First, I established a regular rhythm (Fig 4.1Bi – Bii; n = 16). Stimulation of the L5/L6 ventral roots evoked a slow tonic depolarization of electrotonic potentials that was potentiated with each successive stimuli of the stimulus train (Fig 4.1Bi). The evoked rhythmic bursts coincided with the onset of the stimulus train, although one or two cycles and a tonic discharge usually outlasted the stimulus train. Similar to other reports (Bonnot et al., 2009), I found that evoking a rhythm using ventral root stimulation was much less reliable than using other approaches such as dorsal root stimulation or pharmacological activation (Whelan et al., 2000). In my hands, ventral root stimulation produced rhythmic activity in ~25% of preparations. The mean frequency of the rhythm was 1.51 ± 0.17 Hz (mean ± SD) with a phase of 162° and a vector length of 0.80 (n = 16; Rayleigh's test, $P < 0.001$; Fig 4.1Biii). Of the preparations that produced bouts of rhythmicity, 7 of 16 produced coordinated (segmental L2 and L2–L5 locomotor activity) (Fig 4.1Bi – Bii), whereas the remaining 9 preparations produced

segmental L2 alternation with little or no L5 bursting. Because of this I focused on analysis of segmental L2 alternating activity.

4.2.1.2 Addition of DA abolishes a ventral root-evoked locomotor-like rhythm

In my first set of experiments, I bath applied 50 μM DA and found that the ventral root-evoked rhythmic activity was abolished in all preparations (n = 5; Fig 4.2A). In Figure 4.2C I have produced a representative set of spectrograms illustrating ventral root-evoked rhythmic activity before and following the addition of DA. The inhibition of the ventral root-evoked response is not likely due to hyperpolarization of the motoneurons, since DA increased the tonic discharge of the L2 neurograms (Fig 4.2Aii). Also, previous work has shown that 50 μM DA has a net depolarizing effect on motoneurons (Han et al., 2007). Washing with 500–700 ml of regular aCSF restored the power and frequency of ventral root-evoked rhythmic activity and slow depolarization of the electrotonic potentials to control levels (Fig 4.2Aiii and D).

4.2.1.3 Addition of DA abolishes a locomotor-like rhythm induced by stimulation of the sciatic nerve

To confirm that these DAergic effects could be replicated following stimulation of a peripheral nerve vs. a ventral root, I applied a stimulus to a portion of exposed sciatic nerve where the ventral roots were left intact but the dorsal roots were cut (Fig 4.3A; n = 3). Stimulation of the sciatic nerve (5 pulses, 4 Hz, 50–100 μA) resulted in rhythmic bursting from the recorded neurograms (3/3 preparations; Fig 4.3B). After bath application of DA, sciatic nerve stimulation could not produce any detectable rhythmic bursting (3/3 preparations; Fig 4.3Bii). Consistent with the effect of DA on ventral root-evoked bursting, I observed an increase in tonic discharge

in ventral root neurograms (compare Fig 4.3Bi with 4.3Bii). In a separate set of control experiments I cut the ventral roots after eliciting a depolarizing burst and, as expected, the depolarizing response was abolished (2 preparations; data not shown).

4.2.1.4 Addition of DA abolishes long-latency depolarizing events

It was found that a train of pulses applied to the ventral root could elicit long latency depolarizing events with an average latency to peak of ~143 ms (Bonnot et al., 2009). The emergence of these slow long-latency responses was found to be highly correlated with the ability of ventral root stimulation to elicit locomotion (Bonnot et al., 2009). Taking this into consideration, I placed a stimulating electrode at the tip of the L5 ventral root and recorded long-latency depolarizing responses from the adjacent L6 ventral root, which were superimposed on a slow depolarization (Fig. 4.3Ci, 104 ± 26.74 ms, range: 71–175 ms, n = 3). In the presence of DA these slow long-latency responses were blocked (Fig 4.3Cii), consistent with my observation that DA abolished ventral root-evoked rhythmicity.

Taking these findings together (sections 4.2.1.3 and 4.2.1.4), the most parsimonious conclusion is that the inhibitory actions of DA during ventral root-evoked locomotion are on the recurrent collateral pathways, which have access to the CPG network. In the next set of experiments I sought to test whether the actions of DA were due to an inhibition of the excitatory recurrent collateral pathway.

4.2.2 Ventral root-evoked entrainment of burst activity in disinhibited cords

Stimulation of lumbar ventral roots with trains of pulses can entrain a purely excitatory rhythm, otherwise known as a disinhibited rhythm (Bonnot et al., 2009; Machacek & Hochman, 2006).

These reports provide evidence for the existence of an excitatory recurrent collateral pathway having access to the CPG network. Consequently, I tested whether the effects of DA during ventral root stimulation are mediated, at least in part, by inhibiting transmission of an excitatory recurrent collateral pathway onto the CPG network.

4.2.2.1 DA application disrupts ventral root entrainment of burst activity in disinhibited cords

After establishing a disinhibited rhythm by adding the glycine receptor antagonist strychnine (2 μM), $GABA_A$ antagonist picrotoxin (50 μM), and $GABA_B$ antagonist CGP (50 μM) to the isolated spinal cord (Mandadi et al., 2009), I measured the natural occuring frequency of rhythmic bursts to determine the optimal frequency for the stimulus trains. Once the entrainment frequency was determined, I then used this frequency to apply a 5-pulse, 4Hz stimulus (50–100 μA) to the L5 or L6 ventral root (Fig. 4.4A). As illustrated in Figure 4.4Bi, under control conditions, nearly all of the stimulus trains were able to entrain disinhibited bursting. However, when DA was added to the bath, the probability that each stimulus train successfully entrained the disinhibited rhythm and evoked a burst was significantly reduced (Fig. 4.4Bii, C, and Eii; n = 6; $P < 0.0001$). These data suggest that during DA application, stimulation of excitatory recurrent collateral pathways and subsequent transmission onto CPG networks is depressed.

4.2.3 Contribution of D_1/D_2 agonists to ventral root-evoked locomotion

I next examined which DA receptor families contribute to the inhibition of the presumed excitatory recurrent excitatory pathway. Given that Zhu and colleagues (2007) found a predominate expression of D_2 – like receptors within the ventral horn and motoneurons of the

mouse lumbar spinal cord, I hypothesized that activation of the D_2 – like receptor family was involved in the DAergic inhibition of ventral-root rhythmic activity.

4.2.3.1 D_2 – like agonist reproduced the effects of DA on ventral root-evoked rhythmic activity

After establishing a consistent ventral root-evoked rhythm, I bath applied either a D_1 or D_2 – like agonist in separate experiments to isolate which DA receptor family contributed to the DAergic inhibition of ventral root-evoked rhythmic activity (Fig 4.5). After bath application of the D_1 – like agonist SKF-81297 (20 μM), no observable changes in the normalized power or frequency of the ventral root-evoked rhythm were observed (Fig 4.5A – D; n = 5). However, upon application of the D_2 – like agonist quinpirole (20 μM), the ventral root-evoked rhythm was significantly depressed in all experiments (Fig 4.5E – H; n = 5). Specifically, I observed a 69% decrease in normalized power, suggesting that activation of the D_2 – like family most likely underlies the effects seen during DA application. Wash with 800 ml of regular aCSF was unable to completely restore rhythmic activity to control levels.

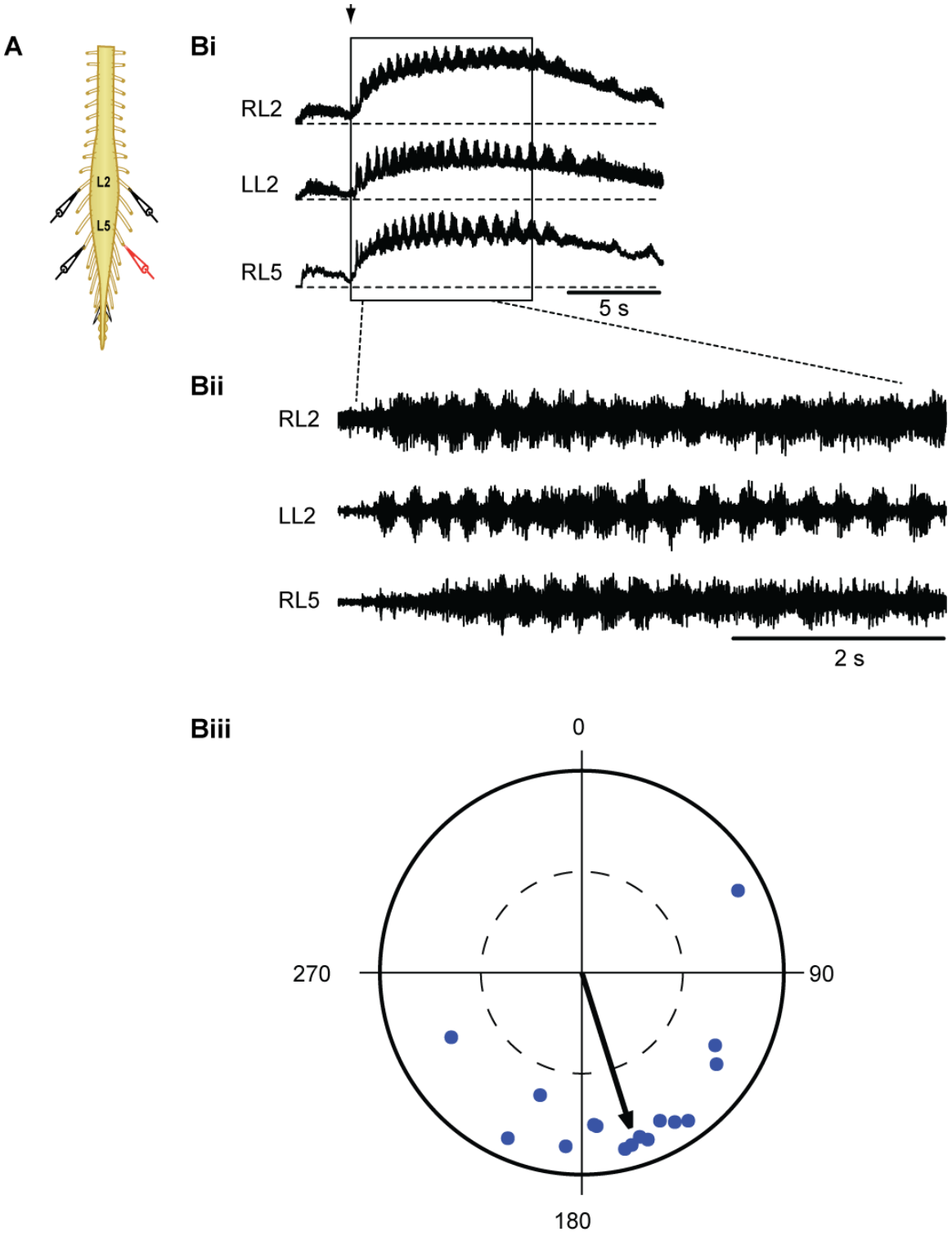
A
L2
L5
Bi
RL2
LL2
RL5
5 s
Bii
RL2
LL2
RL5
2 s
Biii
0
270
90
180

Fig. 4.1 Schematic diagram of the isolated spinal cord preparation

A: Schematic diagram of the isolated spinal cord preparation. Recording [black electrodes; segmental right (RL2) and left L2 (LL2) and left L5 (LL5) ventral roots] and stimulation sites (red electrode). Stimulation trains were applied to the L5 ventral root (4 Hz, 5–10 μA, 10 s; n = 5) once every 3 min. B: neurograms illustrating a locomotor-like sequence following stimulation of the L5 ventral root. Neurogram recordings (Bi) were filtered using a low-pass filter (DC; 1 kHz) to illustrate slow depolarization (arrow represents the start of stimulation) and are expanded (Bii) (100 Hz–1 kHz) to focus on rhythmic bursting. Circular plot summarizes results from several experiments (Biii; n = 15). Each dot represents a single experiment with associated phase and vector length. Arrow represents the mean phase and vector length. Phase is represented in degrees (0–360°).

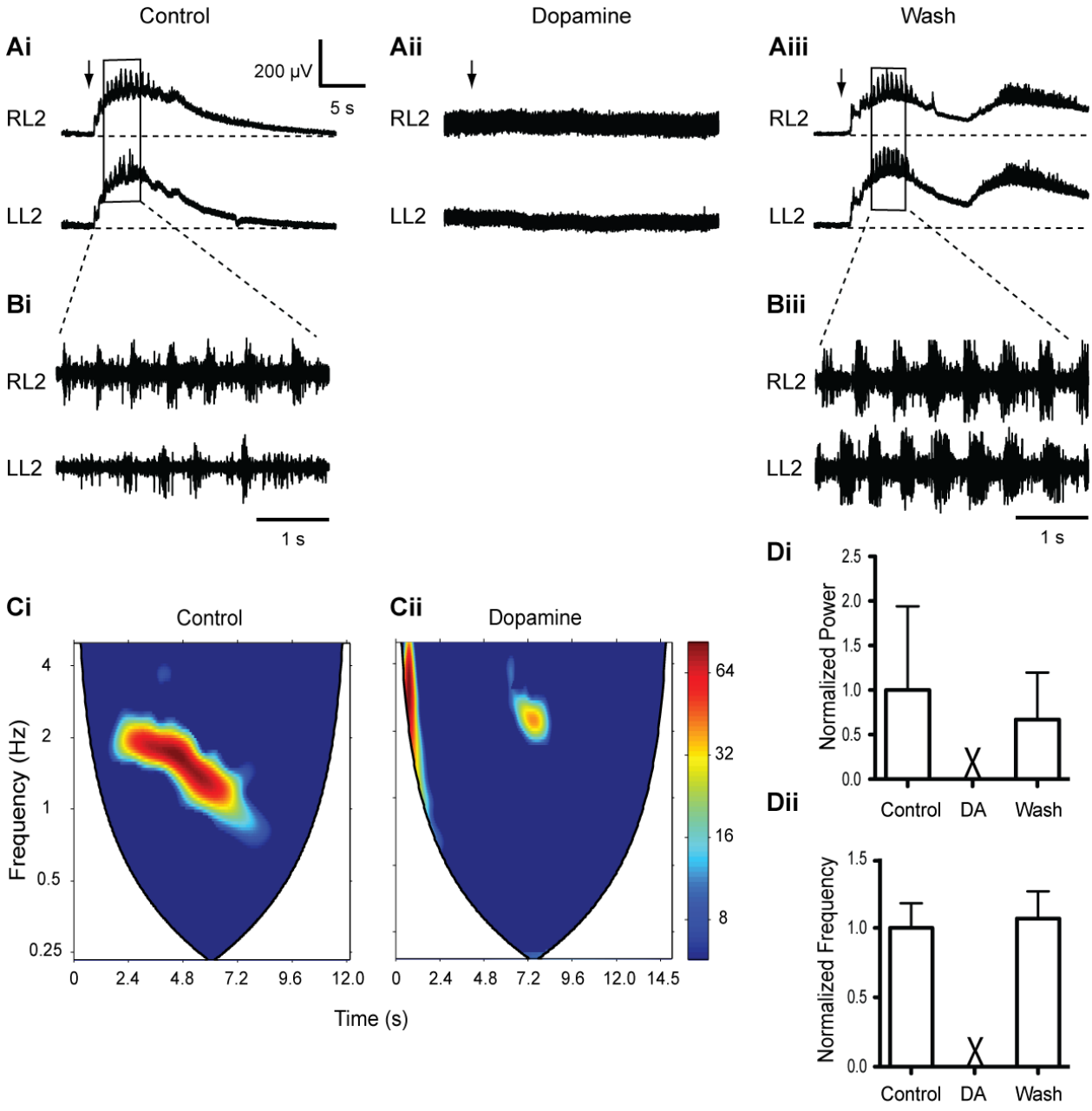
Control
Dopamine
Wash
Ai
Aii
Aiii
200 µV
5 s
RL2
LL2
Bi
Biii
1 s
Ci
Cii
Frequency (Hz)
Time (s)
Di
Dii
Normalized Power
Normalized Frequency
Control
DA
Wash

Figure 4.2. Activation of rhythmic activity by stimulation of ventral roots is abolished by application of DA.

A: DC recordings from RL2 and LL2 ventral roots under control conditions (Ai), addition of DA (Aii), and wash with 500 ml of regular aCSF (Aiii) following stimulation of the L5 ventral root (n = 5). B: alternating activity between the left and right sides under control (Bi) and wash conditions (Bii) is highlighted by expansion of the boxed areas in A. Traces were band-pass filtered (100 Hz–1 kHz). C: cross-wavelet spectrograms of segmental L2 neurogram recordings during ventral root-evoked rhythmic activity under control (Ci) and DA (50 μM) conditions (Cii). Power in the cross-wavelet spectra is shown in a color-coded logarithmic scale at right (see Methods Chapter 2) Note: spectrogram time scales vary depending on the length of a rhythmic bout. High-power regions were abolished with the addition of DA compared with control. D: graphs illustrating normalized power (Di) and normalized frequency (Dii). Error bars represent SD. Note: there are no bars associated with DA application because no rhythmic activity was evoked.

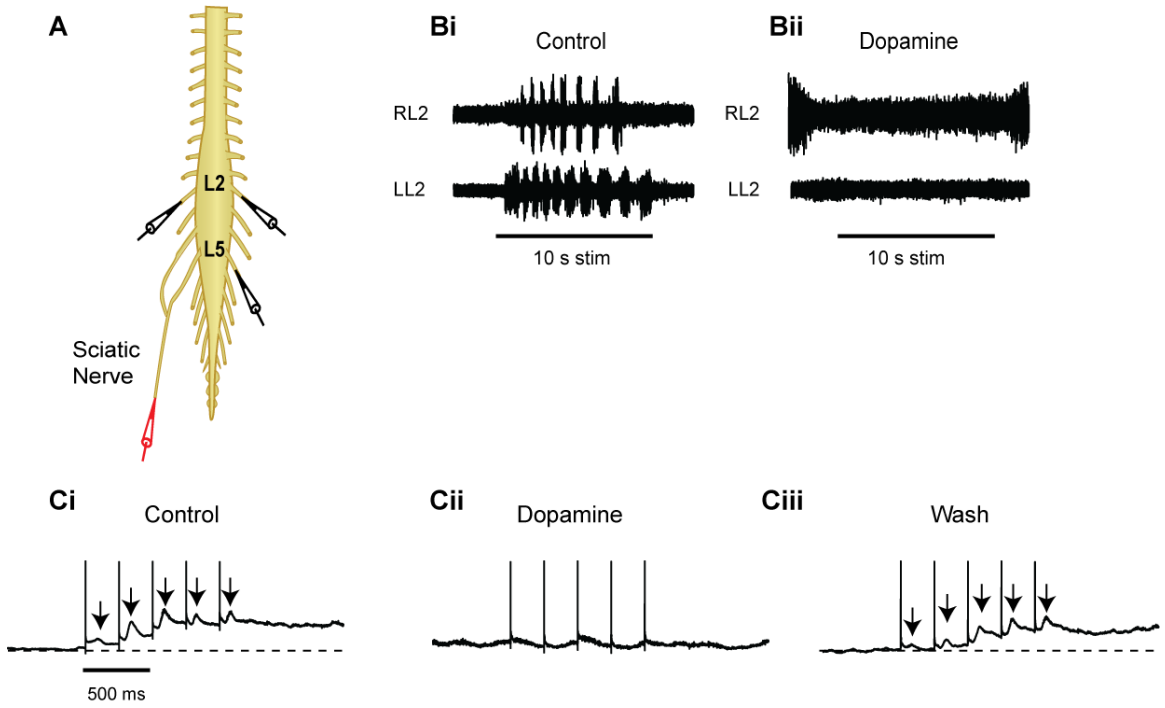
A
L2
L5
Sciatic
Nerve
Bi
Control
RL2
LL2
10 s stim
Bii
Dopamine
RL2
LL2
10 s stim
Ci
Control
500 ms
Cii
Dopamine
Ciii
Wash

Figure 4.3: DAergic modulation extends to peripheral nerve stimulation and inhibits long-latency depolarizations.

A: schematic of the isolated spinal cord preparation with the cut sciatic nerve dissected free. B: stimulation of the sciatic nerve (4Hz, 10s, dorsal roots cut) evoked rhythmic bursts of activity under control conditions (Bi) but not when DA was bath applied (Bii). C: average of 5 DC recordings of the right L6 ventral root during a 4Hz stimulus train (5 stimuli, 50–100 μA; n = 3) applied to the right L5 ventral root under control and DA conditions and following wash. Under control conditions, each stimulus of the stimulus train evoked a slow long latency depolarizing potential (indicated by arrows) that were superimposed on a tonic depolarization (Ci). In the presence of DA, the ability of each stimulus to evoke slow long-latency potentials was abolished (Cii). Washout restored the long-latency potentials (Ciii).

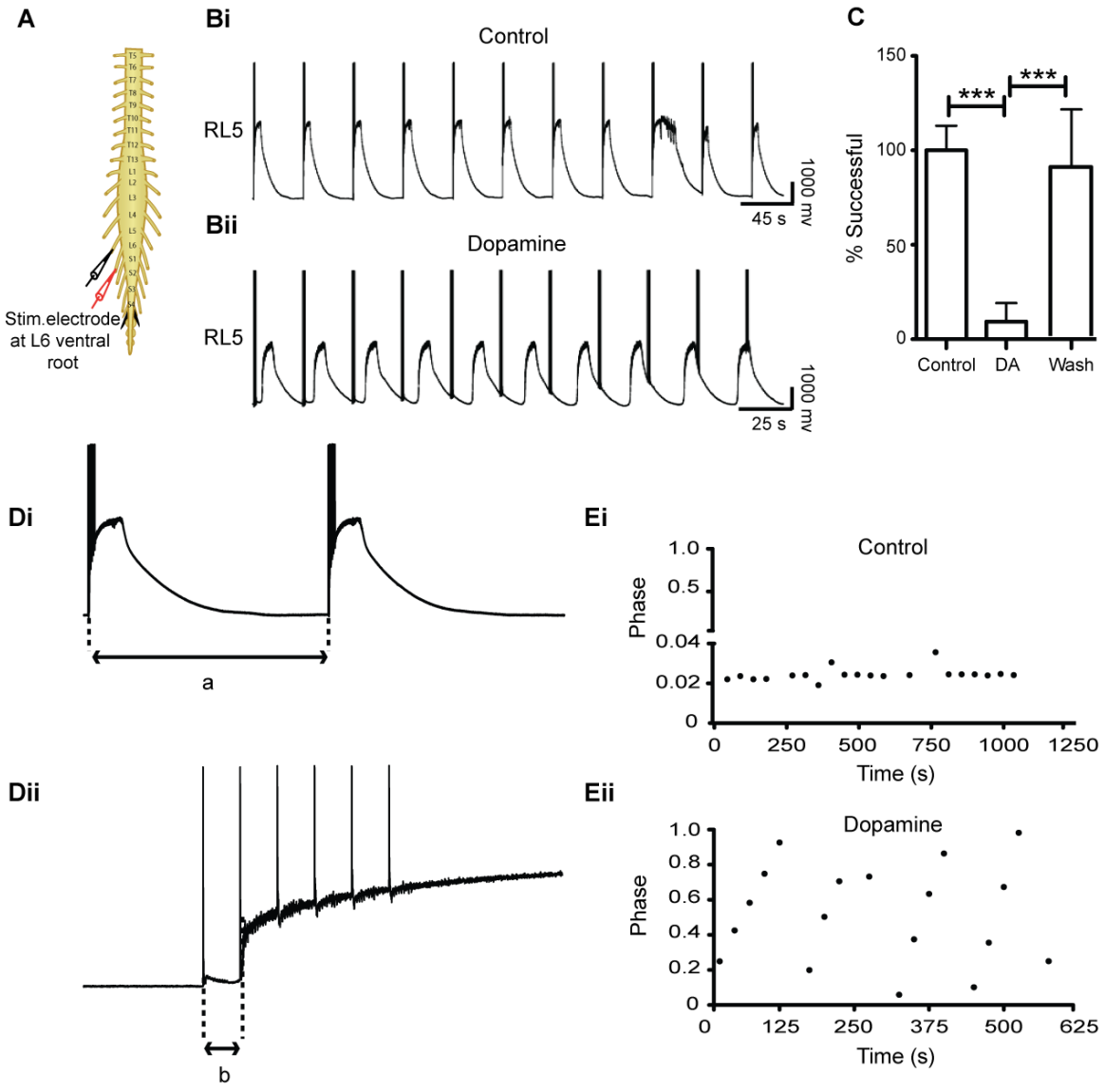
A
Bi
Control
RL5
1000 mv
45 s
Bii
Dopamine
RL5
1000 mv
25 s
Stim.electrode
at L6 ventral
root
C
150
100
50
0
% Successful
***
***
Control
DA
Wash
Di
a
Dii
b
Ei
Control
Phase
1.0
0.5
0.04
0.02
0
0
250
500
750
1000
1250
Time (s)
Eii
Dopamine
Phase
1.0
0.8
0.6
0.4
0.2
0
0
125
250
375
500
625
Time (s)

Figure 4.4: The probability of ventral root-evoked entrainment of disinhibited cords decreases in the presence of DA.

A: schematic diagram of an isolated spinal cord preparation illustrating stimulation (L6 ventral root; red) and recording sites (adjacent L5 ventral root; black) B: comparison in which stimulation of the L6 ventral root (5 pulses, 4 Hz, 50–100 μA) was able to entrain disinhibited rhythmic bursting under control (Bi) but not DA conditions (Bii). C: graph illustrating the percentage of ventral root stimulation-evoked bursts in the presence of strychnine, picrotoxin, and CGP-35348 vs. the percentage of evoked bursts following the addition of DA (1-way repeated-measures ANOVA, ***P < 0.0001; n = 6). Error bars represent SD. D: illustration depicting parameters measured to obtain phase value: a, cycle period of entrainment stimulus train delivered to the L6 ventral root (Di); b, time to burst onset of adjacent L5 ventral root relative to the beginning of the stimulus train (Dii). E: graph illustrates a disinhibited rhythm entrained by ventral root stimulation. Illustrated are plots of phase (b/a) vs. time (1 representative experiment) depicting 2 sequences of rhythmic activity taken before and after application of DA. The endogenous frequency of the disinhibited rhythm was strongly entrained by delivering a stimulus train once every 45 s, indicated by the nearly constant phase value through the sequence (Ei). The endogenous frequency of the disinhibited rhythm increased in the presence of DA such that a stimulus train needed to be delivered once every 25 s (Eii). The progressive increase in phase indicates that in the presence of DA, the disinhibited rhythm was no longer entrained by ventral root stimulation.

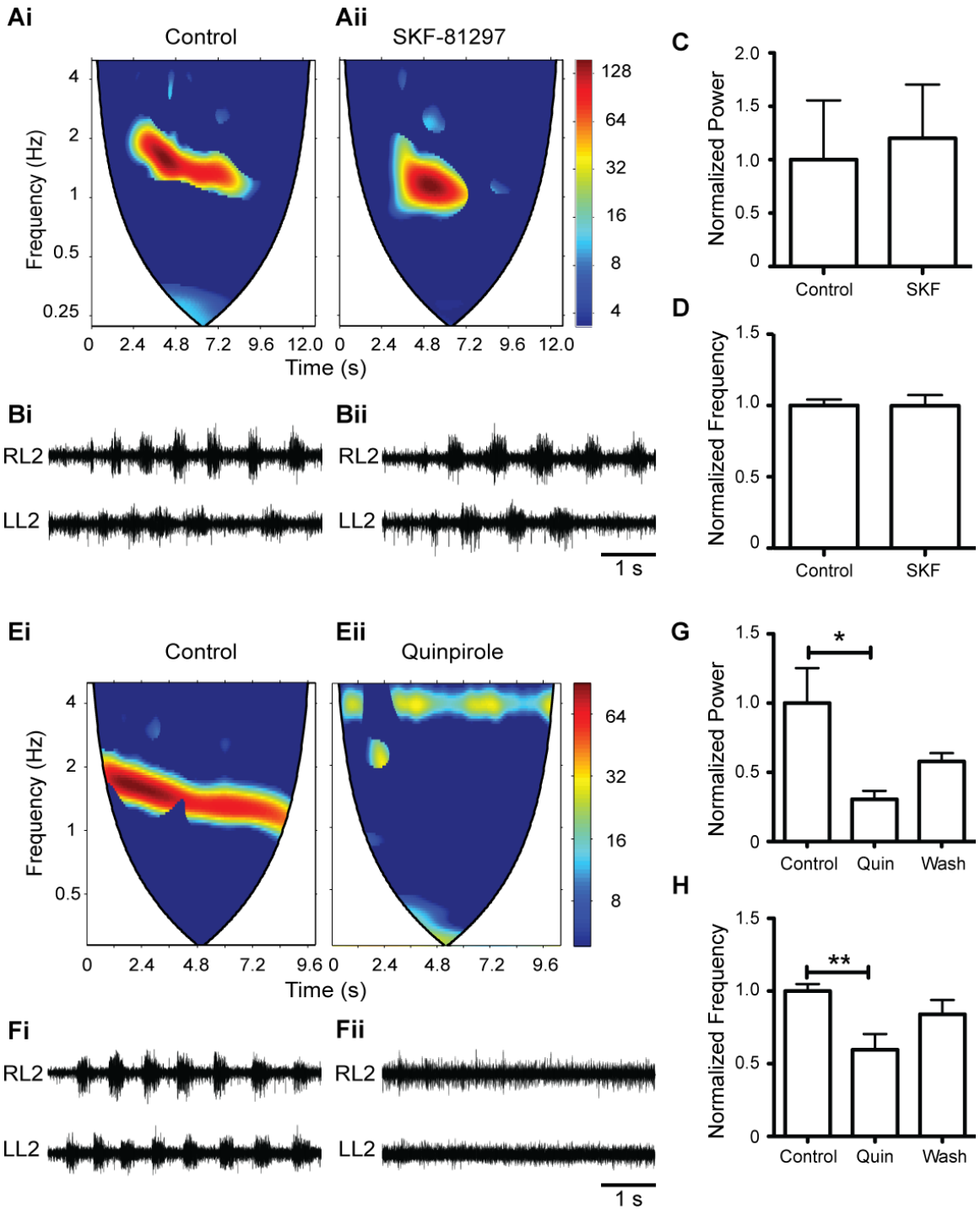
Ai
Control
Aii
SKF-81297
Frequency (Hz)
4
2
1
0.5
0.25
0
2.4
4.8
7.2
9.6
12.0
Time (s)
128
64
32
16
8
4
Bi
RL2
LL2
Bii
RL2
LL2
1 s
C
Normalized Power
2.0
1.5
1.0
0.5
0
Control
SKF
D
Normalized Frequency
1.5
1.0
0.5
0
Control
SKF
Ei
Control
Eii
Quinpirole
Frequency (Hz)
4
2
1
0.5
0
2.4
4.8
7.2
9.6
Time (s)
64
32
16
8
Fi
RL2
LL2
Fii
RL2
LL2
1 s
G
Normalized Power
*
1.5
1.0
0.5
0
Control
Quin
Wash
H
Normalized Frequency
**
1.5
1.0
0.5
0
Control
Quin
Wash

Figure 4.5: Application of D_2 – like receptor agonist depresses ventral root-evoked rhythmic activity, whereas D_1 – like receptor agonist does not.

A: cross-wavelet spectrograms of segmental L2 neurogram recordings under control conditions (Ai) and with the addition of D_1 – like receptor agonist SKF-81297 (20 μM; Aii). B: raw traces of L2 neurogram recordings under control conditions (Bi) or addition of SKF-81297 (Bii) (same experiment as A). C and D: graphs show normalized power (C) and normalized frequency (D) under control and SKF-81297 conditions ($P < 0.05$, paired t-test; $n = 9$). Error bars represent SD. E: cross-wavelet spectrograms of segmental L2 neurogram data under control conditions (Ei) and with the addition of D_2 – like receptor agonist quinpirole (20 μM; Eii). F: raw traces of L2 neurogram recordings under control conditions (Fi) and following bath application of quinpirole (Fii) (same experiment as E). G and H: graphs show normalized power (G) and normalized frequency (H) under control and quinpirole conditions ($P < 0.05$, 1-way repeated-measures ANOVA; $n = 5$). Error bars represent SD. Note: in 3/5 experiments, rhythmic activity persisted in the presence of quinpirole; however, activity was depressed from control levels. Therefore, we report the normalized power and normalized frequency scores for these experiments in G and H. All raw traces depicted illustrate the first 5 s of a 10-s stimulus train.

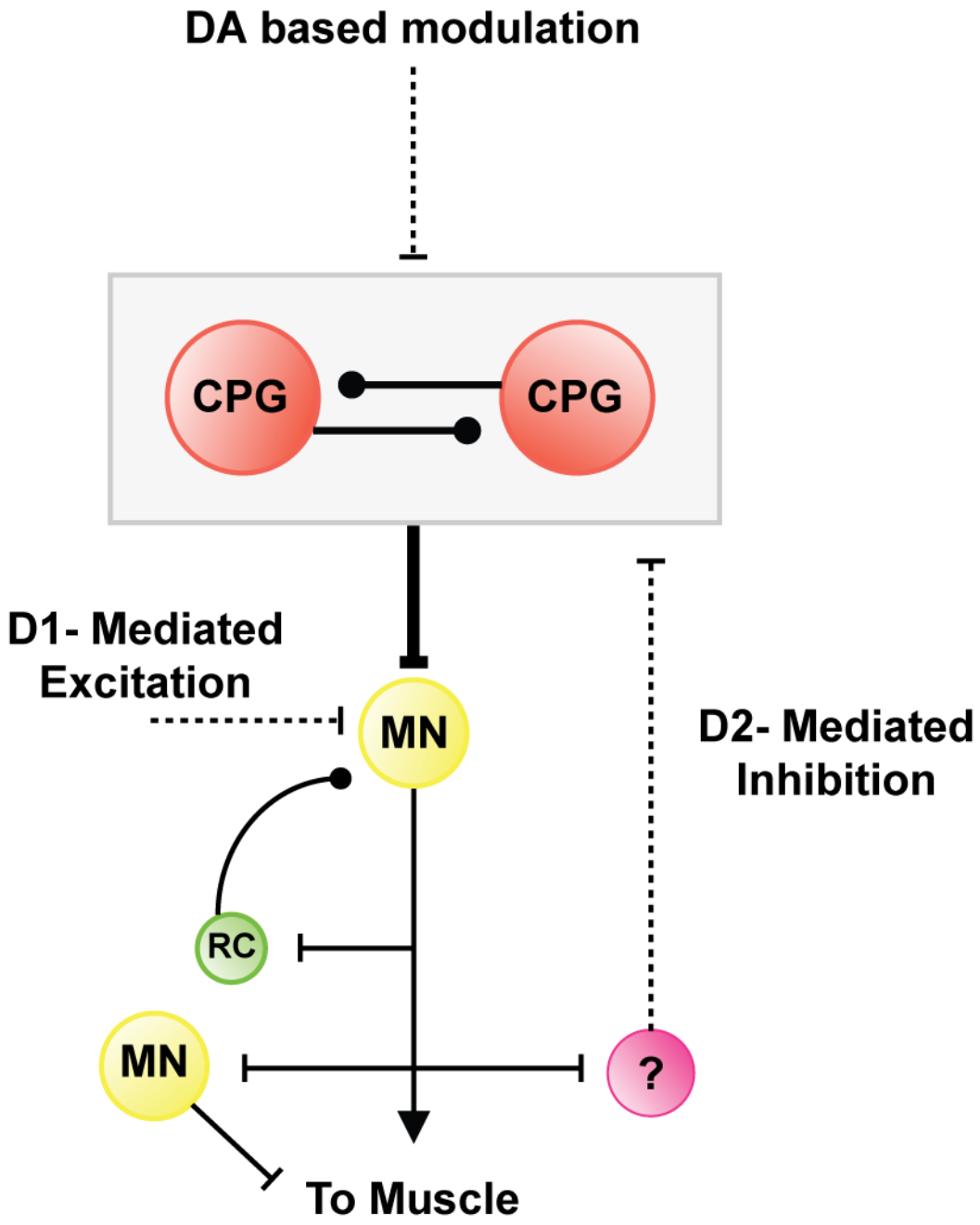
DA based modulation
CPG
CPG
D1- Mediated
Excitation
MN
D2- Mediated
Inhibition
RC
MN
?
To Muscle

Figure 4.6: DA exerts activation dependent modulation over locomotor CPG networks.

Taking together my previous findings (Chapter 3) with the current work, my results suggest that pharmacological activation of CPG networks is facilitated by DA by increasing the amplitude of the bursts and the stability of the rhythm. In addition, my work suggests that activation of CPG networks by excitatory recurrent collateral pathways is inhibited by a D_2 – like receptor-mediated pathway. Excitatory and inhibitory synaptic connections are shown by lines and small circles, respectively. Dashed lines represent putative sites of DA modulation. The question mark represents an unidentified excitatory interneuron that receives excitatory drive from recurrent motor axon collaterals. MN, motoneuron; RC, Renshaw cell.

4.3 DISCUSSION

4.3.1 General remarks

The current results, together with my previous work (Chapter 3), suggest that DA exerts activation specific modulation of spinal cord CPG output. My data suggest that DA, via a D_2 based signaling system, blocks a recurrent excitatory pathway that likely projects onto the CPG. On the other hand, when the CPG is already active by way of 5-HT, NMA drug application, DA promotes a more regular rhythm and increases burst amplitude (Chapter 3; see Figure 4.6 for summary diagram).

4.3.2 Control of recurrent excitatory feedback by DA

Several studies illustrate that stimulation of recurrent collaterals from motoneurons can elicit network activity (Bonnot et al., 2009; Hanson & Landmesser, 2003; Mentis et al., 2005; Wenner & O'Donovan, 1999). Our work shows that DA inhibits locomotor activity evoked from presumed recurrent collaterals. Several lines of evidence support this conclusion. First, I found that DA reversibly abolished long-latency potentials evoked following ventral root stimulation. Bonnot and colleagues (2009) found that ventral root stimulation evoked similar slow long latency potentials, likely through a polysynaptic pathway, and that the presence of the potentials correlated highly with the ability to elicit locomotion. DAergic inhibition of these long-latency potentials is not locomotor dependent, suggesting that the pathway may lie outside the CPG itself. Second, when fast inhibitory transmission was blocked, DA reduced entrainment of the disinhibited rhythm by ventral root stimulation. This suggests that DA is acting on an excitatory pathway that can access the CPG and rules out a role for Renshaw cells under these conditions.

My data does not exclude a role for Renshaw cells when inhibitory blockers are absent. DA could disinhibit GABA/glycinergic projections onto Renshaw cells allowing them to inhibit motoneuronal drive. Indeed, it has been demonstrated that Renshaw cells normally receive inhibitory drive during the active portion of L2 rhythmic bursting in the neonatal mouse (Nishimaru et al., 2006). However, there is no data suggesting selective depression by DA of inhibitory pathways within the spinal cord, and evidence suggests that Renshaw cells receive both excitatory and inhibitory inputs during locomotor activity (Nishimaru et al., 2006).

A possible need for the regulation of the excitatory pathway may stem from the fact that DA and other monoamines increase the input-output ratio of motoneurons (Han et al., 2007; Rekling et al., 2000). For example DA boosts the spike output of motoneurons by increasing excitatory glutamatergic transmission, decreasing I_A, and decreasing the SK_{ca} based conductances in neonatal mice (Han et al., 2007; Han & Whelan, 2009). The net increase in motoneuron spike output following DA administration could explain the need to decrease the gain of the recurrent excitatory pathway. In other areas of the brain where recurrent positive feedback exists, such as the CA3 region of the hippocampus (Bains, Longacher, & Staley, 1999) or neurons in the cortex (Douglas et al., 1995), gain is regulated to ensure that the dynamic firing range of neurons is maintained.

My work shows that the DAergic inhibition of the recurrent excitatory pathway is at least partly mediated by D_2 - like receptor mechanisms. This concurs with evidence showing expression of D_2 – like receptors within the ventral and dorsal horns of the mouse spinal cord (Zhu et al., 2007). My work has not identified the downstream D_2-mediated signaling mechanism but one possibility is the metabotropic glutamate (mGluR) 1 class of receptors which have been shown to contribute to the excitatory ventral root activation of locomotor networks (O'Donovan

et al., 2010). Evidence suggesting this as a possibility comes from the basal ganglia where mGluR activity is closely regulated by D_1 and D_2 receptors (Conn, Battaglia, Marino, & Nicoletti, 2005). The depressive effects on recurrent excitatory pathways using D_2 agonists are consistent with the effects of D_2 actions in other systems within the spinal cord (Gordon & Whelan, 2006b; Millan, 2002; Whelan et al., 2000). Recent work by Clemens et al., (2012) has found a concentration dependent effect of DA on spinal circuits in *Xenopus* embryos. Specifically they demonstrated that low doses of DA preferentially activated D_2-like receptors due to the higher binding affinity of DA to the D_2 receptors (Clemens et al., 2012). Higher doses then activated the D_1-like system producing an excitatory effect on CPG function and overcoming the D_2 inhibitory effects (Clemens et al., 2012). However, in the excitatory recurrent pathway, it appears that it is a primarily D_2 based signaling pathway and the D_1 system has a minor role to play in modulating the rhythm.

Ventral root afferents in mouse have been found to contain C fibers (Biscoe, Nickels, & Stirling, 1982), but their functional role and connectivity within the spinal cord remains ambiguous (Hildebrand, Karlsson, & Risling, 1997). While they appear to be present in the ventral roots, it is not clear where they enter the cord, and evidence suggests that few if any fibers are observed at the peripheral nervous system/CNS border (Hildebrand et al., 1997). Another possibility for ventral root bursting discussed by O'Donovan and colleagues is that the ventral root stimulation may elevate extracellular K^+ concentrations in the ventral horn (Bonnot et al., 2009; Marchetti, Beato, & Nistri, 2001). In this scenario, D_2 agonists would inhibit network interneurons, countering the effects of increases in extracellular K^+ in promoting bursting. However the kainate/AMPA blocker NBQX could block ventral root-evoked activation of the network, while permitting dorsal root-evoked rhythmic activity, suggesting that the

network itself was not in a dormant state (Bonnot et al., 2009). Similarly, in the same report it was found that mGluR1 antagonists could depress the rhythm. Thus, the most parsimonious hypothesis is that the observed excitatory responses are caused by recurrent collaterals projecting via interposed interneurons onto the CPG.

4.3.3 Relation to actions of other monoamines

It is interesting that a closely related catecholamine, NA, has different effects compared to DA (Machacek & Hochman, 2006). In contrast to the effects of NA (Machacek & Hochman, 2006), DA appears to decrease the gain of the recurrent excitatory pathway. In this regard, DA appears to share an inhibitory regulatory role with 5-HT (Machacek & Hochman, 2006). These data also suggest that the actions of DA are not likely due to conversion to NA and are also supported by the replication of DA's effects by D_1 and D_2 agonists. Differential effects of monoamines have been observed in many areas of the brain and spinal cord as well as invertebrate networks (Miles & Sillar, 2011). For example, NA and 5-HT were observed to mutually enhance group II afferent transmission but were also observed to act in an antagonistic fashion (Jankowska, Hammar, & Chojnicka, 2000). When one considers commissural interneurons, monoamines have been shown to have contrasting effects depending on the pathway being activated (Hammar, Bannatyne, Maxwell, Edgley, & Jankowska, 2004). For example 5-HT facilitated group II input onto these cells, but NA inhibited transmission. On the other hand both 5-HT and NA facilitated reticulospinal input onto commissural interneurons. 5-HT has been shown to have heterogeneous effects on mouse commissural interneurons depending on whether they descended or bifurcated after crossing the midline (Zhong, Díaz-Ríos, & Harris-Warrick, 2006).

4.3.4 Functional considerations

The modulatory effects of DA on motoneurons are biased towards increasing the input-output spike rates (Han et al., 2007; Han & Whelan, 2009). Overall this acts to robustly promote rhythmic motor output. A possible consequence is that the gain of the recurrent excitatory pathway from motoneurons onto rhythm generating populations of interneurons could increase to a point where the drive could lead to destabilization of the rhythmic pattern. However, it is important to emphasize that the functional effects of DA will likely differ depending on several variables, concentration at the synapse, intrinsic properties of the neurons, specific pathways, receptor distribution, and the state of the second messenger system (Clemens et al., 2012). Data from adult animals suggests that DA can potentiate stepping (Lapointe et al., 2009) which suggests conserved modulatory mechanisms during development. On the other hand the ventral root-evoked depolarizing responses in mice may represent a functionally immature excitatory circuit. Certainly we see evidence for differences in circuitry during development (Hanson & Landmesser, 2003; Mentis, Siembab, Zerda, O'Donovan, & Alvarez, 2006). These caveats, which are interesting in their own right, remain to be tested. The current work certainly provides evidence that DA can exert complex changes in spinal network function that are dependent on the mode of activation. A hypothesis for further investigation is whether DA can functionally depress excitatory recurrent collateral transmission onto ventral horn interneurons.

Chapter Five: Dopamine modulates postinhibitory rebound in motoneurons of the neonatal mouse

5.1 INTRODUCTION

The final behavioral output of any CPG network is the result of a combination of network properties together with the underlying synaptic interactions and inherent cellular properties of component CPG neurons (Calabrese, 1995; 1998; Harris-Warrick, 2010; Pirtle & Satterlie, 2007; Prinz, Bucher, & Marder, 2004). Therefore, when monoamines such as DA alter network output, one can hypothesize that the mechanistic basis of these actions occurs at network, synaptic, and cellular levels. Previous studies, including work published by our lab have demonstrated that DA can exert diverse and complex actions on locomotor rhythms (Gordon & Whelan, 2006b; Humphreys & Whelan, 2012; Kemnitz, 1997; Kemnitz et al., 1995; McPherson & Kemnitz, 1994; Schotland et al., 1995; Whelan et al., 2000). Specifically addressing drug-evoked locomotor rhythms, I found that DA can potentiate rhythmic activity. One possible target DA may be acting upon to promote rhythmicity is the cellular property of postinhibitory rebound (PIR), which is the depolarization that occurs at the offset of a hyperpolarizing event before the membrane potential returns to its initial value (Perez-Reyes, 2003). PIR contributes to the generation of stable rhythmic motor patterns (Angstadt & Friesen, 1993; Angstadt, Grassmann, Theriault, & Levasseur, 2005; Marder & Bucher, 2001; Merrywest, McDearmid, Kjaerulff, Kiehn, & Sillar, 2003; Peck, Nakanishi, Yaple, & Harris-Warrick, 2001; Wang et al., 2011).

To gain insight as to how one intrinsic membrane property, namely PIR, contributes to neuronal discharge during complex ongoing behaviors such as locomotion, it may be helpful to revisit the early work of Thomas Graham-Brown over a century ago (T. G. Brown, 1911). Brown proposed the “half-center” model of locomotor rhythm generation to account for how the CPG generates rhythmic alternating flexor-extensor activity. It is likely that PIR contributes to the generation of a stable, alternating burst pattern by promoting rebound bursting among the half-

center neurons that are experiencing inhibition, thereby ensuring alternation between reciprocally connected networks.

PIR has been well described in putative CPG interneurons and motoneurons, in both vertebrate and invertebrate locomotor systems (Angstadt et al., 2005; Angstadt & Friesen, 1993; Bertrand & Cazalets, 1998; Wang et al., 2011; Wilson et al., 2005). Key ionic contributions to the initiation of PIR are the HCN current (I_h), and the low-voltage activated calcium currents. I_h becomes activated at membrane potentials below -60 mV, and permits an influx of Na^+ and K^+ which depolarize the membrane potential toward threshold for firing action potentials (Robinson & Siegelbaum, 2003). I_T (Cav3) and I_L (L – Type Ca^{2+} channels, specifically the Cav1.3 isoform) grouped together can be called the low voltage activated (LVA) calcium channels because they become activated by small depolarizations in the membrane potential (Perez-Reyes, 2003). This can lead to the influx of calcium and the generation of low-threshold spikes, which can trigger bursts of action potentials. Interestingly, several cases have been published demonstrating that the PIR response, more specifically I_h and I_T , are prime candidates for monoaminergic modulation (Angstadt et al., 2005; Harris-Warrick et al., 1995; Merrywest et al., 2003; Wang et al., 2011).

In the mammal, most work regarding PIR has been focused at the level of the motoneurons (Bertrand & Cazalets, 1998; Harris-Warrick et al., 1995; Kjaerulff & Kiehn, 2001; Rekling et al., 2000). This may not be surprising given that the motoneurons are key in sculpting the final output of the CPG network and indeed more recently are being postulated to form part of the CPG itself (O'Donovan et al., 2010). Additionally, PIR may assume an important regulatory role over the contraction of skeletal muscle by contributing to the build up of tetanic contractile force in flexor and extensor motoneuron pools. In order for steady and sustained

muscle contractions, muscles must reach a tetanized state whereby motor units are stimulated at a sufficiently high frequency of action potentials. Inability to reach or sustain tetanus during contraction would result in very weak muscle contraction. Therefore, by providing a boost at the start of motoneuron activation, PIR would contribute to the twitch summation and ultimately contractile force.

Previous work published by our lab has demonstrated that pre-existing 5-HT, NMA-evoked locomotor rhythms convert into a much slower, more stabilized rhythm when in the presence of DA (Chapter 3; Fig 3.1). Specifically, the alternation between the left and right halves of the spinal cord, as well the alternation of flexor-extensor equivalent motoneuron pools became much more defined and rhythmic. However, the mechanisms underlying this stabilization are not yet clear. Given that we know monoamines can modulate PIR (Angstadt et al., 2005; Harris-Warrick et al., 1995; Merrywest et al., 2003; Wang et al., 2011), and that PIR plays a role in the burst discharge of motoneurons during fictive locomotion (Bertrand & Cazalets, 1998), I sought to investigate the mechanistic actions of DA by testing whether DA could modulate the PIR response at the motoneuronal level in the neonatal mouse. Utilizing the whole-cell patch clamp technique, I first examined the presence of PIR in putative motoneurons of the neonatal mouse. Next, I tested the effect of DA on the PIR response. Finally, I explored the ionic basis of the observed PIR response.

5.2 RESULTS

5.2.1 Presence of PIR in the neonatal mouse

As previously mentioned, PIR is an immediate depolarizing neuronal membrane response that occurs as a hyperpolarizing influence is being lifted, prior to the membrane potential returning to rest. In all experiments, two protocols were used to investigate the presence of PIR in putative motoneurons. First, the voltage dependency of PIR was tested by delivering a series of hyperpolarizing current steps (500 ms), of increasing amplitude (from -10 pA to -190 pA) at a constant holding potential of around -60 mV. This will be referred to as the "hyperpolarizing protocol" in subsequent text. Second, the time dependency of the hyperpolarizing current pulse was investigated by delivering a series of current steps of increasing duration (200 ms to 2100 ms). These current steps hyperpolarized cells between -77 mV and -95 mV, from a set holding potential of -65 mV. This will be referred to as the "duration protocol".

Motoneurons from neonatal mice (P1-P3) were identified based on morphological and electrophysiological parameters. I sought to record from ventrally located (lamina IX), large diameter cells (> 20 μm) (Fig 5.1Ai). To help confirm that I was indeed recording from motoneurons, in 2 experiments, targeted cells were back filled with Alexa 488 dye, the slices were preserved in paraformaldehyde (PFA) and mounted with Fluromound. Motoneurons were then identified with an Olympus BX51 microscope (Fig 5.1Aii). The electrophysiological criteria used to identify motoneurons were rheobase, input resistance, and repetitive firing capacity. Upon achieving whole cell current clamp configuration, the membrane potential was set to -60 mV by injecting a bias current, ranging from -102 pA to + 40 pA. Rheobase was defined as the injected current necessary to elicit the first action potential. The average rheobase current of 68.8 ± 10.8 pA (n = 11) while under control conditions was consistent with that of previous findings

published by our lab (Han et al., 2007). I also measured input resistance as an indication of motoneuron identity, which I found to be on average 378.1 ± 47.7 MΩ. This value is higher than what was previously published for neonatal mice (age P0-P3) (Han & Whelan, 2009; Nakanishi & Whelan, 2010), however given that motoneurons are a highly diversified heterogeneous population, I did not omit cells based on this criteria. Only cells that were considered unhealthy were excluded (see Methods section 2.1.3). Finally, I took into account the ability of the targeted cells to fire repetitively, which is a classic signature of motoneurons (Lee & Heckman, 2001; Miles, 2005; Rekling et al., 2000). In response to depolarizing current steps, all cells tested possessed the ability to repetitively fire with successive excitatory stimulation.

I recorded from a total of 25 putative motoneurons, 15 of which demonstrated a PIR response. Of the 10 cells that did not elicit a PIR response under control conditions, application of DA did not further unmask a PIR response. Therefore, these cells were not included for further analysis. Intrinsic property values (defined in Methods) were recorded from all cells (except those under the influence of TTX) including cells that did not exhibit a PIR response, (n = 17; Table 5.1). All experiments were performed in the presence of synaptic blockade.

5.2.1.1 Utilizing the hyperpolarizing protocol to explore the presence of PIR

Using the hyperpolarizing protocol, I observed 2 different PIR response phenotypes under control conditions (no DA). In 5 out of 8 cells, I observed the PIR reach spike threshold and evoke bursts of spikes in response to hyperpolarizing current steps (Fig 5.1Bi – BiiB). In the remaining 3 cells, I observed a subthreshold response (Fig 5.1Ci – CiiC), regardless of the amplitude of the hyperpolarizing stimulus. Although this rebound response did not reach Na^+ spike threshold, the amplitude of the PIR increased with increasing hyperpolarization.

5.2.1.2 Utilizing the duration protocol to explore the presence of PIR

While exploring the duration dependency of PIR, I observed that 4 out of 10 cells reached spiking under control conditions (data not shown). Three of the four cells that reached spiking threshold demonstrated burst firing capabilities under control conditions. The remaining one cell elicited a single spike upon release of the hyperpolarizing current pulse. Of the 6 cells that did not reach Na^+ spike threshold, the amplitude of the PIR response increased with increasing duration of the hyperpolarizing pre-pulse (Fig 5.1Di-Dii).Taken together, these findings indicate that the PIR response (subthreshold vs. suprathreshold) is varied among neonatal mouse motoneurons. Additionally, I found that the ability of the PIR response to reach Na^+ spike threshold was more dependent upon the voltage level, rather than duration, of the hyperpolarizing pre-pulse.

5.2.2 The modulatory effects of DA on the PIR response evoked using the hyperpolarization protocol

In the next set of experiments, I made use of the hyperpolarizing protocol to explore how (1) DA altered the PIR response in cells that reached threshold under control conditions and (2) how DA altered the PIR response in cells that did not reach threshold under control conditions. See Table 5.2 for the recorded intrinsic properties of cells under control and DA conditions.

5.2.2.1 DA increased the firing frequency of the PIR response

Recall that while under control conditions, I observed a PIR response that was strong enough to elicit spikes in 5 out of 8 cells, while applying the hyperpolarization protocol (5.2.1.1). To investigate the effects of DA application, I first measured the firing frequency evoked after the

release of a hyperpolarizing pre-pulse that forced the cell to approximately -100 mV. I calculated the firing frequency over the remainder of the recording sweep (Fig 5.2A; 4.4 sec; Fig 5.2A). Interestingly, I found that DA increased the firing frequency in 3 out of 5 cells by an average of 186 % ± 18% (Fig 5.2A-C). Of the remaining 2 cells, 1 cell experienced a 25% decrease, and 1 saw a 43% decrease in firing frequency when compared to control conditions. Previous work published by our lab demonstrated that DA could increase the firing frequency of motoneurons after a depolarizing current step (Han et al., 2007). My current work adds to this data, and suggests that DA also increases the firing frequency of motoneurons evoked after a hyperpolarizing current step in the majority of cells tested.

5.2.2.2 DA shifted the activation threshold for PIR in the depolarizing direction

To further quantify DA's effects on firing frequency, I took a measure of the first spike instantaneous frequency, which was defined as the reciprocal of the first interspike interval (Hz) (n = 4). Interestingly, when taking a closer look at the threshold voltage at which PIR firing commenced, I observed that DA application shifted the threshold of PIR activation in the depolarizing direction in 3 out of 4 cells (Fig 5.2C). In two of the 3 cells, DA pushed the activation for PIR threshold into a more physiological range (< 78 mV) (Engbers et al., 2011) and the third cell saw DA shift the threshold of PIR activation from -124 mV (control) to -94 mV (DA; 24% decrease). In the remaining cell, there was a 7 mV increase in the PIR threshold from -81 mV (control) to -88 mV (DA). Collectively, my results suggest that in the majority of cells, DA increases the firing frequency by shifting the threshold for PIR activation in the depolarizing direction.

5.2.2.3 DA converted one non-spiking cell into a spiking cell, and enhanced the PIR response in two non-spiking cells

Contrary to data published in the lamprey (Wang et al., 2011), the PIR response was increased by DA application in 3/3 cells that did not spike under control conditions while utilizing the hyperpolarizing protocol. In fact, 1 of the 3 non-spiking cells converted into a spiking cell in the presence of DA.

In the remaining 2 cells which maintained a subthreshold PIR response, DA increased the average peak PIR amplitude from 1.0 mV to 3.1 mV after a hyperpolarizing step forced the cells to the same voltage (approximately -103 mV; data not shown). Interestingly, unlike the cells which did reach Na^+ spike threshold while under control conditions (5.2.2.1; $n = 5$; Fig 5.2C), I observed that the onset of subthreshold PIR activity for these two cells occurred well within the physiological range under *both* control and DA conditions, (Engbers et al., 2011). The application of DA further shifted the activation of the subthreshold PIR activity in the depolarizing direction for both cells (Fig 5.2D). One cell saw a 16% decrease in threshold for PIR activation (-71 mV; control to -60 mV; DA) and the other cell saw a 4% decrease (-65 mV; control to -63 mV; DA). Collectively, this data demonstrates that DA enhanced the subthreshold PIR response elicited by the hyperpolarizing protocol.

5.2.3 The modulatory effects of DA on the PIR response evoked using the duration protocol

In the next set of experiments, I made use of the duration protocol to explore how (1) DA altered the PIR response in cells that reached threshold under control conditions and (2) how DA altered the PIR response in cells that did not reach threshold under control conditions.

5.2.3.1 DA increased the firing frequency

Under control conditions, I observed that 4 out of 10 cells exhibited a PIR response that was strong enough to trigger Na^+ spikes while applying the duration protocol (section 5.2.1.2). In order to quantify the DAergic effects on these cells, I first looked at whether DA could modulate firing frequency. Firing frequency was calculated for the remainder of each sweep, following each hyperpolarizing pre-pulse (Fig 5.3A; range 4.4 s to 2.5 s). As illustrated in Figure 5.3A, application of DA increased the average firing frequency when compared to control conditions (n = 4). Specifically, this effect was seen in 3/4 cells, with an average firing frequency of 0.30 Hz under control increased to an average firing frequency of 0.77 Hz under DA (increase of 262 %). In the remaining cell, DA application caused a decrease in average firing frequency from 1.1 Hz (control) to 0.85 Hz (DA, 21 % decrease).

5.2.3.2 DA increased the first spike instantaneous firing frequency

To further quantify the effects on firing frequency, I took a measure of the first spike instantaneous frequency (Fig 5.3B; n = 3). Similar to my findings while using the hyperpolarization protocol, I found that 2/3 cells saw an increase in first spike instantaneous frequency from an average of 0.44 Hz (control) to 1.87 Hz upon application of DA. The remaining cell saw a decrease in the first spike instantaneous frequency from 2.72 Hz (control) to 1.59 Hz (DA; 42 % decrease). This was also the same cell that did not see an increase in firing frequency upon DA application. Taken together, these findings indicate that of the cells in which DA increased the firing frequency, that one of the mechanisms by which DA had its effects was on increasing the frequency of the first spike instantaneous interval.

5.2.3.3 DA reduced the duration of the hyperpolarizing current step necessary to evoke a spike

Under control conditions, I observed 4 out of 10 cells that reached spike threshold (sec 5.2.1.2). It took an average of 600-700 ms for these cells to begin to spike following a hyperpolarizing pre-pulse. While in the presence of DA, these cells began to spike after an average hyperpolarizing pre-pulse of only 200-300 ms (Fig 5.3C and D; $n = 4$; $P < 0.01$). These results provide further evidence that DA increased the initiation of PIR, and that this was possibly accomplished by reducing the activation time necessary for ionic conductances that mediate the PIR response.

5.2.3.4 DA converted non-spiking cells into spiking cells

Of the 6 cells that did not spike under control conditions, 4 were converted into spiking cells while in the presence of DA. The remaining 2 cells that did not convert into spiking cells saw an increase in the average subthreshold PIR amplitude per hyperpolarizing pulse duration (Fig 5.3E). The most parsimonious conclusion based on this work is that DA may enhance the PIR response by increasing ionic conductances that mediate the rebound response.

5.2.4 The amplitude of the PIR response is enhanced with the application of DA

To demonstrate the effects of DA on the amplitude of the PIR conductance, I performed the next set of experiments in the presence of TTX (1 μM) to eliminate Na^+ spikes. I was able to detect a PIR response in 4 out of 8 cells tested under these conditions. In 4 out of 4 cells that exhibited a PIR response, DA enhanced the amplitude of the rebound depolarization while using both the hyperpolarizing and duration protocols as seen in Figure 5.4 (same cell as in A and B).

5.2.4.1 DA enhanced the amplitude of the PIR response evoked by the hyperpolarization protocol

Figure 5.4A illustrates the relative change of the PIR amplitude in relation to hyperpolarizing current steps. On average, DA increased the peak PIR amplitude from 1.4 ± 0.8 mV under control conditions to 3.1 mV ± 1.2 mV after a hyperpolarizing pre-pulse forced cells to approximately the same membrane voltage (-103 mV). To further quantify these results, I have fit a linear regression to all the voltage points reached in both control and dopamine conditions and found that the slopes of the regression lines were significantly different (Fig 5.4C; $n = 4$; $P < 0.0001$). The PIR response was abolished with the application of I_T antagonist Ni^{2+} (100 μM). The ionic basis of the PIR response will be further discussed in section 5.2.5.

5.2.4.2 DA enhanced the amplitude of the PIR response evoked by the duration protocol

As with the hyperpolarization protocol, application of DA while utilizing the duration protocol increased the amplitude of the PIR response (Fig 5.4B). The effect of altering the duration of the pre-pulse under control and DA conditions is summarized in Figure 5.4D. On average, the amplitude of the PIR response under DA conditions increased across every duration of the hyperpolarizing pre-pulse. In some cases, DA significantly increased the average PIR response ($n = 4$; $P < 0.05$). Therefore, the data presented in 5.2.4.1 and 5.2.4.2 suggest that PIR response is enhanced while in the presence of DA.

5.2.5 The ionic basis for the PIR response in putative motoneurons

In the next set of experiments, I investigated the possible involvement of I_T and I_h in the PIR response of neonatal mouse motoneurons by using both the hyperpolarization and duration protocols. I_T becomes activated at relatively hyperpolarized membrane potentials near threshold

for spiking (Perez-Reyes, 2003). Therefore, I hypothesized that this channel subtype may possibly contribute to the PIR response. Additionally, I investigated a possible contribution of I_h to the rebound response. The presence of I_h is traditionally associated with a characteristic voltage "sag" of a slowly depolarizing membrane potential during a long hyperpolarizing pulse (Bertrand & Cazalets, 1998; Serrano, Martínez-Rubio, & Miller, 2007), and therefore may become activated during the time course of the duration protocol that I have used to explore the PIR response.

5.2.5.1 Involvement of T-type Ca^{2+} channels

Figure 5.5A depicts a representative motoneuron in which the PIR response was abolished by the T-type Ca^{2+} channel blocker Ni^{2+} (100 μM). The ability of Ni^{2+} to block the PIR response was seen in 6 cells of the 8 cells tested (4/4 cells in the TTX experiments from section 5.2.4; 2/4 cells in the experiments without TTX from sections 5.2.2 and 5.2.3 with a maximum hyperpolarization voltage set to approximately -100 mV).

In the remaining 2 cells tested without TTX, but with Ni^{2+} application, 1 cell saw a decrease of 45 % in firing frequency and the other cell saw no change. Figure 5.5D illustrates the total number of PIR events (mV) vs hyperpolarization level (max to approximately -100 mV; min set to approximately -65 mV) of the 2 cells in which Ni^{2+} did not block the PIR response, at both the subthreshold and suprathreshold level. This graph illustrates two important observations. First, at the subthreshold level within physiological range, there are fewer PIR events with the application of Ni^{2+} when compared to the DA conditions. Secondly, at the suprathreshold level, once again there are fewer PIR events under Ni^{2+} conditions than there are compared to DA conditions. Collectively, this data suggests that even when Ni^{2+} does not abolish the PIR response entirely, it

does decrease the frequency of PIR events that occur. The fact that the PIR response persisted in these 2 cells suggests the presence of at least one other contributing current to the PIR response, which I now turn my attention to.

5.2.5.2 Involvement of HCN channels

To test for a possible involvement of I_h in the 2 cells where Ni^{2+} did not sufficiently abolish the PIR response, I applied the commonly used I_h current blocker ZD 7288 (50 μM) (Gasparini & DiFrancesco, 1997; Harris & Constanti, 1995). The remaining PIR response was abolished in both cells by application of ZD 7288, as illustrated for the motoneuron in Figure 5.6. Collectively, the combined effects of Ni^{2+} and ZD 7288 on the PIR response of putative motoneurons indicate that I_T and I_h can both contribute to different components of the PIR response.

5.2.6 DA induced conditional oscillations in membrane potential

In previous work, our lab has published that DA is necessary, but not sufficient, to induce oscillatory activity in a group of interneurons that possess conditional oscillatory properties while under synaptic blockade (Han et al., 2007). Targeted interneurons only exhibited oscillatory activity when DA (50 μM) was added to a cocktail of NMDA (20 μM), 5-HT (20 μM) and TTX (1μM). When added alone, DA was unable to induce oscillations in this particular group of interneurons. Interestingly in my current work, when I added DA alone to motoneurons, I observed that DA depolarized the membrane potential between 3 to 7 mV in all cells (n = 11), which led to the emergence of oscillatory activity in 4 out of 11 cells. This oscillatory activity became visible within 5 – 10 min after DA application (Fig 5.7). In an attempt to quantify this

data, I analyzed two parameters of the oscillatory activity: cycle period (s), and burst duration (s), while keeping the bias current held steady. Although oscillatory activity was quite varied, all cells demonstrated patterned burst activity, and 3 of the 4 cells exhibited intermitant single spiking activity between bouts of bursting (see Table 5.3 for individual cell characteristics). Average cycle periods ranged from 6 s to 95 s, with average burst duration lasting anywhere between of 1.8 s to 48.8 s. All cells were held at rest, ranging from -65 mV to -58 mV.

As previously stated, 3 of the 4 cells demonstrated burst oscillations with intermitant bursts of action potentials (Fig 5.7A – C). The average cycle period for these 3 cells was 19.3 s ±11.7 with average burst duration of 9.6 s ±7.3. The remaining cell displayed a much different pattern of oscillatory activity, characterized by a much longer cycle period (average: 97.5 s) and much longer burst duration (average: 48.4 s; Fig 5.7D). The variability between cells may partly be explained by the fact that these recordings were made unsystematically, as this unexpected finding was uncovered during the course of our experiments. Nonetheless, it is interesting that application of DA alone can induce different types of oscillatory activity in a handful of cells.

Chapter Five: FIGURES

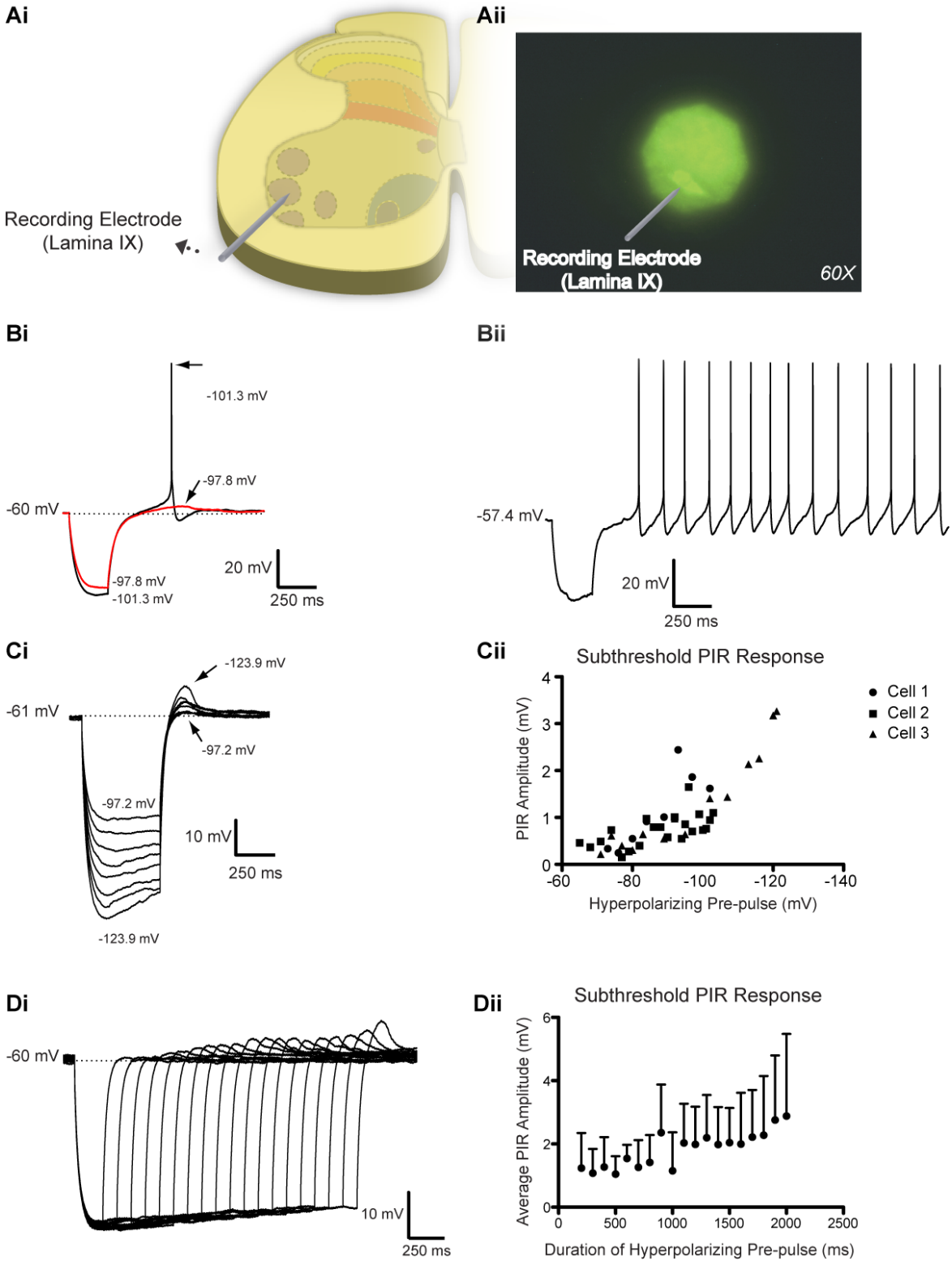

Figure 5.1: PIR response in putative neonatal mouse motoneurons

A: schematic diagram illustrating spinal cord cross-section and recording set up used during experiments (Ai). Example of a targeted putative motoneuron based on cell diameter and cell size, located in the ventral horn of a lumbar transverse slice. Cell was backfilled with Alexa 488 dye and identified with an Olympus BX51 microscope (Aii). B: PIR experimentally induced by injecting negative current pulses gave rise to a spike (Bi) and then a burst of spikes when the strength of the stimulus was increased (Bii). Note, the hyperpolarization level reached was similar in Bii to Bi (~ 100 mV). C: in certain cases cells did not reach threshold for spike or burst firing under control conditions (no TTX; 3/8 cells). However, with the holding potential kept constant at -60 mV, a series of hyperpolarizing current pulses of increasing strength (-20 pA to -140 pA) demonstrated that the PIR response increased in amplitude with more negative membrane potentials reached during the prepulse. Cii: data compiled from the 3 cells that did not reach Na^+ spike threshold. D: The PIR response was also dependent on the duration of the hyperpolarizing stimulus pulse. With a holding potential kept constant at -60 mV, a series of current pulses of increasing duration (200 - 2100ms) was delivered. The representative cell in Di depicts that the PIR response increased in amplitude with longer stimulus pulses (6/10 cells). Graph represents the averaged PIR amplitude per hyperpolarizing pulse duration (Dii) (n = 6; Error bars = SD).

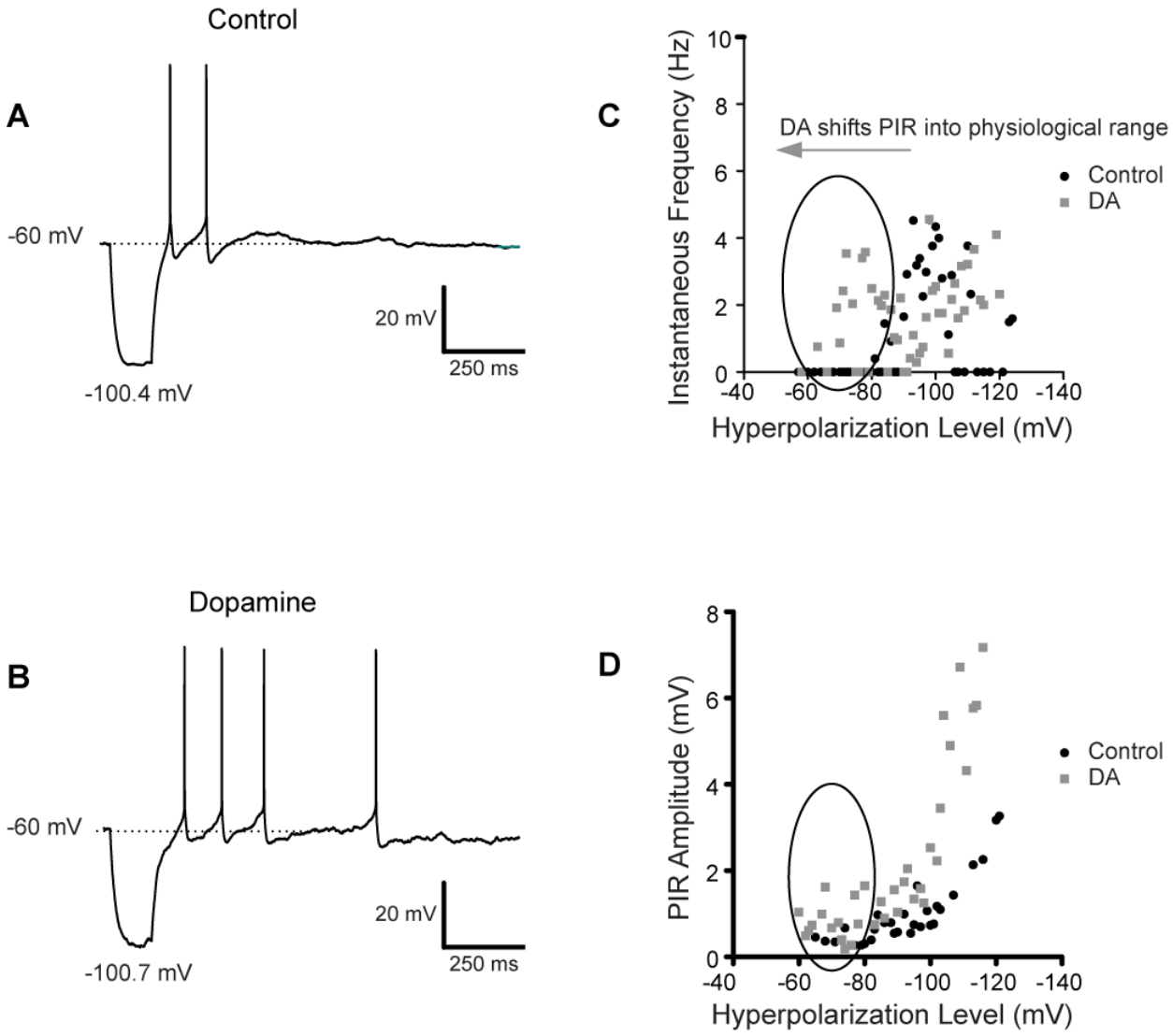
Control
A
-60 mV
20 mV
250 ms
-100.4 mV
C
DA shifts PIR into physiological range
Control
DA
Instantaneous Frequency (Hz)
Hyperpolarization Level (mV)
Dopamine
B
-60 mV
20 mV
250 ms
-100.7 mV
D
Control
DA
PIR Amplitude (mV)
Hyperpolarization Level (mV)

Figure 5.2: The effects of DA on spiking and non-spiking cells explored by using the hyperpolarization protocol

A – B: representative cell showing the firing frequency evoked after a hyperpolarizing pre-pulse forced the cell to -100 mV under control (A) and DA conditions (B) (-54 pA control; -65 pA DA; 200 ms; n = 5). Holding potential was kept constant at -60 mV. C: First instantaneous firing frequency plotted against hyperpolarizing voltage level for both control and DA conditions (n = 4). Note that DA shifts the threshold for PIR in the depolarizing direction indicated by circle. D: plotted is the subthreshold PIR amplitude against hyperpolarization level under both control and DA conditions (n = 2). Note: PIR responses were observed under both control and DA conditions, however DA further shifts the threshold for PIR in the depolarizing direction indicated by circle. Additionally, the PIR amplitude was increased with application of DA.

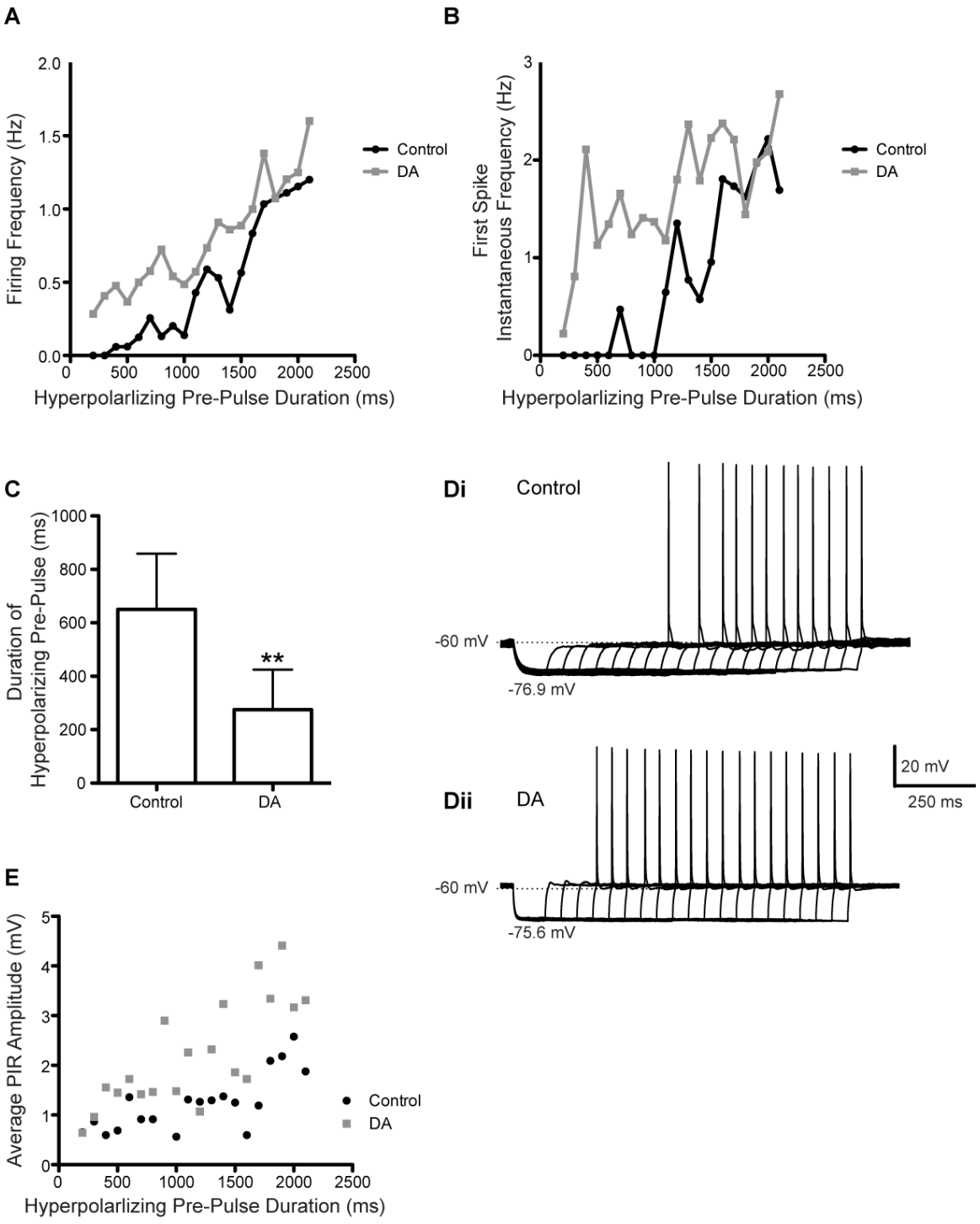
A
Firing Frequency (Hz)
2.0
1.5
1.0
0.5
0.0
0
500
1000
1500
2000
2500
Hyperpolarlizing Pre-Pulse Duration (ms)
Control
DA
B
First Spike Instantaneous Frequency (Hz)
3
2
1
0
Hyperpolarlizing Pre-Pulse Duration (ms)
Control
DA
C
Duration of Hyperpolarizing Pre-Pulse (ms)
1000
800
600
400
200
0
**
Control
DA
Di
Control
-60 mV
-76.9 mV
Dii
DA
-60 mV
-75.6 mV
20 mV
250 ms
E
Average PIR Amplitude (mV)
5
4
3
2
1
0
Hyperpolarlizing Pre-Pulse Duration (ms)
Control
DA

Figure 5.3: The effects of DA on spiking and non-spiking cells explored by using the duration protocol

A – B: graphs represent the average firing frequency (A; n = 4) and average first spike instantaneous firing frequency (B; n = 3) vs duration of hyperpolarizing prepulse (200 – 2100 ms) for both control and DA conditions. C: graph illustrates the relative change in the duration of the hyperpolarizing pre-pulse necessary to evoke the first spike for both control and DA conditions (n = 4; $P < 0.01$; paired t-test). D: raw traces illustrate that spiking commenced with less time spent with the same hyperpolarizing voltage under DA conditions. E: graph shows that average subthreshold PIR amplitude reached higher values under DA conditions compared to control values at all tested pulse durations.

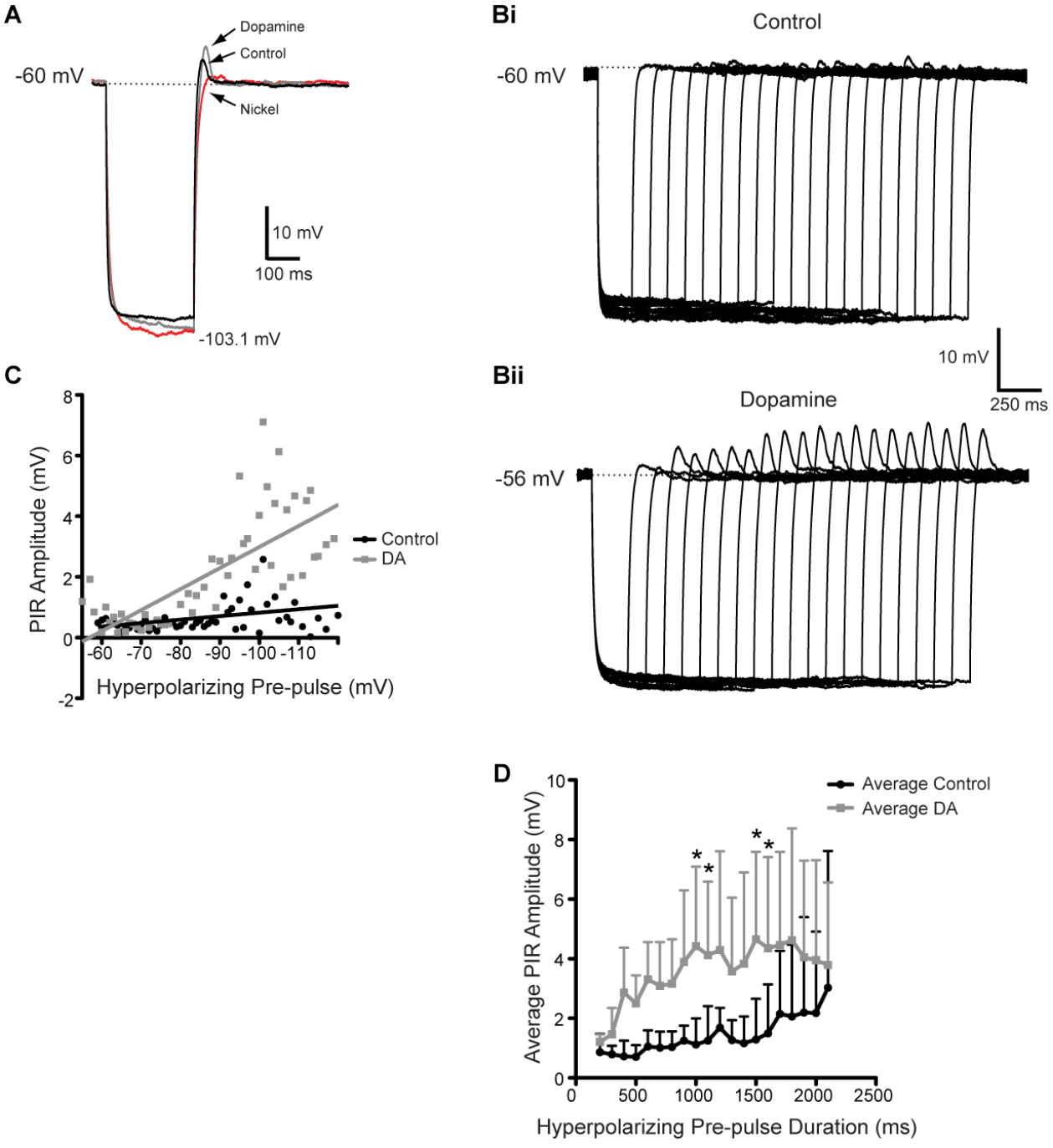
A
Dopamine
Control
-60 mV
Nickel
10 mV
100 ms
-103.1 mV
Bi
Control
-60 mV
10 mV
250 ms
Bii
Dopamine
-56 mV
C
PIR Amplitude (mV)
Control
DA
Hyperpolarizing Pre-pulse (mV)
D
Average Control
Average DA
Average PIR Amplitude (mV)
Hyperpolarizing Pre-pulse Duration (ms)

Figure 5.4: DA modulation of the PIR response

A – C: under conditions where TTX was included in the aCSF, PIR amplitude was markedly increased after bath application of DA (50 μM) (B is same cell as in A; $n = 4$). Holding potential was kept constant at -60 mV. D: plot depicts linear regression of all points for PIR amplitude as a function of hyperpolarizing prepulse under control (black) and DA (grey) conditions (same cell as in A – C). D: graph shows PIR amplitude reached higher values under DA conditions compared to control values at all tested pulse durations. ($n = 4$; $P < 0.05$, Two-way repeated measures ANOVA), data plotted as means; error bars = SD.

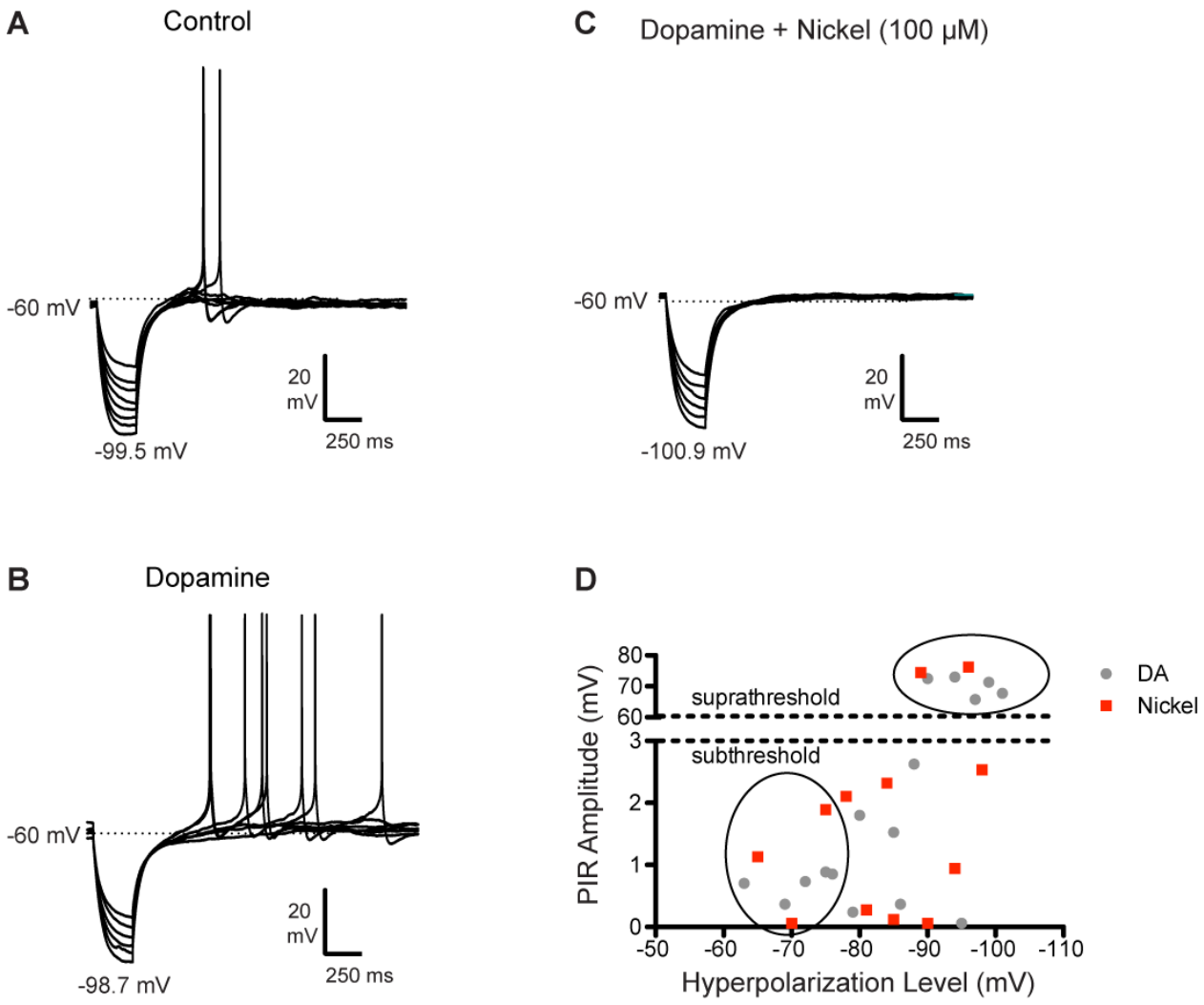
A
Control
-60 mV
-99.5 mV
20
mV
250 ms
C
Dopamine + Nickel (100 µM)
-60 mV
-100.9 mV
20
mV
250 ms
B
Dopamine
-60 mV
-98.7 mV
20
mV
250 ms
D
PIR Amplitude (mV)
80
70
60
3
2
1
0
suprathreshold
subthreshold
-50
-60
-70
-80
-90
-100
-110
Hyperpolarization Level (mV)
DA
Nickel

Figure 5.5: T-type Ca^{2+} channels contribute to the PIR response

A – C: a PIR response was induced in a representative motoneuron using a hyperpolarizing step protocol until the cell reached approximately -100 mV (-10 pA steps x 500 ms hyperpolarizing pulse). Holding potential was kept constant at -60 mV. Cell depicted after control conditions (A) and with the application of DA (B). After 100 μM Ni^{2+} application, the PIR response was abolished in 6 out of 8 cells (C). Note: same cell in A through C. D: for the remaining cells, the graph represents the total PIR events (plotted as PIR amplitude; both subthreshold and suprathreshold responses, n = 2) against hyperpolarizing voltage reached during experiments. The number of PIR events was higher under DA conditions for both subthreshold and suprathreshold levels than it was under Ni^{2+} conditions. Note: the number of PIR events within physiological range was also higher under DA conditions than compared to Ni^{2+} conditions.

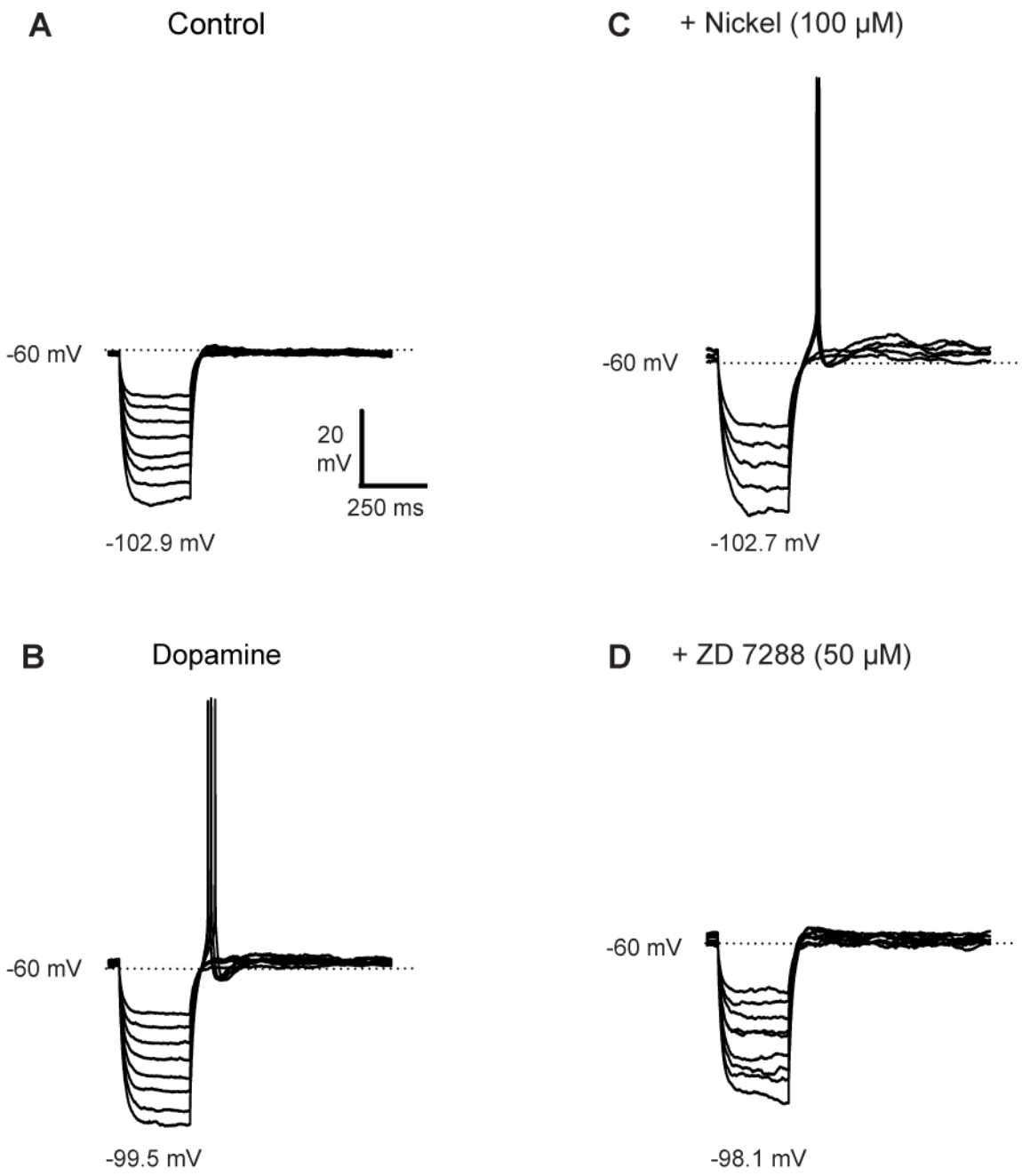
A
Control
-60 mV
20
mV
250 ms
-102.9 mV
C
+ Nickel (100 µM)
-60 mV
-102.7 mV
B
Dopamine
-60 mV
-99.5 mV
D
+ ZD 7288 (50 µM)
-60 mV
-98.1 mV

Figure 5.6: A small subset of cells demonstrated an I_h component of the PIR response

A: a PIR response was induced in a representative motoneuron using a hyperpolarizing step protocol until the cell reached approximately -100 mV (-10 pA steps x 500-ms hyperpolarizing pulse). Holding potential was kept constant at -60 mV. B: application of DA enhanced the subthreshold PIR response. C: after Ni^{2+} application, the PIR response was abolished in 6 out of 8 cells. D: for the remaining 2 cells that persisted to spike while in the presence of Ni^{2+}, the addition of ZD-7288 (50 μM) abolished the remaining PIR response. Note: same cell in A through D.

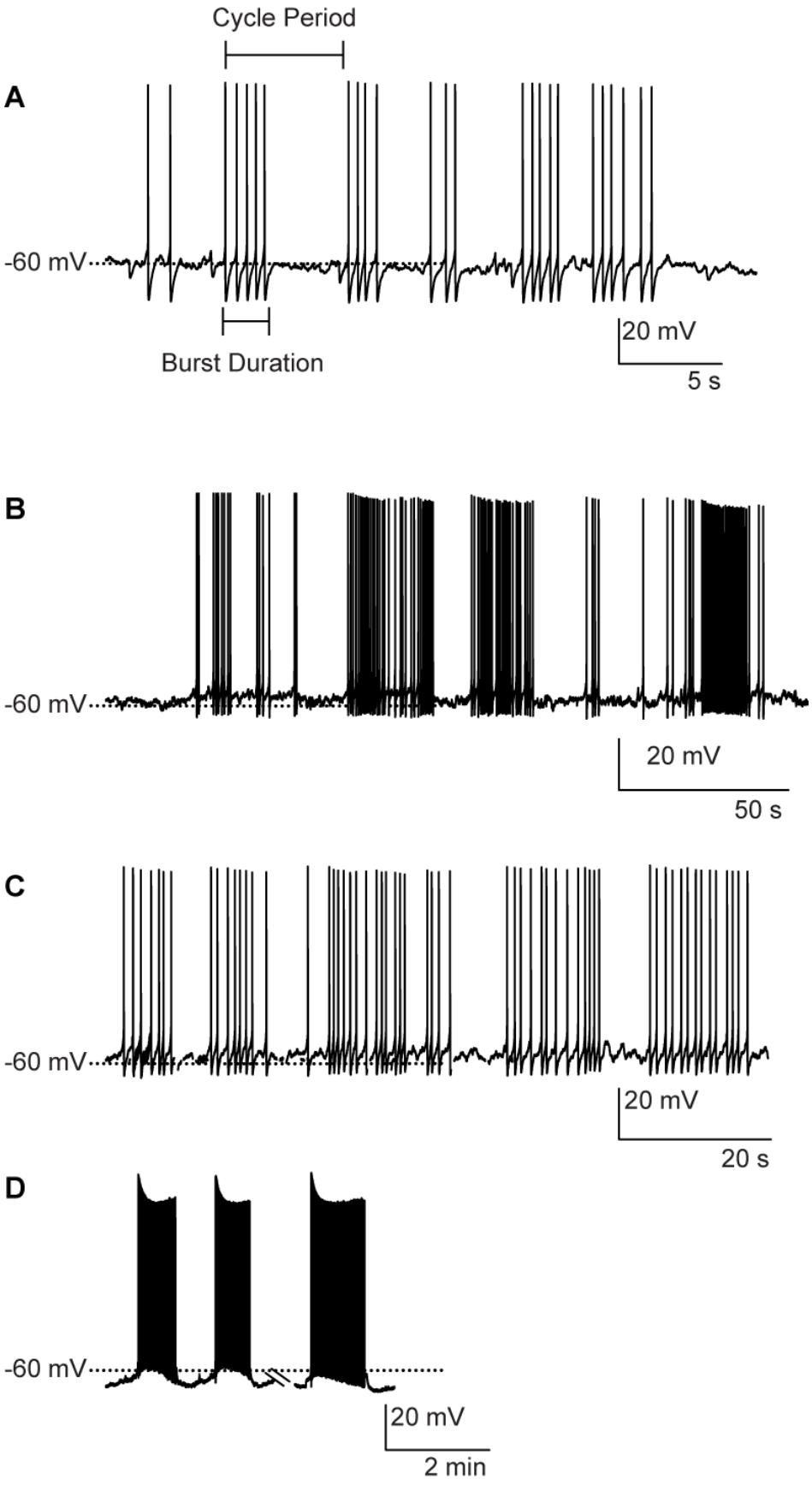
Cycle Period
A
-60 mV
Burst Duration
20 mV
5 s
B
-60 mV
20 mV
50 s
C
-60 mV
20 mV
20 s
D
-60 mV
20 mV
2 min

Figure 5.7: DA induced conditional bursting in a small subset of cells

In 4/10 cells, application of DA induced conditional bursting in putative motoneurons. All synaptic transmission was blocked. A: cycle period was calculated by measuring the time (s) from the onset of one burst to the onset of the subsequent burst. Burst duration was calculated by marking the beginning and end of each burst to calculate the average burst duration. A – C: the average cycle period for these 3 cells was 19.3 s ±11.7 with average burst duration of 9.6 s ±7.3. D: the average cycle period for this cell was 97.5 s with an average burst duration of 48.4 s.

Chapter Five: TABLES

Table 5.1: Motoneuron intrinsic properties recorded from untreated (no DA) cells

	Control (*n* = 11)		Control no PIR (*n* = 6)		
Property	**Mean**	**SE**	**Mean**	**SE**	***P* Value**
Action Potential					
Amplitude, mV	65.53	2.18	69.01	2.87	NS (0.35)
Time-to-peak, ms	1.56	0.12	1.47	0.10	NS (0.60)
Rheobase current, pA	68.83	10.85	69.83	18.93	NS (0.96)
Afterhyperpolarization					
Amplitude, mV	3.92	0.93	7.46	0.97	< 0.05*
Half-decay time, ms	203.31	11.31	200.60	13.26	NS (0.88)
Input resistance (R_{in}) MΩ	378.05	47.72	316.55	49.52	NS (0.42)

n = number of motoneurons
* indicates significance; NS, not significant

Table 5.2: Motoneurons intrinsic properties recorded from untreated control cells and under DA conditions

	Control (*n* = 11)		DA (*n* = 11)		
Property	**Mean**	**SE**	**Mean**	**SE**	***P* Value**
Action Potential					
Amplitude, mV	65.53	2.18	62.30	1.78	NS (0.14)
Time-to-peak, ms	1.56	0.12	1.85	0.18	NS (0.10)
Rheobase current, pA	68.83	10.85	57.76	9.57	NS (0.19)
Afterhyperpolarization					
Amplitude, mV	3.92	0.93	5.23	0.89	NS (0.27)
Half-decay time, ms	203.31	11.31	198.62	27.26	NS (0.84)
Input resistance (R_{in}) MΩ	378.05	47.72	392.06	66.64	NS (0.73)

Table 5.3 Characteristics of conditionally oscillating motoneurons while in the presence of DA

Cell Number	Average Cycle Period (s)	Average Burst Duration (s)
1 (A)	6.5	1.8
2 (B)	36.0	18.8
3 (C)	15.4	8.7
4 (D)	97.5	48.4

*Letters beside “Cell Number” correspond to cell depicted in figure 5.7

5.3 DISCUSSION

5.3.1 General remarks

In the present study, I explored the existence of the PIR response in putative motoneurons in the neonatal mouse. I first investigated the modulatory effects of DA application on several parameters of this PIR response including firing frequency, first spike instantaneous frequency, and threshold voltage for spike initiation. There were two protocols used to explore both the voltage dependency and the time dependency of the PIR response (Perez-Reyes, 2003). I next examined the underlying PIR conductances by investigating the contribution of I_T and I_h.

5.3.2 PIR in motoneurons of the neonatal mouse

To the best of my knowledge, only a few other studies have investigated the presence and modulation of PIR in neonatal lumbar spinal motoneurons of the rodent (Berger & Takahashi, 1990; Bertrand & Cazalets, 1998; Takahashi & Berger, 1990)). Therefore, my work, although preliminary in nature, adds valuable insight regarding the conditions of expression, the characterization, and the modulation of the PIR response of neonatal mouse motoneurons. First, I noted that roughly 60% of motoneurons exhibited a PIR response, while the remaining population displayed no PIR activity. PIR activity could not further be unmasked with the application of DA in this subpopulation of motoneurons. These results may be accounted for by several possibilities. Motoneurons are a heterogeneous population of cells composed of large diameter α-motoneurons (α-MNs), smaller diameter γ-motoneurons (γ-MNs), and the less defined population of β-motoneurons (β-MNs) (Kanning & Kaplan, 2010). Despite the fact that motoneurons share the same general function i.e., drive muscle contraction, each motoneuron

class innervates distinct targets within the muscle, and has different contractile properties (English & Weeks, 1984). Additionally, different classes of motoneurons can be distinguished based on molecular identity (Ashrafi et al., 2012; Kanning & Kaplan, 2010). These differences in size, molecular identity, and function manifest biophysical consequences accompanied by different compositions of ion channels that support membrane properties such as PIR.

The dependence of the PIR on the level at which the membrane potential reached was investigated by delivering a series of hyperpolarizing pulses of increasing amplitude at a constant holding potential (hyperpolarization protocol; Fig 5.1B). Unlike previous investigations, I did not restrict my measurements to trigger only subthreshold rebound depolarizations (Bertrand & Cazalets, 1998). Instead, I sought to characterize the entirety of the PIR response both as subthreshold and suprathreshold events. My findings indicate that the presence of PIR in neonatal motoneurons is expressed primarily as a suprathreshold event in the majority of cells (5 out of 8) but also as a subthreshold event (3 out of 8) under control conditions. The dependence of the PIR response on the duration of the hyperpolarizing current was also investigated by delivering a series of pulses of increasing duration from a set holding potential (duration protocol; Fig 5.1C). Conversely, I observed that the majority of PIR events remained subthreshold (6 out of 10) upon negative current injections of increasing duration. My findings were consistent with previous reports, such that I found that there was a progressive increase in the PIR response (both at the subthreshold and suprathreshold levels) with more negative membrane levels reached, and with increased pulse durations (Bertrand & Cazalets, 1998; Wang et al., 2011).

One may argue that since some PIR responses reached Na^+ spike threshold and others did not, that this may be dependent upon differences in input resistance across cells. Indeed, on

average, input resistance values were higher for cells that reached Na^+ spike threshold under control conditions for both protocols. However, while input resistance dramatically affects the voltage deflection response to an injected current pulse, it cannot entirely explain my findings. If input resistance was the sole reason why some cells reached Na^+ spike threshold while others did not, then one would expect that the cells with higher input resistance would also exhibit lower rheobase current values; i.e. it would take less current to evoke a spike in these cells. Interestingly, this was not the case as some cells with high input resistance also displayed a high rheobase value. Therefore, additional mechanisms, such as the set level of Na^+ spike threshold (Gao & Ziskind-Conhaim, 1998; Nakanishi & Whelan, 2010), could contribute to the interpretation of my data. Regardless of whether or not cells reached Na^+ spike threshold under control conditions, what is of importance is that qualitatively speaking, the PIR response observed across all cells was increased throughout the course of both the hyperpolarizing and durations protocols. Collectively, these findings provide important insights regarding the capacity of one membrane property, PIR, to evoke action potential firing in motoneurons.

5.3.3 DA modulation of the PIR response

Several studies have documented the targeting of PIR by modulatory systems influencing network operation (Angstadt et al., 2005; Angstadt & Friesen, 1993; Merrywest et al., 2003; Peck et al., 2001; Takahashi & Berger, 1990; Wang et al., 2011). My interest in the DAergic modulation of motoneuronal PIR stems from the actions of DA during a pre-existing drug-evoked locomotor rhythm, in which DA stabilizes network activity and boosts the amplitude of motor output (Chapter 3) (Barriere et al., 2004; Humphreys & Whelan, 2012; Madriaga et al., 2004; Whelan et al., 2000). If PIR were a modulatory target for DA to stabilize a drug-evoked

locomotor rhythm, then one would expect DA to increase the PIR response at the cellular level. Indeed, when I collapse the data obtained using both protocols, specifically regarding data collected from cells that reached Na^+ spike threshold under control conditions, DA increased the firing frequency and first spike instantaneous firing frequency in the majority of cells (Fig 5.2A – C; Fig 5.3A and B). Additionally, I noted that DA increased cellular excitability upon application, as evident by a depolarization of the membrane potential in all cells, which led to the emergence of oscillatory activity in 4 out of 11 cells (Fig 5.7). Collectively, it is possible that the excitatory effects of DA on the burst amplitude of a 5-HT, NMA-evoked locomotor rhythm may be partly attributed to DA's ability to increase PIR at the motoneuronal level.

I also characterized the effects of DA modulation on subthreshold PIR responses. If I collapse the data between the two protocols, 9 cells failed to reach Na^+ threshold under control conditions. However upon application of DA, a suprathreshold response was unmasked in 5 of these 9 cells. Of the 4 cells that remained subthreshold, DA increased the PIR amplitude in all cells (Fig 5.2D). Moreover, when Na^+ spiking was eliminated with the addition of TTX, once again DA increased the PIR amplitude evoked by both protocols in all cells (Fig 5.4). Collectively, these data suggest that DA is enhancing the PIR response at both supra and subthreshold levels in neonatal mouse motoneurons.

Interestingly, these results are in contrast to those reported in the lamprey, in which DA was found to exert depressive effects on the PIR of motoneurons by reducing L-type Cav1.3 and T-type Cav3 calcium channel conductances (Wang et al., 2011). This effect was mediated via activation of D_2 receptors, which have been shown to be present in the lamprey spinal cord (Robertson et al., 2012; Schotland et al., 1995). In line with this data, D_2 receptor activation has been shown to reduce L-type currents in other areas of the rodent central nervous system (Lledo,

Homburger, Bockaert, & Vincent, 1992). Additionally, D_2 receptor activation in the rat powerfully inhibits cellular excitability by augmenting the G-protein regulated inwardly rectifying potassium channels (GIRK), which could possibly affect voltage-dependent membrane properties such as PIR. In all, my results that DA enhances PIR rebound in the mouse, combined with the previously reported results that DA depresses PIR in the lamprey (Wang et al., 2011) adds to the diversity of how membrane properties such as PIR are targeted differently by modulatory systems across different species.

5.3.4 Ionic basis of the PIR response

The PIR phenomena has been extensively studied in many species, from crustaceans (Barrio, Araque, & Buño, 1994), to early vertebrates including the lamprey (Grillner et al., 1995; Wang et al., 2011) and the Xenopus (Roberts & Tunstall, 1990), to mammals such as the rodent (Bertrand & Cazalets, 1998; Wilson et al., 2005). This work, and that of others, has uncovered several mechanisms by which PIR excitation can occur. This includes the presence of a small outward current carried by K^+ ions, otherwise known as the M-current (Barrio et al., 1994) (Constanti, Adams, & Brown, 1981), LVA Ca^{2+} channels including L-type Cav1.2 and T-type Cav3 (Bertrand & Cazalets, 1998; Grillner et al., 1995; Perez-Reyes, 2003; Wang et al., 2011; Wilson et al., 2005), Ca^{2+} activated Cl^- currents (Owen, Segal, & Barker, 1984), and inward rectifying currents (Chandler, Hsaio, Inoue, & Goldberg, 1994; Pape, 1996; Robinson & Siegelbaum, 2003). Among these various mechanisms, two of them may explain my current results based on the pharmacology of the observed PIR response: (1) LVA channels (specifically a T-type component; I_T) and (2) inward rectifying channels HCN (I_h). My results are supported by several other lines of evidence in which both LVA currents and inward rectifying currents are

present in neurons that generate PIR (Berger & Takahashi, 1990; Bertrand & Cazalets, 1998; Takahashi & Berger, 1990). Interestingly, it appears that these two conductances do not contribute equally to the generation of the PIR response in the neonatal mouse. Furthermore, my results differ from a previous report in the neonatal rat in which the predominate current generating the PIR response in motoneurons was I_h (Bertrand & Cazalets, 1998). Abolishment of PIR in my work was mainly due to application of low concentrations of Ni^{2+} (100 μM), a relatively selective T-type antagonist (6/8 cells; Fig 5.4 and 5.5). For cells in which Ni^{2+} did not completely abolish the PIR response (n = 2), further application of the specific I_h channel blocker ZD-7288 (50 μM) did block the remaining rebound depolarization. This suggests that there was a small I_h component to the PIR response in some cells. Although my results highlight I_T as the main contributing influence to the observed PIR response in the neonatal mouse, this is not to say that later in development this would remain true. Work published in the mouse demonstrated that I_T is abundant in motoneurons at embryonic day 14, but steadily declines postnatally to become undetectable past P7–P8 (Mynlieff & Beam, 1992). Similar findings have been found in the developing chick (McCobb, Best, & Beam, 1989). For both species, the decrease in I_T coincides with the phase of motoneuronal cell death and the onset of synapse elimination. Additionally, further work is necessary to explore the possibility that some other mechanisms, such as Ca^{2+} activated Cl^- currents, may contribute to the PIR response in neonatal mice.

5.3.5 Physiological involvement of PIR during locomotion

An important question that arises with regards to previously published work is whether the rebound that is induced experimentally is likely to occur and be expressed during ongoing drug-induced locomotion. When a series of hyperpolarizing pulses of increasing amplitude were

delivered, I observed that DA caused a depolarizing shift in threshold voltage for spiking in 3 of the 4 cells. Upon further examination, I found that DA pushed the threshold voltage for spike initiation into a more physiological range in 2 of these 3 cells (Fig 5.2C). This is an important consideration for two reasons: (1) it is a well established fact that motoneurons receive local inhibitory synaptic input from Renshaw cell mediated pathways and Ia inhibitory interneurons, as well as descending input from the brainstem regions (Rekling et al., 2000). Although inhibitory input onto motoneurons functions to regulate firing, it is important to respect that hyperpolarization levels reached during experimentation do not always reflect those seen naturally during locomotion; (2) in order for experimental work to provide insight on real motor behavior, experimental voltage-dependent rebound responses should align with physiological voltage levels recorded during ongoing behavior (Bertrand & Cazalets, 1998; Engbers et al., 2011). In the present study, I was careful to include a range of hyperpolarizing voltage levels that were consistent with those reported in the rat during ongoing drug-evoked locomotion (Bertrand & Cazalets, 1998). Therefore, the PIR events observed in my study are likely within the voltage range for expression and participation of PIR responses present during fictive locomotion.

The present study demonstrates what a key role DA can play at the level of motoneuronal output by enhancing the PIR response. The effects of DA on motoneurons; i.e. depolarizing the membrane potential, increasing firing frequency, shifting the threshold voltage in the depolarizing direction, and enhancing subthreshold PIR amplitude, suggest that DAergic modulation of PIR is likely part of the mechanistic basis by which DA exerts actions on during fictive locomotion.

Chapter Six: Low threshold calcium channels modulate locomotor activity in the mouse

6.1 INTRODUCTION

The origin of alternating rhythmic locomotor output produced by spinal CPG circuits is still not fully understood. Two competing mechanisms have been proposed to underlie rhythm production: (1) networks can be driven by endogenously oscillating or conditionally oscillating neurons that function as "pacemaker neurons" and (2) rhythms emerge from resultant synaptic interconnections among neurons that are not themselves inherently rhythmic (Harris-Warrick, 2010; Marder & Thirumalai, 2002; Ramirez, Tryba, & Peña, 2004). Traditionally, these dichotomizing models for rhythmogenesis have been placed into "either/or" categories based on the presence of pacemaker or emergent properties, even though it has been recognized by some that a hybrid of rhythm generating mechanisms would potentially be more robust (Brocard, Tazerart, & Vinay, 2010; Harris-Warrick, 2010; Ivanchenko, Thomas Nowotny, Selverston, & Rabinovich, 2008). Along these lines, a novel approach to the study of rhythmogenesis has recently been put forth by Harris-Warrick (2010) whereby he suggests thinking in terms of rhythmogenic ionic *currents* rather than by rhythmogenic circuits or neurons. Indeed, there are a number of key ionic conductances such as $I_{Na(P)}$ (Tazerart et al., 2007; Zhong et al., 2007), Ca^{2+}-activated nonselective cation currents (I_{CAN}) (Zhang et al., 1995), I_h currents (Peck et al., 2006), $I_{K(Ca)}$ (Manira et al., 1994), I_A (Hess & Manira, 2001) present in both "pacemaker-driven" and "emergent-network" driven CPG circuits. Generally speaking, these ionic conductances (and their modulation) help shape rhythmogenesis by supporting different intrinsic membrane properties that mediate burst initiation, prolonged firing, and burst termination. This fresh outlook may be extremely valuable for the future elucidation of locomotor network operation.

Locomotor rhythmogenesis manifested in *in vitro* preparations is a signature behavior consisting of left-right alternating discharge within the same spinal segment, and alternation of the ipsilateral flexor and extensor muscles groups (Whelan et al., 2000). In terms of rhythmogenic ionic currents, conductances can assist the neuronal transitions between activated and inhibited states necessary to support alternating discharge. As previously discussed (Chapter 5), the LVA T-type (Cav3) Ca^{2+} current (I_T) contributes to the generation of rebound depolarizations such as PIR that likely help facilitate alternating left-right, flexor-extensor activity amongst reciprocally connected groups of neurons. Multiple lines of evidence suggest that I_T is involved in locomotor rhythm generation (Anderson et al., 2012; Bertrand & Cazalets, 1998; Wang et al., 2011; Wilson et al., 2005). What designates T-type Ca^{2+} channels as invaluable key players during locomotor rhythmogenesis is their ability to generate nonlinear responses to subthreshold changes in voltage, mediated by a fast activating – fast inactivating channel conductance which is normally inactivated at rest, and which recovers during bouts of membrane hyperpolarization (Catterall et al., 2003; Harris-Warrick, 2010; Perez-Reyes, 2003). Therefore, T-type Ca^{2+} channel availability increases upon increasing membrane hyperpolarization (Perez-Reyes, 2003), such as that which occurs throughout a period of inhibition during alternating left-right or flexor-extensor discharge.

My previous work has implicated an important role for I_T within the motoneuronal class of cells of the neonatal mouse (Chapter 5). Specifically, I demonstrated that PIR expressed in this population of cells was largely due to the presence of I_T, and that the addition of DA boosted the PIR effect. While this work provides important insights regarding the cellular function of I_T at the level of motoneurons, it does not speak to the role of I_T at the network level during ongoing locomotor-like behavior. Therefore in the current study, I hypothesized that T-type Ca^{2+}

channels play an important role in supporting the emergence and maintenance of an ongoing locomotor rhythm evoked by bath application of 5-HT, NMA, and DA.

It should be noted that some studies have already begun to address this issue by focusing at the level of rhythmically active interneurons[1]. Of particular focus has been the Hb9 class of interneurons (Anderson et al., 2012; Hinckley et al., 2005; Kwan et al., 2009; Wilson et al., 2005), likely due to their conditional bursting properties which are resultant of T-type mediated PIR (Wilson et al., 2005). Although Hb9 cells are unlikely candidates to be solely responsible for rhythm generation (Kwan et al., 2009) their rhythmic bursting has been correlated to locomotion (Hinckley et al., 2005; Kwan et al., 2009).

Given that we know that T-type Ca^{2+} channels possess unique kinetic and voltage dependent properties that support aspects of rhythmogenesis (Perez-Reyes, 2003), and that I_T has demonstrated functionally relevant roles both in a class of conditional oscillatory Hb9 (Anderson et al., 2012; Hinckley et al., 2005; Kwan et al., 2009; Wilson et al., 2005) and at the level of motor output (Wang et al., 2011) (Chapter 5), I sought to examine the role for I_T during ongoing locomotor activity elicited by bath application of 5-HT, NMA, and DA. My work demonstrates that antagonizing T-type Ca^{2+} channels with low (50 – 75 μM) concentrations of Ni^{2+} significantly slows the frequency of the locomotor rhythm. At higher concentrations of Ni^{2+} (100 – 300 μM), the locomotor-like rhythm becomes severely disrupted and eventually converts into a synchronous rhythm. This finding persisted despite mid-sagittal sectioning of the spinal cord, indicating that T-type Ca^{2+} channels are not only expressed on commissurally projecting interneurons, but also on ipsilaterally projecting interneuronal circuitry. Finally, my work demonstrates that application of specific Cav3 agonist, L-Cysteine, exerts the opposite effect on

[1] It should be noted that at the time of this work, another group replicated, expanded on, and published our findings. This will be discussed further the Discussion Section of Chapter 6.

rhythm, thereby increasing the frequency. Collectively, this work points to an important role for T-type Ca^{2+} channels in mediating alternating locomotor-like activity in the neonatal mouse.

6.2 RESULTS

6.2.1 T-type Ca^{2+} channels are key contributors to the maintenance of ongoing locomotor activity

In contrast to high voltage activated (HVA) Ca^{2+} channels, LVA Ca^{2+} channels of the Cav3 family are resistant to most organic Ca^{2+} channel blockers, such as the dihydropyridines that block L-type; peptide toxins, such as the snail toxin ω-conotoxin GVIA that blocks N-type; and the spider toxin ω-agatoxin-IVA that blocks P-type channels (Catterall et al., 2003; Miljanich & Ramachandran, 1995; Perez-Reyes, 2003). However, T-type Ca^{2+} channels display are relatively sensitive to Ni^{2+}, with many studies reporting IC_{50} values of ~300 μM in neurons (Perez-Reyes, 2003). Cav3.2 channels are most sensitive to Ni^{2+} block (IC_{50} 10-50 μM) while Cav3.1 and 3.3 are roughly 20 fold less sensitive (Lee, Gomora, Cribbs, & Perez-Reyes, 1999; Perez-Reyes, 2003). Therefore, in my first set of experiments, I tested for the involvement of I_T in maintaining ongoing drug induced locomotion by applying varying concentrations of Ni^{2+}.

6.2.1.1 Blocking T-type Ca^{2+} Channels with Ni^{2+} disrupts a fictive locomotor rhythm in a concentration dependent manner

To determine the extent to which I_T was involved in maintaining ongoing locomotor output in the neonatal mouse, I first activated the CPG network by combined bath application of 5-HT (10 μM), NMA (5 μM) and DA (50 μM) (Jiang et al., 1999; Whelan et al., 2000). Once a regular rhythm was established (within 10-15 min of drug application; Fig 6.1Ai) I applied Ni^{2+} at varying concentrations (42, 56, 72, 100, 133, 178, 238, and 319 μM; n = 40) and observed effects on rhythm frequency and stability as monitored by extracellular suction electrodes on

lumbar ventral roots (Fig 6.1B - D). Application of low Ni^{2+} (56 – 72 μM) slowed the rhythm frequency in all preparations tested (Fig 6.1B; 72 μM; n = 11). At intermediate concentrations of Ni^{2+} (100 – 133 μM) the alternating locomotor-like rhythm not only demonstrated a slower frequency, but started to become highly unorganized, as evident by a disruption of left-right and flexor-extensor alternation, and the emergence of occasional bouts of synchronous bursting across all ventral roots (100 μM; Fig 6.1C). At high concentrations of Ni^{2+} (178 – 319 μM) the emergence of a fully developed synchronous rhythm was observed, evident by large amplitude synchronous neurogram bursts across all recorded ventral roots (L2-L2 & L2-L5; 238 μM; Fig 6.1D). Additionally, the frequency of the synchronous rhythm was significantly slower than the control 5-HT, NMA, DA-evoked rhythm. At the end of these experiments, I constructed a dose-response relationship between the effects of Ni^{2+} concentration on rhythm frequency (Fig 6.1E and F) and found that the IC_{50} for Ni^{2+} was 126 μM. This concentration is consistent with previous finding (Anderson et al., 2012) and well within range of affinities of Ni^{2+} to exert relatively selective block of T- type Ca^{2+} channels, likely on the Cav3.2 isoform (Lee et al., 1999; Perez-Reyes, 2003).

Regardless of the Ni^{2+} concentration, the left-right and flexor-extensor alternation was re-established in all preparations following wash with ~500 – 600 ml aCSF including 5-HT, NMA and DA. These data suggest that the CPG rhythm generator, which governs rhythm frequency, is sensitive to Ni^{2+} application, likely by antagonizing the actions of T-type Ca^{2+} channels.

6.2.1.2 I_T antagonist amiloride replicated the effects of Ni^{2+} on a drug-evoked locomotor rhythm

It has been shown that Ni^{2+} blocks not only T-Type Ca^{2+} channels but also R-Type channels (Cav2.3) as well (Huguenard, 1996; Todorovic & Lingle, 1998; Tsien, Lipscombe, Madison,

Bley, & Fox, 1988; Zamponi, Bourinet, & Snutch, 1996). Therefore, in an attempt to provide further evidence that the actions of Ni^{2+} on rhythm frequency and stability were indeed due to blocking T-type channels, I tested another putatively selective T-type antagonist amiloride (500 μM; n = 2) (Tang, Presser, & Morad, 1988; Tytgat, Vereecke, & Carmeliet, 1990). Within 10 min of application, the alternating drug-evoked rhythm began to slow down and eventually converted into one of synchrony (data not shown). This effect was very similar to what was observed with Ni^{2+} application, thereby providing further evidence in support of T-type Ca^{2+} channels contributing to the maintenance of alternating locomotor activity.

In recent years, some progress has been made regarding advanced pharmacological tools for studying T-type Ca^{2+} channels (Lory & Chemin, 2007; McGivern, 2006). Some of the most widely used T-type antagonists to come from this work are mibefradil (Clozel, Ertel, & Ertel, 1997), it's closely related derivative NNC 55-0396 (Huang, 2004), and the recently discovered TTA-P2 (Choe et al., 2011; Uebele et al., 2009). Therefore, I tested the effectiveness of these drugs to block I_T during ongoing drug-evoked locomotor activity. Interestingly, when I individually applied T-type antagonists mibefradil (2-10 μM), NNC-55-0396 (10 μM), and TTA-P2 (3-10 μM), in contrast to my previous findings there were no observable changes in rhythm frequency or stability. These data were unexpected and difficult to interpret given my findings with other T-type antagonists Ni^{2+} and amiloride (see Discussion). However, although I was unable to replicate the effects of Ni^{2+} and amiloride with the newer pharmacological agents, this does not necessarily mean that T-type Ca^{2+} channels do not contribute to rhythmogenesis. This interpretation will be expanded upon in my Discussion. For a full review of the T-type antagonists used and their effectiveness related to the current work, see Table 6.1.

6.2.1.3 Removal of the dorsal horn permits the actions of Ni^{2+} at lower concentrations

Three things T-type antagonists such as mibefradil, NNC-55-0396 and TTA-P2 have in common are that they are (1) organic, (2) heavy-molecular weighted, (3) hydrophobic molecules. Hence, it is possible that these drugs may have a difficult time diffusing through the spinal tissue far enough to reach the CPG circuitry. Bearing in mind that CPG circuitry resides within the ventral horn of the spinal cord (Kjaerulff & Kiehn, 1996), and that the dorsal horn is not necessary to evoke rhythmic CPG motor output, I designed a set of experiments whereby I removed the dorsal horn tissue from the isolated spinal cord preparation to create better access for I_T antagonists (Fig 6.2A – Aii). In this preparation, the ventral circuitry remained intact and motor output could still be recorded from the ventral roots.

In my first set of experiments, I tested the effects of Ni^{2+} on the dorsal-horn removed isolated spinal cord preparation. After removing between 100 – 250 microns of dorsal horn tissue, I applied the rhythmogenic cocktail of 5-HT, NMA, DA to the dorsal-horn removed and isolated spinal cord preparation. In 4 out of 6 preparations, bath application of drugs elicited alternating locomotor-like activity. The rhythm was slower in frequency and less stable than what I observed in an intact isolated spinal cord preparation (compare Fig 6.2B with 6.1Ai). Nevertheless, once an alternating rhythm was established, 30 minutes were given to allow for the rhythm to stabilize. Next I applied varying low concentrations of Ni^{2+} ranging from 50 μM – 75 μM. Interestingly, upon application of Ni^{2+} (50 μM), the rhythm began to slow down and become highly disorganized in the dorsal horn removed preparation. When similar concentrations of Ni^{2+} (56 μM) were applied to the intact preparation, there was no significant change in rhythm frequency or stability. At 75 μM Ni^{2+}, the drug-evoked alternating rhythm of the dorsal horn-removed preparation converted into one of synchrony (Fig 6.2Ci). This effect was not seen in the

intact preparation until after 100 μM of Ni^{2+} had been applied. Collectively, these data suggest that by removing the dorsal horn, better access was created for Ni^{2+} to block I_T present in the interneurons of the CPG circuitry.

6.2.1.4 Removal of the dorsal horn does not permit the actions of mibefradil

Given that the frequency of the locomotor-like rhythm slowed down and eventually became synchronous with lower concentrations of Ni^{2+} when applied to the dorsal horn-removed preparation, I next sought to test whether the removal of the dorsal horn tissue from the isolated spinal cord preparation would in fact assist the diffusion of mibefradil into the cord. As in my previous experiments, I first generated a 5-HT, NMA, DA-evoked locomotor rhythm from the dorsal horn-removed preparation. Unlike with the application of Ni^{2+} however, application of 3 μM mibefradil, did not exert any changes to the locomotor frequency or rhythmicity (n = 1). I will further address this finding in my Discussion.

6.2.2 T-type agonist L-Cysteine potentiates the frequency of the locomotor rhythm

Given that Ni^{2+} and amiloride significantly slow the frequency of a drug-evoked locomotor rhythm, presumably by antagonizing T-type Ca^{2+} channels, I next sought to examine whether potentiating the activity of T-type Ca^{2+} channels, and therefore enhancing presence of I_T, would augment the frequency of a fictive locomotor rhythm. The endogenous reducing agent L-Cysteine (100 – 200 μM) has recently been shown to potentiate I_T in dorsal root ganglion cells (Nelson, Joksovic, Perez-Reyes, & Todorovic, 2005). Therefore, I applied L-Cysteine to a drug-evoked fictive locomotor rhythm in order to test whether augmenting I_T could increase rhythm frequency.

Application of 100 μM L-Cysteine did not alter fictive locomotor rhythm parameters. However within 10 – 15 min of application of 200 μM L-Cysteine, the frequency of the fictive locomotor rhythm began to increase on average from 0.29 Hz (± 0.02) to 0.35 Hz (± 0.01), until reaching steady state within 20-30 min (Fig 6.3C; $n = 6$; $P < 0.05$). These data provide further evidence that the locomotor cycle frequency is sensitive to the modulation of I_T. Moreover, in view of the fact that agonizing and antagonizing T-type Ca^{2+} channels modulates the speed of the rhythm, I suspect that I am targeting T-type Ca^{2+} channels expressed on pre-motor interneurons involved in rhythm generation, rather than targeting motoneurons exclusively. In the next set of experiments I further explored likely candidate populations of interneurons that may express T-type Ca^{2+} channels.

6.2.3 T-type Ca^{2+} channel involvement in the circuitry underlying flexor-extensor and left-right alternation

Left-right hindlimb alternation as seen during locomotion, is mediated by a group of spinal neurons called commissural interneurons (CINs) that cross the ventral commissure and provide reciprocal coordination between the left and right sides of the spinal cord (Fong et al., 2009; Kiehn, 2006). CINs are classified into two main groups: (1) intersegmental CINs which have long axons that extend at least two segments (2) intrasegmental CINs (sCINs) which cross the midline but stay within the same segment. It is likely that sCINs are directly involved in coordinating segmental homogenous muscles whereas, CINs that descend multiple segments once they cross the midline (also known as dCINs, part of the intersegmental population) are thought to play a role in binding flexor-extensor synergies across the spinal cord (Kiehn et al., 2008). dCINs and sCINs have been studied extensively, and have been shown to be rhythmically

active during locomotion. dCINs and sCINs are composed of both glutamatergic and glycinergic neuronal types that terminate in a monosynaptic and polysynaptic fashion onto flexor and extensor motoneurons (Kiehn, 2006). If inhibitory input to contralateral motoneurons is blocked, such that only excitatory input remains, then the remaining excitatory input will convert the normally alternating rhythm between the left and right halves of the spinal cord into a "synchronous" rhythm (Kiehn & Butt, 2003). In other words, both limb flexor and extensor muscles will fire simultaneously ultimately turning a walking pattern into a hopping one.

It has been demonstrated in the mouse (Yunker et al., 2003), rat (Mynlieff & Beam, 1992), and chick (McCobb et al., 1989), that T-type Ca^{2+} channels are expressed throughout the ventral and dorsal regions of the spinal cord as early as embryonic day 14. Therefore, it is entirely possible that dCINs and sCINs of neonatal mice (P0-P3) possess an I_T component. Given that my data demonstrates a disruption of left-right and flexor-extensor alternation while in the presence of T-type channel blockade (Fig 6.1D), I hypothesized that I_T is potentially expressed amongst the dCIN and sCINs population of cells. In the next set of experiments, I sought to test this hypothesis.

6.2.3.1 T-type Ca^{2+} channels are likely expressed on commissural-projecting and ipsilaterally projecting populations of interneurons

In an attempt to localize which CPG interneurons express I_T, I performed a mid-sagittal sectioning of the spinal cord after it had been transferred to the recording chamber (Fig 6.4A – Ai; n = 5). A spinal cord that has been mid-sagittally cut will no longer have intact crossed connections via commissural interneurons, therefore the left-right alternation will no longer be representative of any locomotor network drive. However, the ipsilateral circuitry that is

responsible for flexor-extensor alternation will still be intact in both halves of the spinal cord (see Whelan et al., 2000). In these experiments, after mid-sagittal sectioning, the rhythmogenic drugs (DA, 5-HT, NMA) were administered. A rhythmic flexor-extensor alternation in the divided spinal cord emerged, thereby providing evidence that the ipsilateral circuitry necessary for flexor-extensor activity was still intact (Fig 6.4B). These results have been previously published by Whelan and colleagues (2000). Interestingly, in the presence of Ni^{2+} (200 μM), the remaining flexor-extensor alternation generated by the divided spinal cord converted into a much slower, synchronous rhythm (Fig 6.4Bi), despite having been mid-sagittally sectioned. These results provide preliminary evidence that T-type conductances are expressed and modulate both contralaterally and ipsilaterally projecting interneuronal networks in the neonatal mouse.

Chapter Six: FIGURES

Representative Control

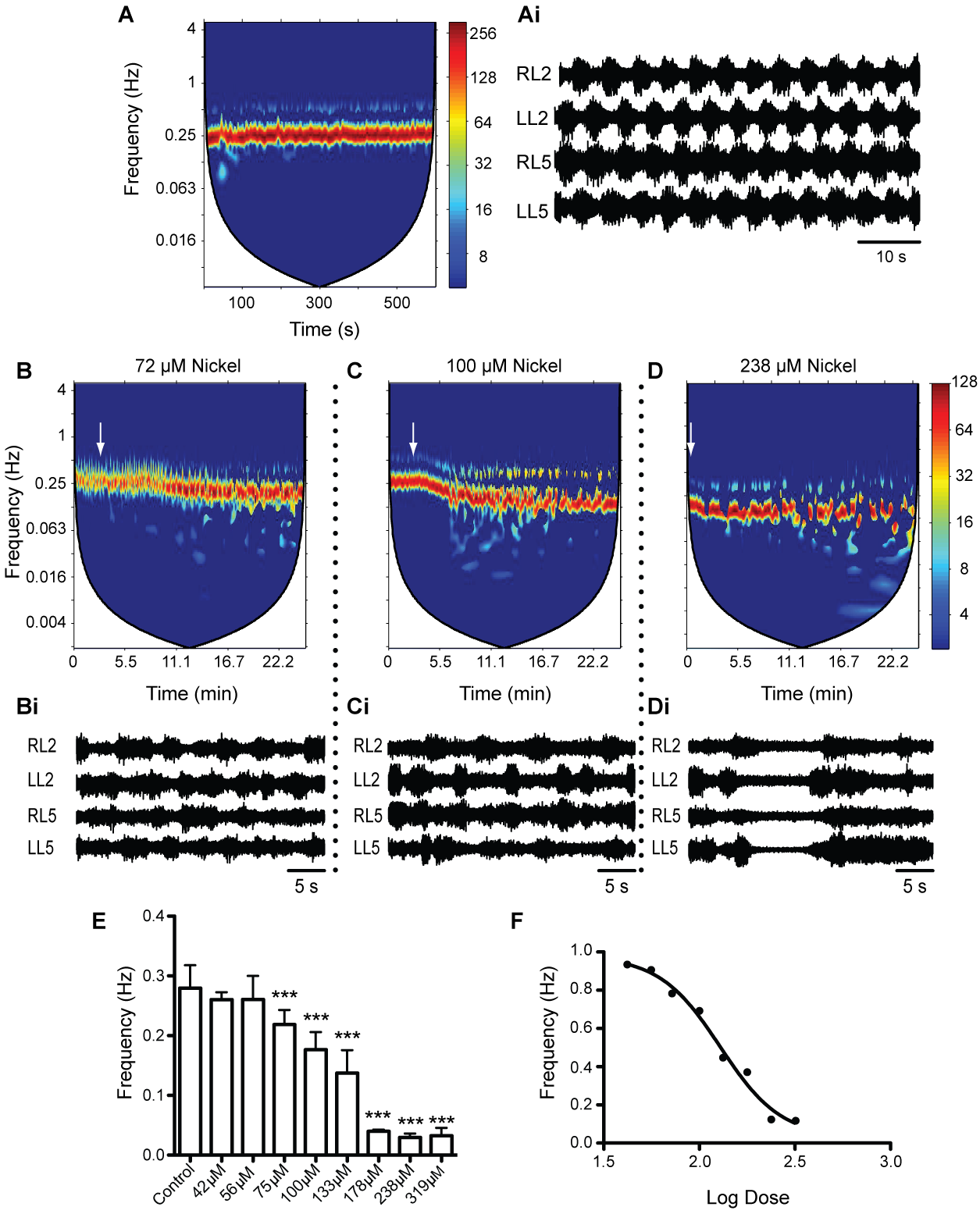

Figure 6.1: Blocking T-type Ca^{2+} channels with Ni^{2+} disrupts fictive locomotion in a concentration-dependent manner.

A: cross – wavelet spectrogram of the L2-L2 neurogram recordings depicting a representative 5-HT, NMA, DA-evoked locomotor rhythm over a 10 minute period. Raw traces from the right and left L2 and L5 neurogram recordings under control conditions with 5-HT, NMA and DA (Ai). Note: Ai is the same experiment as shown in A. B – D: cross – wavelet spectrogram of L2-L2 neurograms (25 min total) illustrating changes to the high power frequency band upon application of 72 μM Ni^{2+} (B), 100 μM Ni^{2+} (C), and 238 μM Ni^{2+} (D). Note: white arrows in spectrograms B – D indicate the point in time when Ni^{2+} was added during each experiment. Bi – Di: raw traces from the right and left L2 and L5 neurogram recordings illustrating the effects of 72 μM Ni^{2+} (Bi), 100 μM Ni^{2+} (Ci), and 238 μM Ni^{2+} (Di) to a 5-HT, NMA, DA-evoked locomotor rhythm. Raw traces are taken from same experiments in B – D. E: graph of the average frequency of bursts recorded following application of varying concentrations of Ni^{2+} (One-way ANOVA; $P < 0.001$). Error bars represent the SD. F: graph of the dose-response relationship between varying concentrations of Ni^{2+} and rhythm frequency.

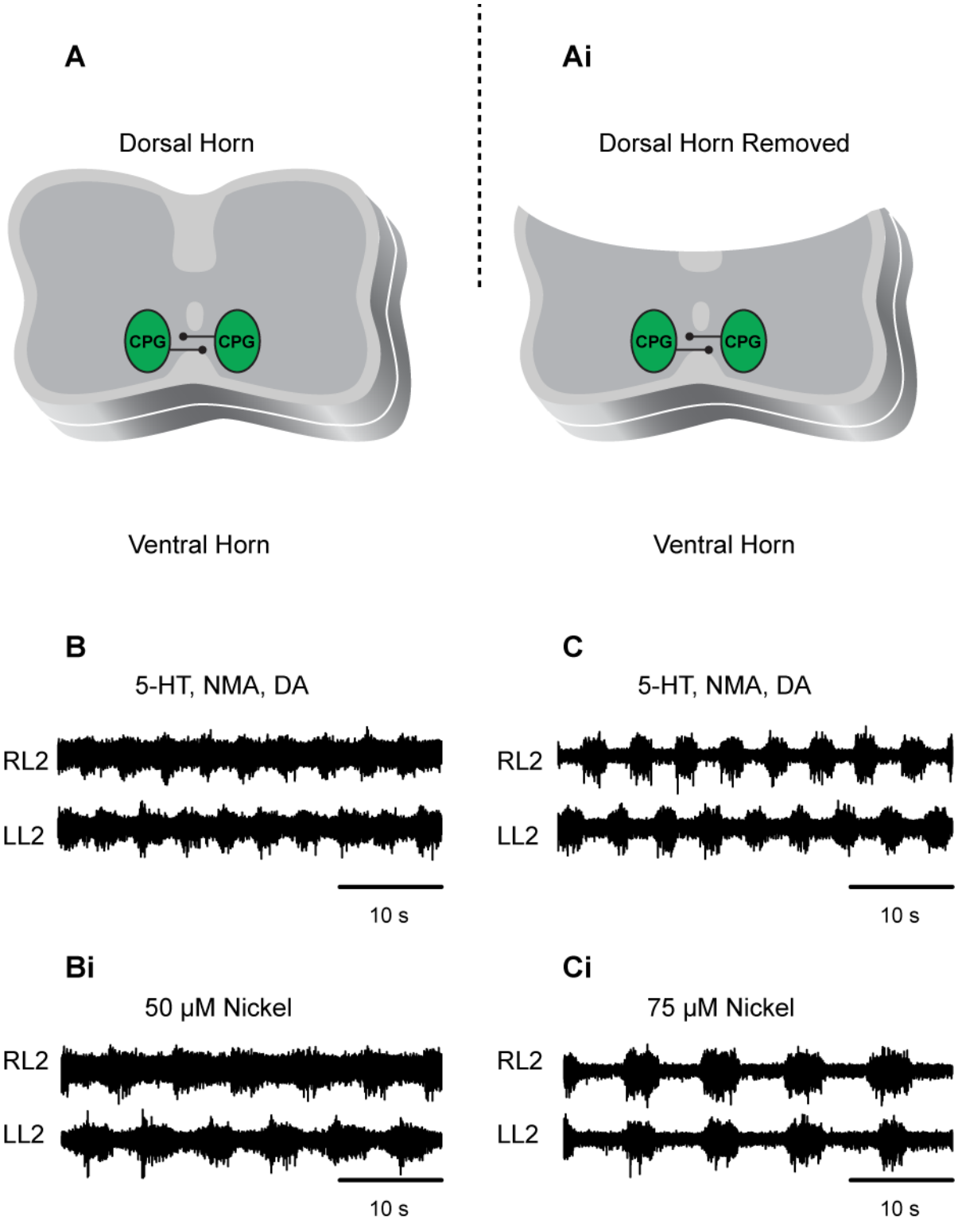
A
Dorsal Horn
CPG
CPG
Ventral Horn
Ai
Dorsal Horn Removed
CPG
CPG
Ventral Horn
B
5-HT, NMA, DA
RL2
LL2
10 s
C
5-HT, NMA, DA
RL2
LL2
10 s
Bi
50 µM Nickel
RL2
LL2
10 s
Ci
75 µM Nickel
RL2
LL2
10 s

Figure 6.2: Removal of the dorsal horn permits the actions of Ni^{2+} at lower concentrations.

A: schematic diagrams illustrating a cross sectional view of the intact spinal cord and CPG network at the lumbar level (A) and with 100 – 250 microns of the dorsal horn tissue removed (Ai). Note: In the dorsal horn removed preparation, the ventral horn and associated CPG interneuronal projections are still intact. B: raw traces from the right and left L2-L2 neurogram recordings under control conditions in the presence of 5-HT, NMA, DA (B) and with the addition of 50 μM Ni^{2+} (Bi). C: raw traces from the right and left L2-L2 neurogram recordings under control conditions with 5-HT, NMA, DA (C) and with the addition of 75 μM Ni^{2+} (Ci). Traces from B and C are taken from separate experiments.

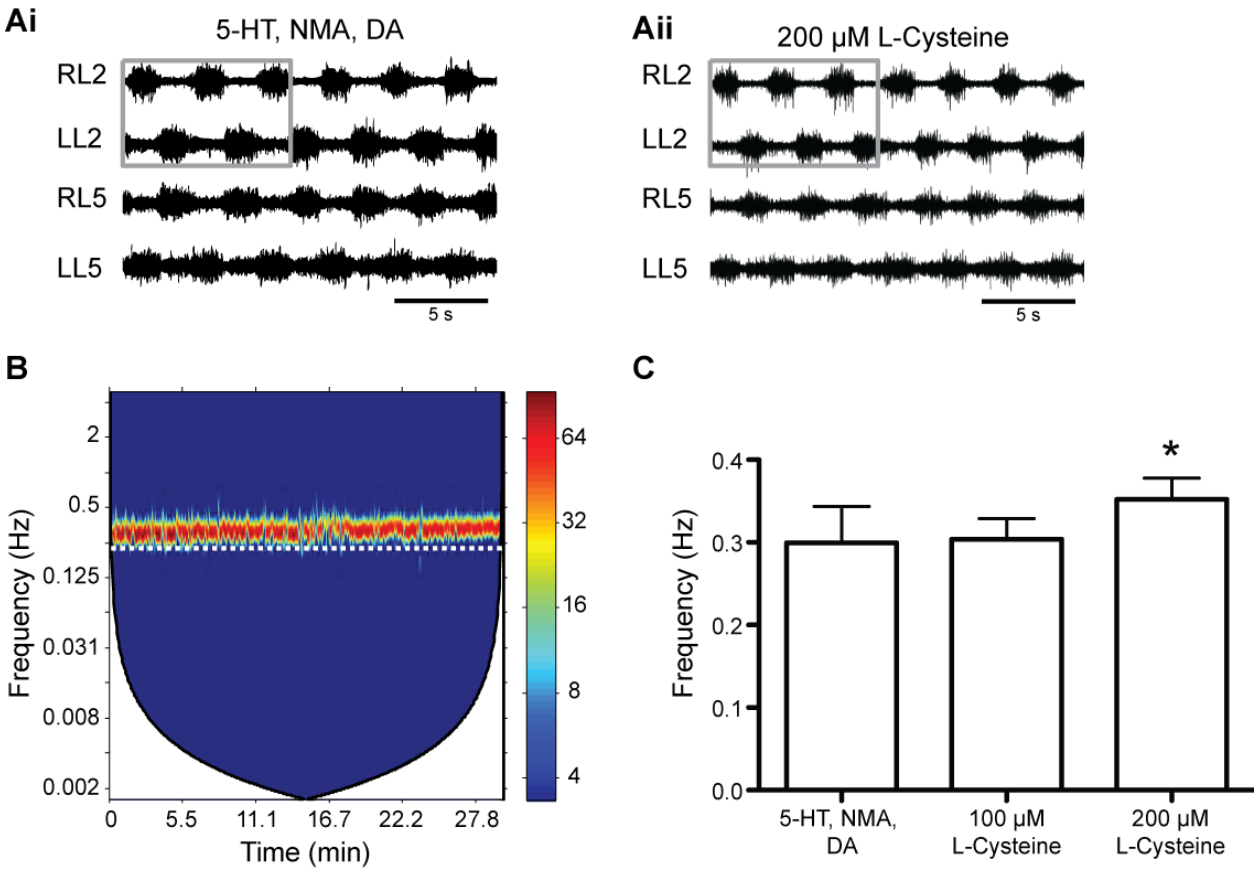
Ai
5-HT, NMA, DA
RL2
LL2
RL5
LL5
5 s
Aii
200 µM L-Cysteine
RL2
LL2
RL5
LL5
5 s
B
Frequency (Hz)
2
0.5
0.125
0.031
0.008
0.002
0
5.5
11.1
16.7
22.2
27.8
Time (min)
64
32
16
8
4
C
Frequency (Hz)
0.4
0.3
0.2
0.1
0.0
*
5-HT, NMA, DA
100 µM L-Cysteine
200 µM L-Cysteine

Figure 6.3: T-type Ca^{2+} channel agonist L-Cysteine increases the frequency of a 5-HT, NMA, DA-evoked locomotor rhythm.

A: raw traces of the left and right L2 and L5 ventral root neurograms illustrating changes in rhythm frequency under 5-HT, NMA, DA (control) conditions (Ai), and with the addition of L-Cysteine (200 μM) (Aii). Grey box is identical in both traces, and has been placed around the first three bursts of the right L2 recordings under control and L-Cysteine conditions. B: cross – wavelet spectrogram of L2-L2 neurograms (30 min) illustrating changes to the high power frequency band upon application of L-Cysteine. Dotted line indicates control baseline and is meant to highlight the change in frequency of the high power frequency band from 0.29 Hz to 0.35 Hz (same experiment as A). C: graph comparing rhythm frequency under control conditions and with the addition of 100 μM and 200 μM L-Cysteine ($P < 0.05$; one-way ANOVA; $n = 6$). Error bars indicate SD.

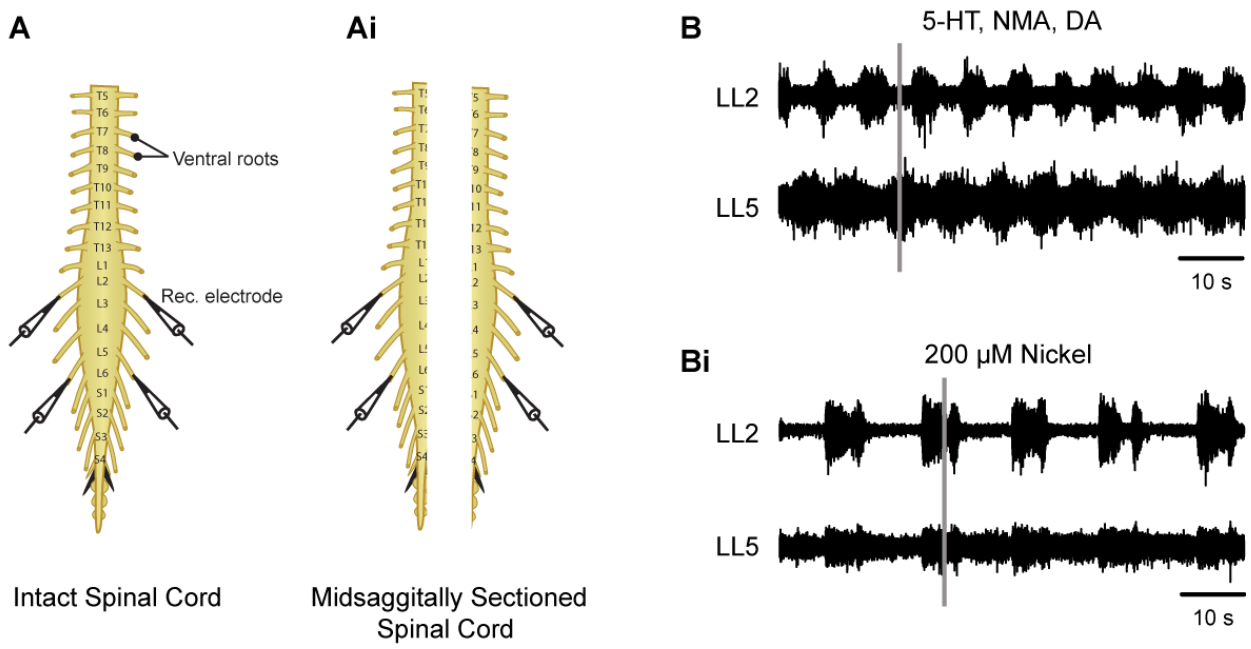
A
Ai
B
Bi
Ventral roots
Rec. electrode
Intact Spinal Cord
Midsaggitally Sectioned Spinal Cord
5-HT, NMA, DA
LL2
LL5
10 s
200 µM Nickel
LL2
LL5
10 s

Figure 6.4: Ni^{2+} application to a mid-sagittally-sectioned spinal cord converts an alternating rhythm between flexors and extensors into a synchronous rhythm.

A: schematic diagrams illustrating the intact isolated spinal cord and recording set up (A) and the isolated spinal cord that has been mid-sagittally sectioned (Ai). B: raw traces from the left L2-L5 (LL2, LL5) neurogram recordings under 5-HT, NMA, DA conditions (control) (B) and with the addition of 200 μM Ni^{2+} (Bi). Grey line indicates the presence of an alternating rhythm (B) and synchronous bursting (Bi).

Chapter Six: TABLES

Table 6.1: T-type Ca^{2+} channel antagonists and their effectiveness related to the current work

I_T Antagonist	**Concentration**	**Effect on locomotor rhythm**
Ni^{2+}	42 – 319 μM	Yes
Amiloride	500 μM	Yes
Mibefradil	2 – 10 μM	No
NNC 55-0396	10 μM	No
TTA-P2	3 – 10 μM	No

6.3 DISCUSSION

6.3.1 General remarks

In the present study, I examined the role of I_T in the generation and maintenance of an ongoing drug-evoked locomotor rhythm in the neonatal mouse. Here, I provide evidence that pharmacologically blocking I_T alters several aspects of a drug-evoked rhythm, including rhythm frequency and the alternation of left-right and flexor-extensor activity in the neonatal mouse isolated spinal cord. Specifically, I found that in a dose-dependent manner the I_T antagonist Ni^{2+} slows the rhythm frequency, and eventually converts an alternating rhythm into one of synchrony. These data support an important role for I_T in the generation and maintenance of a fictive drug-evoked locomotor rhythm. Combined with my previous findings (Chapter 5), I_T appears to be a crucial current both at the rhythm-generating layer of the CPG network, and at the level of motor output.

6.3.2 Contribution of I_T to the emergence and maintenance of drug-evoked fictive locomotion

When the modulation of a particular ion channel exerts visible changes to the frequency or pattern of fictive locomotor output, it suggests that that ion channel plays an important role within the CPG network. The relative accessibility and simplicity of the lamprey spinal cord have allowed for experimental and modeling studies to investigate the role for I_T during fictive swimming behavior (Grillner, Wallén, Hill, Cangiano, & Manira, 2001; Matsushima et al., 1993; Tegnér et al., 1997). This pioneering work revealed an important role for I_T contributing to the stabilization of a fictive locomotor swimming rhythm, likely through the promotion of burst

initiation in classes of excitatory interneurons (Grillner et al., 2001; Matsushima et al., 1993; Tegnér et al., 1997).

Within the mammalian spinal cord, I_T has been studied within the context of Hb9 interneurons (Anderson et al., 2012; Wilson et al., 2005; Ziskind-Conhaim, Wu, & Wiesner, 2008). However at the time the current work was conducted, the role of I_T in the generation and maintenance of mammalian locomotor-like behavior had not been investigated. In all likelihood this has been because of issues identifying selective I_T antagonists. In recent years, Ni^{2+} has been found to possess a high affinity for Cav3.2 with lower affinity for Cav3.1 and 3.3 (Lee et al., 1999; Perez-Reyes, 2003). Several lines of evidence suggest that in both slice and midsagittaly sectioned preparations, Ni^{2+} (100 μM) is effective in suppressing drug-induced (NMA, 5-HT, DA) TTX-resistant voltage oscillations of Hb9 interneurons and motoneurons (Wilson et al., 2005; Ziskind-Conhaim et al., 2008). It was concluded from this work that Ni^{2+} was most likely antagonizing Cav3 channels, which was further supported by the voltage dependency of the oscillatory response (Wilson et al., 2005; Ziskind-Conhaim et al., 2008). Based on this work, low concentrations Ni^{2+} should provide an effective method for testing the effects of I_T on locomotor pattern generation.

Using the midsaggitally sectioned spinal cord preparation, Ziskind-Conhaim et al., (2008) observed that at both the Hb9 interneuronal and motoneuronal levels, Ni^{2+} application not only reduced the amplitude of drug-induced voltage oscillations, but simultaneously reduced the frequency of the membrane oscillations within both neuronal populations. Their observations were made in the presence of fast synaptic blockers and TTX, thereby effectively isolating Hb9 interneurons and motoneurons from any network influence. It is possible that synaptically isolated neurons may operate differently while under the influence of the CPG network (Berg,

Alaburda, & Hounsgaard, 2007). Therefore, my current work expands on the existing findings that Ni^{2+} slows the frequency of voltage oscillations at the cellular level (Wilson et al., 2005; Ziskind-Conhaim et al., 2008), by demonstrating that Ni^{2+} also produced a similar decrease in rhythm frequency generated at the level of the CPG network (Fig 6.1B) Moreover, the importance of T-type Ca^{2+} channels within the context of the CPG network was highlighted by the fact that blocking I_T converted a left-right, flexion-extension alternating rhythm into one of synchrony (Fig 6.1D). Collectively, this work suggests T-type Ca^{2+} channels contribute to rhythmogenesis and CPG network output in the neonatal mouse spinal cord.

6.3.3 The effects of Ni^{2+} are not mediated by R-type Ca^{2+} channels

The potential for T-type Ca^{2+} channels to exert a rhythmogenic and modulatory influence on fictive locomotor patterns was also recognized by another group (Anderson et al., 2012). Unfortunately, Dr. Whelan and I were unaware that the current data was being replicated and expanded upon at the time of our experimentation. However, since Anderson and colleagues (2012) were able to publish their findings, my data can now be considered an in-depth replication of published work. Additionally, a number of experiments were identical between my current work and the published work of Anderson and colleagues (2012), and therefore we can consider this a validation of my results. For example, Anderson et al., (2012) found that increasing concentrations of Ni^{2+} slow the frequency of a drug-evoked locomotor rhythm. Additionally, they reported that with high enough concentrations of Ni^{2+}, a synchronous rhythm would emerge.

Throughout the course of my experiments, I became aware of some important caveats regarding the exclusive use of Ni^{2+} as the sole I_T antagonist in my studies. Specifically at this time, I recognized that my results were somewhat ambiguous based on two important issues: (1)

the high voltage activated R-type Ca^{2+} channels (Cav2.3) display a similar sensitivity to low concentrations of Ni^{2+} that T-type Ca^{2+} do (Huguenard, 1996; Kang, Moon, Joo, & Lee, 2007; Perez-Reyes, 2003; Randall & Tsien, 1997; Todorovic & Lingle, 1998; Tsien et al., 1988; Zamponi et al., 1996) and (2) even after removing the dorsal horn tissue from the isolated spinal cord, presumably increasing drug accessibility, I could not replicate the effects of Ni^{2+} with any other commonly used T-type antagonists other than amiloride (see below).

To address the first potential caveat, that the Ni^{2+} effects on rhythm frequency and alternation were mediated by R-type Ca^{2+} channels rather than the hypothesized T-type Ca^{2+} channels, I proposed an experiment (Humphreys & Whelan, 2009) whereby I would apply the highly specific R-type Ca^{2+} blocker SNX-482 (Newcomb et al., 1998) during a drug-evoked fictive locomotor rhythm and monitor subsequent changes to rhythm parameters. However prior to testing the R-type Ca^{2+} channel blocker, Anderson and colleagues (2012) published their manuscript, which included the previously proposed experiment. It was found that application of R-type Ca^{2+} blocker SNX-487 (100 nM) did not disturb a drug-evoked fictive locomotor rhythm, thereby suggesting that the observed reduction in rhythm frequency, and the eventual conversion from an alternating rhythm into a synchronous rhythm upon Ni^{2+} application was likely mediated by blocking I_T. Thus, by examining for a possible R-type contribution to the effects observed upon Ni^{2+} application to rhythm frequency and alternation, Anderson and colleagues (2012) reduced some of the initial ambiguity within my own data.

6.3.4 Caveats related to T-type Ca^{2+} channel pharmacology

During the course of my experiments, the only additional I_T antagonist that reproduced the same effects observed with Ni^{2+} application was amiloride (500 μM). Although amiloride

was initially manufactured to target epithelial Na^+ channels in the management of hypertension and congestive heart failure (Bull & Laragh, 1968; Ramsay et al., 1983) the ability of amiloride to block T-type Ca^{2+} channels has well been documented (Hirano, Fozzard, & January, 1989; Tang et al., 1988; Tytgat et al., 1990). Even though amiloride is considered a traditional pharmacological agent for identifying T-type Ca^{2+} channels in more recent work, significant differences in the IC_{50} for amiloride have been reported (Herrington & Lingle, 1992; Tang et al., 1988). Additionally, the IC_{50} for amiloride in blocking mouse Cav3 channels is ~ 25-fold higher than what has been reported in humans (Lacinová, Klugbauer, & Hofmann, 2000; Williams et al., 2002). A recent study in human Cav3 channels demonstrated that amiloride preferentially blocks Cav3.2 channels (Lopez-Charcas, Rivera, & Gomora, 2012), however the discrepancies between Cav3 channels in human and the mouse still remain. Therefore, I sought to find an additional I_T antagonist to reproduce the effects of Ni^{2+}.

After it's discovery in the 1990's, mibefradil became known as the first selective, organic I_T blocker (Clozel et al., 1997). However, it was later demonstrated that mibefradil could block a number of other ion channels, namely HVA Ca^{2+} channels (Viana et al., 1997), Na^+ channels (Eller et al., 2000), K^+ channels (Liu et al., 1999) and Cl^- channels (Nilius et al., 1997). This finding led to the development of a more stable analogue of mibefradil, NNC 55-0396 (Huang, 2004; Li, Hansen, Huang, Keyser, & Taylor, 2006). NNC 55-0396 displays an acute IC_{50} of ~ 7 μM in order to block recombinant T-type channels expressed in human embryonic kidney 293 (HEK293). Additionally, up to 100 μM NNC 55-0396 has been shown to exert no detectable effect on HVA currents, at least in a line of insulin secreting cells (Huang, 2004; Li et al., 2006). Therefore, in an attempt to reproduce the actions of Ni^{2+} on a drug-evoked fictive locomotor

rhythm, I tested the effects of both mibefradil and NNC 55-0396, plus a relatively new I_T antagonist TTA-P2 (Choe et al., 2011; Uebele et al., 2009).

In contrast to data collected by Anderson et al., (2012), when I applied NNC 55-0396 in my current work there were no observable changes to the ongoing drug-evoked locomotor rhythm. This was also true upon application of mibefradil and TTA-P2 (Table 6.1). When one considers the extra tissue present in en bloc preparations compared to slice tissues, it becomes plausible that the lack of effect could be the result of a drug penetration issue. In agreement with this hypothesis, mibefradil, NNC 55-0396, and TTA-P2 all have a molecular weight greater than 550 g/mol and are hydrophobic. Along these lines, amiloride mimicked the effects of Ni^{2+} which may be due to fact that this drug is lipophilic and has a lower molecular weight (less than 300 g/mol) (Kleyman & Cragoe, 1988).

It should be noted that the working concentrations for the I_T antagonists used in this study were based on known IC_{50} curves for these drugs, which were established by performing whole-cell patch clamp recordings in either the slice preparation or cultured cells (Choe et al., 2011; Clozel et al., 1997; Huang, 2004; Shipe et al., 2008; Uebele et al., 2009). It should also be noted that Anderson and colleagues required 100 μM NNC 55-0396 to observe an effect vs. my working concentration of 10 μM NNC 55-0396. Therefore, one possible explanation for the discrepancy between my data and that published was that my working concentration was too low and was unable to diffuse through the spinal tissue to the layer of the CPG network. However on the other hand, Anderson and colleagues (2012) were using a working concentration of NNC 55-0396 (100 μM) that was ~ 15 times higher than the reported IC_{50} (~ 7 μM) for this I_T antagonist (Huang, 2004). Therefore, another possibility to explain the discrepancies in my data and that of Anderson et al., (2012) is that Anderson and colleagues were observing non-specific actions of

NNC 55-0396 application. Interestingly, a lack of specificity may explain why Anderson et al., (2012) reported that NNC 55-0396 irreversibly abolished motor output all together. These findings are in contrast to the effects of Ni^{2+} application in that even upon high concentrations (> 300 μM, Fig 6.1), Ni^{2+} did not abolish motor output. Instead, maximal concentrations Ni^{2+} consistently converted a stable alternating 5-HT, NMA, DA-evoked rhythm into a synchronous rhythm, which was re-established once again as an alternating rhythm upon wash. Therefore, based on the fact that Anderson and colleagues (2012) required a concentration of NNC 55-0396 that was ~15 times higher than the reported IC_{50}, in addition to the fact that at this concentration, NNC 55-0396 irreversibly abolished motor output, suggests that the latter of the two explanations for the discrepancies between my data and that published is more likely.

To further rule out potential drug diffusion problems, I utilized a dorsal-horn removed preparation. Indeed, lower concentrations of Ni^{2+} achieved the same effects on the drug-evoked rhythm (i.e. slower frequency and an eventual conversion to synchrony). However, mibefradil still exerted no effect. These results could be interpreted in one of two ways: (1) either mibefradil was still not penetrating the cord or (2) mibefradil successfully reached the CPG network and did not exert any changes to the locomotor rhythm by blocking I_T. However, given my results with Ni^{2+} and amiloride, plus my results that T-type agonist L-Cysteine had the reverse effect and potentiated the frequency of a drug-evoked rhythm (Fig 6.3), the latter interpretation is less likely.

In a final attempt to solidify a role for T-type Ca^{2+} channels in rhythmogenesis and maintenance of ongoing locomotion, I decided to use green fluorescent protein (GFP) tagged small interference ribonucleic acid (siRNA) to knockdown Cav3.1, Cav3.2 and Cav3.3

expression[2]. The experimental protocol required intrathecal injections of siRNA at birth (P0) and pups were sacrificed 4 days later (P4). During these experiments (n = 17), a 5-HT, NMA, DA-evoked rhythm was evoked. Once the rhythm stabilized, 100 μM Ni^{2+} was applied. In all injected preparations examined, application of Ni^{2+} resulted in a disruption of the drug-induced locomotor rhythm, suggesting that the siRNA was not successful in knocking down Cav3 expression. My electrophysiological findings were confirmed by a complete lack of GFP expression in injected spinal cords. One possible explanation for my negative data is due to fact that the intrathecal space of neonatal mice is extremely small. Unlike other studies that have utilized intrathecal injections of neonatal mice (Fedorova, Battini, Prakash-Cheng, Marras, & Gusella, 2006), I injected mice using a 30 gauge needle attached to a Hamilton syringe, rather than a ultra-fine needle attached to an microsyringe. Therefore it is entirely possible the siRNA injections were unsuccessful. Another possibility is that the siRNA used was not pure. One way to address this potential issue would be to utilize HEK cell technology to over-express Cav3 channels, and then subsequently test whether addition of the same GFP tagged siRNA used in my work would knockdown Cav3 expression.

In summary, my results, and those of Anderson and colleagues (2012) provide evidence that T-type Ca^{2+} channels play an important role in locomotor rhythmogenesis. Although the effects of Ni^{2+} and amiloride on a fictive locomotor rhythm could not be replicated by other T-type pharmacology in my current work, Anderson and collegeaues (2012) found that 100 μM NNC 55-0396 was capable of abolishing a drug-evoked locomotor rhythm. To further elucidate the role of T-type Ca^{2+} channels during mammalian locomotor behavior, our future experiments will extend my current *in vitro* findings in the neonatal mouse, to *in vivo* work in the adult.

[2] Dr. Whelan and I would like to acknowledge Dr. Gerald Zamponi for providing us with the siRNA constructs.

Recently, our lab published a report documenting the advantages of using the adult mouse decerebrate preparation (Nakanishi & Whelan, 2012), and we are fully equipped to perform experiments with this preparation. A major advantage of this preparation is the ability to directly record from neurons in the spinal cord of adult mouse decerebrate preparation during sustained bouts of stepping *in vivo*, while in the absence of anesthetic drugs. Therefore, the adult mouse decerebrate preparation is a highly attractive model for studying the role of T-type Ca^{2+} channels in locomotion throughout development.

Chapter Seven: General discussion

7.1 GENERAL DISCUSSION

7.1.1 General remarks

Rhythmic motor behaviors such as chewing, respiration, and locomotion are under the control of dedicated networks of interneurons called central pattern generators (CPGs) (Grillner, 2006; Kiehn, 2006). Although the mechanisms supporting rhythm generation have not fully been elucidated, neuromodulatory influences upon CPGs endow these networks the ability to produce a wide range of network configurations that enable behavioral flexibility. The ability of neuromodulators such as the monoamine transmitters 5HT, NA, and DA to modulate CPG circuits has been of long standing interest in the field of motor control. Much of what we know regarding the monoaminergic modulation of mammalian locomotor spinal circuits has been derived from studies investigating the role of 5HT and NA. In comparison, the exact role for DA has been largely understudied. Therefore, the goal of my work was to shed light on the ability of DA to function as a neuromodulator of mammalian locomotor CPG circuits. Based on what we know regarding DA's diverse actions within the mammalian brain (Missale et al., 1998; Neve et al., 2004), and given that there is a widespread distribution of DA receptors within the spinal cord, I hypothesized that DA could exert complex neuromodulatory actions on mammalian locomotor rhythm generating spinal circuitry. Below I will discuss my work in relation to previous findings regarding DA's effects on network function.

7.1.2 DA is an important regulator of CPG network function

My electrophysiology results using the isolated spinal cord confirm and extend previous work (Barriere et al., 2004; Gordon & Whelan, 2006b; Jiang et al., 1999; Madriaga et al., 2004; Schotland et al., 1995; Whelan et al., 2000) implicating a role for DA as a potent modulator of locomotor CPG circuits. Assessment of my *in vitro* isolated spinal cord experiments reveals two distinct roles for DA in modulating locomotor CPG network output. First, DA can act as a powerful facilitator of CPG network output in the neonatal mouse if the network has been pre-activated by 5-HT and NMA. Second, DA can exert an inhibitory break on CPG network function, which may ultimately help to ensure the emergence of stable rhythmic output by controlling for possible hyper-excitability of CPG networks. The opposing roles for DA that have emerged from my work will be further discussed in the following section.

7.1.2.1 Opposing effects of DA in other CPG systems: what we can learn from invertebrate models

Much of our understanding on mammalian network function is based on pioneering experiments performed on invertebrate preparations (Dickinson, 2006; Harris-Warrick et al., 1998; Marder, 2012; Peck et al., 2001). In a recent review, Marder (2012) urges today's researchers to stop "reinventing the wheel" when it comes to circuit modulation, but instead to start drawing upon available knowledge obtained using small-circuit animals. Clearly important lessons can be learned from examining less complex networks. Therefore I will briefly discuss my findings in relation to the actions of DA in smaller circuit animals, namely the crustacean stomatogastric ganglion.

My work features the widespread actions of DA on the locomotor CPG network within a mammalian model system. Specifically, I have shown that DA facilitates some avenues of CPG recruitment while it inhibits others. At first, the opposing actions of DA on CPG network function were surprising (Chapter 3 vs. Chapter 4). How can one neuromodulator function to stabilize network output, and then function to completely shut down network activity all together? This question may be difficult to answer in a complex neural system such as that of the mammal. Interestingly, the opposing actions of DA are not unique to the complex neural system of the neonatal mouse. Indeed, there is a wealth of knowledge characterizing the conflicting actions of DA on CPG circuit parameters in the stomatogastric ganglion of the lobster *Panulirus interruptus* (Harris-Warrick et al., 1998). The stomatogastric ganglion (STG) of the lobster is a small ganglion of 30 neurons that controls rhythmic feeding movements of the foregut (Harris-Warrick, Marder, Selverston, & Moulins, 1992). The STG is composed of two CPG networks, the slow gastric mill and the pyloric network which functions to control rhythmic pumping and filtering movements of the foregut. The pyloric network is composed of only 14 neurons and is one of the best understood CPG networks, such that under certain experimental conditions, all the composite neurons and synaptic connections have been mapped out (Harris-Warrick et al., 1998; Marder & Thirumalai, 2002). DA has been shown to modulate nearly all the cellular and synaptic properties of the pyloric network, and often does so by exerting opposing effects on components of the CPG (Harris-Warrick et al., 1998). Given that the final output of any CPG network is the combination of network properties, intrinsic cellular properties and synaptic interactions of the circuit (Calabrese, 1995; 1998; Harris-Warrick, 2010; Pirtle & Satterlie, 2007; Prinz et al., 2004) it would be useful to draw upon readily available knowledge from the STG

regarding how DA modulates ionic conductances and synaptic properties. By doing so, we can begin to appreciate DA's function in a more complex CPG network.

A common target of DAergic modulation in the pyloric network is the K^+ current I_A, which is an important determinant of cycle frequency and phasing activity of cells that compose the pyloric network (Kloppenburg, Levini, & Harris-Warrick, 1999). DA has been shown to modulate I_A in nearly every pyloric neuron, but the underlying mechanisms are different (Harris-Warrick et al., 1998; Kloppenburg et al., 1999). A primary example comes from the rhythm-generating core of the pyloric network, which is composed of the anterior burster (AB) cell type and two pyloric dilator (PD) neurons. These cells are electrically coupled together and function as the major pacemakers for network function. DA has been shown to inhibit PD neuronal activity which contributes to a reduction in spike frequency of this cell type by enhancing I_A (Kloppenburg et al., 1999), while simultaneously exciting the AB neuron cell type by reducing the maximal conductance of I_A. In addition to differentially modulating two distinct cell types, DA can exert opposing actions within an individual neuron of the STG by acting on the different ionic conductances expressed (Harris-Warrick et al., 1998).

The second major mechanism subject to opposing neuromodulatory actions of DA is the ability of DA to alter the synaptic interactions that connect the network together. Several lines of evidence in the pyloric network highlight the ability of DA to strengthen some synaptic connections and weaken others (Johnson & Harris-Warrick, 1990; Johnson, Peck, & Harris-Warrick, 1993; 1994). Taken together, it is thought that the final motor output of the pyloric network is a *population response* of all the composite neurons and synapses to the actions of DA and other modulators present. Since my findings demonstrate that DA drives opposing changes in network function within the mammalian system, it therefore provides incentive for future

studies to explore the actions of DA on the underlying synaptic connections and intrinsic properties of the spinal cord network in the mouse.

7.1.2.2 Conflicting actions of DA: possible explanations

There are several possible reasons why DA exerts conflicting actions on the underlying cellular and synaptic properties that give rise to network function. First, DA's opposing actions on CPG network components may simply mirror remnants of ongoing developmental processes that give rise to potentially non-specific effects of second messenger systems. A consequence of DAergic activation of metabotropic receptors is the initiation of a sequence of biochemical events that modify proteins, enzymes, and ion channels (Greengard, 2001; Missale et al., 1998; Neve et al., 2004). For example, DA differentially modulates the activity of the effector protein adenylate cyclase in either an excitatory or inhibitory fashion depending on the activation of either D_1 – like and/or D_2 – like receptors respectively, which has important down stream effects (Greengard, 2001). With regards to my work in the neonatal mouse, it is entirely possible that these down stream effects differ between the neuronal populations that comprise the CPG network, and may be in place to help fine tune CPG development. Second, the concentration of exogenously applied DA in my experiments may account for differences in network output. This point highlights a caveat within the experimental paradigm I and many other labs have adopted. Although exogenous application of modulators such as DA allows for researchers to infer what their physiological role may be, it does not reproduce the distinct concentration profile critical for the proper expression of modulator actions that would normally be seen by neural stimulation *in vivo* (Brezina, 2010; Marder, 2012). Third, and perhaps the most compelling reason why DA may exert opposing modulatory actions on CPG network function may be to stabilize the newly

modulated state of the CPG network in order to prevent *over-modulation* and potentially disorganized output (Harris-Warrick & Johnson, 2010). This notion of "over-modulation" has recently been put forth by Harris-Warrick and Johnson (2010) and suggests that while the presence of neuromodulators, such as DA, endow CPG networks with essential behavioral flexibility, there is the coincident risk that neuromodulators may decrease network efficiency. Over-modulated networks may become unstable and cease to function appropriately. Interestingly, this may explain my findings that DA can facilitate some aspects of network function, but also provide an "inhibitory break" via recurrent collateral pathways (Chapter 4; Fig 4.6) If seen from this perspective, this may be an example of DA constraining it's own modulatory influence in an attempt to limit the systems' flexibility and therefore maintain stable motor output.

7.1.3 Global modulation of monoaminergic systems

In my work, the ability of DA to stabilize a 5-HT, NMA-evoked locomotor rhythm highlights two very important roles for DA in the modulation of neonatal mouse CPG circuits: (1) DA can function as an independent neuromodulator, such that DA's actions alone exert changes to the ongoing rhythm frequency, stability and burst amplitude, (2) When put into context, my findings are consistent with a potentially bigger picture - one that reflects on the ability of monoaminergic systems to interact *globally* in order to produce a behavioral effect, in this case locomotion. The collective effort made by monoaminergic systems to inhibit incoming sensory information, such as nociceptive information (Basbaum & Fields, 1984; Garraway & Hochman, 2001; Jacobs & Fornal, 1993) is a primary example of how these transmitter systems function in tandem in order to produce a global effect, as this is achieved through activation of 5-

HTergic receptors 5-HT_{1A} and 5-HT_{1B}, NAergic receptor α_2, and DAergic receptor D_2 – like receptors (Kiritsy-Roy et al., 1994; Pertovaara, 1993; Zemlan, Murphy, & Behbehani, 1994, Clemens & Hochman, 2004). Therefore, while it was my goal to elucidate the exclusive role of DA as a neuromodulator of neonatal mouse spinal circuits, it must be acknowledged that under physiological conditions, DA works in tandem with multiple other neuromodulators (i.e. monoamines, amino acids, and peptides) (Miles & Sillar, 2011). Therefore, it is necessary to briefly discuss my findings regarding DA in relation to other monoaminergic systems during locomotion.

An immense amount of data has accumulated to show how monoaminergic systems together exert global modulatory effects on behaviors such as locomotion (Brezina, 2010). From this work, we have learned what combinations of monoamine transmitters best evoke locomotor-like activity within a desired model system. In the mouse for example, my work and that of others (Jiang et al., 1999; Whelan et al., 2000) has shown that combined application of 5-HT and NMA can produce varied bouts of rhythmic alternation. This induced activity is often disorganized, such that it is not well synchronized between the two halves of the spinal cord (Whelan et al., 2000). It is for this reason that I chose to use the "5-HT and NMA" combination of exogenous drugs (Chapter 3; Fig 3Bi) to spotlight the additive effects of DA (Chapter 3; Fig 3Bii and Biii). In the neonatal rat, however, 5-HT and NMA either added individually or in combination consistently evokes stable locomotor-like activity (Cazalets et al., 1992; Cowley & Schmidt, 1994b; Kudo & Yamada, 1987b). This discrepancy between species is likely due to differences in receptor distribution within the CPG network. Interestingly, the ability of 5-HT and NMA to sometimes induce locomotor-like activity in the neonatal mouse appears to be lost in a more mature mouse preparation (age P6 and older), as the addition of DA is necessary at this

point in time to induce locomotor-like activity (Jiang et al., 1999). Therefore throughout development, it is a combination of monoamine transmitters plus excitatory amino acids that is best able to produce stable rhythmic alternating locomotor-like activity, at least in the mouse. It remains unknown in the mature rat what combination of monoamines effectively elicits locomotor-like activity.

At a cellular level, several lines of study have examined the complementary actions of monoaminergic systems by focusing on the ability of monoamine transmitters to similarly modulate cellular mechanisms in order to achieve the stable behavioral output. Indeed, work in the STG of the lobster (Peck et al., 2001) and the lamprey (Wang et al., 2011) have demonstrated that 5-HT and DA can exert the same effects on different ionic conductances that govern different cellular firing patterns, in order to achieve a specific motor output. On the other hand, this is not always the case. For example, a study in the lamprey (Schotland et al., 1995) has shown that both 5-HT and DA function to reduce the intrinsic cellular property of AHPs in CPG interneurons, however what is remarkable about this finding is that the cellular mechanisms by which DA and 5-HT exert their complementary actions on AHPs were distinctly different. Furthermore, numerous reports have documented the ability of monoaminergic systems to exert differential effects on the neuronal behavior of sensory-motor circuits (Calejesan, Ch'ang, & Zhuo, 1998; Martin, Gupta, Loo, Rohde, & Basbaum, 1999). This does not mean that, under these circumstances, monoaminergic systems do not function in tandem. Instead, perhaps this demonstrates a degree of flexibility within monoaminergic systems. Specifically, this may be a way of coordinating the modulation of multiple transmitters within the sensory-motor circuit in an attempt to avoid over-modulation and to maintain functional circuit performance during modulation. If the desired output of a system is stable motor behavior, such as locomotion,

regardless of which direction monoaminergic systems exert their individual effects at the cellular and synaptic level, if stable locomotor like activity is induced then they have done their job.

In summary, monoamines have the powerful ability to independently tweak different cellular and synaptic properties in order to achieve a desired behavioral output. The idea of "global modulation" is often not acknowledged, as we typically see studies highlighting the function of a particular neuromodulator within a neural system (Cazalets et al., 1992; Clemens & Hochman, 2004; Dunbar et al., 2010). While knowledge regarding the individual modulatory roles for monoamine transmitters is not without its value, it is necessary to keep in mind that their actions are never executed alone within a circuit. This may be important for the future development of monoaminergic treatment therapies for individuals who have suffered from spinal cord injury.

7.1.4 DA in the brain

The discovery over 50 years ago that DA was not merely just an intermediate in the biosynthesis of catecholamine transmitters NA and adrenaline, but also a functional transmitter in the CNS (Carlsson, 1957) was of great importance in our understanding of monoamine function (Björklund & Dunnett, 2007a; Carlsson, Lindqvist, & Magnusson, 1957; J. R. Cooper, Bloom, & Roth, 2003; Greengard, 2001; Missale et al., 1998; Sibley, 1999). DAergic systems in the brain have been the subject of extensive investigation, mainly because several neurological and psychiatric diseases, notably Parkinsonism, schizophrenia, Attention Deficit Hyperactivity Disorder (ADHD), and drug abuse, have been linked to dysregulation of DA transmission (Beaulieu & Gainetdinov, 2011; Missale et al., 1998). Studies examining DA receptor function, and the subsequent downstream intracellular signaling mechanisms, have led to the development

of clinical applications for the treatment of various DA-related disorders. Indeed, this knowledge has led to the improvement of new paradigms for understanding the role of DA at a systems level. Such frameworks can provide the opportunity to comprehend the interactions between DA and other systems, such as the locomotor CPG network in the spinal cord.

The work presented in my thesis highlights the ability of DA to exert diverse and complex actions on the emergence and maintenance of locomotor activity. These effects are mediated through the activation of two distinct DA receptor families. While D_2 – like receptor activation did contribute to the stabilizing effect of DA during a pre-existing locomotor rhythm and decreased the rhythm frequency, it was the activation of this DA receptor family that was solely responsible for shutting down locomotor-like behavior during ventral root-evoked locomotion (Fig 4.2) Therefore, D_2 – like receptors appear to occupy a very important role in spinal cord motor function. Interestingly, this is not the first account of D_2 – like receptors exerting complex physiological actions within the CNS in relation to movement. Below is a brief discussion regarding the role of DA in the brain, specifically the basal ganglia, and how this knowledge relates to my findings in the spinal cord.

7.1.4.1 The role of DA receptors in the basal ganglia

The fact most brain dopamine is confined to the basal ganglia has provided the impetus to explore this group of nuclei in the control of movement (Clark & White, 1987; J. R. Cooper et al., 2003; Jackson & Westlind-Danielsson, 1994; Missale et al., 1998). The main components of the basal ganglia are illustrated in Figure 7.1.

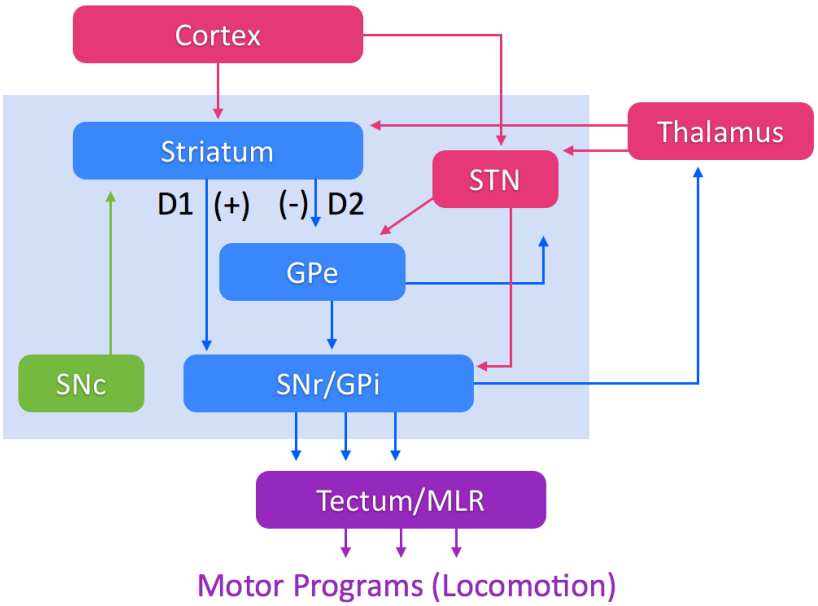

Figure 7.1 The organization of the basal ganglia.
The striatum, globus pallidus externa (GPe), globus pallidus interna (GPi) and substantia nigra pars reticulata (SNr) consist of GABAergic neurons (blue). SNr and GPi collectively represent the output of the basal ganglia, and send projections of neurons to different motor centers such as the tectum, and the mesencephalic locomotor region (MLR), and also the thalamus. The indirect pathway is represented by striatal projections (which express D2 receptors) to the GPe, the subthalamic nucleus (STN), and the output level (SNr/GPi). The direct pathway is represented by striatal projections onto the SNr/Gpi, which express D1 receptors. Excitatory glutamatergic neurons are in pink. Inhibitory pathways are in blue. The major source of DA is the substantia nigra pars compacta (SNc) (green).

The striatum serves as the major "input layer" of the basal ganglia, as it receives many projections from different brain regions. The major "output layer" of the basal ganglia is composed of two nuclei, the globus pallidus interna (GPi) and the substantia nigra pars reticulata (SNr), and will be referred to collectively as pallidal output from here on out. Pallidal nuclei give rise to tonically active GABAergic neurons that project to different motor centers in the brainstem, such as the mesencephalic locomotor region (MLR) (Swanson, 2000; Swanson, Mogenson, Gerfen, & Robinson, 1984). These neurons are tonically active at rest, and therefore

maintain a continuous level of inhibition over different motor centers during resting conditions (Grillner, Hellgren, Ménard, Saitoh, & Wikström, 2005; Ménard, Auclair, Bourcier-Lucas, Grillner, & Dubuc, 2007; Takakusaki, Saitoh, Harada, & Kashiwayanagi, 2004). In order to initiate a motor program, motor centers need to be released from pallidal inhibition. This requires an inhibition of pallidal output from the striatum (Grillner et al., 2005; Grillner, Wallén, Saitoh, Kozlov, & Robertson, 2008; Ménard et al., 2007) and is accomplished via activation of D_1 – like receptors on striatal projection neurons. Striatal projections are categorized into one of two types, one which projects directly to the pallidal output layer of the basal ganglia and express D_1 – like receptors. The second type of striatal neuronal projections express D_2 – like receptors and indirectly project to the pallidal output layer by way of the globus pallidus externa (GPe) – subthalamic nucleus (STN) route (Fig 7.1). Remarkably, the highly organized structure and intricate workings of the basal ganglia has been conserved throughout the vertebrate phylogeny (Grillner, Robertson, & Stephenson-Jones, 2013; Stephenson-Jones, Ericsson, Robertson, & Grillner, 2012; Stephenson-Jones, Samuelsson, Ericsson, Robertson, & Grillner, 2011).

7.1.4.1.1 D_1 – like receptors

In this system, activation of D_1 – like receptors are primarily involved in the initiation of motor behavior, such as locomotion, via a disinhibition of pallidal output to motor centers. Indeed, it has been demonstrated that in wild type mice, administration of selective D_1 – like agonist SKF-81297 resulted in increased locomotor activity (Xu et al., 1994). Perhaps even more interesting was the finding that when the D_1 – like antagonist SCH-23390 was administered, wild type mice exhibited hypoactivity and immobility (Xu et al., 1994). Moreover, D_1 receptor activation has been shown to mediate increases in other motor activities, such as grooming

behavior (Zhang, Zhou, & Weiss, 1994). Therefore, it appears that activation of D_1 – like receptors are key to the descending control of locomotor activity and other motor behaviors. These findings are in agreement with my own work, such that I have found D_1 – like agonist SKF-81297 to facilitate 5-HT, NMA-evoked locomotor-like activity (Chapter 3; Fig 3.2Bi), while SCH-23390 application disrupted a 5-HT, NMA locomotor-like rhythm (data not shown).

7.1.4.1.2 D_2 – like receptors

Locomotion and other motor behaviors are inhibited by way of D_2 – like receptor activation on the indirect projection pathway of the basal ganglia. Activation of D_2 – like receptors lower the excitability of the GPe, which in turn reduces tonic inhibition of the STN. Therefore, the activity of the STN increases and ultimately enhances inhibitory output onto motor centers. This has been the "classical" role for the D_2 – like receptors within the basal ganglia. However, just as I have found in the spinal cord, it is now widely accepted that the role for D_2 – like receptors in the brain is much more complex than originally thought (Beaulieu & Gainetdinov, 2011; Missale et al., 1998; Sibley, 1999). Unlike D_1 – like receptors, which are exclusively expressed postsynaptically, D_2 – like receptors in the brain have presynaptic *and* postsynaptic localizations and functions (De Mei, Ramos, Iitaka, & Borrelli, 2009; Missale et al., 1998; Sibley, 1999; Wolf & Roth, 1990). DAergic nerve terminals throughout many regions of the brain, including the striatum, possess presynaptic D_2 receptors termed autoreceptors that generally serve as an important negative feedback mechanism (Wolf et al., 1990; Beaulieau et al., 2011). Stimulation of D_2 autoreceptors results in a decreased DA synthesis and release, and can dramatically slow the firing rate of DA neurons (De Mei et al., 2009; Missale et al., 1998; Sibley, 1999; Wolf & Roth, 1990). Indeed it is largely the activation of D_2 autoreceptors in the

striatum that leads to the reduction in locomotor activity (Jackson & Westlind-Danielsson, 1994; Missale et al., 1998). This contrasts with the mechanisms by which DA inhibits locomotion in my own work given that there is very little evidence for the expression of D_2 autoreceptors in the spinal cord, specifically in the ventral horn where the motor circuits reside. Instead, a presynaptic expression of D_3 and D_4 receptors have been reported on primary afferent terminals and descending projections from the A11, both of which are mostly restricted to the dorsal horn (Levant, 1997).

Just as I have found in the spinal cord, there is a dual functionality for D_2 – like receptors in the brain. Several lines of evidence have reported that stimulation of postsynaptic D_2 receptors slightly increases locomotor ability (Missale et al., 1998; Sibley, 1999). Furthermore, studies utilizing gene targeting approaches have demonstrated that knocking out the D_2 receptors reduced several measures of locomotor ability as tested in a series of open field tests (Kelly et al., 1998). Taken together with my findings in the spinal cord, which are consistent with those in the brain, it appears that both DA receptor signaling systems can facilitate and inhibit locomotion.

7.1.4.2 Significance of DA in the brain and spinal cord

It is clear that in both the brain and spinal cord, the presence of DA is important for the production and maintenance of stable locomotor activity. This is highlighted in the brain by several pathological conditions such as Parkinson's disease (PD), which is characterized by a loss of nigrostriatal DAergic neurons (Albanese, 1990). Parkinsonian patients display symptoms such as tremor at rest, slowness of movement, and rigidity of the head and neck. The administration of the DA agonists and the DA precursor L-DOPA are effective in alleviating

symptoms of PD, including rescuing some locomotor function. Interestingly, my work demonstrates that the administration of DA and DA agonists to a pre-existing unstable locomotor-like rhythm at the level of the spinal cord is also capable of securing stable rhythmic output from locomotor CPG circuits. Collectively this work highlights the importance of DA as a facilitator of locomotion both in the brain and at the level of the spinal cord. Moreover, it appears that neural systems in the brain and spinal cord achieve fine control over motor activity by balancing a dynamic interplay between excitation and inhibition which is in part mediated by the activation of D_1 – like and D_2 – like receptors.

7.1.5 Potential mechanisms by which DA potentiates locomotor network activity

7.1.5.1 Postinhibitory rebound

As previously discussed, the half-center model of CPG organization is reliant upon reciprocal inhibitory connections in order to generate stable rhythmic output, and was first proposed by Brown in order to explain the flexion and extension phases of cat locomotion (T. G. Brown, 1914). Many efforts have gone into investigating the dynamics supporting alternation of the half-centers in an attempt to understand why each neuron makes it's transition between activated and inhibited states (Jankowska, Jukes, Lund, & Lundberg, 1967a; 1967b; McCrea & Rybak, 2007; Skinner, Kopell, & Marder, 1994). It has been found that network, synaptic, and intrinsic membrane properties contribute to the potentiation of rhythmicity generated by reciprocally coupled networks (Calabrese, 1998; Harris-Warrick, 2010; Pirtle & Satterlie, 2007; Prinz et al., 2004). Given that the intrinsic membrane property of PIR produces an excitation upon release of inhibition, it is believed that PIR contributes to the phase transitioning between the half-centers. Evidence from the swimming CPG of the *Clione limacina* suggests that the

strength of PIR is increased by the presence of 5-HT, and that this is correlated with the acceleration of swimming behavior (Satterlie & Norekian, 1995). Additionally my work and that of others in the neonatal mouse demonstrates that blocking T-type Ca^{2+} channels, a crucial conductance underlying the expression of PIR (Chapter 5), significantly slows down and can disrupt an ongoing locomotor rhythm (Chapter 6) (Anderson et al., 2012). Therefore, it is possible that the DAergic modulation of PIR at the level of the motoneuron, as I have demonstrated in my work (Chapter 5) could have important downstream effects which likely result in the enhanced build up of tetanic contractile force in flexor and extensor motoneuron pools. Since DA can increase the PIR capacity of motoneurons, then it is possible that DA could increase the PIR capacity of interneurons that comprise the CPG network. Moreover, the fact that DA increases the firing frequency of the PIR response at the cellular level (Fig 5.2 A – C; Fig 5.3 A and B) suggests the possibility that this could be one of the mechanisms DA acts upon to promote the stabilization of a pre-existing 5-HT, NMA induced locomotor rhythm (Humphreys & Whelan, 2012; Kiehn & Kjaerulff, 1996; Madriaga et al., 2004; Whelan et al., 2000).

7.1.5.2 Recurrent collateral pathways

Rhythmogenesis has been traditionally thought of as being produced by networks of spinal interneurons, while motoneurons serve solely as the "final common output" of the system (Kiehn, 2006). However, multiple lines of evidence from the developing spinal cord are now challenging this dogma, suggesting that motoneurons are indeed part of the rhythm generating circuitry (Hanson & Landmesser, 2003; O'Donovan et al., 2010; Wenner & O'Donovan, 2001). It is now well recognized that stimulation of motor axons in ventral roots or muscle nerves can lead to the activation of the CPG network via excitatory recurrent collateral pathways (Chapter 4)

(Bonnot et al., 2009; Humphreys & Whelan, 2012; Machacek & Hochman, 2006; Mentis et al., 2005). Based on my current findings, that DA application enhances the PIR response and therefore firing frequency of motoneurons, (Chapter 5), I speculate that the firing frequency of recurrent collaterals would increase as well. This would further suggest that via recurrent collateral pathways, DA's actions on PIR could potentially *strengthen* feedback loops onto the CPG network thereby contributing to the stabilizing effect observed during a pre-existing locomotor rhythm (Chapter 3). It should be noted that in response to ventral root stimulation, recurrent collaterals release an excitatory amino acid (Mentis et al., 2005; Nishimaru et al., 2005; O'Donovan et al., 2010) that activate mGluR receptors on postsynaptic interneurons which are presumably part of the CPG. Without a negative feedback mechanism in place, the DAergic increase in motoneuronal PIR could send the CPG network into overdrive via overly excited recurrent collaterals. Therefore, I propose that the D_2 – like receptor-mediated depression of CPG activity I observed in my work (Chapter 4), together with the 5-HT receptor-mediated depression of recurrent collateral pathways observed by Machacek and colleagues (2006), is in place in order to prevent over-excitability of CPG network function. Accordingly, by increasing the firing capacity of motoneurons and subsequently that of recurrent collaterals, DA's overall action in this context would result in a stabilizing effect on network function.

Although my published work has demonstrated that DA application during ventral root stimulation completely shuts down CPG network activity (Chapter 4) (Humphreys & Whelan, 2012), this may be an extreme reflection of what happens under physiological conditions. That is not to say that DA does not depress recurrent collateral activity under physiological conditions, but it is unlikely that a complete shut down of network function would occur. One must keep in mind that this extreme effect of DA could very likely be dependent upon the mode of activation.

During the course of these experiments, the electrical stimulus (4 Hz; 2-10 μA) that was used to evoke a response likely recruited a synchronous activation of all motor axons, not normally seen *in vivo*. Additionally this was not a robust method of recruiting locomotor-like activity, as it was only successful in ~ 25% of my preparations, a finding that was consistent with other reports (Bonnot et al., 2009). This suggests that while recurrent collateral pathways indeed have access to the CPG network, their primary function is likely *not* to recruit network function but perhaps rather to *modulate* it. Finally, the concentration of DA that was bath applied (50 μM) during the course of ventral root-evoked locomotion vs. the concentration that would actually be released synaptically following physiological activation of recurrent collaterals is noteworthy. Experimental DA application most likely activates not only all DA receptors (D_1-D_5), but possibly cross activates other monoaminergic receptors such as 5-HT (Madriaga et al., 2004). Furthermore, what we do know is that DA has been shown to potentiate network function during a pre-existing locomotor rhythm (Humphreys & Whelan, 2012; Kiehn & Kjaerulff, 1996; Madriaga et al., 2004; Whelan et al., 2000), and that these effects carry on throughout development as DA and it's agonists have been shown to potentiate stepping in the adult mouse (Lapointe et al., 2009).

7.1.6 Future directions

In order to further establish how DA functions within the spinal cord, the following future studies are necessary:

(i) *To determine whether or not endogenous DA release can enhance locomotor stability, which was observed upon exogenous DA application*. This could be accomplished with two different approaches: (1) by blocking DA reuptake within the *in vitro*

isolated spinal cord preparation or (2) by using an *in vivo* adult mouse model combined with an optogenetic approach to activate the A11 region which has been hypothesized to be the sole source of spinal DA (although this is subject to debate at the moment (Barraud et al., 2010)). The latter experiments are being carried out in our lab currently.

(ii) *To further understand the importance of D_2 – like receptor activation during locomotion by using a D_2 knockout mouse*. The aim of this study would be to utilize the D_2 knockout mouse *in vitro* isolated spinal cord preparation and repeat the 5-HT, NMA-evoked locomotor experiments (Chapter 3) and the ventral root stimulation experiments (Chapter 4).

(iii) *To further ascertain the effects of DA on I_T and I_h, which mediate PIR in motoneurons*. This would be accomplished using the whole cell patch configuration, under voltage clamp conditions.

(iv) *To demonstrate the actions of DA on the PIR response of ventrally located* ***interneurons*** *that may comprise the locomotor CPG, such as the Hb9 cell type* (Han et al., 2007). These studies would expand on my data at the level of the motoneurons and provide valuable information relating to DA's role in the rhythmogenesis and maintenance of locomotor activity.

(v) *To further investigate the role for T-type Ca^{2+} channels during locomotor behavior*. As previously discussed, these studies will utilize the adult decerebrate mouse preparation (Chapter 6). These studies will not only further our understanding for a role of I_T in the emergence and maintenance of locomotion, but will expand our knowledge of I_T throughout locomotor development.

7.1.7 Final conclusion

While the initiation and maintenance of locomotion is highly dependant upon the presence of DA within the CNS, most studies have aimed at understanding DA's functional role within the brain (Anzalone et al., 2012; Beaulieu & Gainetdinov, 2011; Björklund & Dunnett, 2007b; Missale et al., 1998; Neve et al., 2004; Sibley, 1999). The relatively small number of neuroscientists that have targeted DA's function within CPG networks have focused on invertebrate or lower vertebrate systems (Harris-Warrick et al., 1998; Schotland et al., 1995). Accordingly, there is a relatively large gap in our knowledge of how DA modulates the mammalian locomotor CPG.

The research presented in this thesis highlights the ability of the monoamine transmitter, DA, to potently modulate of CPG network function. These studies improve our knowledge of DA by providing a detailed account of how DA modulates different intrinsic properties of motoneurons, namely PIR, and provide insight as to DA's effects on network function. Since the activation of DAeric receptors can both facilitate and inhibit network function at the level of the spinal cord, control of DA receptor activation may provide new therapeutic strategies for individuals who have suffered spinal cord injury, specifically those who have experienced a loss of descending monoaminergic control.

WORK CITED

Akagi, H., Konishi, S., Otsuka, M., & Yanagisawa, M. (1985). The role of substance P as a neurotransmitter in the reflexes of slow time courses in the neonatal rat spinal cord. *British journal of pharmacology*, *84*(3), 663–673.

Albanese, A. (1990). Extrapyramidal system, motor Ganglia and movement disorders. *Reviews in the neurosciences*, *2*(3), 145–164. doi:10.1515/REVNEURO.1990.2.3.145

Alvarez, F. J., Pearson, J. C., Harrington, D., Dewey, D., Torbeck, L., & Fyffe, R. E. (1998). Distribution of 5-hydroxytryptamine-immunoreactive boutons on alpha-motoneurons in the lumbar spinal cord of adult cats. *The Journal of comparative neurology*, *393*(1), 69–83.

Anderson, T. M., Abbinanti, M. D., Peck, J. H., Gilmour, M., Brownstone, R. M., & Masino, M. A. (2012). Low-threshold calcium currents contribute to locomotor-like activity in neonatal mice. *Journal of neurophysiology*, *107*(1), 103–113. doi:10.1152/jn.00583.2011

Angstadt, J. D., & Friesen, W. O. (1993). Modulation of swimming behavior in the medicinal leech. I. Effects of serotonin on the electrical properties of swim-gating cell 204. *Journal of comparative physiology. A, Sensory, neural, and behavioral physiology*, *172*(2), 223–234.

Angstadt, J. D., Grassmann, J. L., Theriault, K. M., & Levasseur, S. M. (2005). Mechanisms of postinhibitory rebound and its modulation by serotonin in excitatory swim motor neurons of the medicinal leech. *Journal of comparative physiology. A, Sensory, neural, and behavioral physiology*, *191*(8), 715–732. doi:10.1007/s00359-005-0628-6

Anzalone, A., Lizardi-Ortiz, J. E., Ramos, M., De Mei, C., Hopf, F. W., Iaccarino, C., et al. (2012). Dual control of dopamine synthesis and release by presynaptic and postsynaptic dopamine D2 receptors. *The Journal of neuroscience : the official journal of the Society for Neuroscience*, *32*(26), 9023–9034. doi:10.1523/JNEUROSCI.0918-12.2012

Ashrafi, S., Lalancette-Hébert, M., Friese, A., Sigrist, M., Arber, S., Shneider, N. A., & Kaltschmidt, J. A. (2012). Wnt7A identifies embryonic γ-motor neurons and reveals early postnatal dependence of γ-motor neurons on a muscle spindle-derived signal. *The Journal of neuroscience : the official journal of the Society for Neuroscience*, *32*(25), 8725–8731. doi:10.1523/JNEUROSCI.1160-12.2012

Ayali, A., Johnson, B. R., & Harris-Warrick, R. M. (1998). Dopamine Modulates Graded and Spike-Evoked Synaptic Inhibition Independently at Single Synapses in Pyloric Network of Lobster. *Journal of …*.

Bains, J. S., Longacher, J. M., & Staley, K. J. (1999). Reciprocal interactions between CA3 network activity and strength of recurrent collateral synapses. *Nature neuroscience*, *2*(8), 720–726. doi:10.1038/11184

Baldessarini, R. J., & Fischer, J. E. (1978). Trace amines and alternative neurotransmitters in the central nervous system. *Biochemical Pharmacology*, *27*(5), 621–626. doi:10.1016/0006-2952(78)90495-1

Ballion, B., Branchereau, P., Chapron, J., & Viala, D. (2002). Ontogeny of descending serotonergic innervation and evidence for intraspinal 5-HT neurons in the mouse spinal cord. *Developmental Brain Research*, *137*(1), 81–88. doi:10.1016/S0165-3806(02)00414-5

Barbeau, H., & Rossignol, S. (1991). Initiation and modulation of the locomotor pattern in the adult chronic spinal cat by noradrenergic, serotonergic and dopaminergic drugs. *Brain research*, *546*(2), 250–260.

Barbeau, H., Chau, C., & Rossignol, S. (1993). Noradrenergic agonists and locomotor training affect locomotor recovery after cord transection in adult cats. *Brain research bulletin*, *30*(3-4), 387–393.

Barraud, Q., Obeid, I., Aubert, I., Barriere, G., Contamin, H., McGuire, S., et al. (2010). Neuroanatomical study of the A11 diencephalospinal pathway in the non-human primate. *PloS one*, *5*(10), e13306. doi:10.1371/journal.pone.0013306

Barriere, G., Mellen, N., & Cazalets, J.-R. (2004). Neuromodulation of the locomotor network by dopamine in the isolated spinal cord of newborn rat. *The European journal of neuroscience*, *19*(5), 1325–1335. doi:10.1111/j.1460-9568.2004.03210.x

Barrio, L. C., Araque, A., & Buño, W. (1994). Participation of voltage-gated conductances on the response succeeding inhibitory synaptic potentials in the crayfish slowly adapting stretch receptor neuron. *Journal of neurophysiology*, *72*(3), 1140–1151.

Basbaum, A. I., & Fields, H. L. (1984). Endogenous pain control systems: brainstem spinal pathways and endorphin circuitry. *Annual review of neuroscience*, *7*, 309–338. doi:10.1146/annurev.ne.07.030184.001521

Basbaum, A. I., Zahs, K., Lord, B., & Lakos, S. (1988). The fiber caliber of 5-HT immunoreactive axons in the dorsolateral funiculus of the spinal cord of the rat and cat. *Somatosensory research*, *5*(3), 177–185.

Beaulieu, J.-M., & Gainetdinov, R. R. (2011). The Physiology, Signaling, and Pharmacology of Dopamine Receptors. *Pharmacological reviews*.

Berg, R. W., Alaburda, A., & Hounsgaard, J. (2007). Balanced inhibition and excitation drive spike activity in spinal half-centers. *Science (New York, N.Y.)*, *315*(5810), 390–393. doi:10.1126/science.1134960

Berger, A. J., & Takahashi, T. (1990). Serotonin enhances a low-voltage-activated calcium current in rat spinal motoneurons. *The Journal of neuroscience : the official journal of the Society for Neuroscience*, *10*(6), 1922–1928.

Berry, M. D. (2004). Mammalian central nervous system trace amines. Pharmacologic amphetamines, physiologic neuromodulators. *Journal of neurochemistry*, *90*(2), 257–271. doi:10.1111/j.1471-4159.2004.02501.x

Bertrand, S., & Cazalets, J. R. (1998). Postinhibitory rebound during locomotor-like activity in neonatal rat motoneurons in vitro. *Journal of neurophysiology*, *79*(1), 342–351.

Biel, M., Wahl-Schott, C., Michalakis, S., & Zong, X. (2009). Hyperpolarization-Activated Cation Channels: From Genes to Function. *Physiological Reviews*, *89*(3), 847–885. doi:10.1152/physrev.00029.2008

Biostatistical Analysis. (2009). *Biostatistical Analysis* (5(null) ed.). Prentice Hall.

Biscoe, T. J., Nickels, S. M., & Stirling, C. A. (1982). Numbers and sizes of nerve fibres in mouse spinal roots. *Quarterly journal of experimental physiology (Cambridge, England)*, *67*(3), 473–494.

Björklund, A., & Dunnett, S. B. (2007a). Fifty years of dopamine research. *Trends in neurosciences*, *30*, 185–187.

Björklund, A., & Dunnett, S. B. (2007b). Dopamine neuron systems in the brain: an update. *Trends in neurosciences*, *30*(5), 194–202. doi:10.1016/j.tins.2007.03.006

Bonnot, A., Chub, N., Pujala, A., & O'Donovan, M. J. (2009). Excitatory actions of ventral root stimulation during network activity generated by the disinhibited neonatal mouse spinal cord. *Journal of neurophysiology*, *101*(6), 2995–3011. doi:10.1152/jn.90740.2008

Bonnot, A., Whelan, P. J., Mentis, G. Z., & O'Donovan, M. J. (2002). Locomotor-like activity generated by the neonatal mouse spinal cord. *Brain research. Brain research reviews*, *40*(1-3), 141–151.

Bortolozzi, A., Díaz-Mataix, L., Scorza, M. C., Celada, P., & Artigas, F. (2005). The activation of 5-HT receptors in prefrontal cortex enhances dopaminergic activity. *Journal of neurochemistry*, *95*(6), 1597–1607. doi:10.1111/j.1471-4159.2005.03485.x

Bras, H., Cavallari, P., Jankowska, E., & McCrea, D. (1989). Comparison of effects of monoamines on transmission in spinal pathways from group I and II muscle afferents in the cat. *Experimental Brain Research*, *76*(1), 27–37. doi:10.1007/BF00253620

Braun, A. R., & Chase, T. N. (1986). Obligatory D-1/D-2 receptor interaction in the generation of dopamine agonist related behaviors. *European journal of pharmacology*, *131*(2-3), 301–306.

Brezina, V. (2010). Beyond the wiring diagram: signalling through complex neuromodulator networks. *Philosophical transactions of the Royal Society of London. Series B, Biological sciences*, *365*(1551), 2363–2374. doi:10.1098/rstb.2010.0105

Brocard, F., Tazerart, S., & Vinay, L. (2010). Do Pacemakers Drive the Central Pattern Generator for Locomotion in Mammals? *The Neuroscientist*, *16*(2), 139–155. doi:10.1177/1073858409346339

Brown, T. G. (1911). The Intrinsic Factors in the Act of Progression in the Mammal. *Proceedings of the Royal Society of London Series B*.

Brown, T. G. (1914). On the nature of the fundamental activity of the nervous centres; together with an analysis of the conditioning of rhythmic activity in progression, and a theory of the evolution of function in the nervous system. *The Journal of physiology*, *48*(1), 18–46.

Brownstone, R. M., & Wilson, J. M. (2008). Strategies for delineating spinal locomotor rhythm-generating networks and the possible role of Hb9 interneurones in rhythmogenesis. *Brain research reviews*, *57*(1), 64–76. doi:10.1016/j.brainresrev.2007.06.025

BULL, M. B., & LARAGH, J. H. (1968). Amiloride: a potassium-sparing natriuretic agent. *Circulation*, 45–53.

Burchett, S. A., & Hicks, T. P. (2006). The mysterious trace amines: protean neuromodulators of synaptic transmission in mammalian brain. *Progress in neurobiology*, *79*(5-6), 223–246. doi:10.1016/j.pneurobio.2006.07.003

Burke, R. E., Degtyarenko, A. M., & Simon, E. S. (2001). Patterns of locomotor drive to motoneurons and last-order interneurons: clues to the structure of the CPG. *Journal of neurophysiology*, *86*(1), 447–462.

Butt, S. J. B., Harris-Warrick, R. M., & Kiehn, O. (2002). Firing properties of identified interneuron populations in the mammalian hindlimb central pattern generator. *The Journal of neuroscience : the official journal of the Society for Neuroscience*, *22*(22), 9961–9971.

Calabrese, R. L. (1995). Oscillation in motor pattern-generating networks. *Current opinion in neurobiology*, *5*(6), 816–823.

Calabrese, R. L. (1998). Cellular, synaptic, network, and modulatory mechanisms involved in rhythm generation. *Current opinion in neurobiology*, *8*(6), 710–717.

Calejesan, A. A., Ch'ang, M. H. C., & Zhuo, M. (1998). Spinal serotonergic receptors mediate facilitation of a nociceptive reflex by subcutaneous formalin injection into the hindpaw in rats. *Brain research*, *798*(1-2), 46–54. doi:10.1016/S0006-8993(98)00394-1

Carlsson, A., Lindqvist, M., & Magnusson, T. (1957). 3,4-Dihydroxyphenylalanine and 5-hydroxytryptophan as reserpine antagonists. *Nature*, *180*(4596), 1200–1200. doi:10.1038/1801200a0

Catterall, W. A., Striessnig, J., Snutch, T. P., & Perez-Reyes, E. (2003). International Union of Pharmacology. XL. Compendium of Voltage-Gated Ion Channels: Calcium Channels. *Pharmacological ….*

Cazalets, J. R., Sqalli-Houssaini, Y., & Clarac, F. (1992). Activation of the central pattern generators for locomotion by serotonin and excitatory amino acids in neonatal rat. *The Journal of physiology*, *455*, 187–204.

Cazalets, J.-R., Gardette, M., & Hilaire, G. (2000). Locomotor Network Maturation Is Transiently Delayed in the MAOA-Deficient Mouse. *Journal of ….*

Chandler, S. H., Hsaio, C. F., Inoue, T., & Goldberg, L. J. (1994). Electrophysiological properties of guinea pig trigeminal motoneurons recorded in vitro. *Journal of ….*

Choe, W., Messinger, R. B., Leach, E., Eckle, V. S., Obradovic, A., Salajegheh, R., et al. (2011). TTA-P2 Is a Potent and Selective Blocker of T-Type Calcium Channels in Rat Sensory Neurons and a Novel Antinociceptive Agent. *Molecular Pharmacology*, *80*(5), 900–910. doi:10.1124/mol.111.073205

Christie, K. J., & Whelan, P. J. (2005). Monoaminergic Establishment of Rostrocaudal Gradients of Rhythmicity in the Neonatal Mouse Spinal Cord. *Journal of neurophysiology*, *94*(2), 1554–1564. doi:10.1152/jn.00299.2005

Clarac, F., Vinay, L., Cazalets, J. R., Fady, J. C., & Jamon, M. (1998). Role of gravity in the development of posture and locomotion in the neonatal rat. *Brain research. Brain research reviews*, *28*(1-2), 35–43.

Clark, D., & White, F. J. (1987). Review: D1 dopamine receptor?the search for a function: A critical evaluation of the D1/D2 dopamine receptor classification and its functional implications. *Synapse (New York, N.Y.)*, *1*(4), 347–388. doi:10.1002/syn.890010408

Clemens, S., & Hochman, S. (2004). Conversion of the Modulatory Actions of Dopamine on Spinal Reflexes from Depression to Facilitation in D3 Receptor Knock-Out Mice. *The Journal of neuroscience*.

Clemens, S., Belin-Rauscent, A., Simmers, J., & Combes, D. (2012). Opposing modulatory effects of D1- and D2-like receptor activation on a spinal central pattern generator. *Journal of neurophysiology, 107*(8), 2250-2259.

Clemens, S., Rye, D., & Hochman, S. (2006). Restless legs syndrome: revisiting the dopamine hypothesis from the spinal cord perspective. *Neurology*, *67*(1), 125–130. doi:10.1212/01.wnl.0000223316.53428.c9

Clozel, J. P., Ertel, E. A., & Ertel, S. I. (1997). Discovery and main pharmacological properties of mibefradil (Ro 40-5967), the first selective T-type calcium channel blocker. *Journal of hypertension. Supplement : official journal of the International Society of Hypertension*, *15*(5), S17–25.

Conn, P. J., Battaglia, G., Marino, M. J., & Nicoletti, F. (2005). Metabotropic glutamate receptors in the basal ganglia motor circuit. *Nature Reviews Neuroscience*, *6*(10), 787–798. doi:10.1038/nrn1763

Connell, L. A., & Wallis, D. I. (1988). Responses to 5-hydroxytryptamine evoked in the hemisected spinal cord of the neonate rat. *British journal of pharmacology*, *94*(4), 1101–1114.

Connell, L. A., & Wallis, D. I. (1989). 5-hydroxytryptamine depolarizes neonatal rat motorneurones through a receptor unrelated to an identified binding site. *Neuropharmacology*, *28*(6), 625–634. doi:10.1016/0028-3908(89)90142-1

Constanti, A., Adams, P. R., & Brown, D. A. (1981). Why do barium ions imitate acetylcholine? *Brain research*, *206*(1), 244–250. doi:10.1016/0006-8993(81)90125-6

Cooper, J. R., Bloom, F. E., & Roth, R. H. (2003). *The Biochemical Basis of Neuropharmacology*. Oxford University Press, USA.

Cowley, K. C., & Schmidt, B. J. (1994a). Some limitations of ventral root recordings for monitoring locomotion in the in vitro neonatal rat spinal cord preparation. *Neuroscience letters*, *171*(1-2), 142–146.

Cowley, K. C., & Schmidt, B. J. (1995). Effects of inhibitory amino acid antagonists on reciprocal inhibitory interactions during rhythmic motor activity in the in vitro neonatal rat spinal cord. *Journal of neurophysiology*.

Cowley, K. C., & Schmidt, B. J. (1997). Regional Distribution of the Locomotor Pattern-Generating Network in the Neonatal Rat Spinal Cord. *Journal of neurophysiology*.

Cowley, K. C., & Schmidt, B. J. (1994b, February 17). A comparison of motor patterns induced by N-methyl-d-aspartate, acetylcholine and serotonin in the in vitro neonatal rat spinal cord. *Neuroscience letters*. Retrieved February 17, 2013, from https://login.ezproxy.lib.ucalgary.ca/login?url=http://library.ucalgary.ca/rdd-subject?s=25

De Mei, C., Ramos, M., Iitaka, C., & Borrelli, E. (2009). Getting specialized: presynaptic and postsynaptic dopamine D2 receptors. *Current Opinion in Pharmacology*, *9*(1), 53–58. doi:10.1016/j.coph.2008.12.002

Delpy, A., Allain, A. E., & Meyrand, P. (2008). NKCC1 cotransporter inactivation underlies embryonic development of chloride-mediated inhibition in mouse spinal motoneuron - Delpy - 2008 - The Journal of Physiology - Wiley Online Library. *The Journal of …*.

Delvolvé, I., Gabbay, H., & Lev-Tov, A. (2001). The motor output and behavior produced by rhythmogenic sacrocaudal networks in spinal cords of neonatal rats. *Journal of neurophysiology*, *85*(5), 2100–2110.

Dickinson, P. S. (2006). Neuromodulation of central pattern generators in invertebrates and vertebrates. *Current opinion in neurobiology*, *16*(6), 604–614. doi:10.1016/j.conb.2006.10.007

Dong, Y., Cooper, D., Nasif, F., Hu, X.-T., & White, F. J. (2004). Dopamine modulates inwardly rectifying potassium currents in medial prefrontal cortex pyramidal neurons. *The Journal of neuroscience : the official journal of the Society for Neuroscience*, *24*(12), 3077–3085. doi:10.1523/JNEUROSCI.4715-03.2004

Dougherty, K. J., & Kiehn, O. (2010). Firing and cellular properties of V2a interneurons in the rodent spinal cord. *The Journal of neuroscience : the official journal of the Society for Neuroscience*, *30*(1), 24–37. doi:10.1523/JNEUROSCI.4821-09.2010

Douglas, R. J., Koch, C., Mahowald, M., Martin, K. A., & Suarez, H. H. (1995). Recurrent excitation in neocortical circuits. *Science (New York, N.Y.)*, *269*(5226), 981–985.

Dunbar, M. J., Tran, M. A., & Whelan, P. J. (2010). Endogenous extracellular serotonin modulates the spinal locomotor network of the neonatal mouse. *The Journal of physiology*, *588*(Pt 1), 139–156. doi:10.1113/jphysiol.2009.177378

Ramsay, L.E., Thomas, J.P., Thomson, W.H., & Smith, B.S., (1983). Comparison of thiazides and amiloride in treatment of moderate hypertension. *British medical journal (Clinical research ed.)*, *287*(6392), 614–615.

Eller, P., Berjukov, S., Wanner, S., Huber, I., Hering, S., Knaus, H. G., Toth, G., Kimball S.D., & Striessnig, J., (2000). High affinity interaction of mibefradil with voltage-gated calcium and sodium channels. *British journal of pharmacology*, *130*(3), 669–677. doi:10.1038/sj.bjp.0703352

Elliott, P., & Wallis, D. I. (1992). Serotonin and L-norepinephrine as mediators of altered excitability in neonatal rat motoneurons studied in vitro. *Neuroscience*, *47*(3), 533–544.

Engberg, I., & Lundberg, A. (1969). An electromyographic analysis of muscular activity in the hindlimb of the cat during unrestrained locomotion. *Acta physiologica Scandinavica*, *75*(4), 614–630.

Engbers, J., Anderson, D., Tadayonnejad, R., Mehaffey, W.H., Molineux, M.L., & Turner, R.W., (2011). Distinct roles for IT and IH in controlling the frequency and timing of rebound spike responses. *The Journal of physiology, 589.22*, 5391-5413.

English, A. W., & Weeks, O. I. (1984). Compartmentalization of single muscle units in cat lateral gastrocnemius. *Experimental Brain Research*, *56*(2), 361–368. doi:10.1007/BF00236292

Fedirchuk, B., & Dai, Y. (2004). Monoamines increase the excitability of spinal neurones in the neonatal rat by hyperpolarizing the threshold for action potential production. *The Journal of physiology*, *557*(Pt 2), 355–361. doi:10.1113/jphysiol.2004.064022

Fedorova, E., Battini, L., Prakash-Cheng, A., Marras, D., & Gusella, G. L. (2006). Lentiviral gene delivery to CNS by spinal intrathecal administration to neonatal mice. *The journal of gene medicine*, *8*(4), 414–424. doi:10.1002/jgm.861

Fischer, J. E., & Baldessarini, R. J. (1971). False neurotransmitters and hepatic failure. *Lancet*, *2*(7715), 75–80.

Fleetwood-Walker, S. M., Hope, P. J., & Mitchell, R. (1988). Antinociceptive actions of descending dopaminergic tracts on cat and rat dorsal horn somatosensory neurones. *The Journal of physiology*, *399*, 335–348.

Fong, A. J., Roy, R. R., Ichiyama, R. M., Lavrov, I., Courtine, G., Gerasimenko, Y., et al. (2009). Recovery of control of posture and locomotion after a spinal cord injury: solutions staring us in the face. *Progress in brain research*, *175*, 393–418. doi:10.1016/S0079-6123(09)17526-X

Forssberg, H., & Grillner, S. (1973). The locomotion of the acute spinal cat injected with clonidine i.v. *Brain research*, *50*(1), 184–186.

Fortier, P. A., Smith, A. M., & Rossignol, S. (1987). Locomotor deficits in the mutant mouse, Lurcher. *Experimental Brain Research*, *66*(2), 271–286. doi:10.1007/BF00243304

Freedman, S. B., Patel, S., Marwood, R., Emms, F., Seabrook, G. R., Knowles, M. R., & McAllister, G. (1994). Expression and pharmacological characterization of the human D3 dopamine receptor. *The Journal of pharmacology and experimental therapeutics*, *268*(1), 417–426.

Gallagher, J. P., Inokuchi, H., & Shinnick-Gallagher, P. (1980). Dopamine depolarisation of mammalian primary afferent neurones. *Nature*, *283*(5749), 770–772.

Gao, B. X., & Ziskind-Conhaim, L. (1998). Development of ionic currents underlying changes in action potential waveforms in rat spinal motoneurons. *Journal of neurophysiology*, *80*(6), 3047–3061.

Garraway, S. M., & Hochman, S. (2001). Modulatory actions of serotonin, norepinephrine, dopamine, and acetylcholine in spinal cord deep dorsal horn neurons. *Journal of neurophysiology*, *86*(5), 2183–2194.

Gasparini, S., & DiFrancesco, D. (1997). Action of the hyperpolarization-activated current (Ih) blocker ZD 7288 in hippocampal CA1 neurons. *Pflügers Archiv European Journal of Physiology*, *435*(1), 99–106. doi:10.1007/s004240050488

Gerin, C. G., Hill, A., Hill, S., Smith, K., & Privat, A. (2010). Serotonin release variations during recovery of motor function after a spinal cord injury in rats. *Synapse (New York, N.Y.)*, *64*(11), 855–861. doi:10.1002/syn.20802

Gerin, C., & Privat, A. (1998). Direct evidence for the link between monoaminergic descending pathways and motor activity:: II. A study with microdialysis probes implanted in the ventral horn of the spinal cord. *Brain research*, *794*(1), 169–173.

Gerin, C., Becquet, D., & Privat, A. (1995). Direct evidence for the link between monoaminergic descending pathways and motor activity. I. A study with microdialysis probes implanted in the ventral funiculus of the spinal cord. *Brain research*, *704*(2), 191–201.

Gordon, I. T., & Whelan, P. J. (2006a). Deciphering the organization and modulation of spinal locomotor central pattern generators. *The Journal of experimental biology*, *209*(Pt 11), 2007–2014. doi:10.1242/jeb.02213

Gordon, I. T., & Whelan, P. J. (2006b). Monoaminergic control of cauda-equina-evoked locomotion in the neonatal mouse spinal cord. *Journal of neurophysiology*, *96*(6), 3122–3129. doi:10.1152/jn.00606.2006

Gordon, I. T., & Whelan, P. J. (2008). Brainstem modulation of locomotion in the neonatal mouse spinal cord. *The Journal of physiology*, *586*(10), 2487–2497. doi:10.1113/jphysiol.2007.148320

Gorelova, N., Seamans, J. K., & Yang, C. R. (2002). Mechanisms of dopamine activation of fast-spiking interneurons that exert inhibition in rat prefrontal cortex. *Journal of neurophysiology*, *88*(6), 3150–3166. doi:10.1152/jn.00335.2002

Gosgnach, S., Pierani, A., Jessell, T. M., & Goulding, M. (2004). Genetic Identification of Spinal Interneurons that Coordinate Left-Right Locomotor Activity Necessary for Walking Movements. *Neuron*, *42*, 375–386.

Goulding, M. (2009). Circuits controlling vertebrate locomotion: moving in a new direction. *Nature Reviews Neuroscience*, *10*(7), 507–518. doi:10.1038/nrn2608

Greengard, P. (2001). The Neurobiology of Slow Synaptic Transmission. *Science (New York, N.Y.)*, *294*(5544), 1024–1030. doi:10.1126/science.294.5544.1024

Grillner, S. (1975). Locomotion in vertebrates: central mechanisms and reflex interaction. *Physiological Reviews*, *55*(2), 247–304.

Grillner, S. (1981). *Control of Locomotion in Bipeds, Tetrapods, and Fish*. *Comprehensive Physiology*. Hoboken, NJ, USA: John Wiley & Sons, Inc. doi:10.1002/cphy.cp010226

Grillner, S. (2003). The motor infrastructure: from ion channels to neuronal networks. *Nature Reviews Neuroscience*, *4*(7), 573–586. doi:10.1038/nrn1137

Grillner, S. (2006). Biological pattern generation: the cellular and computational logic of networks in motion. *Neuron*, *52*(5), 751–766. doi:10.1016/j.neuron.2006.11.008

Grillner, S., Deliagina, T., Ekeberg O, Manira, el, A., Hill, R. H., Lansner, A., et al. (1995). Neural networks that co-ordinate locomotion and body orientation in lamprey. *Trends in neurosciences*, *18*(6), 270–279.

Grillner, S., Hellgren, J., Ménard, A., Saitoh, K., & Wikström, M. A. (2005). Mechanisms for selection of basic motor programs--roles for the striatum and pallidum. *Trends in neurosciences*, *28*(7), 364–370. doi:10.1016/j.tins.2005.05.004

Grillner, S., Robertson, B., & Stephenson-Jones, M. (2013). The evolutionary origin of the vertebrate basal ganglia and its role in action-selection. *The Journal of physiology*. doi:10.1113/jphysiol.2012.246660

Grillner, S., Wallén, P., Hill, R., Cangiano, L., & Manira, el, A. (2001). Ion channels of importance for the locomotor pattern generation in the lamprey brainstem-spinal cord. *The Journal of physiology*, *533*(Pt 1), 23–30.

Grillner, S., Wallén, P., Saitoh, K., Kozlov, A., & Robertson, B. (2008). Neural bases of goal-directed locomotion in vertebrates—An overview. *Brain research reviews*, *57*(1), 2–12. doi:10.1016/j.brainresrev.2007.06.027

Hammar, I., Bannatyne, B. A., Maxwell, D. J., Edgley, S. A., & Jankowska, E. (2004). The actions of monoamines and distribution of noradrenergic and serotoninergic contacts on different subpopulations of commissural interneurons in the cat spinal cord. *The European journal of neuroscience*, *19*(5), 1305–1316. doi:10.1111/j.1460-9568.2004.03239.x

Han, P., & Whelan, P. J. (2009). Modulation of AMPA currents by D(1)-like but not D(2)-like receptors in spinal motoneurons. *Neuroscience*, *158*(4), 1699–1707. doi:10.1016/j.neuroscience.2008.11.040

Han, P., Nakanishi, S. T., Tran, M. A., & Whelan, P. J. (2007). Dopaminergic modulation of spinal neuronal excitability. *The Journal of neuroscience : the official journal of the Society for Neuroscience*, *27*(48), 13192–13204. doi:10.1523/JNEUROSCI.1279-07.2007

Hanson, M. G., & Landmesser, L. T. (2003). Characterization of the Circuits That Generate Spontaneous Episodes of Activity in the Early Embryonic Mouse Spinal Cord. *The Journal of neuroscience*.

Harris, N. C., & Constanti, A. (1995). Mechanism of block by ZD 7288 of the hyperpolarization-activated inward rectifying current in guinea pig substantia nigra neurons in vitro. *Journal of neurophysiology*, *74*, 2366–2378.

Harris-Warrick, R. M. (2010). General principles of rhythmogenesis in central pattern generator networks. *Progress in brain research*, *187*, 213–222. doi:10.1016/B978-0-444-53613-6.00014-9

Harris-Warrick, R. M., & Johnson, B. R. (2010). Checks and balances in neuromodulation. *Frontiers in behavioral neuroscience*, *4*. doi:10.3389/fnbeh.2010.00047

Harris-Warrick, R. M., Coniglio, L. M., Levini, R. M., Gueron, S., & Guckenheimer, J. (1995). Dopamine modulation of two subthreshold currents produces phase shifts in activity of an identified motoneuron. *Journal of neurophysiology*, *74*(4), 1404–1420.

Harris-Warrick, R. M., Johnson, B. R., Peck, J. H., Kloppenburg, P., Ayali, A., & Skarbinski, J. (1998). Distributed effects of dopamine modulation in the crustacean pyloric network. *Annals of the New York Academy of Sciences*, *860*, 155–167.

Harris-Warrick, R. M., Marder, E., Selverston, A. I., & Moulins, M. (1992). Dynamic Biological Networks: The Stomatogastric Nervous System - Ronald M. Harris-Warrick - Google Books. *MIT Press*.

Herrington, J., & Lingle, C. J. (1992). Kinetic and pharmacological properties of low voltage-activated Ca2+ current in rat clonal (GH3) pituitary cells. *Journal of neurophysiology*.

Hess, D., & Manira, el, A. (2001). Characterization of a high-voltage-activated IA current with a role in spike timing and locomotor pattern generation. *Proceedings of the National Academy of Sciences*, *98*(9), 5276–5281. doi:10.1073/pnas.091096198

Hildebrand, C., Karlsson, M., & Risling, M. (1997). Ganglionic axons in motor roots and pia

mater. *Progress in neurobiology*, *51*(2), 89–128.
Hille, B. (2001). *Ion Channels of Excitable Membranes*. Sinauer Associates.
Hinckley, C. A., Hartley, R., Wu, L., Todd, A., & Ziskind-Conhaim, L. (2005). Locomotor-like rhythms in a genetically distinct cluster of interneurons in the mammalian spinal cord. *Journal of neurophysiology*, *93*(3), 1439–1449. doi:10.1152/jn.00647.2004
Hirano, Y., Fozzard, H. A., & January, C. T. (1989). Characteristics of L- and T-type Ca2+ currents in canine cardiac Purkinje cells. *… of Physiology-Heart and …*.
Hochman, S., & Schmidt, B. J. (1998). Whole cell recordings of lumbar motoneurons during locomotor-like activity in the in vitro neonatal rat spinal cord. *Journal of neurophysiology*, *79*(2), 743–752.
Hodgkin, A. L., & Huxley, A. F. (1952). A quantitative description of membrane current and its application to conduction and excitation in nerve. *The Journal of physiology*, *117*(4), 500–544.
Holstege, J. C., Van Dijken, H., Buijs, R. M., Goedknegt, H., Gosens, T., & Bongers, C. M. (1996). Distribution of dopamine immunoreactivity in the rat, cat and monkey spinal cord. *The Journal of comparative neurology*, *376*(4), 631–652. doi:10.1002/(SICI)1096-9861(19961223)376:4<631::AID-CNE10>3.0.CO;2-P
Hongo, T., Jankowska, E., & Lundberg, A. (1965). Effects evoked from the rubrospinal tract in cats. *Experientia*, *21*(9), 525–526.
Hounsgaard, J., Hultborn, H., Jespersen, B., & Kiehn, O. (1988). Bistability of alpha-motoneurones in the decerebrate cat and in the acute spinal cat after intravenous 5-hydroxytryptophan. *The Journal of physiology*, *405*, 345–367.
Hoyer, D., Hannon, J. P., & Martin, G. R. (2002). Molecular, pharmacological and functional diversity of 5-HT receptors. *Pharmacology, biochemistry, and behavior*, *71*(4), 533–554.
Huang, L. (2004). NNC 55-0396 [(1S,2S)-2-(2-(N-[(3-Benzimidazol-2-yl)propyl]-N-methylamino)ethyl)-6-fluoro-1,2,3,4-tetrahydro-1-isopropyl-2-naphtyl cyclopropanecarboxylate dihydrochloride]: A New Selective Inhibitor of T-Type Calcium Channels. *Journal of Pharmacology and Experimental Therapeutics*, *309*(1), 193–199. doi:10.1124/jpet.103.060814
Hughes, V. (2013, January 24). Mapping brain networks: Fish-bowl neuroscience. *Nature*, pp. 466–468. doi:10.1038/493466a
Huguenard, J. R. (1996). Low-threshold calcium currents in central nervous system neurons. *Annual review of physiology*, *58*, 329–348.
Humphreys, J. M., & Whelan, P. J. (2012). Dopamine exerts activation-dependent modulation of spinal locomotor circuits in the neonatal mouse. *Journal of neurophysiology*, *108*(12), 3370–3381. doi:10.1152/jn.00482.2012
Humphreys, J. M., & Whelan, P. J. (2009, October 18). T-type calcium channel blockade modulates drug evoked locomotion. *Society For Neurosci Abstract*. Chicago.
Irons, T. D., Kelly, P. E., Hunter, D. L., Macphail, R. C., & Padilla, S. (2013). Acute administration of dopaminergic drugs has differential effects on locomotion in larval zebrafish. *Pharmacology, biochemistry, and behavior*, *103*(4), 792–813. doi:10.1016/j.pbb.2012.12.010
Ivanchenko, M. V., Thomas Nowotny, Selverston, A. I., & Rabinovich, M. I. (2008). Pacemaker and network mechanisms of rhythm generation: Cooperation and competition. *Journal of Theoretical Biology*, *253*(3), 452–461. doi:10.1016/j.jtbi.2008.04.016

Jackson, D. M., & Westlind-Danielsson, A. (1994). Dopamine receptors: Molecular biology, biochemistry and behavioural aspects. *Pharmacology & Therapeutics*, *64*(2), 291–370. doi:10.1016/0163-7258(94)90041-8

Jacobs, B. L., & Fornal, C. A. (1993). 5-HT and motor control: a hypothesis. *Trends in neurosciences*, *16*(9), 346–352. doi:10.1016/0166-2236(93)90090-9

Jaeger, C., Teitelman, G., Joh, T., Albert, V., Park, D., & Reis, D. (1983). Some neurons of the rat central nervous system contain aromatic-L-amino-acid decarboxylase but not monoamines. *Science (New York, N.Y.)*, *219*(4589), 1233–1235. doi:10.1126/science.6131537

Jankowska, E. (2001). Spinal interneuronal systems: identification, multifunctional character and reconfigurations in mammals. *The Journal of physiology*, *533*(Pt 1), 31–40.

Jankowska, E., Hammar, I., & Chojnicka, B. (2000). Effects of monoamines on interneurons in four spinal reflex pathways from group I and/or group II muscle afferents. *European Journal of …*, *12*, 701–714.

Jankowska, E., Jukes, M. G., Lund, S., & Lundberg, A. (1967a). The effect of DOPA on the spinal cord. 6. Half-centre organization of interneurones transmitting effects from the flexor reflex afferents. *Acta physiologica Scandinavica*, *70*(3), 389–402.

Jankowska, E., Jukes, M. G., Lund, S., & Lundberg, A. (1967b). The effect of DOPA on the spinal cord. 5. Reciprocal organization of pathways transmitting excitatory action to alpha motoneurones of flexors and extensors. *Acta physiologica Scandinavica*, *70*(3), 369–388.

Jiang, Z., Carlin, K. P., & Brownstone, R. M. (1999). An in vitro functionally mature mouse spinal cord preparation for the study of spinal motor networks. *Brain research*, *816*(2), 493–499.

Johnson, B. R., & Harris-Warrick, R. M. (1990). Aminergic modulation of graded synaptic transmission in the lobster stomatogastric ganglion. *The Journal of neuroscience : the official journal of the Society for Neuroscience*, *10*(7), 2066–2076.

Johnson, B. R., Kloppenburg, P., & Harris-Warrick, R. M. (2003). Dopamine Modulation of Calcium Currents in Pyloric Neurons of the Lobster Stomatogastric Ganglion. *Journal of ….*

Johnson, B. R., Peck, J. H., & Harris-Warrick, R. M. (1993). Amine modulation of electrical coupling in the pyloric network of the lobster stomatogastric ganglion. *Journal of comparative physiology. A, Sensory, neural, and behavioral physiology*, *172*(6), 715–732.

Johnson, B. R., Peck, J. H., & Harris-Warrick, R. M. (1994). Differential modulation of chemical and electrical components of mixed synapses in the lobster stomatogastric ganglion. *Journal of comparative physiology. A, Sensory, neural, and behavioral physiology*, *175*(2), 233–249.

Johnson, B. R., Schneider, L. R., Nadim, F., & Harris-Warrick, R. M. (2005). Dopamine Modulation of Phasing of Activity in a Rhythmic Motor Network: Contribution of Synaptic and Intrinsic Modulatory Actions. *Journal of neurophysiology*, *94*(5), 3101–3111. doi:10.1152/jn.00440.2005

Jordan, L. M., & Schmidt, B. J. (2002). Propriospinal neurons involved in the control of locomotion: potential targets for repair strategies? *Progress in brain research*, *137*, 125–139.

Jordan, L. M., Brownstone, R. M., & Brian, R. N. (1992). Control of functional systems in the brainstem and spinal cord. *Current opinion in neurobiology*, *2*, 794–801.

Kang, H.-W., Moon, H.-J., Joo, S.-H., & Lee, J.-H. (2007). Histidine residues in the IS3-IS4 loop are critical for nickel-sensitive inhibition of the Cav2.3 calcium channel. *FEBS letters*, *581*(30), 5774–5780. doi:10.1016/j.febslet.2007.11.045

Kanning, K. C., & Kaplan, A. (2010). Motor neuron diversity in development and disease. … *review of neuroscience*.

Katz, P. S. (1995). Intrinsic and extrinsic neuromodulation of motor circuits. *Current opinion in neurobiology*, *5*(6), 799–808.

Kelly, M. A., Rubinstein, M., Phillips, T. J., Lessov, C. N., Burkhart-Kasch, S., Zhang, G., et al. (1998). Locomotor activity in D2 dopamine receptor-deficient mice is determined by gene dosage, genetic background, and developmental adaptations. *The Journal of neuroscience : the official journal of the Society for Neuroscience*, *18*(9), 3470–3479.

Kemnitz, C. P. (1997). Dopaminergic modulation of spinal neurons and synaptic potentials in the lamprey spinal cord. *Journal of neurophysiology*, *77*(1), 289–298.

Kemnitz, C. P., Strauss, T. R., Hosford, D. M., & Buchanan, J. T. (1995). Modulation of swimming in the lamprey, Petromyzon marinus, by serotonergic and dopaminergic drugs. *Neuroscience letters*, *201*(2), 115–118.

Kiehn, O. (2006). Locomotor circuits in the mammalian spinal cord. *Annual review of neuroscience*, *29*(1), 279–306. doi:10.1146/annurev.neuro.29.051605.112910

Kiehn, O., & Butt, S. J. B. (2003). Physiological, anatomical and genetic identification of CPG neurons in the developing mammalian spinal cord. *Progress in neurobiology*, *70*(4), 347–361.

Kiehn, O., Kjaerulff, O., Tresch, M. C., & Harris-Warrick, R. M. (2000). Contributions of intrinsic motor neuron properties to the production of rhythmic motor output in the mammalian spinal cord. *Brain research bulletin*, *53*(5), 649–659.

Kiehn, O., & Kjaerulff, O. (1996). Spatiotemporal characteristics of 5-HT and dopamine-induced rhythmic hindlimb activity in the in vitro neonatal rat. *Journal of neurophysiology*, *75*(4), 1472–1482.

Kiehn, O., Hultborn, H., & Conway, B. A. (1992). Spinal locomotor activity in acutely spinalized cats induced by intrathecal application of noradrenaline. *Neuroscience letters*, *143*(1-2), 243–246.

Kiehn, O., Quinlan, K. A., Restrepo, C. E., Lundfald, L., Borgius, L., Talpalar, A. E., & Endo, T. (2008). Excitatory components of the mammalian locomotor CPG. *Brain research reviews*, *57*(1), 56–63. doi:10.1016/j.brainresrev.2007.07.002

Kiehn, O., Sillar, K. T., Kjaerulff, O., & McDearmid, J. R. (1999). Effects of noradrenaline on locomotor rhythm-generating networks in the isolated neonatal rat spinal cord. *Journal of neurophysiology*, *82*(2), 741–746.

Kiritsy-Roy, J. A., Shyu, B. C., Danneman, P. J., Morrow, T. J., Belczynski, C., & Casey, K. L. (1994). Spinal antinociception mediated by a cocaine-sensitive dopaminergic supraspinal mechanism. *Brain research*, *644*(1), 109–116.

Kjaerulff, O., & Kiehn, O. (1996). Distribution of Networks Generating and Coordinating Locomotor Activity in the Neonatal Rat Spinal Cord In Vitro : A Lesion Study. *The Journal of neuroscience*, *16*(18), 5777–5794.

Kjaerulff, O., & Kiehn, O. (2001). 5-HT modulation of multiple inward rectifiers in motoneurons in intact preparations of the neonatal rat spinal cord. *Journal of neurophysiology*, *85*(2), 580–593.

Kleyman, T. R., & Cragoe, E. J. (1988). Amiloride and its analogs as tools in the study of ion transport. *The Journal of Membrane Biology*, *105*(1), 1–21.

Kloppenburg, P., Levini, R. M., & Harris-Warrick, R. M. (1999). Dopamine Modulates Two

Potassium Currents and Inhibits the Intrinsic Firing Properties of an Identified Motor Neuron in a Central Pattern Generator Network. *Journal of neurophysiology*. *81*(1), 29-38.
Koblinger, K., Krajacic, A., Nakanishi, S. T., & Whelan, P. J. (2012). Characterization of A11 neurons projecting to the spinal cord of adult mice. *Society For Neurosci Abstract*.
Komori, K., Fujii, T., Karasawa, N., & Yamada, K. (1991). Some neurons of the mouse cortex and caudo-putamen contain aromatic L-amino acid decarboxylase but not monoamines. *Acta histochemica et* cytochemica.
Kopin, I. J., Fischer, J. E., Musacchio, J., & Horst, W. D. (1964). Evidence for a false neurocemhical transmitter as a mechanism for the hypotensive effect of monoamines oxidase inhibitors. *Proceedings of the National Academy of Sciences of the United States of America*, *52*, 716–721.
Kremer, E., & Lev-Tov, A. (1997). Localization of the spinal network associated with generation of hindlimb locomotion in the neonatal rat and organization of its transverse coupling system. *Journal of neurophysiology*, *77*(3), 1155–1170.
Kriellaars, D. J., Brownstone, R. M., Noga, B. R., & Jordan, L. M. (1994). Mechanical entrainment of fictive locomotion in the decerebrate cat. *Journal of neurophysiology*, *71*(6), 2074–2086.
Kudo, N., & Yamada, T. (1987a). N-Methyl-d,l-aspartate-induced locomotor activity in a spinal cord-indlimb muscles preparation of the newborn rat studied in vitro. *Neuroscience letters*, (75), 43–48.
Kudo, N., & Yamada, T. (1987b). N-methyl-D,L-aspartate-induced locomotor activity in a spinal cord-hindlimb muscles preparation of the newborn rat studied in vitro. *Neuroscience letters*, *75*(1), 43–48.
Kwan, A. C., Dietz, S. B., Webb, W. W., & Harris-Warrick, R. M. (2009). Activity of Hb9 Interneurons during Fictive Locomotion in Mouse Spinal Cord. *The Journal of Neuroscience*, *29*(37), 11601–11613. doi:10.1523/JNEUROSCI.1612-09.2009
Lacinová, L., Klugbauer, N., & Hofmann, F. (2000). Regulation of the calcium channel alpha(1G) subunit by divalent cations and organic blockers. *Neuropharmacology*, *39*(7), 1254–1266.
Lafreniere-Roula, M., & McCrea, D. A. (2005). Deletions of rhythmic motoneuron activity during fictive locomotion and scratch provide clues to the organization of the mammalian central pattern generator. *Journal of neurophysiology*, *94*(2), 1120–1132. doi:10.1152/jn.00216.2005
LaHoste, G. J., Henry, B. L., & Marshall, J. F. (2000). Dopamine D1 Receptors Synergize with D2, But Not D3 or D4, Receptors in the Striatum without the Involvement of Action Potentials. *The Journal of Neuroscience, 20* (17), 6666-6671.
Lambert, A. M., Bonkowsky, J. L., & Masino, M. A. (2012). The conserved dopaminergic diencephalospinal tract mediates vertebrate locomotor development in zebrafish larvae. *The Journal of neuroscience : the official journal of the Society for Neuroscience*, *32*(39), 13488–13500. doi:10.1523/JNEUROSCI.1638-12.2012
Lapointe, N. P., Rouleau, P., Ung, R. V., & Guertin, P. A. (2009). Specific role of dopamine D1 receptors in spinal network activation and rhythmic movement induction in vertebrates. *The Journal of physiology*, *587*(7), 1499–1511. doi:10.1113/jphysiol.2008.166314
Lee, J.-H., Gomora, J. C., Cribbs, L. L., & Perez-Reyes, E. (1999). Nickel Block of Three Cloned T-Type Calcium Channels: Low Concentrations Selectively Block α1H. *Biophysical Journal*, *77*(6), 3034–3042. doi:10.1016/S0006-3495(99)77134-1

Lee, R. H., & Heckman, C. J. (2001). Essential role of a fast persistent inward current in action potential initiation and control of rhythmic firing. *Journal of neurophysiology*, *85*(1), 472–475.

Levant, B. (1997). The D3 dopamine receptor: neurobiology and potential clinical relevance. *Pharmacological reviews*, *49*(3), 231–252.

Li, M., Hansen, J. B., Huang, L., Keyser, B. M., & Taylor, J. T. (2006). Towards Selective Antagonists of T-Type Calcium Channels: Design, Characterization and Potential Applications of NNC 55-0396. *Cardiovascular drug reviews*, *23*(2), 173–196. doi:10.1111/j.1527-3466.2005.tb00164.x

Liu, J., & Jordan, L. M. (2005). Stimulation of the parapyramidal region of the neonatal rat brain stem produces locomotor-like activity involving spinal 5-HT7 and 5-HT2A receptors. *Journal of neurophysiology*, *94*(2), 1392–1404. doi:10.1152/jn.00136.2005

Liu, J.-H., Bijlenga, P., Occhiodoro, T., Fischer-Lougheed, J., Bader, C. R., & Bernheim, L. (1999). Mibefradil (Ro 40-5967) inhibits several Ca 2+and K +currents in human fusion-competent myoblasts. *British journal of pharmacology*, *126*(1), 245–250. doi:10.1038/sj.bjp.0702321

Lledo, P. M., Homburger, V., Bockaert, J., & Vincent, J. D. (1992). Differential G protein-mediated coupling of D2 dopamine receptors to K+ and Ca2+ currents in rat anterior pituitary cells. *Neuron*, *8*(3), 455–463.

Lopez-Charcas, O., Rivera, M., & Gomora, J. C. (2012). Block of Human CaV3 Channels by the Diuretic Amiloride. *Molecular Pharmacology*, *82*(4), 658–667. doi:10.1124/mol.112.078923

Lory, P., & Chemin, J. (2007). Towards the discovery of novel T-type calcium channel blockers. *Expert opinion on therapeutic targets*, *11*(5), 717–722. doi:10.1517/14728222.11.5.717

Lundberg, A. (1969). Convergence of excitatory and inhibitory action on interneurones in the spinal cord. [UCLA Forum Med Sci. 1969] - PubMed - NCBI. *UCLA forum in medical sciences*.

Lundberg, A. (1979). Multisensory control of spinal reflex pathways. *Progress in brain research*, *50*, 11–28. doi:10.1016/S0079-6123(08)60803-1

Machacek, D. W., & Hochman, S. (2006). Noradrenaline unmasks novel self-reinforcing motor circuits within the mammalian spinal cord. *The Journal of neuroscience : the official journal of the Society for Neuroscience*, *26*(22), 5920–5928. doi:10.1523/JNEUROSCI.4623-05.2006

MacLean, J. N., Cowley, K. C., & Schmidt, B. J. (1998). NMDA receptor-mediated oscillatory activity in the neonatal rat spinal cord is serotonin dependent. *Journal of neurophysiology*, *79*(5), 2804–2808.

Madriaga, M. A., McPhee, L. C., Chersa, T., Christie, K. J., & Whelan, P. J. (2004). Modulation of locomotor activity by multiple 5-HT and dopaminergic receptor subtypes in the neonatal mouse spinal cord. *Journal of neurophysiology*, *92*(3), 1566–1576. doi:10.1152/jn.01181.2003

Mandadi, S., Nakanishi, S. T., Takashima, Y., Dhaka, A., Patapoutian, A., McKemy, D. D., & Whelan, P. J. (2009). Locomotor networks are targets of modulation by sensory transient receptor potential vanilloid 1 and transient receptor potential melastatin 8 channels. *Neuroscience*, *162*(4), 1377–1397. doi:10.1016/j.neuroscience.2009.05.063

Manira, el, A., Pombal, M. A., & Grillner, S. (1997). Diencephalic projection to reticulospinal neurons involved in the initiation of locomotion in adult lampreys Lampetra fluviatilis. *The*

Journal of comparative neurology, *389*(4), 603–616.
Manira, el, A., Tegnér, J., & Grillner, S. (1994). Calcium-dependent potassium channels play a critical role for burst termination in the locomotor network in lamprey. *Journal of neurophysiology*, *72*(4), 1852–1861.
Marchetti, C., Beato, M., & Nistri, A. (2001). Alternating rhythmic activity induced by dorsal root stimulation in the neonatal rat spinal cord in vitro. *The Journal of physiology*.
Marder, E. (2012). Neuromodulation of neuronal circuits: back to the future. *Neuron*, *76*(1), 1–11. doi:10.1016/j.neuron.2012.09.010
Marder, E., & Bucher, D. (2001). Central pattern generators and the control of rhythmic movements. *Current biology : CB*, *11*(23), R986–96.
Marder, E., & Thirumalai, V. (2002). Cellular, synaptic and network effects of neuromodulation. *Neural Networks*.
Martin, W. J., Gupta, N. K., Loo, C. M., Rohde, D. S., & Basbaum, A. I. (1999). Differential effects of neurotoxic destruction of descending noradrenergic pathways on acute and persistent nociceptive processing. *Pain*, *80*(1-2), 57–65.
Matsushima, T., Tegnér, J., Hill, R. H., & Grillner, S. (1993). GABAB receptor activation causes a depression of low- and high-voltage-activated Ca2+ currents, postinhibitory rebound, and postspike afterhyperpolarization in lamprey neurons. *Journal of neurophysiology*, *70*(6), 2606–2619.
McCobb, D. P., Best, P. M., & Beam, K. G. (1989). Development alters the expression of calcium currents in chick limb motoneurons. *Neuron*, *2*(6), 1633–1643.
McCrea, A. E., Stehouwer, D. J., & Van Hartesveldt, C. (1997). Dopamine D1 and D2 antagonists block L-DOPA-induced air-stepping in decerebrate neonatal rats. *Brain research. Developmental brain research*, *100*(1), 130–132.
McCrea, D. A., & Rybak, I. A. (2007). Modeling the mammalian locomotor CPG: insights from mistakes and perturbations. *Progress in brain research*, *165*, 235–253. doi:10.1016/S0079-6123(06)65015-2
McCrea, D. A., & Rybak, I. A. (2008). Organization of mammalian locomotor rhythm and pattern generation. *Brain research reviews*, *57*(1), 134–146. doi:10.1016/j.brainresrev.2007.08.006
McGivern, J. G. (2006). Pharmacology and drug discovery for T-type calcium channels. *CNS & neurological disorders drug targets*, *5*(6), 587–603.
McLean, D. L., Merrywest, S. D., & Sillar, K. T. (2000). The development of neuromodulatory systems and the maturation of motor patterns in amphibian tadpoles. *Brain research bulletin*, *53*(5), 595–603.
McPherson, D. R., & Kemnitz, C. P. (1994). Modulation of lamprey fictive swimming and motoneuron physiology by dopamine, and its immunocytochemical localization in the spinal cord. *Neuroscience letters*, *166*(1), 23–26.
Mentis, G. Z., Alvarez, F. J., Bonnot, A., Richards, D. S., Gonzalez-Forero, D., Zerda, R., & O'Donovan, M. J. (2005). Noncholinergic excitatory actions of motoneurons in the neonatal mammalian spinal cord. *Proceedings of the National Academy of Sciences of the United States of America*, *102*(20), 7344–7349. doi:10.1073/pnas.0502788102
Mentis, G. Z., Siembab, V. C., Zerda, R., O'Donovan, M. J., & Alvarez, F. J. (2006). Primary afferent synapses on developing and adult Renshaw cells. *The Journal of neuroscience : the official journal of the Society for Neuroscience*, *26*(51), 13297–13310. doi:10.1523/JNEUROSCI.2945-06.2006

Merrywest, S. D., McDearmid, J. R., Kjaerulff, O., Kiehn, O., & Sillar, K. T. (2003). Mechanisms underlying the noradrenergic modulation of longitudinal coordination during swimming in Xenopus laevis tadpoles. *The European journal of neuroscience*, *17*(5), 1013–1022.

Ménard, A., Auclair, F., Bourcier-Lucas, C., Grillner, S., & Dubuc, R. (2007). Descending GABAergic projections to the mesencephalic locomotor region in the lamprey Petromyzon marinus. *The Journal of comparative neurology*, *501*(2), 260–273. doi:10.1002/cne.21258

Miles, G. B. (2005). Mechanisms underlying the early phase of spike frequency adaptation in mouse spinal motoneurones. *The Journal of physiology*, *566*(2), 519–532. doi:10.1113/jphysiol.2005.086033

Miles, G. B., & Sillar, K. T. (2011). Neuromodulation of vertebrate locomotor control networks. *Physiology (Bethesda, Md.)*, *26*(6), 393–411. doi:10.1152/physiol.00013.2011

Miljanich, G. P., & Ramachandran, J. (1995). Antagonists of neuronal calcium channels: structure, function, and therapeutic implications. *Annual review of pharmacology and toxicology*, *35*, 707–734. doi:10.1146/annurev.pa.35.040195.003423

Millan, M. J. (2002). Descending control of pain. *Progress in neurobiology*.

Missale, C., Nash, S. R., Robinson, S. W., Jaber, M., & Caron, M. G. (1998). Dopamine receptors: from structure to function. *Physiological Reviews*, *78*(1), 189–225.

Mor, Y., & Lev-Tov, A. (2007). Analysis of rhythmic patterns produced by spinal neural networks. *Journal of neurophysiology*, *98*(5), 2807–2817. doi:10.1152/jn.00740.2007

Mynlieff, M., & Beam, K. G. (1992). Characterization of voltage-dependent calcium currents in mouse motoneurons. *Journal of neurophysiology*, *68*(1), 85–92.

Nakajima, K., Matsuyama, K., & Mori, S. (1998). Prenatal administration of para-chlorophenylalanine results in suppression of serotonergic system and disturbance of swimming movements in newborn rats. *Neuroscience research*, *31*(2), 155–169.

Nakanishi, S. T., & Whelan, P. J. (2010). Diversification of Intrinsic Motoneuron Electrical Properties During Normal Development and Botulinum Toxin–Induced Muscle Paralysis in Early Postnatal Mice. *Journal of neurophysiology*.

Nakanishi, S. T., & Whelan, P. J. (2012). A decerebrate adult mouse model for examining the sensorimotor control of locomotion. *Journal of neurophysiology*, *107*(1), 500–515. doi:10.1152/jn.00699.2011

Nelson, M. T., Joksovic, P. M., Perez-Reyes, E., & Todorovic, S. M. (2005). The endogenous redox agent L-cysteine induces T-type Ca2+ channel-dependent sensitization of a novel subpopulation of rat peripheral nociceptors. *The Journal of neuroscience : the official journal of the Society for Neuroscience*, *25*(38), 8766–8775. doi:10.1523/JNEUROSCI.2527-05.2005

Neve, K. A., Seamans, J. K., & Trantham-Davidson, H. (2004). Dopamine Receptor Signaling. *Journal of receptors and signal tranduction*, *37*(3), 165-205.

Newcomb, R., Szoke, B., Palma, A., Wang, G., Chen, X. H., Hopkins, W., et al. (1998). Selective peptide antagonist of the class E calcium channel from the venom of the tarantula Hysterocrates gigas. *Biochemistry*, *37*(44), 15353–15362. doi:10.1021/bi981255g

Nilius, B., Prenen, J., Kamouchi, M., Viana, F., Voets, T., & Droogmans, G. (1997). Inhibition by mibefradil, a novel calcium channel antagonist, of Ca 2+- and volume-activated Cl −channels in macrovascular endothelial cells. *British journal of pharmacology*, *121*(3), 547–555. doi:10.1038/sj.bjp.0701140

Nishimaru, H., Restrepo, C. E., & Kiehn, O. (2006). Activity of Renshaw cells during

locomotor-like rhythmic activity in the isolated spinal cord of neonatal mice. *The Journal of neuroscience : the official journal of the Society for Neuroscience*, *26*(20), 5320–5328. doi:10.1523/JNEUROSCI.5127-05.2006

Nishimaru, H., Takizawa, H., & Kudo, N. (2000). 5-Hydroxytryptamine-induced locomotor rhythm in the neonatal mouse spinal cord in vitro. *Neuroscience letters*, *280*(3), 187–190.

Noga, B. R., Kettler, J., & Jordan, L. M. (1988). Locomotion produced in mesencephalic cats by injections of putative transmitter substances and antagonists into the medial reticular formation and the pontomedullary locomotor strip. *The Journal of neuroscience : the official journal of the Society for Neuroscience*, *8*(6), 2074–2086.

Nowycky, M. C., Fox, A. P., & Tsien, R. W. (1985). Three types of neuronal calcium channel with different calcium agonist sensitivity. *Nature*, *316*(6027), 440–443.

O'Donovan, M. J., Bonnot, A., Mentis, G. Z., Chub, N., Pujala, A., & Alvarez, F. J. (2010). Mechanisms of excitation of spinal networks by stimulation of the ventral roots. *Annals of the New York Academy of Sciences*, *1198*(1), 63–71. doi:10.1111/j.1749-6632.2010.05535.x

Owen, D. G., Segal, M., & Barker, J. L. (1984). A Ca-dependent Cl– conductance in cultured mouse spinal neurones. *Nature*, *311*(5986), 567–570. doi:10.1038/311567a0

Pape, H. C. (1996). Queer current and pacemaker: the hyperpolarization-activated cation current in neurons. *Annual review of physiology*, *58*, 299–327. doi:10.1146/annurev.ph.58.030196.001503

Pearson, K. G. (2001). Could enhanced reflex function contribute to improving locomotion after spinal cord repair? *The Journal of physiology*, *533*(Pt 1), 75–81.

Pearson, K. G. (2004). Generating the walking gait: role of sensory feedback. In *Progress in Brain Research* (Vol. 143, pp. 123–129). Elsevier. doi:10.1016/S0079-6123(03)43012-4

Peck, J. H., Gaier, E., Stevens, E., Repicky, S., & Harris-Warrick, R. M. (2006). Amine modulation of Ih in a small neural network. *Journal of neurophysiology*, *96*(6), 2931–2940. doi:10.1152/jn.00423.2005

Peck, J. H., Nakanishi, S. T., Yaple, R., & Harris-Warrick, R. M. (2001). Amine modulation of the transient potassium current in identified cells of the lobster stomatogastric ganglion. *Journal of neurophysiology*, *86*(6), 2957–2965.

Perez-Reyes, E. (2003). Molecular Physiology of Low-Voltage-Activated T-type Calcium Channels. *Physiological Reviews*, 1–46.

Pertovaara, A. (1993). Antinociception induced by alpha-2-adrenoceptor agonists, with special emphasis on medetomidine studies. *Progress in neurobiology*, *40*(6), 691–709.

Philippson, M. (1905). L'autonomie et la centralisation dans le systéme nerveux des animaux. *Trav Lab Physiol Inst Solvay*, (1), 1–208.

Pirtle, T. J., & Satterlie, R. A. (2007). The role of postinhibitory rebound in the locomotor central-pattern generator of Clione limacina. *Integrative and comparative biology*, *47*(4), 451–456. doi:10.1093/icb/icm085

Prinz, A. A., Bucher, D., & Marder, E. (2004). Similar network activity from disparate circuit parameters. *Nature neuroscience*, *7*(12), 1345–1352. doi:10.1038/nn1352

Qu, S., Ondo, W. G., Zhang, X., Xie, W. J., & Pan, T. H. (2006). Projections of diencephalic dopamine neurons into the spinal cord in mice - Springer. *Experimental brain research, 168,* 152-156.

Ramirez, J.-M., Tryba, A. K., & Peña, F. (2004). Pacemaker neurons and neuronal networks: an integrative view. *Current opinion in neurobiology*, *14*(6), 665–674. doi:10.1016/j.conb.2004.10.011

Randall, A. D., & Tsien, R. W. (1997). Contrasting biophysical and pharmacological properties of T-type and R-type calcium channels. *Neuropharmacology*, *36*(7), 879–893. doi:10.1016/S0028-3908(97)00086-5

Rekling, J. C., Funk, G. D., Bayliss, D. A., Dong, X. W., & Feldman, J. L. (2000). Synaptic control of motoneuronal excitability. *Physiological Reviews*, *80*(2), 767–852.

Renshaw, B. (1941). Influence of discharge of motoneurons upon excitation of neighboring motoneurons. *Journal of neurophysiology*.

Ridet, J. L., Sandillon, F., Rajaofetra, N., Geffard, M., & Privat, A. (1992). Spinal dopaminergic system of the rat: light and electron microscopic study using an antiserum against dopamine, with particular emphasis on synaptic incidence. *Brain research*, *598*(1-2), 233–241.

Roberts, A., & Tunstall, M. J. (1990). Mutual Re-excitation with Post-Inhibitory Rebound: A Simulation Study on the Mechanisms for Locomotor Rhythm Generation in the Spinal Cord of Xenopus Embryos. *The European journal of neuroscience*, *2*(1), 11–23. doi:10.1111/j.1460-9568.1990.tb00377.x

Roberts, A., SOFFE, S. R., WOLF, E. S., Yoshida, M., & ZHAO, F. Y. (1998). Central Circuits Controlling Locomotion in Young Frog Tadpoles. *Annals of the New York Academy of Sciences*, *860*(1 NEURONAL MECH), 19–34. doi:10.1111/j.1749-6632.1998.tb09036.x

Robertson, B., Huerta-Ocampo, I., Ericsson, J., Stephenson-Jones, M., Pérez-Fernández, J., Bolam, J. P., et al. (2012). The dopamine D2 receptor gene in lamprey, its expression in the striatum and cellular effects of D2 receptor activation. *PloS one*, *7*(4), e35642. doi:10.1371/journal.pone.0035642

Robinson, R. B., & Siegelbaum, S. A. (2003). Hyperpolarization-activated cation currents: from molecules to physiological function. *Annual review of physiology*.

Rossignol, S., Chau, C., Brustein, E., Bélanger, M., Barbeau, H., & Drew, T. (1996). Locomotor capacities after complete and partial lesions of the spinal cord. *Acta neurobiologiae experimentalis*, *56*(1), 449–463.

Rybak, I. A., Shevtsova, N. A., Lafreniere-Roula, M., & McCrea, D. A. (2006). Modelling spinal circuitry involved in locomotor pattern generation: insights from deletions during fictive locomotion. *The Journal of physiology*, *577*(Pt 2), 617–639. doi:10.1113/jphysiol.2006.118703

Saito, K., Ito, S., Kitazawa, T., & Ohga, A. (1982). Selective inhibition by methusergide of the monosynaptic reflex discharge in the isolated spinal cord of the newborn rat. *Brain research*, *251*(1), 117–125. doi:10.1016/0006-8993(82)91279-3

Satterlie, R. A., & Norekian, T. P. (1995). Serotonergic modulation of swimming speed in the pteropod mollusc Clione limacina. III. Cerebral neurons. *Journal of experimental biology*.

Sautel, F., Griffon, N., Lévesque, D., Pilon, C., Schwartz, J. C., & Sokoloff, P. (1995). A functional test identifies dopamine agonists selective for D3 versus D2 receptors. *Neuroreport*, *6*(2), 329–332.

Schmidt, B. J., & Jordan, L. M. (2000). The role of serotonin in reflex modulation and locomotor rhythm production in the mammalian spinal cord. *Brain research bulletin*, *53*(5), 689–710.

Schotland, J., Shupliakov, O., Wikström, M., Brodin, L., Srinivasan, M., You, Z. B., et al. (1995). Control of lamprey locomotor neurons by colocalized monoamine transmitters. *Nature*, *374*(6519), 266–268. doi:10.1038/374266a0

Selverston, A. I., & Moulins, M. (1985). Oscillatory neural networks. *Annual review of physiology*, *47*, 29–48. doi:10.1146/annurev.ph.47.030185.000333

Serrano, G. E., Martínez-Rubio, C., & Miller, M. W. (2007). Endogenous motor neuron

properties contribute to a program-specific phase of activity in the multifunctional feeding central pattern generator of Aplysia. *Journal of neurophysiology*, *98*(1), 29–42. doi:10.1152/jn.01062.2006

Seth, P., Gajendiran, M., Maitra, K. K., Ross, H. G., & Ganguly, D. K. (1993). Evidence for D1 dopamine receptor-mediated modulation of the synaptic transmission from motor axon collaterals to Renshaw cells in the rat spinal cord. *Neuroscience letters*, *158*(2), 217–220.

Shapovalov, A. I. (1975). Neuronal organization and synaptic mechanisms of supraspinal motor control in vertebrates. In *Reviews of Physiology* (Vol. 72, pp. 1–54). Berlin/Heidelberg: Springer-Verlag. doi:10.1007/BFb0031545

Sherrington, C. S. (1910). Flexion-reflex of the limb, crossed extension-reflex, and reflex stepping and standing. *The Journal of physiology*, *40*(1-2), 28–121.

Shipe, W. D., Barrow, J. C., Yang, Z.-Q., Lindsley, C. W., Yang, F. V., Schlegel, K.-A. S., et al. (2008). Design, synthesis, and evaluation of a novel 4-aminomethyl-4-fluoropiperidine as a T-type Ca2+ channel antagonist. *Journal of medicinal chemistry*, *51*(13), 3692–3695. doi:10.1021/jm800419w

Sibley, D. R. (1999). New insights into dopaminergic receptor function using antisense and genetically altered animals. *Annual review of pharmacology and toxicology*, *39*, 313–341. doi:10.1146/annurev.pharmtox.39.1.313

Sickles, A. E., Stehouwer, D. J., & Van Hartesveldt, C. (1992). Dopamine D1 and D2 antagonists block L-dopa-elicited air-stepping in neonatal rats. *Brain research. Developmental brain research*, *68*(1), 17–22.

Skinner, F. K., Kopell, N., & Marder, E. (1994). Mechanisms for oscillation and frequency control in reciprocally inhibitory model neural networks. *Journal of Computational Neuroscience*, *1*(1-2), 69–87. doi:10.1007/BF00962719

Smith, J. C., & Feldman, J. L. (1987). In vitro brainstem-spinal cord preparations for study of motor systems for mammalian respiration and locomotion. *Journal of neuroscience methods*, *21*(2-4), 321–333.

Smith, J. C., Feldman, J. L., & Schmidt, B. J. (1988). Neural mechanisms generating locomotion studied in mammalian brain stem-spinal cord in vitro. *FASEB journal : official publication of the Federation of American Societies for Experimental Biology*, *2*(7), 2283–2288.

Sokoloff, P., Andrieux, M., Besançon, R., Pilon, C., Martres, M. P., Giros, B., & Schwartz, J. C. (1992). Pharmacology of human dopamine D3 receptor expressed in a mammalian cell line: comparison with D2 receptor. *European journal of pharmacology*, *225*(4), 331–337.

Staley, K. J., Longacher, M., Bains, J. S., & Yee, A. (1998). Presynaptic modulation of CA3 network activity. *Nature neuroscience*, *1*(3), 201–209. doi:10.1038/651

Steeves, J. D., & Jordan, L. M. (1980). Localization of a descending pathway in the spinal cord which is necessary for controlled treadmill locomotion. *Neuroscience letters*, *20*(3), 283–288.

Steinbusch, H. W. (1981). Distribution of serotonin-immunoreactivity in the central nervous system of the rat-cell bodies and terminals. *Neuroscience*, *6*(4), 557–618.

Stephenson-Jones, M., Ericsson, J., Robertson, B., & Grillner, S. (2012). Evolution of the basal ganglia: dual-output pathways conserved throughout vertebrate phylogeny. *The Journal of comparative neurology*, *520*(13), 2957–2973. doi:10.1002/cne.23087

Stephenson-Jones, M., Samuelsson, E., Ericsson, J., Robertson, B., & Grillner, S. (2011). Evolutionary conservation of the basal ganglia as a common vertebrate mechanism for action selection. *Current biology : CB*, *21*(13), 1081–1091. doi:10.1016/j.cub.2011.05.001

Strauss, I., & Lev-Tov, A. (2003). Neural pathways between sacrocaudal afferents and lumbar pattern generators in neonatal rats. *Journal of neurophysiology*, *89*(2), 773–784. doi:10.1152/jn.00716.2002

Surmeier, D. J., & Kitai, S. T. (1993). D1 and D2 dopamine receptor modulation of sodium and potassium currents in rat neostriatal neurons. *Progress in brain research*, *99*, 309–324.

Svensson, E., Woolley, J., Wikström, M., & Grillner, S. (2003). Endogenous dopaminergic modulation of the lamprey spinal locomotor network. *Brain research*, *970*(1-2), 1–8.

Swanson, L. W. (2000). Cerebral hemisphere regulation of motivated behavior. *Brain research*, *886*(1-2), 113–164.

Swanson, L. W., Mogenson, G. J., Gerfen, C. R., & Robinson, P. (1984). Evidence for a projection from the lateral preoptic area and substantia innominata to the "mesencephalic locomotor region" in the rat. *Brain research*, *295*(1), 161–178.

Takahashi, T., & Berger, A. J. (1990). Direct excitation of rat spinal motoneurones by serotonin. *The Journal of physiology*, *423*, 63–76.

Takakusaki, K., Saitoh, K., Harada, H., & Kashiwayanagi, M. (2004). Role of basal ganglia-brainstem pathways in the control of motor behaviors. *Neuroscience research*, *50*(2), 137–151. doi:10.1016/j.neures.2004.06.015

Takeuchi, Y., Kojima, M., Matsuura, T., & Sano, Y. (1983). Serotonergic innervation on the motoneurons in the mammalian brainstem. Light and electron microscopic immunohistochemistry. *Anatomy and embryology*, *167*(3), 321–333.

Tamae, A., Nakatsuka, T., Koga, K., Kato, G., Furue, H., Katafuchi, T., & Yoshimura, M. (2005). Direct inhibition of substantia gelatinosa neurones in the rat spinal cord by activation of dopamine D2-like receptors. *The Journal of physiology*, *568*(Pt 1), 243–253. doi:10.1113/jphysiol.2005.091843

Tang, C., Presser, F., & Morad, M. (1988). Amiloride selectively blocks the low threshold (T) calcium channel. *Science (New York, N.Y.)*, *240*(4849), 213–215. doi:10.1126/science.2451291

Tartas, M., Morin, F., Barriere, G., Goillandeau, M., Lacaille, J.-C., Cazalets, J.-R., & Bertrand, S. S. (2010). Noradrenergic modulation of intrinsic and synaptic properties of lumbar motoneurons in the neonatal rat spinal cord. *Frontiers in neural circuits*, *4*, 4–16. doi:10.3389/neuro.04.004.2010

Tazerart, S., Viemari, J.-C., Darbon, P., Vinay, L., & Brocard, F. (2007). Contribution of persistent sodium current to locomotor pattern generation in neonatal rats. *Journal of neurophysiology*, *98*(2), 613–628. doi:10.1152/jn.00316.2007

Tegnér, J., Hellgren-Kotaleski, J., Lansner, A., & Grillner, S. (1997). Low-Voltage-Activated Calcium Channels in the Lamprey Locomotor Network: Simulation and Experiment. *Journal of neurophysiology*, *77*(4), 1795–1812.

Todorovic, S. M., & Lingle, C. J. (1998). Pharmacological Properties of T-Type Ca2+ Current in Adult Rat Sensory Neurons: Effects of Anticonvulsant and Anesthetic Agents. *Journal of neurophysiology*.

Tresch, M. C., & Kiehn, O. (2000). Motor coordination without action potentials in the mammalian spinal cord. *Nature neuroscience*, *3*(6), 593–599. doi:10.1038/75768

Tsien, R. W., Lipscombe, D., Madison, D. V., Bley, K. R., & Fox, A. P. (1988). Multiple types of neuronal calcium channels and their selective modulation. *Trends in neurosciences*, *11*(10), 431–438.

Tytgat, J., Vereecke, J., & Carmeliet, E. (1990). Mechanism of cardiac T-type Ca channel

blockade by amiloride. *The Journal of pharmacology and experimental therapeutics*, *254*(2), 546–551.
Uebele, V. N., Nuss, C. E., Fox, S. V., Garson, S. L., Cristescu, R., Doran, S. M., et al. (2009). Positive Allosteric Interaction of Structurally Diverse T-Type Calcium Channel Antagonists. *Cell Biochemistry and Biophysics*, *55*(2), 81–93. doi:10.1007/s12013-009-9057-4
Vergara, C., Latorre, R., Marrion, N. V., & Adelman, J. P. (1998). Calcium-activated potassium channels. *Current opinion in neurobiology*, *8*(3), 321–329.
Viana, F., Van den Bosch, L., Missiaen, L., Vandenberghe, W., Droogmans, G., Nilius, B., & Robberecht, W. (1997). Mibefradil (Ro 40-5967) blocks multiple types of voltage-gated calcium channels in cultured rat spinal motoneurones. *Cell calcium*, *22*(4), 299–311.
Wang, D., Grillner, S., & Wallén, P. (2011). 5-HT and dopamine modulates CaV1.3 calcium channels involved in postinhibitory rebound in the spinal network for locomotion in lamprey. *Journal of neurophysiology*, *105*(3), 1212–1224. doi:10.1152/jn.00324.2009
Wang, M. Y., & Dun, N. J. (1990). 5-Hydroxytryptamine responses in neonate rat motoneurones in vitro. *The Journal of physiology*, *430*, 87–103.
Weil-Fugazza, J., & Godefroy, F. (1993). Dorsal and ventral dopaminergic innervation of the spinal cord: functional implications. *Brain research bulletin*, *30*(3-4), 319–324.
Wenner, P., & O'Donovan, M. J. (1999). Identification of an interneuronal population that mediates recurrent inhibition of motoneurons in the developing chick spinal cord. *The Journal of neuroscience : the official journal of the Society for Neuroscience*, *19*(17), 7557–7567.
Wenner, P., & O'Donovan, M. J. (2001). Mechanisms that initiate spontaneous network activity in the developing chick spinal cord. *Journal of neurophysiology*, *86*(3), 1481–1498.
Whelan, P. J., Hiebert, G. W., & Pearson, K. G. (1995). Plasticity of the extensor group I pathway controlling the stance to swing transition in the cat. *Journal of neurophysiology*, *74*(6), 2782–2787.
Whelan, P., Bonnot, A., & O'Donovan, M. J. (2000). Properties of rhythmic activity generated by the isolated spinal cord of the neonatal mouse. *Journal of neurophysiology*, *84*(6), 2821–2833.
Williams, M. E., Washburn, M. S., Hans, M., Urrutia, A., Brust, P. F., Prodanovich, P., et al. (2002). Structure and Functional Characterization of a Novel Human Low-Voltage Activated Calcium Channel. *Journal of neurochemistry*, *72*(2), 791–799. doi:10.1046/j.1471-4159.1999.0720791.x
Wilson, J. M., Hartley, R., Maxwell, D. J., Todd, A. J., Lieberam, I., Kaltschmidt, J. A., et al. (2005). Conditional rhythmicity of ventral spinal interneurons defined by expression of the Hb9 homeodomain protein. *The Journal of neuroscience : the official journal of the Society for Neuroscience*, *25*(24), 5710–5719. doi:10.1523/JNEUROSCI.0274-05.2005
Wilson, R. J. A., Chersa, T., & Whelan, P. J. (2003). Tissue PO2 and the effects of hypoxia on the generation of locomotor-like activity in the in vitro spinal cord of the neonatal mouse. *Neuroscience*, *117*(1), 183–196.
Wilson, R., Vasilakos, K., & Remmers, J. E. (2006). Phylogeny of vertebrate respiratory rhythm generators: The Oscillator Homology Hypothesis. *Respiratory physiology & Neurobiology*, (154), 47–60.
Wolf, M. E., & Roth, R. H. (1990). Autoreceptor Regulation of Dopamine Synthesis. *Annals of the New York Academy of Sciences*, *604*(1 Presynaptic R), 323–343. doi:10.1111/j.1749-6632.1990.tb32003.x

Xu, M., Moratalla, R., Gold, L. H., Hiroi, N., Koob, G. F., Graybiel, A. M., & Tonegawa, S. (1994). Dopamine D1 receptor mutant mice are deficient in striatal expression of dynorphin and in dopamine-mediated behavioral responses. *Cell*, *79*(4), 729–742.

Yang, C. R., Seamans, J. K., & Gorelova, N. (1999). Developing a neuronal model for the pathophysiology of schizophrenia based on the nature of electrophysiological actions of dopamine in the prefrontal cortex. *Neuropsychopharmacology : official publication of the American College of Neuropsychopharmacology*, *21*(2), 161–194. doi:10.1016/S0893-133X(98)00112-2

Yoshida, M., & Tanaka, M. (1988). Existence of new dopaminergic terminal plexus in the rat spinal cord: assessment by immunohistochemistry using anti-dopamine serum. *Neuroscience letters*, *94*(1-2), 5–9.

Yunker, A. M. R., Sharp, A. H., Sundarraj, S., Ranganathan, V., Copeland, T. D., & McEnery, M. W. (2003). Immunological characterization of T-type voltage-dependent calcium channel CaV3.1 (alpha 1G) and CaV3.3 (alpha 1I) isoforms reveal differences in their localization, expression, and neural development. *Neuroscience*, *117*(2), 321–335.

Zamponi, G. W., Bourinet, E., & Snutch, T. P. (1996). Nickel Block of a Family of Neuronal Calcium Channels: Subtype- and Subunit-Dependent Action at Multiple Sites. *The Journal of Membrane Biology*, *151*(1), 77–90. doi:10.1007/s002329900059

Zemlan, F. P., Murphy, A. Z., & Behbehani, M. M. (1994). 5-HT1A receptors mediate the effect of the bulbospinal serotonin system on spinal dorsal horn nociceptive neurons. *Pharmacology*, *48*(1), 1–10.

Zhang, B., Wootton, J. F., & Harris-Warrick, R. M. (1995). Calcium-dependent plateau potentials in a crab stomatogastric ganglion motor neuron. II. Calcium-activated slow inward current. *Journal of neurophysiology*, *74*(5), 1938–1946.

Zhang, S. P., Zhou, L. W., & Weiss, B. (1994). Oligodeoxynucleotide antisense to the D1 dopamine receptor mRNA inhibits D1 dopamine receptor-mediated behaviors in normal mice and in mice lesioned with 6-hydroxydopamine. *The Journal of pharmacology and experimental therapeutics*, *271*(3), 1462–1470.

Zhong, G., Díaz-Ríos, M., & Harris-Warrick, R. M. (2006). Intrinsic and functional differences among commissural interneurons during fictive locomotion and serotonergic modulation in the neonatal mouse. *The Journal of neuroscience : the official journal of the Society for Neuroscience*, *26*(24), 6509–6517. doi:10.1523/JNEUROSCI.1410-06.2006

Zhong, G., Droho, S., Crone, S. A., Dietz, S., Kwan, A. C., Webb, W. W., et al. (2010). Electrophysiological characterization of V2a interneurons and their locomotor-related activity in the neonatal mouse spinal cord. *The Journal of neuroscience : the official journal of the Society for Neuroscience*, *30*(1), 170–182. doi:10.1523/JNEUROSCI.4849-09.2010

Zhong, G., Masino, M. A., & Harris-Warrick, R. M. (2007). Persistent sodium currents participate in fictive locomotion generation in neonatal mouse spinal cord. *The Journal of neuroscience : the official journal of the Society for Neuroscience*, *27*(17), 4507–4518. doi:10.1523/JNEUROSCI.0124-07.2007

Zhu, H., Clemens, S., Sawchuk, M., & Hochman, S. (2007). Expression and distribution of all dopamine receptor subtypes (D1–D5) in the mouse lumbar spinal cord: A real-time polymerase chain reaction and non-autoradiographic in situ hybridization study. *Neuroscience*, *149*(4), 885–897. doi:10.1016/j.neuroscience.2007.07.052

Ziskind-Conhaim, L., Wu, L., & Wiesner, E. P. (2008). Persistent sodium current contributes to induced voltage oscillations in locomotor-related hb9 interneurons in the mouse spinal cord. *Journal of neurophysiology*, *100*(4), 2254–2264. doi:10.1152/jn.90437.2008